



**HAL**  
open science

# Development of tools for the precise control of biological parameters via microfluidics

Camila Betterelli Giuliano

## ► To cite this version:

Camila Betterelli Giuliano. Development of tools for the precise control of biological parameters via microfluidics. Other. Université de Strasbourg, 2022. English. NNT: 2022STRAF037. tel-04271875

**HAL Id: tel-04271875**

**<https://theses.hal.science/tel-04271875>**

Submitted on 6 Nov 2023

**HAL** is a multi-disciplinary open access archive for the deposit and dissemination of scientific research documents, whether they are published or not. The documents may come from teaching and research institutions in France or abroad, or from public or private research centers.

L'archive ouverte pluridisciplinaire **HAL**, est destinée au dépôt et à la diffusion de documents scientifiques de niveau recherche, publiés ou non, émanant des établissements d'enseignement et de recherche français ou étrangers, des laboratoires publics ou privés.

*ÉCOLE DOCTORALE SCIENCES CHIMIQUES (ED222)*

Institut de science et d'ingénierie supramoléculaires (ISIS)

UMR 7006

**THÈSE** présentée par :

**Camila BETTERELLI GIULIANO**

soutenue le : **22 Septembre 2022**

pour obtenir le grade de : **Docteur de l'université de Strasbourg**

Discipline/ Spécialité : Chimie

**Development of tools for the precise control  
of biological parameters via microfluidics**

**Développement d'outils pour le contrôle précis de  
paramètres à intérêts biologiques utilisant la  
microfluidique**

THÈSE dirigée par :

**M. MORAN Joseph**

Professor, Université de Strasbourg

RAPPORTEURS :

**Mme. SIMMCHEN Juliane**

Directrice de Recherche, Technical University of Dresden

**M. GARCIA César**

Directeur de Recherche, Luxembourg Institute of Science and Technology

AUTRES MEMBRES DU JURY :

**Mme. TALY Valérie**

Directrice de Recherche, CNRS

**Mme. SEPULVEDA Julia**

Directrice d'Innovation, Elvsys

**M. MICHEL Patrick Pierre**

Directeur Scientifique, ICM

“Faz meu coração brilhar  
Que o sol já vai chegar  
Trazendo esperança  
Pois afinal a vida é uma dança”

Ó do Forró – ‘A vida é uma dança’

# Acknowledgements

“Gratitude is when memory is stored in the heart and not in the mind.” –  
**Lionel Hampton**

During my Master's thesis, I was surprised to see my friends' short acknowledgement sessions, while I had so much to be thankful for. And once again, the story repeats itself, and I have so many people to thank that I don't even know where to start.

I will dutifully start by acknowledging Elvesys for giving me the opportunity to do my thesis with them. I "personificate" the company and direct my thank you to Julia Sepulveda and Guilhem Velve-Casquillas. The only thing I knew for certain when I started was that everything would change, and so it did. And it was quite a ride! The ups and downs were the most fruitful learning moments, and I finish this career cycle with the certainty that I was fortunate to have done my PhD in such a particular environment. Elvesys has a distinctive culture, and I'm grateful for it. Besides, what other place has a pole dance bar in the office?!

There are so many people in Elvesys that I would like to cite, and I know I will probably end up being unfair, but I cannot not extend my acknowledgements to Jessica, who does not work there anymore but was the best emotional support I could have to cross a pandemic and the difficulties of my first project. And Lisa, who hit the ground running, lending me her super structured scientific mind, so I could make the most of my last months and turn an assortment of almost unrelated experiments into a proper PhD thesis. To Alan, the best problem-solver and most patient engineer I have ever met. Thank you for saving my neck so many times! To Sébastien, the best pole dance buddy I could have asked for. To Christa, for her easy laugh in the corridors (heard and recognisable from every room in the company!) and all great moments spent outside the office. To everyone else at Elvesys, I would like to say that you made my days brighter, and it was a pleasure sharing these past three years with you.

I would like to thank the members of the Protomet Consortium for taking on the challenge of adding an industrial PhD to the mix. A heartfelt thank you to my academic supervisor, Joseph Moran, who agreed to supervise it before the University. If not like that, I would probably not have pursued a doctoral degree. Nonetheless, we all know it is not straightforward to navigate academic and corporate cultures. All exchanges with PIs and other PhDs, the secondments

and the meetings were enriching experiences. It was a pleasure to work with all of you. Lorena, thank you for making everything run so smoothly.

Regardless of how many times you move countries, adapting to a new place is always a mentally-demanding process. It can be made easier by a combination of factors: the support you have back home; and the people you find, and the connections you make, in the new place. I, luckily, have always had both. My parents, Eliana and Vagner, have always supported me and my career, even if they don't have a clue about what I do since I got into university. From their eyes, no dream is too big for me. I also have the privilege to be surrounded (at this point virtually) by remarkable women. My dear friend, Isadora, has never been so close while being far. And I couldn't be more grateful for her presence in my life and her patience with all my podcasts. Rafaela, my Brazilian wife, is the one I run to when I need a reality check. And man, how many of those were needed in these past three years!

Although I have lived abroad many times before, France has been where I stayed the longest and where I found myself the happiest outside Brazil. And that's mainly due to the people I've found myself surrounded by. Besides the crew at Elvsys, I've found myself connected to an incredible community of people who share the same passion (or should I say obsession?) with forró. The Brazilian dance has united us, but the exchanges go far beyond it, and I feel I'm continuously embraced in a warm hug. Dancing has been the best way to celebrate my good lab days and overcome the bad ones. I've seen myself apply my scientific mind to progress quickly as a dancer and, on the other hand, become a better scientist because the joy and the stress relief made my mind sharper.

I've always seen my career as a hybrid between science and business, aiming to gracefully navigate between both worlds. Now, I come to the end of my PhD realising this duality extends far beyond my career, and I am learning to navigate between science and art.

For that, I could not be more grateful.

So, thank you all.

Camila Betterelli Giuliano



# Table of Contents

<b>Acknowledgements.....</b>	<b>3</b>
<b>Abstract.....</b>	<b>5</b>
<b>List of Abbreviations.....</b>	<b>17</b>
<b>CHAPTER 1.....</b>	<b>19</b>
<b>INTRODUCTION.....</b>	<b>19</b>
<b>1. Introduction.....</b>	<b>20</b>
<b>1.1. Introduction to Microfluidics.....</b>	<b>20</b>
<b>1.2. Microfabrication.....</b>	<b>23</b>
1.2.1. Photolithography and Soft-lithography.....	23
<b>1.3. Microfluidics for biological applications.....</b>	<b>25</b>
1.3.1. Microfluidics and drug delivery systems.....	27
<b>1.3.2. Microenvironment monitoring for microfluidic cell culture.....</b>	<b>38</b>
1.3.2.1 Microfluidic Cell Culture.....	38
1.3.2.2. The importance of pH monitoring.....	41
1.3.2.3. Monitoring the microfluidic cell culture environment.....	43
<b>1.4. Aims and Scope of Thesis.....</b>	<b>46</b>
<b>1.5. References.....</b>	<b>47</b>
<b>CHAPTER 2.....</b>	<b>54</b>
<b>MARKET STUDY: ENCAPSULATION-IN-DROPLETS AND MICROENVIRONMENT MONITORING OF MICROFLUIDIC CELL CULTURES.....</b>	<b>54</b>
<b>2.1. Introduction.....</b>	<b>56</b>
2.1.1. Research rationale.....	57
<b>2.2. Research Methodology.....</b>	<b>58</b>

2.2.1.	Competitive Landscape Review .....	58
2.2.2.	Researcher Surveys .....	58
2.2.3.	Market sizing and Financial Analysis .....	59
<b>2.3.</b>	<b><i>Results and Discussion</i></b> .....	<b>60</b>
2.3.1.	Overview of the market assessment .....	60
2.3.2.	Investigation of market demand for Encapsulation in Droplets.....	62
2.3.2.1.	Market Segmentation of applications.....	62
2.3.2.2.	Financial Analysis for Risk Assessment .....	64
2.3.2.3.	Market acceptance and barriers to entry .....	68
2.3.2.4.	Feedback analysis of potential users .....	69
2.3.3.	Determination of technical needs for microenvironment monitoring in microfluidic cell culture	77
2.3.3.1.	Main technical needs .....	78
2.3.3.2.	Refining technical parameters for off-chip pH monitoring.....	81
2.3.3.3.	Main existing solutions .....	83
2.3.3.4.	Financial Analysis for Risk Assessment .....	85
<b>2.4.</b>	<b><i>Conclusions and Outlook</i></b> .....	<b>87</b>
<b>2.5.</b>	<b><i>References</i></b> .....	<b>89</b>
<b>CHAPTER 3.....</b>		<b>100</b>
<b>MICROFLUIDIC-BASED MICROCOMPARTMENTS: PRODUCTION AND ENCAPSULATION .....</b>		<b>100</b>
<b>3.1.</b>	<b><i>Introduction</i></b> .....	<b>102</b>
<b>3.2.</b>	<b><i>Materials and Method</i></b> .....	<b>107</b>
3.2.1.	Microfluidic chip fabrication.....	107
3.2.1.1.	SU-8 Mold fabrication .....	107
3.2.1.2.	PDMS Chip fabrication .....	108
3.2.2.	Channel Characterisation .....	108
3.2.3.	Single Emulsion Formation .....	109
3.2.4.	Encapsulation in single emulsions.....	109



<b>3.2.5. Double Emulsions Production</b>	<b>109</b>
3.2.5.1. Solution Preparation	109
3.2.5.2. Surface Coating	111
3.2.5.3. Double Emulsion Production	112
3.2.5.4. Off-chip dewetting	113
3.2.5.5. Membrane Permeability Assay	113
<b>3.3. Results and Discussion</b>	<b>113</b>
<b>3.3.1. Microfluidic chip fabrication</b>	<b>113</b>
3.3.1.1. Channel characterisation	114
<b>3.3.2. Single-emulsion production</b>	<b>116</b>
3.3.2.1. Encapsulation in single emulsions	117
<b>3.3.3. Double Emulsion Production</b>	<b>119</b>
3.3.3.1. Surface Coating	119
a. Design 1 and 2	119
b. Design 3	120
3.3.3.2. Microfluidic Setup	121
3.3.3.3. DE production with Design 1	122
3.3.3.4. DE production with Design 2	132
3.3.3.5. DE production with Design 3	139
<b>3.4. Discussion</b>	<b>142</b>
3.4.1. DEs were successfully produced in non-specialist settings	142
3.4.2. No dewetting was observed	143
<b>3.5. Conclusion and Outlook</b>	<b>145</b>
<b>3.6. References</b>	<b>146</b>
<b>CHAPTER 4</b>	<b>149</b>
<b>PRODUCTION AND STABILITY OF DOUBLE EMULSIONS FOR ORAL DRUG DELIVERY</b>	<b>149</b>
<b>4.1. Introduction</b>	<b>151</b>
<b>4.2. Materials and Methods</b>	<b>153</b>
4.2.1. Microfluidic Production of Double Emulsions	153

4.2.2.	Image Analysis .....	154
4.2.3.	Encapsulation of compounds of interest .....	154
4.2.3.1.	Production of Large Unilamellar Vesicles (LUVs) .....	154
4.2.3.2.	Encapsulation in Double Emulsions .....	155
4.2.4.	Stability Assays .....	155
4.2.4.1.	DE temperature stability over time .....	155
4.2.4.2.	DE pH stability .....	155
4.2.4.3.	Stability of unloaded and loaded DEs at different mechanical stress conditions .....	156
<b>4.3.</b>	<b>Results.....</b>	<b>156</b>
4.3.1.	Microfluidics as a highly suitable method for reproducible DE production .....	156
4.3.2.	Stability Assays .....	157
4.3.3.	DE stability at different temperatures over time .....	157
4.3.4.	Encapsulation of compounds of interest and stability of loaded DEs over time .....	159
4.3.5.	DE stability at different pH ranges .....	162
4.3.6.	Stability of unloaded and loaded DEs under mechanical stimulus .....	163
<b>4.4.</b>	<b>Discussion.....</b>	<b>165</b>
4.4.1.	Environmental conditions affect loaded and unloaded DEs differently .....	165
4.4.2.	Cargo has considerable effect on long-term DE stability .....	167
4.4.3.	Localisation and properties of cargo are important parameters for DE drug delivery.....	168
<b>4.5.</b>	<b>Conclusion .....</b>	<b>169</b>
<b>CHAPTER 5.....</b>		<b>174</b>
<b>MONITORING ENVIRONMENTAL PARAMETERS IN MICROFLUIDIC CELL</b>		
<b>CULTURE.....</b>		<b>174</b>
<b>5.1.</b>	<b>Introduction.....</b>	<b>176</b>
<b>5.2.</b>	<b>Materials and Methods.....</b>	<b>178</b>
5.2.1.	CO <sub>2</sub> and pH characterisation of media .....	178
5.2.1.1.	Colorimetric Assay.....	178
5.2.1.2.	DMEM/CO <sub>2</sub> Characterisation: Static conditions .....	179

<b>5.2.2. Gas permeability of components .....</b>	<b>179</b>
5.2.2.1. Development of 3D printed flow cell .....	179
5.2.2.2. Gas permeability of different tubing materials .....	180
5.2.2.3. Gas permeability curve of PTFE in static conditions .....	180
5.2.2.4. Gas permeability of the chip in dynamic conditions.....	181
<b>5.2.3. Culturing cells outside the CO<sub>2</sub> incubator .....</b>	<b>181</b>
5.2.3.1. Cell Seeding .....	181
5.2.3.2. Static microfluidic cell culture outside the CO <sub>2</sub> incubator .....	182
5.2.3.3. Intermittent reservoir-to-waste cell culture outside the CO <sub>2</sub> incubator .....	182
5.2.3.4. Intermittent recirculation cell culture outside the CO <sub>2</sub> incubator .....	183
<b>5.3. Results.....</b>	<b>183</b>
<b>5.3.1. The importance of measuring pH in microfluidics.....</b>	<b>183</b>
<b>5.3.2. Design of 3D-printed flow cell .....</b>	<b>184</b>
<b>5.3.3. Characterisation of the effect of CO<sub>2</sub> on DMEM .....</b>	<b>185</b>
<b>5.3.4. Gas permeability of microfluidic components .....</b>	<b>186</b>
5.3.4.1. Gas permeability of Microfluidic tubing .....	186
5.3.4.2. Gas permeability of microfluidic chip .....	190
<b>5.3.5. Culturing cells outside the CO<sub>2</sub> incubator .....</b>	<b>195</b>
5.3.5.1. Static cell cultures on chip .....	195
5.3.5.2. Dynamic cell cultures on chip .....	196
<b>5.4. Discussion.....</b>	<b>202</b>
<b>5.4.1. Colorimetric pH assessment is insufficient for microfluidic cell culture .....</b>	<b>202</b>
<b>5.4.2. The rate of CO<sub>2</sub> diffusion through PTFE varies according to the parameters of the system</b>	<b>203</b>
<b>5.4.3. Off-chip pH sensing flow cell can detect metabolic cycles of cells cultured outside the CO<sub>2</sub> incubator .....</b>	<b>204</b>
<b>5.5. Conclusion and Outlook .....</b>	<b>205</b>
<b>5.6. References.....</b>	<b>206</b>
<b>CHAPTER 6.....</b>	<b>210</b>
<b>Conclusion and Outlook.....</b>	<b>210</b>

<i>Appendices.....</i>	<b>214</b>
<i>Appendix 1 - Chapter 2. [Encapsulation-in-Droplets] Questionnaire for Experts .....</i>	<b>215</b>
<i>Appendix 2 - Chapter 2. [Encapsulation-in-Droplets] Questionnaire for Potential Clients.....</i>	<b>218</b>
<i>Appendix 3 - Chapter 2. [Microenvironment Monitoring] Online Questionnaire</i>	<b>220</b>
<i>Appendix 4 - Chapter 2. [Microenvironment Monitoring] Interview Questionnaire .....</i>	<b>223</b>
<i>Appendix 5 - Chapter 2. A/B Testing - Single-cell Encapsulation.....</i>	<b>225</b>
<i>Appendix 6 - Chapter 2. A/B Testing - High-throughput Encapsulation .....</i>	<b>226</b>
<i>Appendix 7 - Chapter 2. A/B Testing – Cell Encapsulation .....</i>	<b>227</b>
<i>Appendix 8 - Chapter 2. Pilot Pack - pH control without Incubator.....</i>	<b>228</b>
<i>Appendix 9 - Chapter 2. Pilot Pack - CO2 control without Incubator .....</i>	<b>229</b>
<i>Appendix 10 - Chapter 2. Pilot Pack - pH control for cell culture.....</i>	<b>230</b>
<i>Appendix 11 - RÉSUMÉ EN FRANÇAIS .....</i>	<b>231</b>
<i>Appendix 12 – Scientific Outreach activities .....</i>	<b>241</b>
<i>Appendix 13 – Curriculum Vitae.....</i>	<b>242</b>

# List des Tables

Table 1.1. Summary of advantages and drawbacks of Microfluidics .....	22
Table 2.1. Assumptions for financial analysis of different market segments in soft microencapsulation .....	65
Table 2.2. Financial analysis of different market segments in soft microencapsulation.....	65
Table 2.3. Market Sizing for different market segments in soft microencapsulation .....	67
Table 2.4. Paid advertisement price ranges for selected keywords.....	68
Table 2.5. Summary of results of the A/B testing of the webpages.....	71
Table 2.6. Competitors' and substitutes' landscape .....	76
Table 2.7. Results of pilot packs on the website and of the email campaign .....	83
Table 2.8. The landscape of competitors in the microfluidic pH monitoring market.....	84
Table 2.9. Assumptions for financial analysis of different market segments in pH monitoring for microfluidic cell culture .....	85
Table 2.10. Financial analysis of different market segments in pH monitoring for microfluidic cell culture .....	85
Table 2.11. Market Sizing for different market segments in pH monitoring of microfluidic cell cultures.....	86
Table 2.12. Paid advertisement price ranges for selected keywords .....	87
Table 3.1. Protocols according to the SU-8 resin and desired height of the channels.....	107
Table 3.2. The widths and heights obtained from different SU-8 resins compared to the desired measures.....	116
Table 3.3. Numbers of cells encapsulated per droplet for different cell concentrations.....	119
Table 3.4. Comparison between the pressures used in the published e-beam lithography chip and the 25 $\mu\text{m}$ -high and 13 $\mu\text{m}$ -high soft lithography-made chips.....	125
Table 3.5. Results of varying surfactant concentration in double emulsion production.....	126
Table 3.6. Results of varying the composition of the inner and outer phases in double emulsion production. Controls use the standard solutions stated previously.....	127
Table 3.7. Results of varying lipid concentrations in double emulsion production .....	128
Table 3.8. Results of addition of lipid-specific dye, Dil, to the intermediate phase in double emulsion production .....	129
Table 3.9. Results of changing the resistance of the system in double emulsion production .....	129
Table 3.10. The widths and heights obtained from different SU-8 resins compared to the desired measures.....	131
Table 3.11. Results of varying surface treatment concentration in the double emulsion production in Design 1.2. ....	132

Table 3.12. Summary of tested variables and respective results of Design 2.....	135
Table 3.13. Encapsulation efficiencies and production rates of unloaded DEs and loaded DEs .....	136
Table 3.14. Summary of tested variables and respective results of Design 3.....	141
Table 4.1. Composition of the solutions used in the Temperature Assays.....	153
Table 4.2. Pressures and corresponding flow rates used to test the stability of the double emulsions under flow .....	156
Table 4.3. Results of varying POPC LUV concentrations in double emulsion production ...	160
Table 4.4. Encapsulation efficiencies and production rates of unloaded and loaded DEs...	160
Table 5.1. Values used to calculate the coefficient of permeability of PTFE tubing.....	189

# List of figures

Figure 1.1. Physical parameters governing microfluidics.....	21
Figure 1.2. Process of photolithography and soft-lithography.....	24
Figure 1.3. Microfluidics handles biological samples at <i>in vivo</i> length scales. ....	26
Figure 1.4. The rising interest in microfluidics and microfluidic-related biological applications through time. ....	27
Figure 1.5. Overview of different types of emulsions produced via microfluidics and respective templated drug delivery systems. ....	29
Figure 1.6. The most common microchannel geometries for microfluidics droplet formation.. ..	30
Figure 1.7. Schematic of the dripping and jetting regimes according to the capillary number of the continuous phase.....	31
Figure 1.8. Different flow regimes in cross-flow geometries according to the capillary number of the continuous phase.....	32
Figure 1.9. Flow regimes in flow-focusing geometries.....	33
Figure 1.10. Wettability of the surface.....	34
Figure 1.11. Marangoni effect of droplets in the absence or presence of a surfactant.. ..	35
Figure 1.12. Schematic representation of double emulsion formation with consecutive T-junctions.....	37
Figure 1.13. Illustration of the signals in the cell microenvironment.....	39
Figure 1.14. Organ-on-chip systems.....	40
Figure 1.15. Bicarbonate buffering system.....	43
Figure 1.16. Cell culture pH monitoring.....	44
Figure 2.1. Summary of market assessment process for the fields of interest.....	61
Figure 2.2. Segmentation of the encapsulation market.....	63
Figure 2.3. Illustration of the relationship between TAM, SAM and SOM.....	66
Figure 2.4. A/B testing of the landing pages.....	70
Figure 2.5. Profile of interviewees divided by position, location, field and application.....	72
Figure 2.6. Summary of the challenges reported by microfluidicists and non-microfluidicists during interviews.....	73
Figure 2.7. Decision-making process to work with microfluidics.....	74
Figure 2.8. Results of the questionnaire.....	79
Figure 2.9. Profile of interviewees according to position, location, field and application.....	80
Figure 2.10. A/B testing of pH in microfluidic cell culture.....	82
Figure 3.1. Simplified cross-sectional representation of different types of spherical vesicles dispersed in a bulk aqueous solution.....	103

Figure 3.2. DE-templated GUVs.....	104
Figure 3.3. Published designs used for microcompartment production.....	106
Figure 3.4. Microfluidic chip fabrication steps.....	114
Figure 3.5. Schematic of Design 1 and representative inserts of PDMS chips. ....	115
Figure 3.6. Microfluidic single emulsion production.....	117
Figure 3.7. Encapsulation in single emulsions. ....	118
Figure 3.8. a. Schematic of the coating setup. ....	120
Figure 3.9. Schematic of surface coating for Design 3. ....	121
Figure 3.10. a. Schematic of the microfluidic setup for double emulsion production. ....	122
Figure 3.11. Double emulsions production with Design 1. ....	123
Figure 3.12. Size distribution of DEs produced with Design 1. ....	124
Figure 3.13. Surface treatment of Design 1.....	126
Figure 3.14. Design 1.2 was adapted from Design 1. ....	130
Figure 3.15. Double emulsion production with Design 2.....	133
Figure 3.16. Microfluidic DEs size characterisation.....	134
Figure 3.17. Encapsulation of calcein (0.3mM) in DEs produced with Design 2. ....	136
Figure 3.18. Membrane Permeability Assay.....	138
Figure 3.19. Off-chip octanol dewetting assay. ....	139
Figure 3.20. Double emulsion production with Design 3.....	140
Figure 3.21. Size distribution of DEs produced with Design 3. ....	141
Figure 3.22. Membrane permeability assay. ....	142
Figure 4.1. Stability and morphological changes of unloaded DEs at different temperatures..	158
.....	
Figure 4.2. Encapsulation of cargo in DEs. ....	159
Figure 4.3. Stability of loaded DEs over time at RT.. ....	161
Figure 4.4. Morphological alterations of LUVs inside DEs in 24h.....	162
Figure 4.5. DE stability to different pH ranges.....	163
Figure 4.6. Flow profile of the stop-flow regimen for mechanical stimulus.. ....	164
Figure 4.7. Stability of unloaded and loaded DEs at different flow conditions.....	165
Figure 5.1. Phenol Red, as a pH indicator of cell cultures in traditional flasks and microfluidic	
devices.. ....	184
Figure 5.2. 3D-printed flow cell to house pH sensor plug.. ....	185
Figure 5.3. Characterisation of the pH of DMEM in different atmospheric concentrations of CO <sub>2</sub>	
(room air, 0%; CO <sub>2</sub> incubator, 5%), in static conditions. ....	186
Figure 5.4. Gas permeability of different polymeric materials.....	187
Figure 5.5. Gas permeability curve of PTFE tubing of different diameters (1/16" OD, ID = 700	
µm ID; 1/32" OD, ID = 300 µm).....	188



Figure 5.6. Schematic of microfluidic recirculation circuit..	191
Figure 5.7. Continuous and intermittent flow profiles of recirculation experiments..	192
Figure 5.8. Gas permeability of microfluidic devices.	193
Figure 5.9. Gas permeability of PTFE tubing..	194
Figure 5.10. Static microfluidic cell culture outside the CO <sub>2</sub> incubator..	195
Figure 5.11. Reservoir-to-waste microfluidic cell culture.....	197
Figure 5.12. Reservoir-to-waste microfluidic cell culture.....	198
Figure 5.13. Miniaturised recirculation system inside thermalisation chamber for microscope stage top.....	200
Figure 5.14. Microfluidic culture of HEK293 cells in thermalisation chamber with continuous pH monitoring.....	201

# List of Abbreviations

PDMS - polydimethylsiloxane  
μ-TAS - micro total analysis system  
MEMS - microelectromechanical systems  
Re - Reynolds Number  
We - Weber Number  
DEs - Double Emulsions  
PVA - polyvinyl alcohol  
PDADMAC - Poly(diallyldimethylammonium) chloride  
PSS - poly(sodium 4-styrenesulfonate)  
APTES - aminopropyltriethoxysilane  
PTFE - Polytetrafluoroethylene  
PFA - Perfluoroalkoxy alkanes  
PVDF - Polyvinylidene fluoride  
W/O/W - water-in-oil-in-water  
O/W/O - oil-in-water-in-oil  
HEPES - (4-(2-hydroxyethyl)-1-piperazineethanesulfonic acid)  
PIPES - (piperazine-N,N'-bis(2-ethanesulphonic acid)  
MES - (2-(N-morpholino)-ethanesulfonic acid; pKa = 6.0)  
NVB - non-volatile buffers  
MVV - Multivesicular Vesicle  
GUVs - Giant Unilamellar Vesicles  
LUVs - Large Unilamellar Vesicles  
R&D&I - Research, Development and Innovation  
SMEs - Small and Medium-sized Enterprises  
KOL - Key Opinion Leaders  
HTS - high-throughput screening  
OEM - Original Equipment Manufacturer  
TAM - Total Addressable Market  
SAM - Serviceable Available Market  
SOM - Serviceable Obtainable Market  
CAGR - Compound Annual Growth Rate  
IA - inner aqueous solution  
LO- lipid-oil solution  
OA - outer aqueous solution

DOPC - 1,2-dioleoyl-sn-glycero-3-phosphocholine  
POPC - 1-palmitoyl-2-oleoyl-sn-glycero-3-phosphocholine  
FBS - fetal bovine serum  
PS - Penicillin-streptomycin  
SD - Standard Deviation  
OD - Outer diameter  
ID - inner diameter  
DMEM - Dulbecco's Modified Eagle Medium  
MW - Molecular Weight  
FDA - Food and Drug Administration  
CV - coefficient of variation

# CHAPTER 1.

## INTRODUCTION

“...what matters in life is not whether we receive a round of applause; what matters is whether we have the courage to venture forth despite the uncertainty of acclaim.”

— Amor Towles, *A Gentleman in Moscow*

### ABSTRACT

---

This chapter briefly introduces microfluidics, its history and state-of-the-art microfabrication techniques. Moreover, microfluidics applications in biology research are reviewed and summarised, ranging from droplet-microfluidics for oral drug delivery to microenvironmental monitoring of long-term dynamic cell cultures. The chapter concludes by presenting the aims and scope of this dissertation and by briefly outlining the four experimental chapters that follow.

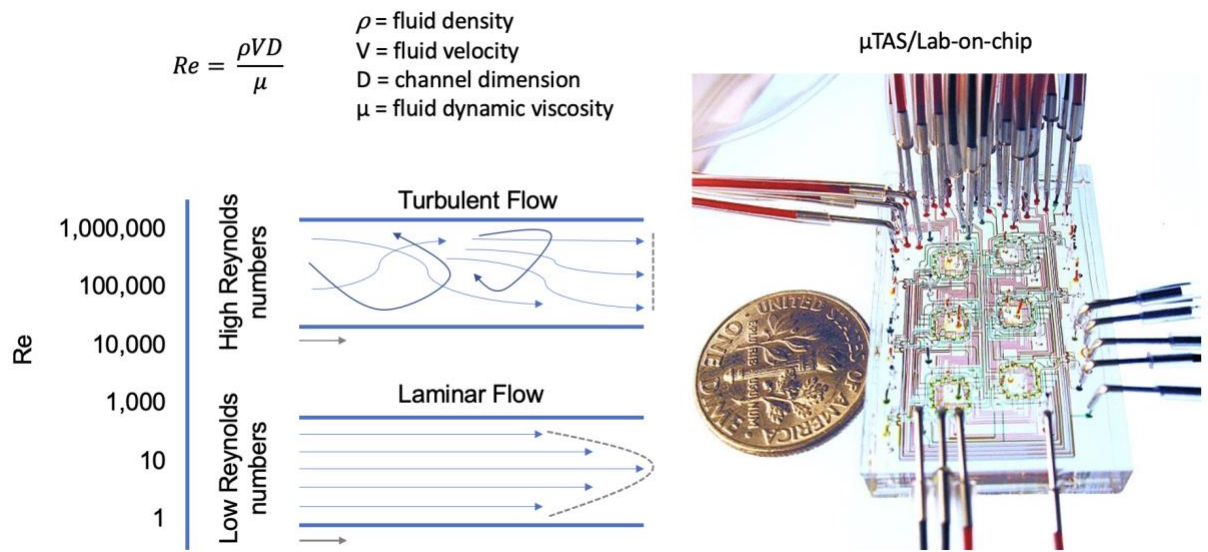
---

# 1. Introduction

## 1.1. Introduction to Microfluidics

Fluids have two well-characterised behaviours: the turbulent and the laminar<sup>1</sup>. These behaviours are represented by the dimensionless Reynolds number,  $Re$ , calculated by the ratio of inertial to viscous forces acting on the fluid flow. At high Reynolds numbers, the predominance is of the turbulent behaviour in which inertial forces dominate over viscous forces, leading to an unpredictable and chaotic flow. Laminar flow happens at low Reynolds numbers, where viscous forces are predominant, and the flow has predictable and parallel patterns<sup>1,2</sup> (Figure 1.1). Microfluidics came forth to take advantage of the controllability of laminar flows.

Microfluidics is a recent technological field that provides tools to handle liquid at the micro-scale. Fluids are driven through microchannels by external flow controllers (e.g. pressure-driven controllers, syringe pumps, or peristaltic pumps). The microchannels are assembled as "chips" by microfabrication techniques, discussed in more detail later, allowing patterns to be made in different materials. Downscaling to the micrometre range favours laminar flow behaviour and confers a high level of control, the use of minute volumes, and high surface-to-volume ratios<sup>2</sup>. Laminar flows can be leveraged for highly controlled delivery of e.g. chemical reagents, soluble factors, or biological samples. Moreover, these physical characteristics allow for fast heat and mass transfer, conferring thermal homogeneity across the working system and highly controllable diffusive mixing and fluid separation<sup>3</sup>.



**Figure 1.1.** Physical parameters governing microfluidics. (Left) The Reynolds number ( $Re$ ) describes the ratio of inertial to viscous forces and characterises the two distinct behaviours of fluids. At high Reynolds numbers ( $Re > 3,500$ ), fluid flow is turbulent, marked by vortices, unstable eddies, and advective mixing. At low Reynolds numbers ( $Re < 2,000$ ), the flow is laminar, moving in parallel lines in a smooth and predictable manner. The velocity flow profile of laminar flows is parabolic, and mixing happens only by diffusion. (Right) A microfluidic chip with connections, compared to the size of a coin. Reproduced from Balagadde *et al.*<sup>4</sup>

The main driving force of flow is a pressure differential. Flow ( $Q$ ) is directly proportional to the pressure difference ( $\Delta P$ ) between the inlet and the outlet of the microfluidic circuit and it is inversely proportional to the resistance ( $R$ ) of the system, e.g. frictional force (Eq. 1). The resistance of a microfluidic system relates to how easy it is to flow liquid through it,<sup>5,6</sup> for example, pulling a liquid through a thick straw is much easier than through a thin one. Resistance is independent of flow rate, being determined by the liquid viscosity, the length of the circuit, and the inner diameter of the tubing<sup>2</sup> (Eq. 3).

$$Q = \frac{\Delta P}{R} \tag{1}$$

$\Delta P$  is defined by Poiseuille's Equation<sup>7</sup>:

$$\Delta P = \frac{8\mu L Q}{\pi r^4} \tag{2}$$

Combining equations (1) and (2):

$$R = \frac{8\mu L}{\pi r^4} \quad (3)$$

in which, Q is the flow rate;  $\Delta P$  is the pressure difference; R is the resistance of the system;  $\mu$  is the fluid viscosity; L is the tubing length; and, r is the tubing inner radius.

The emergence of microfluidics is tightly linked to advancements in microelectronics. The pursuit of microelectromechanical systems (MEMS) to detect chemical and biological weapons in the field led to the creation of the first "laboratory-on-chip" by the US army<sup>8</sup>. Pioneered by the field of semiconductors, the miniaturisation and integration of components started being applied to chemistry assays, culminating in the "micro total analysis system" ( $\mu$ -TAS) concept. The goal was to develop microsystems that could perform all steps of laboratory analysis in a faster and more efficient way when compared to classical assays<sup>9</sup>. As the technology matured over the past 30 years, microfluidics advantages over conventional laboratory assays became more apparent and well-defined, yet, as with any technology, it has its own limitations<sup>10</sup> (Table 1.1.1.). Thus, miniaturising a conventional assay into microfluidics has to provide new insights that were not previously accessible to justify the added labour and potential loss of standardisation in the early stages<sup>11</sup>. This gain in untapped information has been shown to be particularly the case for biological assays.

**Table 1.1.** Summary of advantages and drawbacks of Microfluidics

<b>Microfluidics Advantages</b>	<b>Description</b>	<b>Microfluidics Drawbacks</b>	<b>Description</b>
<b>Less sample and reagent consumption</b>	Microfluidics assays require up to $10^3$ less sample volume	<b>Loss of sample</b>	Enhanced surface adsorption due to high surface-to-area ratio
<b>Enhanced heat transfer</b>	High surface-to-area ratio dissipates heat more effectively	<b>Incompatible with large sample volumes</b>	In micrometre-ranges, 1 ml can take more than 1000 min to be analysed
<b>Laminar Flow</b>	Low sample dissipation	<b>Mismatch with conventional tools</b>	Pipettes work in the microliter-range whereas microfluidic devices are in the nanolitre
<b>Parallelisation</b>	Possibility of running several assays simultaneously	<b>Loss of field standardisation</b>	Results from new assays might be hard to compare
<b>Portability</b>	Miniaturisation of conventional lab-bench assays	<b>Specialised requirements</b>	In early stages, microfluidics require specialised know-how to be implemented

The  $\mu$ -TAS concept and microfluidics tools quickly gained traction in the life sciences field in a wide range of biological applications such as cell sorting<sup>12–14</sup> and detection of rare cells<sup>15,16</sup>, point-of-care diagnostics<sup>17,18</sup>, single-cell studies<sup>19–21</sup>, DNA analysis<sup>22,23</sup>, high throughput screening for drug discovery<sup>24,25</sup>, droplet microfluidics for targeted drug delivery<sup>26–28</sup> and organ-on-chip<sup>29–31</sup>. The versatility of microfluidics as a toolset for biological applications will be explored in later sections.

## 1.2. Microfabrication

To promote laminar flow, the dimensions of the fluid path play a crucial role. Thus, to develop the micron-sized channels required for microfluidics, two lithography techniques were adopted from the semiconductor industry<sup>8</sup>.

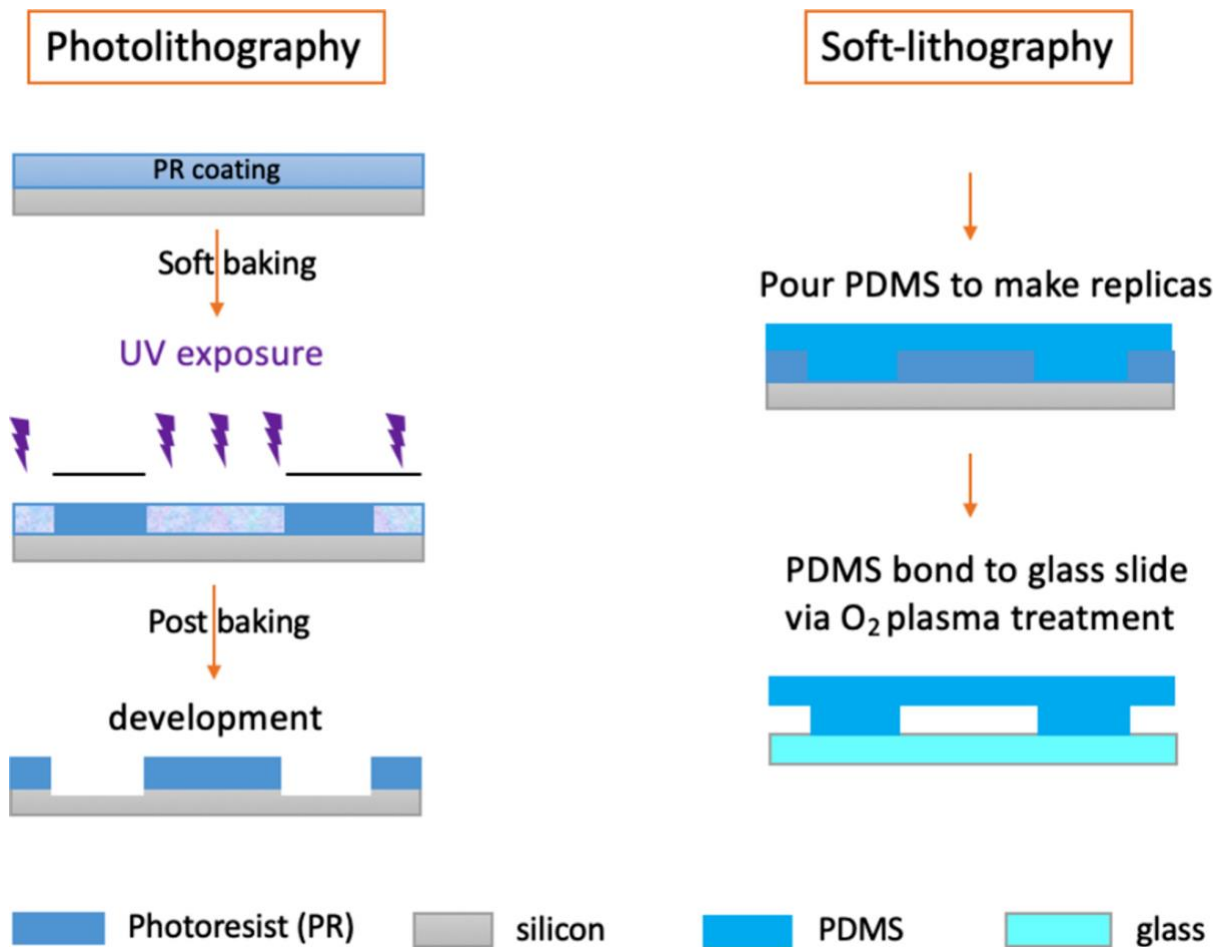
### 1.2.1. Photolithography and Soft-lithography

The term photolithography was first coined by Jay Lathrop and James R. Nall in 1958 in a publication presenting the use of photoresists to pattern germanium<sup>32</sup>. Briefly, the technique consists of spin-coating a thin layer of photoresist, *i.e.* a light-sensitive polymer, on a silicon wafer. The thickness of the layer can be controlled by the speed and time of the spin-coating along with the photoresist composition. After a soft-bake to harden the photoresist and allow placing the patterned photomask on top of it, it is exposed to light at the required wavelength. There are two types of photoresists: the negative photoresist, which crosslinks and remains after exposure to light, and the positive photoresist, which is dissolved when exposed to light. The wafer is baked once again to finish the crosslinking, followed by a process called "development", in which the non-crosslinked photoresist is dissolved, revealing the pattern<sup>2,33</sup> (Figure 1.2, left).

Soft-lithography was developed to handle non-semiconductor materials, which proved difficult with photolithography. It refers to the technique of casting a flexible elastomer onto a master mold<sup>34</sup>. Common soft-lithography techniques that became widespread in the microfluidics fields are replica molding (REM), microtransfer molding ( $\mu$ T), microcontact printing ( $\mu$ CT), and micromolding in capillaries (MIMIC)<sup>35–37</sup>. One of the most common methods to fabricate



microfluidic devices is to combine photolithography to create molds for soft-lithography, which can be used to replicate the desired pattern several times over (Figure 1.2, right).



**Figure 1.2.** Process of photolithography and soft-lithography. In microfluidics, photolithography is used to create molds for soft-lithography. A thin layer of photoresist is spin-coated onto a silicon wafer to the desired height, soft-baked, and then exposed to UV light. Once cross-linked, the photoresist is developed, and the pattern is revealed. The mold is then used to pattern a soft material, such as PDMS. Subsequently, the material is cured and bound to a substrate, such as glass, through surface activation with O<sub>2</sub> plasma treatment. Thus, the channels are closed and form the microfluidic device. Reproduced from Burklund *et al.*<sup>33</sup>

Silicon and glass were the first materials of choice in the early days of microfluidics, still considerably influenced by the microelectronics field. Silicon was widely used in the industry, with well-defined protocols, fabrication methods and resistance to organic solvents, making it a great candidate for  $\mu$ TAS. Nonetheless, silicon was not a cost-effective choice for structures in the micrometre range thus, microfluidic devices made with it had a relatively high cost per unit. Glass is compatible with biological assays due to its non-specific adsorption, but it is gas

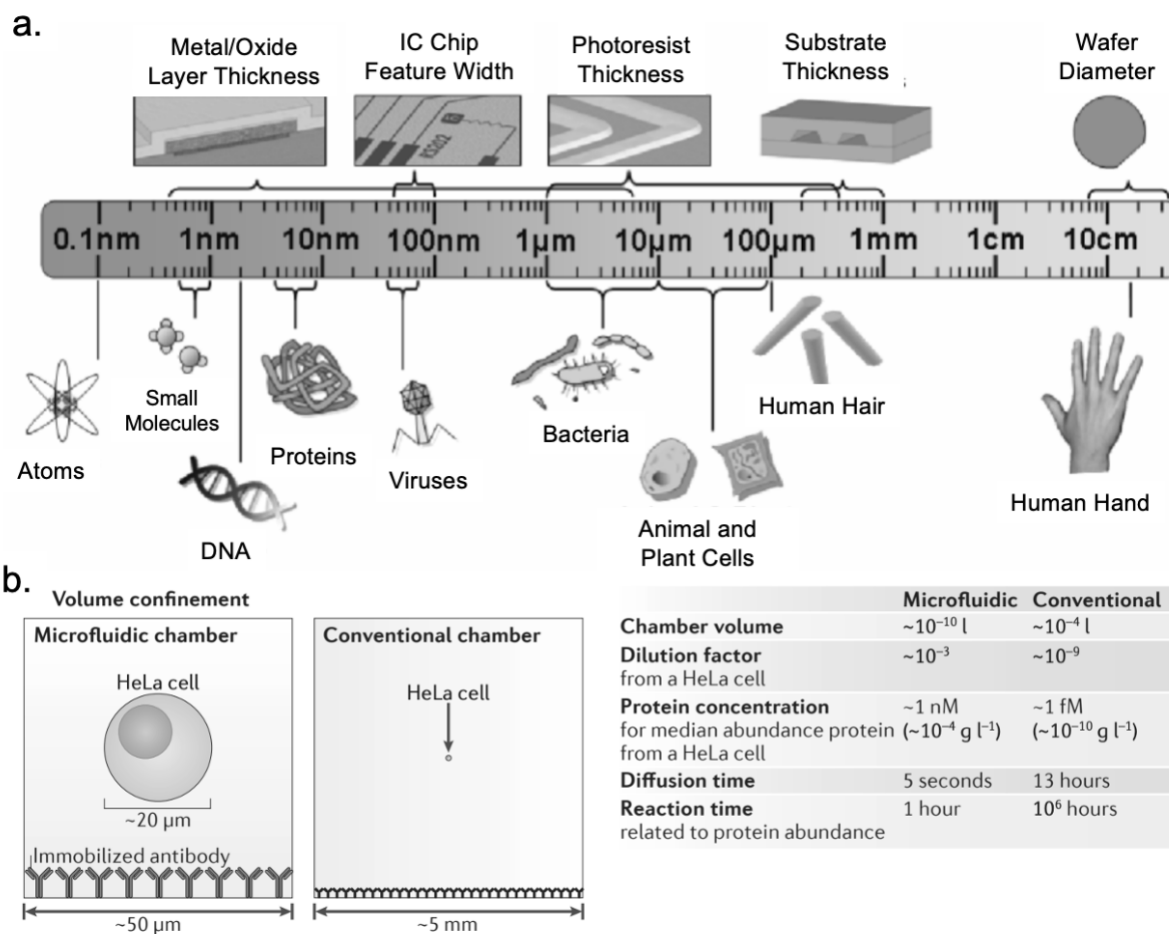
impermeable, an important consideration for life sciences applications involving mammalian cell cultures, which require oxygen to survive. The limitations of these materials prompted a search for something that was cheap, easy to use, malleable, and optically transparent<sup>33</sup>.

Elastomers, such as polydimethylsiloxane (PDMS), gained relevance after the group of George Whitesides at Harvard University introduced a new low-cost microfluidics method<sup>35</sup>. PDMS is a siloxane-based (silicone) two-part polymer produced by mixing a liquid base and a crosslinking agent. Optically transparent to ~300 nm, it has properties very different from those of silicon.<sup>38</sup> It is inherently hydrophobic but can be readily modified to hydrophilic through chemical modification of the surface or high surface energy state using oxygen plasma treatment<sup>39</sup>, although usually for a transient period of time. Considering biological applications, it is non-toxic to cells once cured<sup>40</sup>, compatible with proteins<sup>41</sup>, and relatively permeable to nonpolar gasses, such as O<sub>2</sub>, N<sub>2</sub>, and CO<sub>2</sub><sup>42</sup>.

Although high-compound absorption and low-throughput fabrication are the main disadvantages instigating further investigation into other materials, PDMS and other elastomers are inexpensive, easy to access, and can be subjected to chemical and physical modifications, making them nearly perfect materials for microfluidics in the laboratory-scale. Furthermore, the easiness of fabrication, conferred by soft-lithography and PDMS, has democratized access to microfluidics, moving it from engineering workshops to biology laboratories<sup>11</sup>.

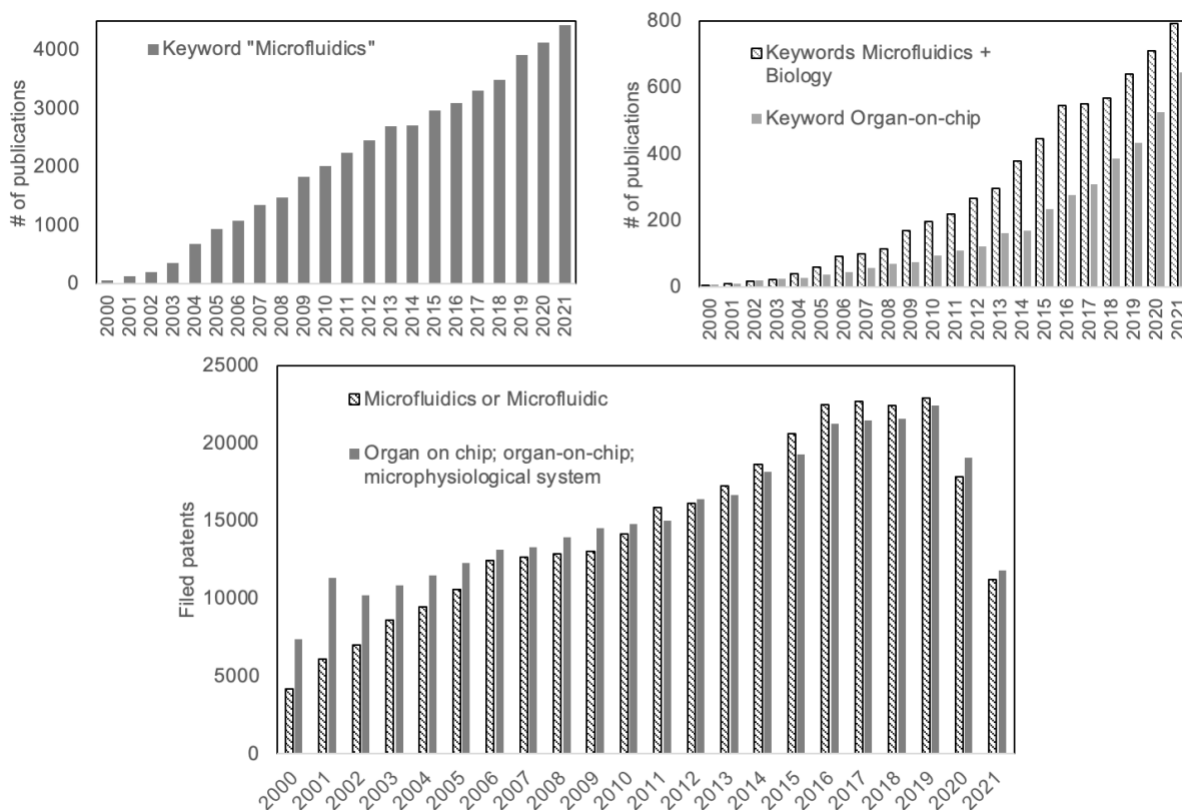
### **1.3. Microfluidics for biological applications**

Microfluidics has gained special relevance within biological applications. Most biological processes involve small-volume liquid transfers at some point, such as blood flowing through small capillaries, molecules crossing the cellular membrane, or oxygen diffusing in the lungs. Thus, microfluidics handles biological samples at *in vivo* length scales<sup>10</sup> (Figure 1.3).



**Figure 1.3.** Microfluidics handles biological samples at *in vivo* length scales. **a.** Approximate length scales of biological and microfabrication components. Reproduced from Sommer *et al.*<sup>10</sup> **b.** Consequences of handling samples at biological scales. Due to the small volumes, proteins of interest are much more concentrated, drastically decreasing the time necessary for detection. Reproduced from Duncombe *et al.*<sup>11</sup>

The technological potential of microfluidics can be easily translated into economic terms. The microfluidics global market was valued at USD17.9 billion in 2020, and it is expected to grow by 16.3% in 2028. The main driver of growth is the rise in clinical studies using cell-based therapies<sup>43</sup>. A PubMed search shows that the number of publications has been steadily increasing for the past 20 years for keywords such as "microfluidics", "microfluidics+biology", and "organ-on-chip". The number of filed patents on the Google Patents database also increased until 2019, reaching over 20,000 requests for keywords "microfluidic or microfluidics" and "organ-on-chip; organ on chip or microphysiological systems" (Figure 1.4). The following decrease might be attributed to repercussions of the COVID-19 pandemic.



**Figure 1.4.** The rising interest in microfluidics and microfluidic-related biological applications through time. The top two panels are the number of publications using the keywords: "Microfluidics" (left), "Microfluidics + Biology" and "Organ-on-chip" (right); from 2000 to 2021. Data gathered from PubMed. The bottom panel is the number of filed patents, *i.e.* number of requests, from 2000 to 2021, mentioning keywords "Microfluidics" or "Microfluidic", and "organ on chip", "organ-on-chip" or "microphysiological systems". Data gathered from Google Patents.

As a tool, microfluidics can be used in a wide range of applications. The following sections will present the two biological applications used in this work to illustrate its versatility. Firstly, droplet microfluidics was employed to develop and test, under physiologically-relevant conditions, an oral drug delivery system based on double emulsions. Then, the microenvironment of microfluidic cell cultures, especially the pH, was monitored and cells were cultivated outside the CO<sub>2</sub> incubator for over 48 h.

### 1.3.1. Microfluidics and drug delivery systems

Patient nonadherence to medication or patient noncompliance is defined as "the extent to which the patients' behaviour matches agreed recommendations from the prescriber<sup>44</sup>". It is a major issue in the healthcare industry, amounting to 1.25 billion euro in costs in Europe alone. It is estimated that 50% of chronic patients do not properly follow long-term treatment, and 10% of hospitalisations of older people are related to medication non-adherence<sup>45</sup>. Among the many possible causes of patient noncompliance, the administration route and undesirable side effects play a major role<sup>44,46-48</sup>. These issues have fuelled the search for novel drug delivery systems that would facilitate adherence to treatment, e.g. changing from intravenous to oral delivery<sup>49,50</sup>; and decreasing adverse effects, e.g. through targeted therapies<sup>51,52</sup>.

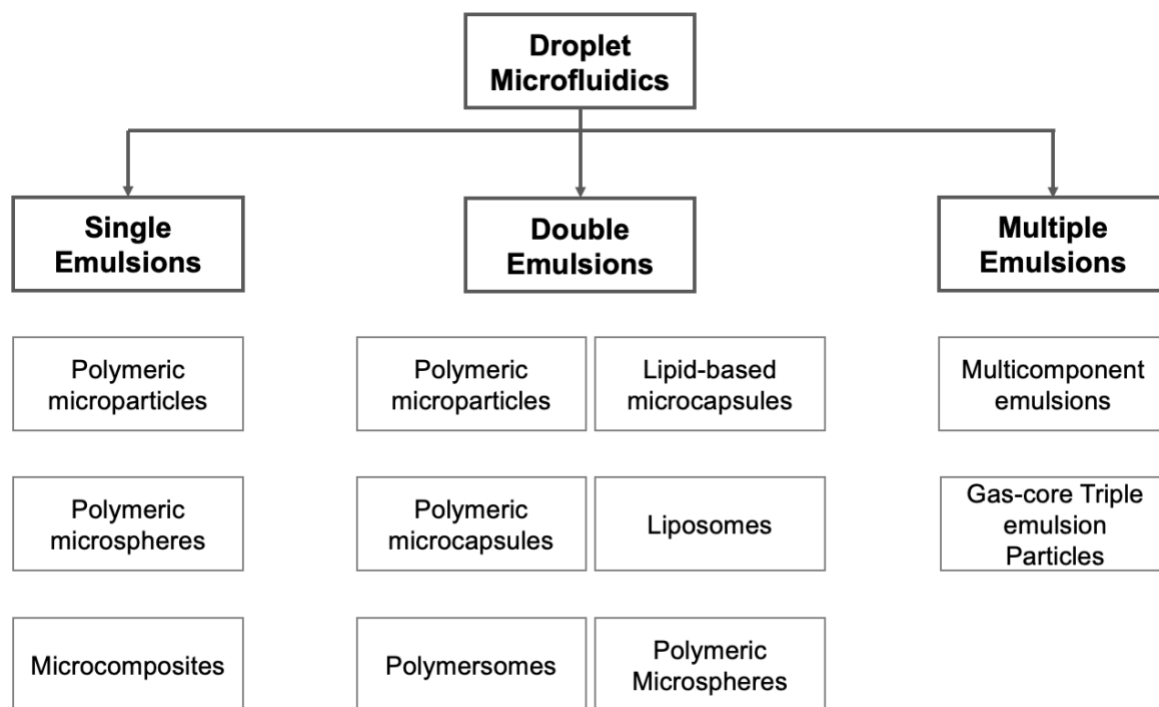
Fostered by the efficient handling of minute volumes and a high level of control, microfluidics has gained space in this field, acting as drug dispensers themselves or in producing drug carriers. Used as direct drug delivery systems, microfluidic devices exploit advancements in the miniaturisation of needles and autonomous and automated systems to dispense drugs in a "smart" manner, using feedback loops for adequate drug dosing. This approach improves patients' comfort and compliance by decreasing administration-related pain and treatment complexity<sup>49,53</sup>. The production of drug carriers via microfluidics assembles complex carriers with precise size and tunable release profiles<sup>53</sup>. These carriers are usually produced by droplet-microfluidics, a technique based on emulsions<sup>53</sup>. Emulsions are homogeneous mixtures of immiscible liquids<sup>54</sup>, such as water-in-oil droplets. For this reason, microfluidic-based carriers can incorporate water-insoluble drugs, which are increasing in number<sup>53</sup>. They also improve the pharmacokinetic profile due to consistent drug concentration and distribution<sup>49</sup>. Droplet-based microfluidics will be discussed in more detail in the following section.

### **1.3.1.1. Droplet microfluidics**

Droplet-based microfluidics involves the generation and manipulation of microdroplets in microfluidic devices<sup>55</sup>. The droplets are formed by driving two immiscible fluids through specific channel geometries, causing one of the fluids (the dispersed phase) to destabilise and be pinched off by the second fluid (the continuous phase). These instabilities are characterised by the Capillary number, the ratio between viscous forces and interfacial tension; and the Weber number, which defines the relationship between inertial forces and surface tension<sup>56</sup>.

Microfluidic droplets' size and production rate can vary from tens to hundreds of micrometres and reach thousands of hertz<sup>57</sup>, with volumes in the pico to nanolitre range. The immiscibility of the phases avoids cross-contamination of material between droplets, allowing for

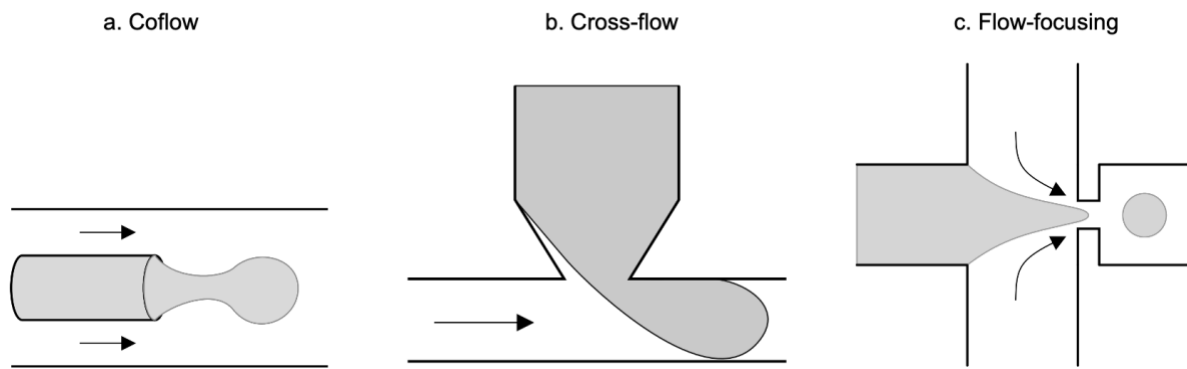
encapsulation of several different samples in the same experiment, down to single cells or even single molecules per droplet<sup>55</sup>. These loaded droplets can be manipulated in several ways, favouring high-throughput analysis. In the drug delivery area, these emulsions are often used as templates for microparticles (Figure 1.5.).



**Figure 1.5.** Overview of different types of emulsions produced via microfluidics and respective templated drug delivery systems. Adapted from Fontana *et al.*<sup>58</sup>

### 1.3.1.1.1. Channels geometries

As previously mentioned, many aspects of droplet formation are linked to the channel geometry and dimensions. To produce single emulsions, there are three well-known geometries when considering soft-lithography-made planar devices: coflow, cross-flow and flow-focusing<sup>6</sup> (Figure 1.6). In all three cases, both fluids are driven independently to the junction, which is designed to ensure the reproducibility of the droplet formation process<sup>59</sup>.

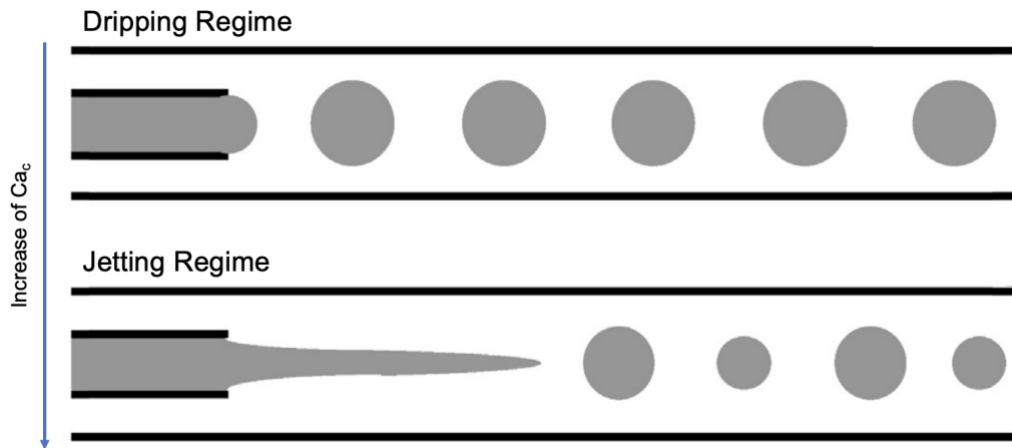


**Figure 1.6.** The most common microchannel geometries for microfluidics droplet formation. Black arrows indicate the direction of the continuous phase. Adapted from Pit *et al.*<sup>60</sup>.

### a. Coflow

The coflow geometry is characterised by the unidirectional flow of both fluids due to coaxial microchannels (Figure 1.6.a.). The dispersed phase is introduced through an inner channel that is concentrically arranged inside an outer channel that flows the continuous phase in the same direction. The droplets are formed at the end of the inner channel, where both fluids meet. The droplet formation can occur with different flow regimes: the dripping regime, in which the droplets are formed at the junction; and the jetting regime, in which the droplet formation occurs further down the post junction channel<sup>61</sup> (Figure 1.7).

The transition between these regimes is governed by different dominant forces. For the dripping regime, the flow rate of the continuous phase is higher, so the viscous forces dominate over the inertial and interfacial forces of the inner phase, resulting in monodisperse droplets at the junction. This regime is thus characterised by the capillary number of the continuous phase<sup>6,56</sup>. In the case of the jetting regime, the disperse phase has a higher flow rate, therefore inertial forces become dominant, characterising the regime by the Weber number of the inner phase<sup>62</sup>.



**Figure 1.7.** Schematic of the dripping and jetting regimes according to the capillary number of the continuous phase. Adapted from Moon *et al.*<sup>63</sup>

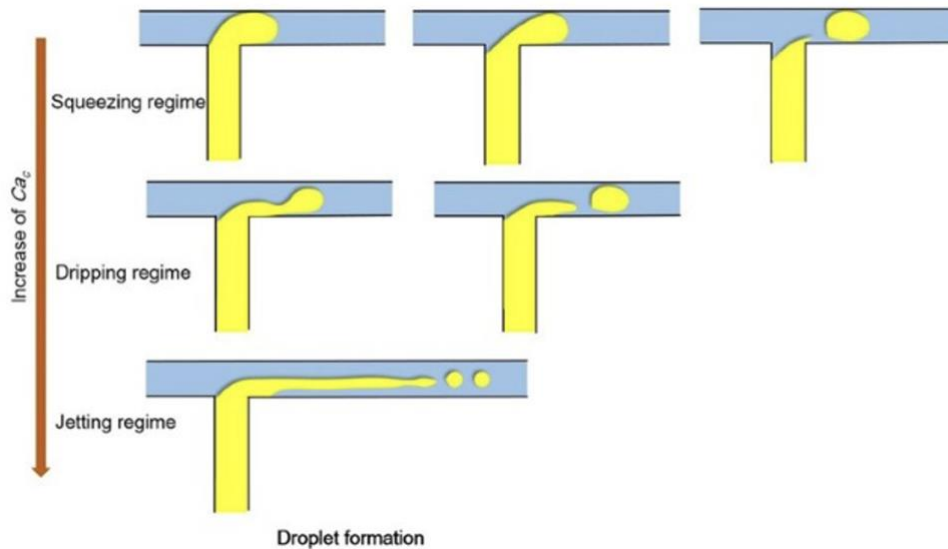
The first reported use of the coflow geometry in the context of microfluidics was Cramer *et al.*<sup>64</sup> The authors placed a capillary inside a rectangular flow cell and studied the forces acting on droplet formation. They identified and characterised the dripping and jetting regimes and the relationship between the properties of the fluids, the flow rates, and the size of the droplets. For example, the size decreases with the decrease in the flow rate of the continuous phase due to viscous shear stress. In contrast, the size increases with the increase of the flow rate of the dispersed phase, as more fluid enters the droplets before breakup<sup>64</sup>.

## b. Cross-Flow

In the cross-flow geometry, the fluids meet at an angle. The most common design is the T-junction with a 90° angle (Figure 1.6.b.), however, other designs are possible. Thorsen *et al.*<sup>65</sup> were the first to use a T-junction to form water droplets in different types of oil.

In addition to the dripping and jetting regimes seen above, the cross-flow geometry also presents a squeezing regime at low capillary numbers, in which the dispersed phase obstructs the continuous phase channel, increasing the upstream pressure. This extra pressure, in turn, squeezes a neck into the dispersed phase, forcing the droplet breakup<sup>66</sup> (Figure 1.8). The main difference between squeezing and dripping is that during the dripping regime, the dispersed phase does not obstruct the continuous phase channel.



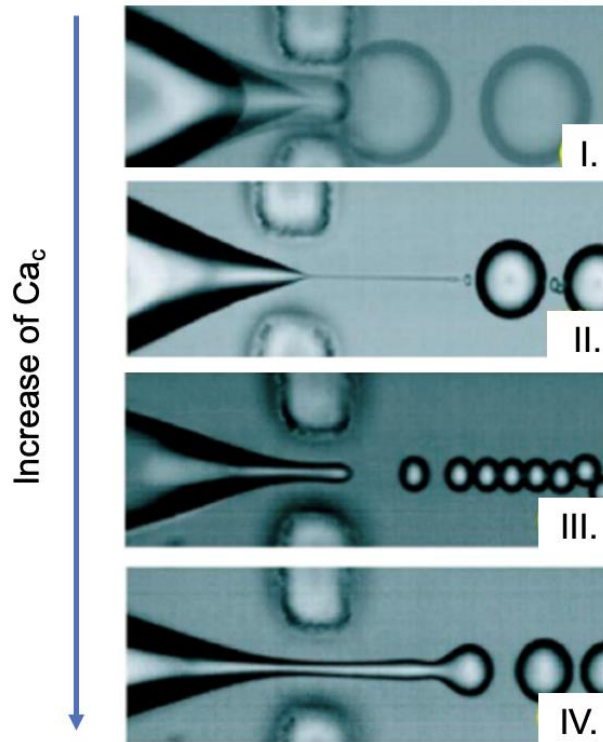


**Figure 1.8.** Different flow regimes in cross-flow geometries according to the capillary number of the continuous phase. Adapted from Liu *et al.*<sup>67</sup>

### c. Flow-focusing

The flow of the dispersed phase is focused by two perpendicular streams of the continuous phase in the flow-focusing geometry (Figure 1.6.c.). The nozzle is usually followed by a constriction, which increases the shear stress in the region. This favours droplet breakup near the junction<sup>60</sup>, which usually generates small droplets<sup>6</sup>. Furthermore, it presents a fourth regime, in addition to the three mentioned in the preceding sections, the thread formation regime<sup>59</sup> (Figure 1.9.II.).

This regime was identified by Anna *et al.*<sup>68</sup> after the addition of surfactants to the droplet generation. It consists in a fine thread of dispersed phase passing through the nozzle and breaking into droplets downstream in the post-junction channel. Due to the several geometrical aspect ratios involved in this design, there is no simple model for droplet prediction as in the previous geometries. However, several experimental and theoretical studies have shown that droplet formation is governed by the channel geometry, flow rate, fluid viscosity, and addition of surfactants<sup>6</sup>.

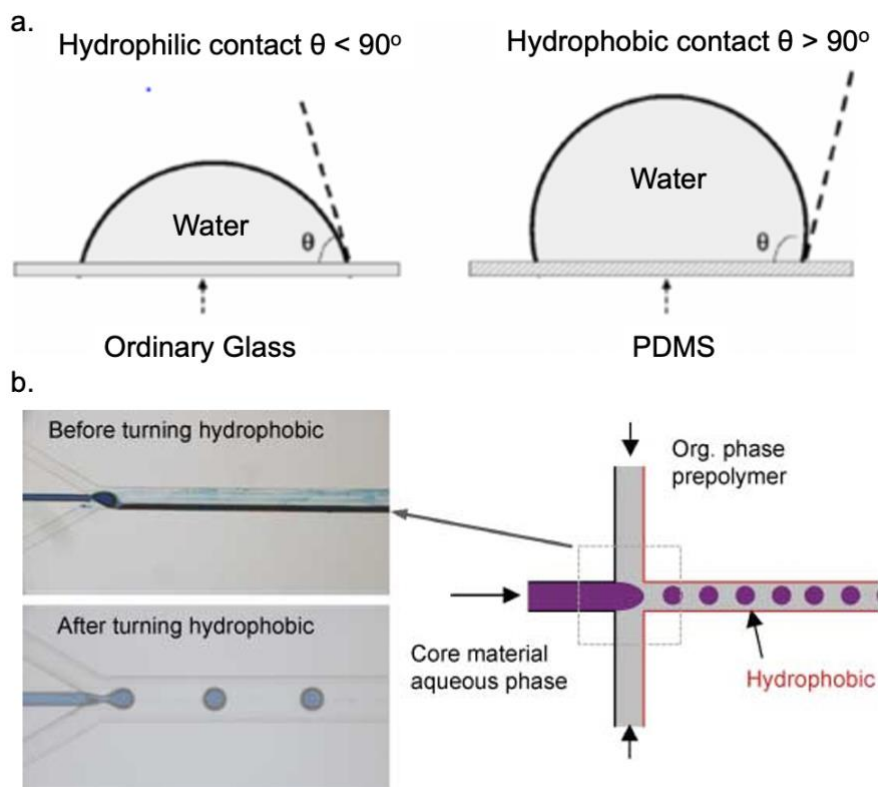


**Figure 1.9.** Flow regimes in flow-focusing geometries. I. Squeezing regime; II. Thread formation regime; III. Dripping regime; IV. Jetting regime. Adapted from Anna *et al.*<sup>68</sup>

### 1.3.1.1.2. Wetting

Besides the physical parameters discussed above, chemical parameters also affect droplet formation and longevity. The wettability of the surface, for example, has a considerable effect on droplet formation. It is important that the continuous phase wets the post-junction channel of the microfluidic device, and, in consequence, repels the dispersed phase to keep droplets from attaching to the channel walls<sup>69</sup>.

PDMS, one of the most common materials for the fabrication of microfluidics devices, is naturally hydrophobic (Figure 1.10.a.). To produce water in oil droplets, PDMS chips do not require any additional steps, unless they are bonded to glass slides. To turn the glass hydrophobic, it is common to treat the channels with a water repellent, such as Aquapel™<sup>70</sup>, before droplet formation to increase the hydrophobicity of the material (Figure 1.10.b.).



**Figure 1.10.** Wettability of the surface. **a.** Contact angle with a water droplet in hydrophilic (ordinary glass) and hydrophobic (PDMS) surfaces. Reproduced from Berthier *et al.*<sup>71</sup> **b.** The wetting effect of the dispersed phase over an untreated surface in droplet formation (before) and over a treated one (after). Adapted from Boskovic *et al.*<sup>69</sup>

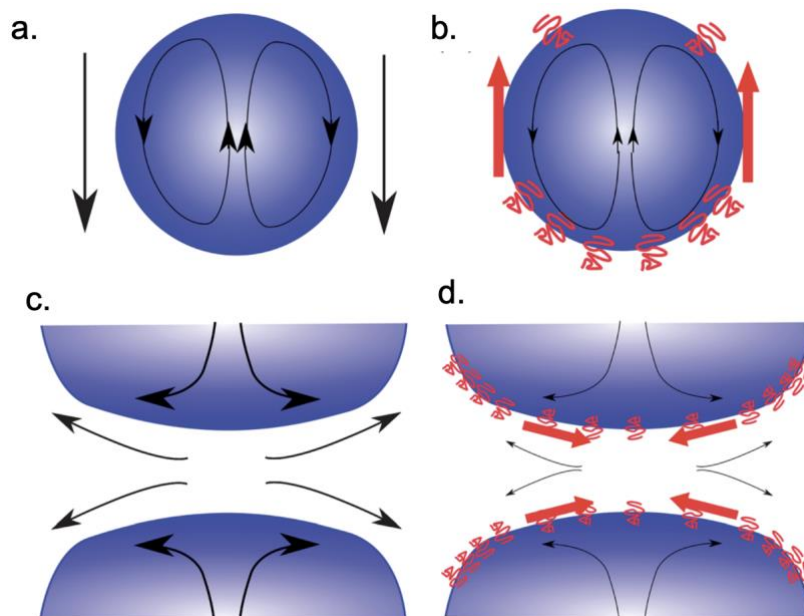
To form oil in water droplets, the PDMS surface needs to be rendered hydrophilic. There are several protocols, for example, coating the surface with polymers such as polyvinyl alcohol (PVA)<sup>72,73</sup>, poly(diallyldimethylammonium) chloride (PDADMAC) and poly(sodium 4-styrenesulfonate) (PSS)<sup>74</sup>; or salinisation with aminopropyltriethoxysilane (APTES)<sup>75</sup> or activating the surface with plasma<sup>76</sup>. It is important to note that the longevity of these treatments is finite and depends on the chemistry of the materials involved. The plasma surface activation, for example, lasts only a few hours and it is usually a pre-treatment for more long-lasting protocols<sup>70</sup>.

### 1.3.1.1.3. Surfactants

Emulsions are metastable systems, i.e. they are kinetically trapped in a local energy minimum, in which the global energy minimum is the complete separation of the fluids<sup>77–80</sup>. Thus, droplets tend to coalesce as an ageing effect. Coalescence is a major issue for any droplet-based application as it completely hinders the advantages conferred by using droplets in the first

place, such as precise encapsulation of compounds, compound isolation, and avoidance of cross-contamination<sup>55</sup>. In order to increase the time they spend in the metastable state, surfactants are employed<sup>80</sup>.

The term surfactant stands for "surface active agent". These molecules have amphiphilic properties, i.e. they are composed of different chemical groups that show an affinity for different immiscible substances, for example, water and oil. Due to this characteristic, and as the name suggests, these molecules arrange themselves at the interfaces of immiscible liquids, avoiding the coalescence of neighbouring droplets by two main mechanisms: the steric repulsion caused by the surfactant molecules at the interface and the slower drainage of the continuous phase between two neighbouring droplets. The latter is due to the dynamic arrangement of the surfactant caused by the Marangoni effect<sup>80</sup> (Figure 1.11). Both mechanisms make it more difficult for droplets to collide, thus avoiding coalescence.



**Figure 1.11.** Marangoni effect of droplets in the absence or presence of a surfactant. **a. and b.** The internal flow of the droplet causes a gradient in surfactant distribution at the surface of the droplet. **c. and d.** The Marangoni effect causes an opposing flow to the continuous phase drainage from the upcoming collision area, slowing it down. Reproduced from Baret, 2011<sup>80</sup>.

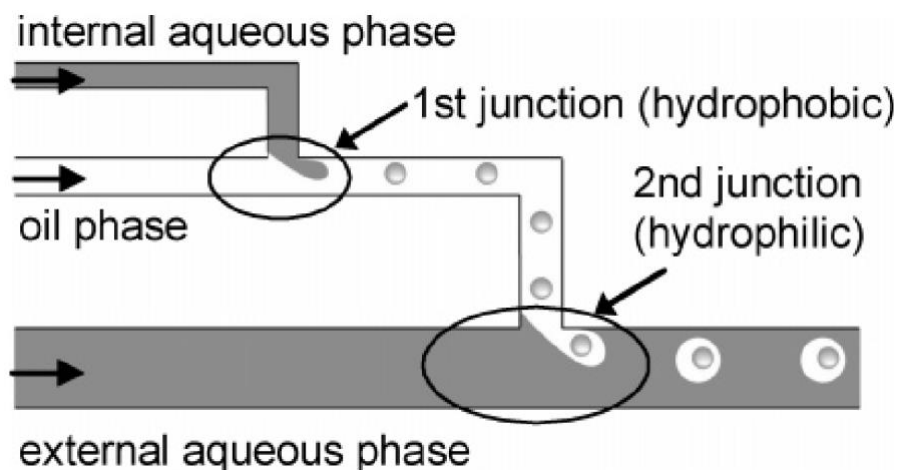
The Marangoni effect is defined as a heterogeneous distribution of surfactant molecules at the interface due to the internal flows of a droplet moving in the continuous phase. This gradient creates an opposing flow to the continuous phase, causing the surface to rigidify, and thus stabilising the droplet (Figure 1.11.b.). Before droplets collide and coalesce, the continuous

phase needs to be drained from the contact area. In the presence of surfactants, the molecules accumulate in this region due to the Marangoni effect, creating an opposing flow to the drainage and slowing it down.

#### **1.3.1.1.4. Double emulsions as oral drug delivery systems**

Double emulsions (DEs) are water-in-oil-in-water (W/O/W, or oil-in-water-in-oil, O/W/O) droplets. They were first reported by Willian Seifriz in 1925 in investigations about oil density<sup>81</sup>. Fifty years later, Matsumoto *et al.*<sup>82</sup> described for the first time the two-step emulsification process to form double emulsions in a reproducible manner. This process consists of mixing two immiscible solutions, forming an emulsion that is, in turn, vigorously stirred in a third solution of similar properties as the inner phase<sup>83</sup>. The rotation speed of each step allows for some control over the size and number of inner droplets within the outer droplet. The two-step emulsification process is still widely used today in the food industry, where DEs are used in low-fat products or as nutrients and flavour additives. However, the resulting populations tend to be polydisperse and encapsulation efficiency low.

The first report of monodisperse microfluidic double emulsions came in 2004<sup>84</sup>. The authors used two approaches to produce DEs: a single chip with two consecutive T-junctions (Figure 1.12), one rendered hydrophobic and the one hydrophilic; and two chips connected by a polytetrafluoroethylene (PTFE) tube, each harbouring a different surface property, either hydrophilic or hydrophobic. This work highlights one of the key points of DE production and one of their main advantages in terms of applications. DEs require a hydrophobic surface to form the W/O emulsion and a hydrophilic surface to form the W/O/W, making them one of the most challenging types of droplets to generate<sup>85</sup>. Nonetheless, requiring opposing properties during formation also implies that DEs carry these opposing properties simultaneously, making them ideal candidates as drug delivery systems for combinatory therapies<sup>58,83</sup>.



**Figure 1.12.** Schematic representation of double emulsion formation with consecutive T-junctions. Reproduced from Okushima *et al.*<sup>84</sup>

Windbergs *et al.*<sup>86</sup> explored this potential by encapsulating the synergistic anticancer drugs, doxorubicin (inner phase) and paclitaxel (intermediate phase), in core-shell microparticles templated from DEs. The ratio of the drugs could be adjusted by the thickness of the oil layer as well as their concentration, by individually changing the composing solutions. This versatility in the formulation is another advantage of employing DEs as drug delivery systems, however, stability is a key issue. This is especially important when considering DEs as oral drug delivery systems. This administration route is favoured by the presence of the oil shell, which promotes intestinal absorption<sup>87</sup>, and their size in the micron range<sup>88</sup>.

To improve DEs stability, surfactants become even more important as, besides preventing the coalescence of one DE with another, it is also necessary to prevent the coalescence of the inner phase with the outer phase, forming a single O/W emulsion. Hence, there are usually two types of surfactants involved in the stabilisation: one, hydrophobic, in the intermediate phase to stabilise the first emulsion, and another, hydrophilic, in the continuous phase, to stabilise the second emulsion<sup>83</sup>. Moreover, surfactants also affect the DEs size and encapsulation efficiency. Surfactant excess has been shown to decrease the size and encapsulation efficiency of DEs due to the migration of the surfactant to the inner phase, affecting the stability balance between the three phases<sup>77</sup>. For drug delivery applications, the biocompatibility of the molecules also needs to be considered. Lipids, due to their amphiphilic and physiological nature, have started to gain relevance as biocompatible surfactants, opening a field of lipid-stabilised double emulsions for biological applications<sup>85,89–91</sup>.

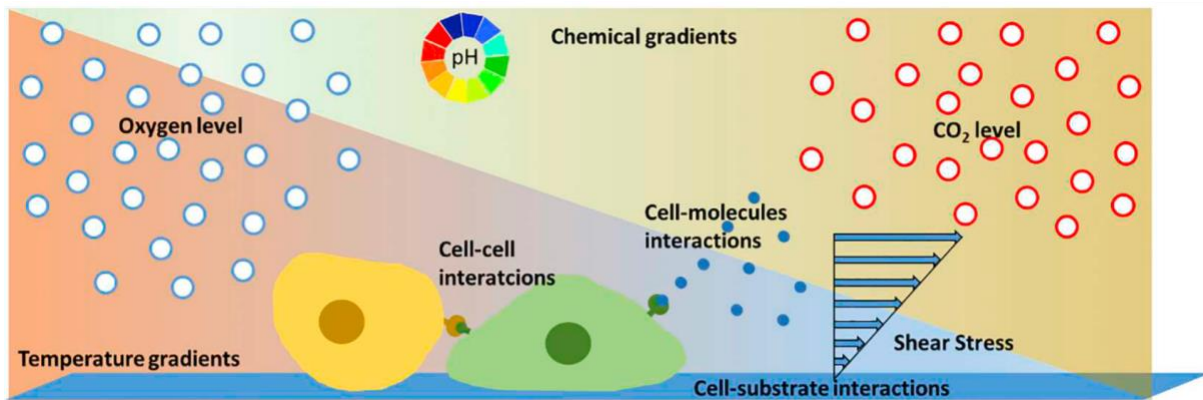
Although promising, DE-based formulations have yet to reach patients. Lipid-stabilised single emulsion oral delivery systems have already crossed the regulatory-approval chasm, treating nausea and diarrhoea, reducing blood pressure, or providing nutritional supplements<sup>92</sup>. Characterisation and optimisation of formulations is the missing piece of the puzzle to unravel the full potential of DEs as oral combinatorial drug delivery systems.

## **1.3.2. Microenvironment monitoring for microfluidic cell culture**

### **1.3.2.1 Microfluidic Cell Culture**

Traditionally, the culture of live cells outside the body is performed in monolayers inside static polymer-coated plastic flasks placed in CO<sub>2</sub> incubators, which maintain a high level of humidity, constant temperature (37 °C), and concentration of CO<sub>2</sub> (5%) for pH buffering. Cell culture provides a platform to study cellular behaviour in a systematic way, with proper isolation of variables and clear experimental design. Experimental work on cultured cells allows investigations that would not be ethical to be conducted in humans while reducing the use of non-analogous animal models. Moreover, the advent of cell culture has been undeniably responsible for historical achievements in the biomedical area, such as the polio vaccine, the connection between viruses and cancer, the emergence of the genetic engineering field, among others<sup>93</sup>.

Nevertheless, it is a reductionist approach that fails to represent the intrinsic complexity of cell differentiation and interaction, tissue function, drug response, and the dynamic and intricate microenvironment present in *in vivo* biology (Figure 1.13). These physical and chemical signals are crucial for cellular development and behaviour, and their absence leads to poor translation between *in vitro* and *in vivo* systems. Furthermore, traditional cell culture protocols are time-consuming and labour-intensive<sup>94</sup>. These limitations profoundly affect the health and pharmaceutical industries, resulting in inefficient and increasingly costly drug development processes. It is estimated that roughly 90% of new drug candidates that reach clinical trials fail due to unforeseen toxicity effects in humans<sup>95,96</sup>. Closing the gap between preclinical and clinical data translation calls for better methods to predict human responses.



**Figure 1.13.** Illustration of the signals in the cell microenvironment. Chemical and temperature gradients, cell-to-cell interactions, molecular signalling from different cell types, and physical stimuli are vital for cell development and behaviour, being poorly represented in traditional cell culture. Reproduced from Coluccio *et al.*<sup>97</sup>

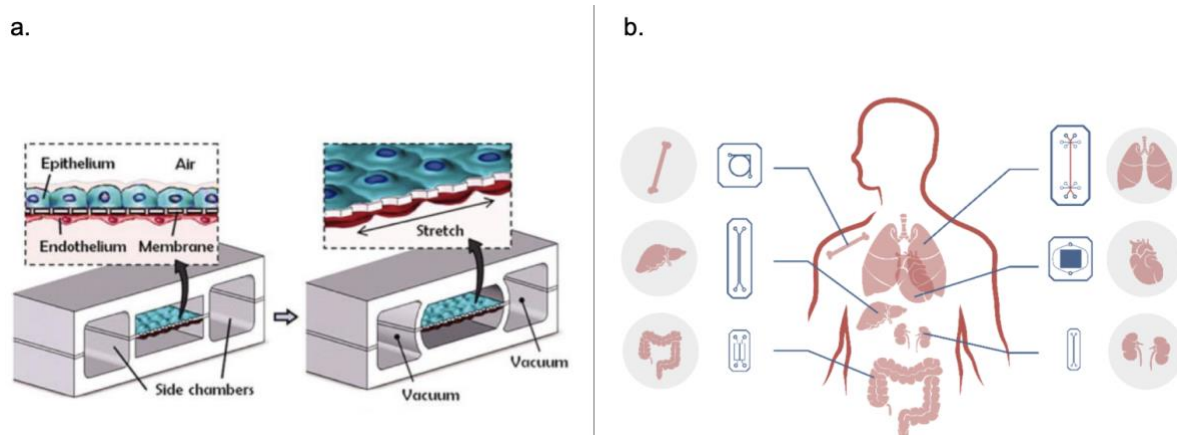
Miniaturising cell cultures into microfluidic systems can address some of the mentioned drawbacks and can also provide other relevant features. The minute volumes dealt with in microfluidics substantially reduce the necessary amount of reagents required for traditional cell culture. Besides directly reducing costs, this is especially advantageous when handling limited or rare samples, such as patient primary cells (those collected directly from patients as opposed to immortalised cell lines<sup>71</sup>). Also, handling smaller quantities of cells decreases the heterogeneity of the culture, so complex cell behaviour is more readily distinguishable. The easiness of fabrication of microfluidics devices provided the foreground for designed co-culture chips. These new devices can reproduce key aspects of the cellular microenvironment, i.e. the co-culture of different types of cells without cross-contamination and replication of physical stimulus and chemical gradients with high spatiotemporal precision due to user-controlled flow<sup>94</sup>. The advent of flowing media continuously or on-demand on top of the cells is of particular interest because, it not only replicates the dynamic environment of the human body, it also automates much of the laborious cell culture practices. Also, microfluidic cell culture profits from the precise addition of compounds of interest or sampling of the microenvironment without much disruption to the cells. Moreover, high throughput can be achieved by parallelising multiple microfluidic devices, in which *in situ* monitoring and analysis can be integrated and performed continuously<sup>94,97</sup>.

The 2010s saw the development of the "organ-on-chip" (OoC) field, building upon the advantages of microfluidic cell culture. Currently one of the most relevant areas of research in microfluidics<sup>8</sup>, it mimics the cellular microenvironment, profiting from the high level of control



plus the possibility of automated monitoring and analysis provided by microfluidics. These specialised *in vitro* cell culture models based on microfluidic devices are structured around three main pillars: reproducing the mechanical and biochemical stimulus of the cellular microenvironment; simulating the 3D microarchitecture of tissues with multiple cell types placed in specific communicating compartments, and replicating functional tissue-tissue interfaces via cell-cell interaction (Figure 1.14.a.). The main goal is to reproduce complex *in vivo* biology to better understand cellular behaviour and metabolism, disease phenotypes, and drug response without the need for insufficient *in vitro* models or imprecise animal models<sup>98</sup>.

Several organ-on-chip devices have been successfully developed, namely, liver<sup>99</sup>, lung<sup>100,101</sup>, kidney<sup>102</sup>, heart<sup>103,104</sup>, intestine<sup>105</sup>, bone<sup>106</sup> and bone marrow<sup>107</sup>, nerve<sup>108</sup>, blood vessels<sup>109,110</sup>, and blood-brain barrier<sup>111</sup> (Figure 1.14.b.). Some have started to demonstrate proofs-of-concept of drug responses closer to human physiology compared to standard *in vitro* models, with the enhanced complexity leading to better cell differentiation and drug transport<sup>112</sup>. As OoC models mature, the interconnection of several OoCs in a "human-on-chip" approach is becoming feasible. These complex systems have been investigated by several groups in different configurations<sup>113–116</sup>. An emerging area that has the potential to deeply change modern medicine is the development of OoC with induced pluripotent stem cells derived from patients. This has the potential to be a paradigm shift in personalised medicine and the development of patient-specific treatments.



**Figure 1.14.** Organ-on-chip systems. **a.** Schematic of the cross-section of a specialised organ-on-chip device, a lung-on-a-chip, highlighting the tissue interface and the vacuum chambers for mechanical stimulus. Reproduced from Huh *et al.*<sup>100</sup> **b.** Illustration of different organ-on-chips, specifically, bone-, liver-, gut-, lung-, heart- and kidney-on-chip. Reproduced from Thomée, 2021.<sup>117</sup>

The increase in complexity of cell cultures enabled by microfluidics has opened the possibility of more in-depth spatiotemporal analysis of cellular development and behaviour. This has further increased the importance of tools such as live-cell imaging<sup>118</sup>, metabolic detection and analysis<sup>119</sup>, and microenvironmental monitoring of parameters such as pH<sup>120</sup>. Consequently, the long-term culturing of cells in OoCs is transitioning from the CO<sub>2</sub> incubator to the microscope stage. As the complexity of the systems increases and the access to more detailed information deepens, enhanced resolution and real-time monitoring of the systems is becoming a clear demand<sup>119,121</sup>. Thus, a growing need to more closely monitor temperature, pH and dissolved O<sub>2</sub>, combined with increasing interest in having a better understanding of the *in situ* metabolic activity, is leading to a plethora of on-chip and off-chip sensing solutions.

### 1.3.2.2. The importance of pH monitoring

As previously mentioned, the gap between preclinical and clinical data is a major concern for the health sector, besides delaying access to treatment for patients. One of the contributing factors to this global issue has been attributed to the variables of microenvironment conditions<sup>122</sup>. Cell lines require a stable pH to grow, as acidic pH can irreversibly inhibit enzymatic activities and the synthesis of DNA, RNA, and protein, thus compromising cell viability<sup>123,124</sup>. pH is defined as the concentration of free H<sup>+</sup> ions in a solution, also called the activity of protons, and can be calculated by the Henderson-Hasselbalch equation (4):

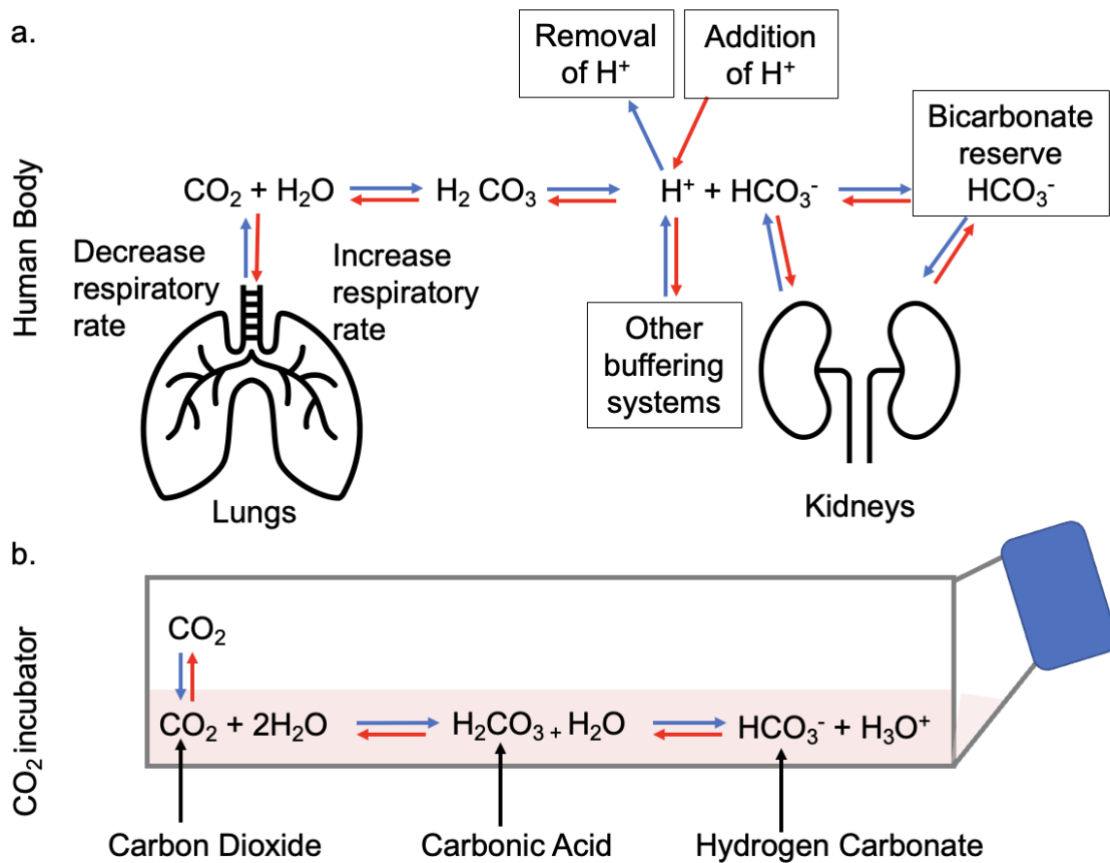
$$pH = pK_a + \log \frac{[B]}{[HB]} \quad (4)$$

in which  $pK_a$  is the acid dissociation constant;  $[HB]$  is the concentration of a compound's protonated form; and  $[B]$  is the concentration of a compound's unprotonated form.

Buffering systems are capable of maintaining the pH constant due to a dynamic equilibrium. The equilibrium between the protonated and unprotonated forms of the buffer can move towards reacting to new free H<sup>+</sup> or releasing H<sup>+</sup> ions to compensate for ions that were added or removed from the surrounding solution. Both mechanisms have the effect of keeping the previous free H<sup>+</sup> concentration constant to a certain extent. If the addition or removal of free H<sup>+</sup> goes beyond a threshold that can be absorbed by the buffer, the pH will change, *i.e.* the buffering capacity of the solution was surpassed<sup>125</sup>. That is why complex organisms, such as mammals, have developed dynamic buffering systems that adjust the concentration of the buffer according to the system's needs. The physiological buffering system is based on the

equilibrium of  $\text{CO}_2/\text{HCO}_3^-$  (bicarbonate buffering system,  $\text{pK}_a = 6.15$ ). The lungs, through the gas exchange of  $\text{CO}_2$ , and the kidneys, through ion transport proteins, are responsible for keeping the ratio of the protonated to unprotonated species of this buffering system in homeostasis and the pH of the organism within the physiological range (Figure 1.15.a.). Cell metabolism leads to acidification of the microenvironment due to the production and release of lactate, which reacts with water to form acid lactic, and  $\text{CO}_2$ , which forms carbonic acid. For this reason, cell culture media usually contains a buffering system to keep pH under physiological conditions<sup>126</sup>. Besides the  $\text{CO}_2/\text{HCO}_3^-$  buffer, media can be buffered by non-volatile buffers (NVB), such as HEPES (4-(2-hydroxyethyl)-1-piperazineethanesulfonic acid) ( $\text{pK}_a = 7.3$ ; 37 °C), PIPES (piperazine-N,N'-bis(2-ethanesulphonic acid);  $\text{pK}_a = 6.7$ ) and MES (2-(N-morpholino)-ethanesulfonic acid;  $\text{pK}_a = 6.0$ )<sup>127,128</sup>.

The bicarbonate buffering system is replicated in cell biology labs with the aid of a  $\text{CO}_2$  incubator. This system works through the equilibrium of  $\text{CO}_2$  from the  $\text{CO}_2$ -rich atmosphere of the incubator, which dissolves in the media and reacts with  $\text{H}_2\text{O}$  forming carbonic acid, and the  $\text{HCO}_3^-$  present in the media (Figure 1.15.b.). Cell culture media come with different concentrations of  $\text{NaHCO}_3$  and require different percentages of  $\text{CO}_2$ . For example, DMEM comes with 44 mM of  $\text{NaHCO}_3$ , which requires approximately 10% of  $\text{CO}_2$  in the atmosphere to maintain the pH close to 7.4.  $\text{CO}_2$  incubators are conventionally set to 5%  $\text{CO}_2$ , which keeps the pH of DMEM around 7.6-7.8. The production of lactic acid and  $\text{CO}_2$  by healthy cells and the buffering capacity of serum, often added to DMEM, partially offsets this difference, allowing the growth of cells with DMEM using conventional  $\text{CO}_2$  concentrations<sup>128</sup>. However, the implications of this adjustment are not well-understood. The intracellular pH of cells is in close equilibrium with the extracellular pH of the microenvironment due to transmembrane ion transporter proteins. Michl. *et al.*<sup>128</sup> studied the effect of extracellular pH change on intracellular pH and concluded that cells re-balance the internal pH based on the external one. Since most  $\text{H}^+$  targets are intracellular, this change can affect intracellular mechanisms and metabolic pathways in unpredictable ways.



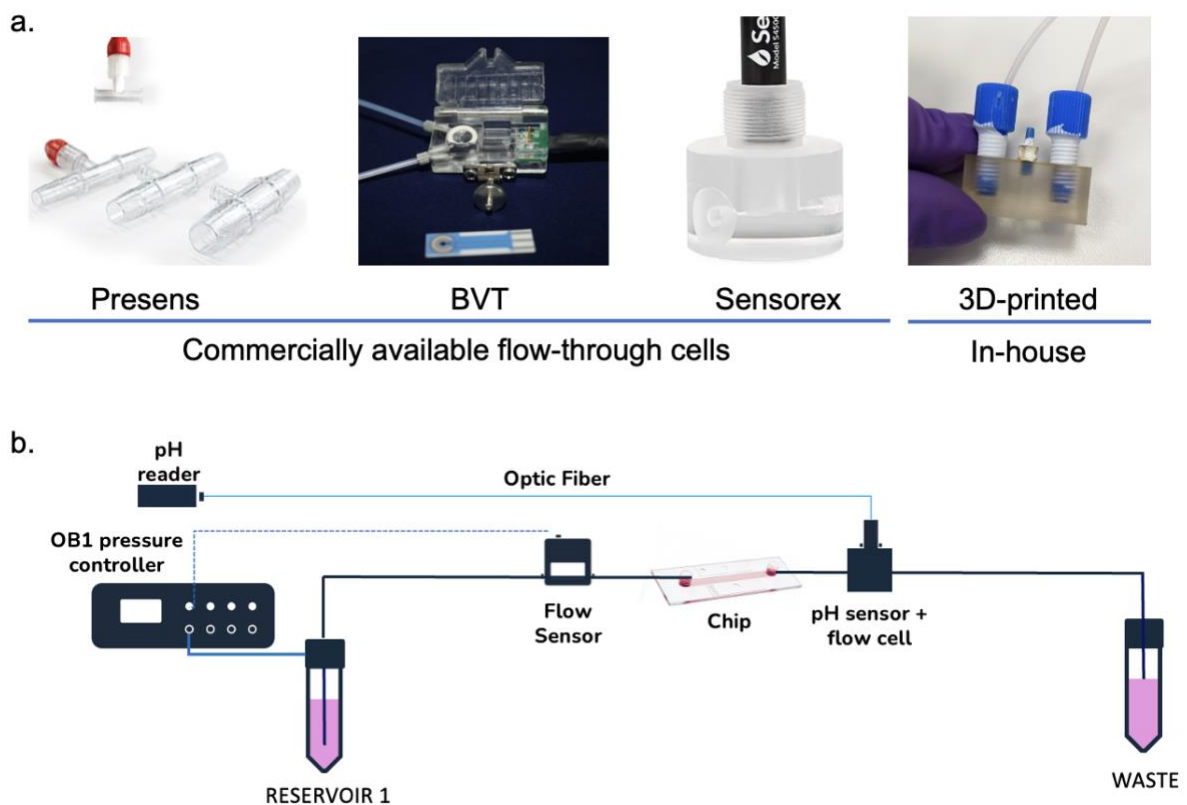
**Figure 1.15.** Bicarbonate buffering system. **a.** Illustration of the bicarbonate buffering system in the human body, highlighting the equilibrium provided by lungs and kidneys. **b.** Bicarbonate buffering system inside the  $\text{CO}_2$ -rich atmosphere of the  $\text{CO}_2$  incubator reacting with the salt present in the media.

When the culturing system is downscaled to micron-range in OoCs, substantially reducing the volumes, the monitoring of pH becomes even more important. Small variations in pH, e.g.  $7.4 \pm 0.3$ , are tolerated in traditional cell culture, however, pH changes faster in microfluidic cell culture due to the much higher cell volume to medium volume ratio, resulting in a more pronounced effect on cell viability. Thus, the closer monitoring of crucial environmental parameters becomes more critical<sup>123</sup>.

### 1.3.2.3. Monitoring the microfluidic cell culture environment

The measurement of metabolic activity in microfluidic cell culture is usually done with on-chip solutions. For example, Weltin *et al.*<sup>129</sup> developed a microphysiometer system in a microfluidic chip with dissolved  $\text{O}_2$  and pH electrochemical sensors inside the culturing chamber. The

authors successfully cultured brain cancer cells with online and continuous measurement of the cells' metabolism. However, these solutions prove to be too complex and costly<sup>130</sup> when the goal is to monitor the cell culture environment, which does not require the same level of detailed information. For that, microfluidic off-chip solutions, such as flow-through cells, are more apt. Flow-through cells can be developed in-house<sup>131–133</sup>, usually 3-D printed<sup>134</sup>, or commercially available<sup>135–139</sup>. The format can vary according to the application, such as T-junctions for HPLC applications or other geometrical structures fitted to house the sensor (Figure 1.16). The main goal is to place the sensors in line with the microfluidic system to allow continuous monitoring.



**Figure 1.16.** Cell culture pH monitoring. **a.** Examples of different flow-through cells for pH monitoring. The first three are commercially available from different suppliers, and the fourth was designed and 3D-printed in-house. **b.** Schematic of a microfluidic setup with an inline flow cell and pH sensor.

A good example is the work of Zhang *et al.*<sup>140</sup> who developed a "physical sensing unit" composed of pH, O<sub>2</sub>, and temperature sensors in a flow-through cell developed in-house. The goal was to monitor the microenvironment of a complex organ-on-chip system. The system was designed as a modular platform to control two organ-on-chips connected to an automated

flow control breadboard. Interestingly, the biomarker sensing unit, *i.e.* the sensors to measure the metabolism, was also off-chip. The platform was validated with a drug screening assay using liver and heart organ-on-chips, exposed to acetaminophen for 5 days and doxorubicin for 24h where cytotoxicity biomarkers were detected and quantified.

Farooqi *et al.*<sup>119</sup> 3-D printed a pH sensing flow-through cell to house an optical pH sensor built with commercially available parts. The sensor measured pH based on the colour of the phenol red present in the media. The goal was to monitor a live-on-chip system also intended to investigate the drug toxicity of doxorubicin. The researchers were able to detect a decrease in pH when cells were exposed to the high concentrations of the drug when compared to the control. The same group performed similar work with a lung-on-chip system<sup>141</sup>, attesting to the robustness of the developed sensing unit. Fibroblasts had pH and O<sub>2</sub> monitored for 3 days in a similar fashion by Ali *et al.*<sup>142</sup> Also using the phenol red of the media, Wu *et al.*<sup>143</sup> designed a high throughput pH sensing unit. It consisted of parallelised microfluidic channels with a sensing chamber connected to optical pH sensors. They performed simulations to define the best shape of the sensing chamber, resulting in an oval shape. The thickness of the PDMS layer was also decreased, to minimise the loss of light transmission. Optical sensors seem to be the most common choice for microfluidics flow-through cells due to their independence of reference electrodes, electrical connections and flow rates. Also, they are not prone to biofouling, corrosion and interference from electrochemical signals from molecules present in the medium<sup>142</sup>.

The important growth of organ-on-chip technologies brought with it an increased need to monitor more closely what was happening inside the system. Several on-chip and off-chip solutions have been designed, and microfluidic flow cells for pH monitoring seem to be the way forward. On-chip sensors are suited for the detection of metabolic activity that can benefit from high spatiotemporal resolution. However, these solutions are too costly and complex for microenvironment monitoring, which does not require the same level of precision. For microenvironment monitoring, flow-through cells with embedded optical sensors which are placed in the microfluidics circuit for real-time and continuous monitoring have been the most common choice.

## 1.4. Aims and Scope of Thesis

As outlined throughout this chapter, microfluidics has a true potential to profoundly change biological investigation. It has indeed already started to do so, but there is still a long way until it becomes a standard tool for life science research.

*The aim of this industrial Ph.D. thesis is to develop microfluidic-based tools for biological applications through two projects:*

- 1) The production and characterisation of double emulsions under physiologically-relevant conditions as oral drug delivery systems.*
- 2) The microenvironmental monitoring of pH in long-term microfluidic cell cultures outside the CO<sub>2</sub> incubator.*

To assess the commercial viability and potential exploitation of the research developed in this industrial thesis, **Chapter 2** describes two market studies: the first is related to the field of compartments and focused on the encapsulation of valuable compounds in droplets; the second analyses the pH monitoring market, considering long-term microfluidic cell culture.

Channel geometry and physicochemical parameters play an important role in the outcome of microfluidics experiments, especially for the production of complex structures such as DEs, as discussed in **Chapter 3**. Several chip heights and designs as well as different surface treatment protocols were tested and adjusted for the best production of DEs and other compartments such as giant unilamellar vesicles and multivesicular vesicles templated from DEs.

Due to their water-in-oil-in-water structure, DEs have the ability to co-localise compounds of opposing properties, i.e., hydrophobic and hydrophilic molecules in the intermediate and inner phase, respectively. **Chapter 4** describes the characterisation of lipid-stabilised DEs produced via microfluidics under physiologically-relevant conditions for oral drug delivery.

**Chapter 5** considers the development of a microfluidic automated solution for the control of environmental parameters. pH is a crucial factor for the growth of cells in culture and is strongly dependent on CO<sub>2</sub> concentration. This chapter discusses the development of an incubator-independent and chip-agnostic microfluidic cell culture system for pH monitoring.

## 1.5. References

1. Brody, J. P., Yager, P., Goldstein, R. E. & Austin, R. H. Biotechnology at low Reynolds numbers. *Biophys. J.* **71**, 3430–3441 (1996).
2. Beebe, D. J., Mensing, G. A. & Walker, G. M. Physics and Applications of Microfluidics in Biology. *Phys. Appl. Microfluid. Biol. Artic. Annu. Rev. Biomed. Eng.* **4**, 261–86 (2002).
3. Nithin Kumar, J., Devaiah, M., Sandeep Kumar, P. & Sudheer Rao, P. *Experimental Investigation of Microstructure and Mechanical Properties of Brass–Iron Joined by TIG Welding Process. Lecture Notes in Mechanical Engineering* (2020). doi:10.1007/978-981-15-1071-7\_35
4. Balagaddé, F. K., You, L., Hansen, C. L., Arnold, F. H. & Quake, S. R. Microbiology: Long-term monitoring of bacteria undergoing programmed population control in a microchemostat. *Science* (80-. ). **309**, 137–140 (2005).
5. Stone, H. A. Introduction to fluid dynamics for microfluidic flows. in *CMOS Biotechnology. Series on Integrated Circuits and Systems.* (eds. Lee, H., Westervelt, R. M. & Ham, D.) 6–29 (Springer, Boston, MA, 2007). doi:https://doi.org/10.1007/978-0-387-68913-5\_2
6. Shang, L., Cheng, Y. & Zhao, Y. Emerging Droplet Microfluidics. *Chem. Rev.* 7964–8040 (2017). doi:10.1021/acs.chemrev.6b00848
7. Pfitzner, J. Poiseuille and his law. *Anaesthesia* **31**, 273–275 (1976).
8. Convery, N. & Gadegaard, N. 30 years of microfluidics. *Micro Nano Eng.* **2**, 76–91 (2019).
9. Manz, A., Graber, N. & Widmer, H. M. Miniaturized Total Chemical Analysis Systems: a Novel Concept for Chemical Sensing. *Sensors Actuators B Chem.* 244–248 (1990).
10. Sommer, G. J. *et al.* Chapter 1 - Introduction to Microfluidics. in *Microfluidics for Biological Applications* (eds. Tian, W.-C. & Finehout, E.) 2–33 (Springer, 2009).
11. Duncombe, T. A., Tentori, A. M. & Herr, A. E. Microfluidics: Reframing biological enquiry. *Nat. Rev. Mol. Cell Biol.* **16**, 554–567 (2015).
12. Sivaramakrishnan, M., Kothandan, R., Govindarajan, D. K., Meganathan, Y. & Kandaswamy, K. Active microfluidic systems for cell sorting and separation. *Curr. Opin. Biomed. Eng.* **13**, 60–68 (2020).
13. Krüger, J. *et al.* Development of a microfluidic device for fluorescence activated cell sorting. *J. Micromechanics Microengineering* **12**, 486 (2002).
14. Warkiani, M. E., Wu, L., Tay, A. K. P. & Han, J. Large-Volume Microfluidic Cell Sorting for Biomedical Applications. *Annu. Rev. Biomed. Eng.* **17**, 1–34 (2015).
15. Chen, Y. *et al.* Rare cell isolation and analysis in microfluidics. *Lab Chip* **14**, 626–645 (2014).
16. Chen, C. L. *et al.* Separation and detection of rare cells in a microfluidic disk via negative selection. *Lab Chip* **11**, 474–483 (2011).
17. Ferguson, B. S. *et al.* Genetic analysis of H1N1 influenza virus from throat swab samples in a microfluidic system for point-of-care diagnostics. *J. Am. Chem. Soc.* **133**, 9129–9135 (2011).
18. Hugo, S., Land, K., Madou, M. & Kido, H. A centrifugal microfluidic platform for point-of-care diagnostic applications. *S. Afr. J. Sci.* **110**, (2014).
19. Mazutis, L. *et al.* Single-cell analysis and sorting using droplet-based microfluidics. *Nat. Protoc.* 2013 85 **8**, 870–891 (2013).
20. Kobel, S., Valero, A., Latt, J., Renaud, P. & Lutolf, M. Optimization of microfluidic single cell trapping for long-term on-chip culture. *Lab Chip* **10**, 857–863 (2010).
21. Segaliny, A. I. *et al.* Functional TCR T cell screening using single-cell droplet microfluidics. *Lab Chip* **18**, 3733–3749 (2018).
22. Sanchez-Freire, V., Ebert, A. D., Kalisky, T., Quake, S. R. & Wu, J. C. Microfluidic single-cell real-time PCR for comparative analysis of gene expression patterns. *Nat. Protoc.*



- 2012 **75** **7**, 829–838 (2012).
23. Bose, S. *et al.* Targeted analysis of nucleotide and copy number variation by exon capture in allotetraploid wheat genome. (2011). doi:10.1186/s13059-015-0684-3
  24. Su, X. *et al.* Microfluidic cell culture and its application in high-throughput drug screening: Cardiotoxicity assay for hERG channels. *J. Biomol. Screen.* **16**, 101–111 (2011).
  25. Hung, P. J., Lee, P. J., Sabounchi, P., Lin, R. & Lee, L. P. Continuous perfusion microfluidic cell culture array for high-throughput cell-based assays. *Biotechnol. Bioeng.* **89**, 1–8 (2005).
  26. Zhang, H., Liu, Y., Wang, J., Shao, C. & Zhao, Y. Tofu-inspired microcarriers from droplet microfluidics for drug delivery. *Sci. China Chem.* 2018 **62**, 87–94 (2018).
  27. Serra, C. A. *et al.* Engineering Polymer Microparticles by Droplet Microfluidics. *J. Flow Chem.* **3**, 66–75 (2013).
  28. Li, Y. *et al.* Composite core-shell microparticles from microfluidics for synergistic drug delivery. *Sci. China Mater.* **60**, 543–553 (2017).
  29. Arik, Y. B. *et al.* Microfluidic organ-on-a-chip model of the outer blood–retinal barrier with clinically relevant read-outs for tissue permeability and vascular structure. *Lab Chip* **21**, 272–283 (2021).
  30. Maoz, B. M. *et al.* A linked organ-on-chip model of the human neurovascular unit reveals the metabolic coupling of endothelial and neuronal cells. *Nat. Biotechnol.* 2018 **36**, 865–874 (2018).
  31. Tao, T. *et al.* Engineering human islet organoids from iPSCs using an organ-on-chip platform. *Lab Chip* **19**, 948–958 (2019).
  32. Nall, J. R. & Lathrop, J. W. Photolithography Fabrication Techniques for Transistors which are an Integral Part of a Printed Circuit. in *Program of Electron Devices Meeting* 117 (1958).
  33. Burklund, A., Tadimety, A., Nie, Y., Hao, N. & Zhang, J. X. *Advances in diagnostic microfluidics. Advances in Clinical Chemistry* **95**, (Elsevier Inc., 2020).
  34. Whitesides, G. M., Ostuni, E., Takayama, S., Jiang, X. & Ingber, D. E. Soft Lithography in biology and biochemistry. (2001).
  35. Duffy, D. C., McDonald, J. C., Schueller, O. J. A. & Whitesides, G. M. Rapid Prototyping of Microfluidic Systems in Poly(dimethylsiloxane). (1998). doi:10.1021/ac980656z
  36. Bharate, S. S. *et al.* Preclinical Development of *Crocus sativus* -Based Botanical Lead IIM-141 for Alzheimer’s Disease: Chemical Standardization, Efficacy, Formulation Development, Pharmacokinetics, and Safety Pharmacology. *ACS Omega* **3**, 9572–9585 (2018).
  37. Rogers, J. A. & Nuzzo, R. G. Recent progress in soft lithography. *Mater. Today* **8**, 50–56 (2005).
  38. Ng, J. M. K., Gitlin, I., Stroock, A. D. & Whitesides, G. M. Components for integrated poly(dimethylsiloxane) microfluidic systems. *Electrophoresis* **23**, 3461–3473 (2002).
  39. Chaudhury, M. K. & Whitesides, G. M. Direct Measurement of Interfacial Interactions between Semispherical Lenses and Flat Sheets of Poly(dimethylsiloxane) and Their Chemical Derivatives. *Langmuir* **7**, 1013–1025 (1991).
  40. Kane, R. S., Takayama, S., Ostuni, E., Ingber, D. E. & Whitesides, G. M. Patterning proteins and cells using soft lithography. *Biomaterials* **20**, 2363–2376 (1999).
  41. Delamarche, E., Bernard, A., Schmid, H., Michel, B. & Biebuyck, H. Patterned Delivery of Immunoglobulins to Surfaces Using Microfluidic Networks. *Science* (80-. ). **276**, 779–781 (1997).
  42. Merkel, T. C., Bondar, V. I., Nagai, K., Freeman, B. D. & Pinnau, I. Gas Sorption, Diffusion, and Permeation in Poly(dimethylsiloxane). *J Polym Sci B Polym Phys* **38**, 415–434 (2000).
  43. Grand View Research. *Microfluidics Market Size, Share & Trends Analysis Report 2021 - 2028.* (2021).
  44. Melnikow, J. & Kiefe, C. Patient compliance and medical research - Issues in methodology. *J. Gen. Intern. Med.* **9**, 96–105 (1994).

45. Cutler, R. L., Fernandez-Llimos, F., Frommer, M., Benrimoj, C. & Garcia-Cardenas, V. Economic impact of medication non-adherence by disease groups: A systematic review. *BMJ Open* **8**, e016982 (2018).
46. Arbit, E. The Physiological Rationale for Oral Insulin Administration. *Diabetes Technol. Ther.* **6**, 510–517 (2004).
47. Düsing, R., Weisser, B., Mengden, T. & Vetter, H. Changes in Antihypertensive Therapy-The Role of Adverse Effects and Compliance. *Blood Press.* **7**, 313–315 (1998).
48. S.K, A. & Vijey Aanandhi, M. An improvement in patient compliance in diabetes mellitus. *Res. J. Pharm. Technol.* **11**, 587–592 (2018).
49. Wood, L. A review on adherence management in patients on oral cancer therapies. *Eur. J. Oncol. Nurs.* **16**, 432–438 (2012).
50. Singh, S. *et al.* Abstract B116: Optimizing a CD71-targeting Probody drug conjugate (PDC) for activity in multiple solid tumor and lymphoma models and for tolerability in nonhuman primates. in *Therapeutic Agents: Biological* **17**, B116–B116 (American Association for Cancer Research, 2018).
51. Vargason, A. M., Anselmo, A. C. & Mitragotri, S. The evolution of commercial drug delivery technologies. *Nat. Biomed. Eng.* **5**, 951–97 (2021).
52. Singh, A. P., Biswas, A., Shukla, A. & Maiti, P. Targeted therapy in chronic diseases using nanomaterial-based drug delivery vehicles. *Signal Transduct. Target. Ther.* **2019** **4**, 1–21 (2019).
53. Riahi, R. *et al.* Microfluidics for advanced drug delivery systems. *Curr. Opin. Chem. Eng.* **7**, 101–112 (2015).
54. Shah, R. K. *et al.* Designer emulsions using microfluidics. *Mater. Today* **11**, 18–27 (2008).
55. Sohrabi, S., Kassir, N. & Keshavarz Moraveji, M. Droplet microfluidics: fundamentals and its advanced applications. *RSC Adv.* **10**, 27560–27574 (2020).
56. Günther, A. & Jensen, K. F. Multiphase microfluidics: From flow characteristics to chemical and materials synthesis. *Lab Chip* **6**, 1487–1503 (2006).
57. Lashkaripour, A., Rodriguez, C., Ortiz, L. & Densmore, D. Performance tuning of microfluidic flow-focusing droplet generators. *Lab Chip* **19**, 1041–1053 (2019).
58. Fontana, F., Ferreira, M. P. A., Correia, A., Hirvonen, J. & Santos, H. A. Microfluidics as a cutting-edge technique for drug delivery applications. *J. Drug Deliv. Sci. Technol.* **34**, 76–87 (2016).
59. Baroud, C. N., Gallaire, F. & Dangla, R. Dynamics of microfluidic droplets. *Lab Chip* **10**, 2032–2045 (2010).
60. Pit, A. M., Duits, M. H. G. & Mugele, F. Droplet Manipulations in Two Phase Flow Microfluidics. *Micromachines* **6**, 1768–1793 (2015).
61. Utada, A. S., Fernandez-Nieves, A., Stone, H. A. & Weitz, D. A. Dripping to jetting transitions in coflowing liquid streams. *Phys. Rev. Lett.* **99**, 1–4 (2007).
62. Utada, A. S. *et al.* Monodisperse double emulsions generated from a microcapillary device. *Science (80-. )*. **308**, 537–541 (2005).
63. Moon, S. K., Cheong, I. W. & Choi, S. W. Effect of flow rates of the continuous phase on droplet size in dripping and jetting regimes in a simple fluidic device for coaxial flow. *Colloids Surfaces A Physicochem. Eng. Asp.* **454**, 84–88 (2014).
64. Cramer, C., Fischer, P. & Windhab, E. J. Drop formation in a co-flowing ambient fluid. *Chem. Eng. Sci.* **59**, 3045–3058 (2004).
65. Thorsen, T., Roberts, R. W., Arnold, F. H. & Quake, S. R. Dynamic pattern formation in a vesicle-generating microfluidic device. *Phys. Rev. Lett.* **86**, 4163–4166 (2001).
66. De menech, M., Garstecki, P., Jousse, F. & Stone, H. A. Transition from squeezing to dripping in a microfluidic T-shaped junction. *J. Fluid Mech.* **595**, 141–161 (2008).
67. Liu, Y. *et al.* A review on emulsification via microfluidic processes. *Front. Chem. Sci. Eng.* **14**, 350–364 (2020).
68. Anna, S. L. & Mayer, H. C. Microscale tipstreaming in a microfluidic flow focusing device. *Phys. Fluids* **18**, 121512 (2006).
69. Boskovic, D. & Loebbecke, S. Synthesis of polymer particles and capsules employing

- microfluidic techniques. *Nanotechnol. Rev.* **3**, 27–38 (2013).
70. Elvira, K. S., Gielen, F., Tsai, S. S. H. & Nightingale, A. M. Materials and methods for droplet microfluidic device fabrication. *Lab Chip* **22**, 859–875 (2022).
  71. Berthier, E., Surfus, J., Verbsky, J., Huttenlocher, A. & Beebe, D. An arrayed high-content chemotaxis assay for patient diagnosis. *Integr. Biol.* **2**, 630–638 (2010).
  72. Deshpande, S., Caspi, Y., Meijering, A. E. C. & Dekker, C. Octanol-assisted liposome assembly on chip. *Nat. Commun.* **7**, 1–9 (2016).
  73. Trantidou, T., Elani, Y., Parsons, E. & Ces, O. Hydrophilic surface modification of pdms for droplet microfluidics using a simple, quick, and robust method via pva deposition. *Microsystems Nanoeng.* **3**, (2017).
  74. Yandrapalli, N., Petit, J., Bäumchen, O. & Robinson, T. Surfactant-free production of biomimetic giant unilamellar vesicles using PDMS-based microfluidics. *Commun. Chem.* **2021 41 4**, 1–10 (2021).
  75. Beal, J. H. L., Bubendorfer, A., Kemmitt, T., Hoek, I. & Mike Arnold, W. A rapid, inexpensive surface treatment for enhanced functionality of polydimethylsiloxane microfluidic channels. *Biomicrofluidics* **6**, 036503 (2012).
  76. Jahangiri, F., Hakala, . Tuuli & Jokinen, V. Long-term hydrophilization of polydimethylsiloxane (PDMS) for capillary filling microfluidic chips. *Microfluid. Nanofluidics* **24**, (2020).
  77. Ficheux, M. F., Bonakdar, L., Leal-Calderon, F. & Bibette, J. Some stability criteria for double emulsions. *Langmuir* **14**, 2702–2706 (1998).
  78. Zhao, C. X., Chen, D., Hui, Y., Weitz, D. A. & Middelberg, A. P. J. Controlled Generation of Ultrathin-Shell Double Emulsions and Studies on Their Stability. *ChemPhysChem* **18**, 1393–1399 (2017).
  79. Leister, N. & Karbstein, H. P. Evaluating the stability of double emulsions— A review of the measurement techniques for the systematic investigation of instability mechanisms. *Colloids and Interfaces* **4**, 8 (2020).
  80. Baret, J. C. Surfactants in droplet-based microfluidics. *Lab Chip* **12**, 422–433 (2012).
  81. Seifriz, W. Studies in Emulsions. I-II. *J. Phys. Chem.* **29**, 587–600 (1925).
  82. Matsumoto, S., Kita, Y. & Yonezawa, D. An attempt at preparing water-in-oil-in-water multiple-phase emulsions. *J. Colloid Interface Sci.* **57**, 353–361 (1976).
  83. Ding, S., Serra, C. A., Vandamme, T. F., Yu, W. & Anton, N. Double emulsions prepared by two–step emulsification: History, state-of-the-art and perspective. *J. Control. Release* **295**, 31–49 (2019).
  84. Okushima, S., Nisisako, T., Torii, T. & Higuchi, T. Controlled production of monodisperse double emulsions by two-step droplet breakup in microfluidic devices. *Langmuir* **20**, 9905–9908 (2004).
  85. Trantidou, T., Regoutz, A., Voon, X. N., Payne, D. J. & Ces, O. A “cleanroom-free” and scalable manufacturing technology for the microfluidic generation of lipid-stabilized droplets and cell-sized multisomes. *Sensors Actuators B Chem.* **267**, 34–41 (2018).
  86. Windbergs, M., Zhao, Y., Heyman, J. & Weitz, D. A. Biodegradable core-shell carriers for simultaneous encapsulation of synergistic actives. *J. Am. Chem. Soc.* **135**, 7933–7937 (2013).
  87. Homayun, B., Lin, X. & Choi, H. J. Challenges and recent progress in oral drug delivery systems for biopharmaceuticals. *Pharmaceutics* **11**, 129 (2019).
  88. Wong, C. Y., Al-Salami, H. & Dass, C. R. Microparticles, microcapsules and microspheres: A review of recent developments and prospects for oral delivery of insulin. *Int. J. Pharm.* **537**, 223–244 (2018).
  89. Czekalska, M. A. *et al.* One-Step Generation of Multisomes from Lipid-Stabilized Double Emulsions. *ACS Appl. Mater. Interfaces* **13**, 6739–6747 (2021).
  90. Torbensen, K., Baroud, C. N., Ristori, S. & Abou-Hassan, A. Tip Streaming of a Lipid-Stabilized Double Emulsion Generated in a Microfluidic Channel. *Langmuir* **37**, 7442–7448 (2021).
  91. Ilaria Clemente *et al.* Exploring the water/oil/water interface of phospholipid stabilized double emulsions by micro-focusing synchrotron SAXS. *RSC Adv.* **9**, 33429–33435

- (2019).
92. Zhong, H., Chan, G., Hu, Y., Hu, H. & Ouyang, D. A comprehensive map of FDA-approved pharmaceutical products. *Pharmaceutics* **10**, 1–19 (2018).
  93. Lyapun, I. N., Andryukov, B. G. & Bynina, M. P. HeLa Cell Culture: Immortal Heritage of Henrietta Lacks. *Mol. Genet. Microbiol. Virol.* **34**, 195–200 (2019).
  94. Mehling, M. & Tay, S. Microfluidic cell culture. *Curr. Opin. Biotechnol.* **25**, 95–102 (2014).
  95. Hoeck, K. How the Right In Vitro Biological Model Can Drive Success in Drug Discovery. <https://home.liebertpub.com/gen> **40**, 19–21 (2020).
  96. Van Norman, G. A. Limitations of Animal Studies for Predicting Toxicity in Clinical Trials: Is it Time to Rethink Our Current Approach? *JACC Basic to Transl. Sci.* **4**, 845–854 (2019).
  97. Coluccio, M. L. *et al.* Microfluidic platforms for cell cultures and investigations. *Microelectron. Eng.* **208**, 14–28 (2019).
  98. Huh, D., Hamilton, G. A. & Ingber, D. E. From 3D cell culture to organs-on-chips. *Trends Cell Biol.* **21**, 745–754 (2011).
  99. Novik, E., Maguire, T. J., Chao, P., Cheng, K. C. & Yarmush, M. L. A microfluidic hepatic coculture platform for cell-based drug metabolism studies. *Biochem. Pharmacol.* **79**, 1036–1044 (2010).
  100. Huh, D. *et al.* Reconstituting organ-level lung functions on a chip. *Science (80-. ).* **328**, 1662–1668 (2010).
  101. Stucki, A. O. *et al.* A lung-on-a-chip array with an integrated bio-inspired respiration mechanism. *Lab Chip* **15**, 1302–1310 (2015).
  102. Jang, K. J. *et al.* Human kidney proximal tubule-on-a-chip for drug transport and nephrotoxicity assessment. *Integr. Biol.* **5**, 1119–1129 (2013).
  103. Grosberg, A., Alford, P. W., McCain, M. L. & Parker, K. K. Ensembles of engineered cardiac tissues for physiological and pharmacological study: Heart on a chip. *Lab Chip* **11**, 4165–4173 (2011).
  104. Kobuszewska, A., Jastrzębska, E., Żukowski, K. & Brzózka, Z. Simulation of hypoxia of myocardial cells in microfluidic systems. *Sci. Reports 2020 101* **10**, 1–11 (2020).
  105. Kim, H. J. & Ingber, D. E. Gut-on-a-Chip microenvironment induces human intestinal cells to undergo villus differentiation. *Integr. Biol.* **5**, 1130–1140 (2013).
  106. Mansoorifar, A., Gordon, R., Bergan, R. C. & Bertassoni, L. E. Bone-on-a-Chip: Microfluidic Technologies and Microphysiologic Models of Bone Tissue. *Adv. Funct. Mater.* **31**, 2006796 (2021).
  107. Torisawa, Y. S. *et al.* Bone marrow-on-a-chip replicates hematopoietic niche physiology in vitro. *Nat. Methods 2014 116* **11**, 663–669 (2014).
  108. Shi, M. *et al.* Glia co-culture with neurons in microfluidic platforms promotes the formation and stabilization of synaptic contacts. *Lab Chip* **13**, 3008–3021 (2013).
  109. Van Der Meer, A. D., Orlova, V. V., Ten Dijke, P., Van Den Berg, A. & Mummery, C. L. Three-dimensional co-cultures of human endothelial cells and embryonic stem cell-derived pericytes inside a microfluidic device. *Lab Chip* **13**, 3562–3568 (2013).
  110. Yu, F., Selva Kumar, N. D., Choudhury, D., Foo, L. C. & Ng, S. H. Microfluidic platforms for modeling biological barriers in the circulatory system. *Drug Discov. Today* **23**, 815–829 (2018).
  111. Booth, R. & Kim, H. Characterization of a microfluidic in vitro model of the blood-brain barrier ( $\mu$ BBB). *Lab Chip* **12**, 1784–1792 (2012).
  112. Bhatia, S. N. & Ingber, D. E. Microfluidic organs-on-chips. *Nat. Biotechnol.* **32**, 760–772 (2014).
  113. Novak, R. *et al.* Robotic fluidic coupling and interrogation of multiple vascularized organ chips. *Nat. Biomed. Eng.* **4**, 407–420 (2020).
  114. Zhang, C., Zhao, Z., Abdul Rahim, N. A., Van Noort, D. & Yu, H. Towards a human-on-chip: Culturing multiple cell types on a chip with compartmentalized microenvironments. *Lab Chip* **9**, 3185–3192 (2009).
  115. Luni, C., Serena, E. & Elvassore, N. Human-on-chip for therapy development and

- fundamental science. *Curr. Opin. Biotechnol.* **25**, 45–50 (2014).
116. Renggli, K., Rousset, N., Lohasz, C., Nguyen, O. T. P. & Hierlemann, A. Integrated Microphysiological Systems: Transferable Organ Models and Recirculating Flow. *Adv. Biosyst.* **3**, 1900018 (2019).
  117. Thomée, E. Development of thermoplastic elastomer microfluidic systems for bio-applications. (University of Strasbourg, 2021).
  118. Schneckenburger, H. & Richter, V. Challenges in 3d live cell imaging. *Photonics* **8**, (2021).
  119. Farooqi, H. M. U., Khalid, M. A. U., Kim, K. H., Lee, S. R. & Choi, K. H. Real-time physiological sensor-based liver-on-chip device for monitoring drug toxicity. *J. Micromechanics Microengineering* **30**, (2020).
  120. Kilic, T., Navae, F., Stradolini, F., Renaud, P. & Carrara, S. Organs-on-chip monitoring: sensors and other strategies. *Microphysiological Syst.* **1**, 1–1 (2018).
  121. Santbergen, M. J. C., van der Zande, M., Bouwmeester, H. & Nielen, M. W. F. Online and in situ analysis of organs-on-a-chip. *TrAC - Trends Anal. Chem.* **115**, 138–146 (2019).
  122. Begley, C. G. & Ellis, L. M. Drug development: Raise standards for preclinical cancer research. *Nature* **483**, 531–533 (2012).
  123. Lu, C. & Verbridge, S. S. Microfluidic methods for molecular biology. *Microfluid. Methods Mol. Biol.* 1–376 (2016). doi:10.1007/978-3-319-30019-1
  124. Morita, T., Nagaki, T., Fukuda, I. & Okumura, K. Clastogenicity of low pH to various cultured mammalian cells. *Mutat. Res. Mol. Mech. Mutagen.* **268**, 297–305 (1992).
  125. Scorpio, R. *Fundamentals of Acids, Bases, Buffers & Their Application to Biochemical Systems*. (Kendall Hunt Pub Co, 2000).
  126. Salis, A. & Monduzzi, M. Not only pH. Specific buffer effects in biological systems. *Curr. Opin. Colloid Interface Sci.* **23**, 1–9 (2016).
  127. Eagle, H. Buffer combinations for mammalian cell culture. *Science (80-. )*. **174**, 500–503 (1971).
  128. Michl, J., Park, K. C. & Swietach, P. Evidence-based guidelines for controlling pH in mammalian live-cell culture systems. *Commun. Biol.* **2019 21 2**, 1–12 (2019).
  129. Weltin, A. *et al.* Cell culture monitoring for drug screening and cancer research: a transparent, microfluidic, multi-sensor microsystem. *Lab Chip* **14**, 138–146 (2013).
  130. Fuchs, S. *et al.* In-line analysis of organ-on-chip systems with sensors: Integration, fabrication, challenges, and potential. *ACS Biomater. Sci. Eng.* **7**, 2926–2948 (2021).
  131. Akin, M. *et al.* A new set up for multi-analyte sensing: At-line bio-process monitoring. *Biosens. Bioelectron.* **26**, 4532–4537 (2011).
  132. Pousti, M., Zarabadi, M. P., Abbaszadeh Amirdehi, M., Paquet-Mercier, F. & Greener, J. Microfluidic bioanalytical flow cells for biofilm studies: a review. *Analyst* **144**, 68–86 (2018).
  133. Chauvet, A., Tibiletti, T., Caffarri, S. & Chergui, M. A microfluidic flow-cell for the study of the ultrafast dynamics of biological systems. *Rev. Sci. Instrum.* **85**, 103118 (2014).
  134. Capel, A. J., Rimington, R. P., Lewis, M. P. & Christie, S. D. R. 3D printing for chemical, pharmaceutical and biological applications. *Nat. Rev. Chem.* **2**, 422–436 (2018).
  135. Krejčí, J. *et al.* The measurement of small flow. *Sensors Actuators, A Phys.* **266**, 308–313 (2017).
  136. Strebl, M. G., Bruns, M. P., Schulze, G. & Virtanen, S. Respirometric In Situ Methods for Real-Time Monitoring of Corrosion Rates: Part II. Immersion. *J. Electrochem. Soc.* **168**, 011502 (2021).
  137. Ahmerkamp, S. *et al.* The effect of sediment grain properties and porewater flow on microbial abundance and respiration in permeable sediments. *Sci. Reports* **2020 101 10**, 1–12 (2020).
  138. Higuera, G. A. *et al.* Supporting data of spatiotemporal proliferation of human stromal cells adjusts to nutrient availability and leads to stanniocalcin-1 expression in vitro and in vivo. *Data Br.* **5**, 84–94 (2015).
  139. Illner, S., Hofmann, C., Löb, P. & Kragl, U. A Falling-Film Microreactor for Enzymatic

- Oxidation of Glucose. *ChemCatChem* **6**, 1748–1754 (2014).
140. Zhang, Y. S. *et al.* Multisensor-integrated organs-on-chips platform for automated and continual in situ monitoring of organoid behaviors. *Proc. Natl. Acad. Sci. U. S. A.* **114**, E2293–E2302 (2017).
  141. Khalid, M. A. U. *et al.* A lung cancer-on-chip platform with integrated biosensors for physiological monitoring and toxicity assessment. *Biochem. Eng. J.* **155**, 107469 (2020).
  142. Ali, S., Shaegh, M., De Ferrari, F. & Zhang, Y. S. A microfluidic optical platform for real-time monitoring of pH and oxygen in microfluidic bioreactors and organ-on-chip devices. *Biomicrofluidics* **10**, 044111 (2016).
  143. Wu, M. H., Lin, J. L., Wang, J., Cui, Z. & Cui, Z. Development of high throughput optical sensor array for on-line pH monitoring in micro-scale cell culture environment. *Biomed. Microdevices* **11**, 265–273 (2009).

## CHAPTER 2.

# MARKET STUDY: ENCAPSULATION-IN-DROPLETS AND MICROENVIRONMENT MONITORING OF MICROFLUIDIC CELL CULTURES

“everyone needs habits of mind that allow them to dance across disciplines.”

— David Epstein, *Range: How Generalists Triumph in a Specialized World*

### ABSTRACT

---

This market study evaluates the two different microfluidic tools for biological applications: encapsulation-in-droplets and microenvironment monitoring for microfluidic cell culture. It is intended to provide industrial contextualisation to the experimental work and scientific evaluation presented in Chapters 4 and 5. The different market approaches used in each study, the "technology push" and the "market pull", are presented and the similarities between scientific and market research are highlighted in the frame of an industrial PhD. Researcher interviews were conducted as a source of primary information to evaluate the limitations and needs in biology research settings; a notable finding is that buying microfluidic equipment is linked to the level of confidence presumed by the researcher in attaining the desired results. Also, most researchers that have crossed this barrier build their own systems and adapt them to existing equipment, such as the CO<sub>2</sub> incubator, which often does not meet the demanding requirements of a fast-evolving field. Finally, an evaluation of each research market size is provided, utilising Google Scholar publication results to quantify the growth of microfluidics in several research areas, defining the microfluidic relevance of each market segment. An estimated market value for each application is subsequently made, ranging from 200,000–3,000,000 EUR per year for encapsulation-in-droplets and approximately 120,000-900,000 EUR for pH monitoring of microfluidic cell culture.

---

### *Contributions*

---

The main part of this market study was performed by Camila Betterelli Giuliano. Dr Leslie Labarre (Elvesys) and Dr Benjamin Garlan (Elvesys) aided with assembling the A/B testing landing pages and sending the mail campaigns. Dr Niels Junius (Elvesys) and Dr Amine Rabehi (Elvesys) aided with contact collecting for researcher interviews and note taking during interviews for Encapsulation. Dr Marine Daieff (Elvesys) and Dr Aurélie Vigne (Elvesys) aided the assembly and review of cell culture questionnaire. Writing of this chapter was done by Camila Betterelli Giuliano. Revision was done by Camila Betterelli Giuliano, Dr Lisa Muiznieks (Elvesys) and Prof. Joseph Moran (Univ. Strasbourg).

---



## 2.1. Introduction

The main lagging indicator in Europe's innovation landscape is the lack of innovative young companies when compared to other developed economies, namely the US. The main identified reason for this gap is the lack of early-stage risk funding<sup>1</sup>. As one way to address this issue and strengthen the economy after the 2008 crisis, the European Commission launched the Horizon 2020 program. The initiative aimed to consolidate Europe's fragmented research, development and innovation (R&D&I) investments across the Union through public-private partnerships<sup>2</sup>. These consortia of academic institutions and small and medium-sized enterprises (SMEs) fostered hybrid PhD formats. This promoted and developed entrepreneurial capabilities in early-stage researchers by pursuing research with direct market relevance, as is the case of this thesis. One of the skills developed during this work was assessing the market relevance of scientific investigations, which consists of better understanding the needs and demands of potential users by means of market research.

Market research follows the principles of scientific research, i.e. it is based on systematic observation and investigation of a topic to validate hypotheses and expand the knowledge base. The main difference is the source of the data and the fact that the results are expected to be actionable. The primary data source for market studies is the potential end-users of the technology in question and key opinion leaders (KOLs) of the field, mainly providing qualitative data through interviews and one-on-one interactions. Primary quantitative data can also be gathered through questionnaires and online tools, such as A/B testing of webpages. Similar to scientific investigations, there is also secondary research based on the literature review of what has been already done in the field of interest. Both data sources are complementary, and the extent to which market research relies more on quantitative or qualitative data gathering tools depends on the questions being asked<sup>3</sup>. Ultimately, the market research should be able to provide enough information on the market size, growth, needs, and accessibility, the competitor technology landscape, and customer needs, values, and behaviour so a go/no-go product investment decision can be made.

Innovation can derive from a developed technology that requires a market, also known as a "technology push", or an identified market need that requires technological innovation, a "market pull". The former is usually associated with disruptive technologies that provide major improvements in the current scenario, while the latter relates to incremental improvements of the current state-of-the-art. Both strategies are complementary when considering how to

maintain the competitive edge of innovative companies<sup>4</sup>. This chapter will discuss the application of both approaches in the context of the projects of this industrial PhD.

### 2.1.1. Research rationale

The research objective of this study was to provide market contextualisation of the scientific research conducted in this thesis on the topic of microfluidic tools for biological applications. This thesis is divided into two main microfluidic tools: droplet microfluidics for the production of complex compartments and pH monitoring of microfluidic cell cultures. Thus, this market contextualisation encompassed a quantitative investigation of the market size and trends, an analysis of the competitive landscape, and interview-based primary research, supplemented with questionnaires and other quantitative tools, to evaluate market needs for the broader field of encapsulation in droplets and the area of microenvironment monitoring for microfluidic cell cultures, mainly focusing on pH.

The core hypothesis of each market study was:

- 1) Encapsulation-in-droplets: Biologists see value in using microfluidic tools to improve the depth of data of their experiments. However, the barrier to adoption is the complexity of microfluidic setups. Therefore, there is a market need for accessible microfluidic tools to ease the transition.**
  
- 2) Microenvironment Monitoring: Biologists would like more detailed information about microenvironment parameters of microfluidic cell cultures without having to integrate sensors into chips. Therefore, there is a market need for a product that can easily monitor these parameters regardless of the chip.**

To validate these hypotheses, the following research questions were investigated:

1. What is the size of these two markets?
2. What microfluidic solutions currently exist on the market?
3. What are the main limitations in microfluidic setups, or what improvements are desired?
4. Do biologists perceive value in the proposed solutions?

## **2.2. Research Methodology**

### **2.2.1. Competitive Landscape Review**

Comprehensive market research and review of competitors were conducted for each of the markets of interest: encapsulation in droplets and microenvironment monitoring of microfluidic cell culture. The research was mainly conducted online, focusing on systems that were intended or could be adapted for microfluidics setups.

### **2.2.2. Researcher Surveys**

Questionnaires were assembled for each of the applications of interest and distributed mainly at conferences. In-depth interviews were performed through video calls with questionnaire respondents and other KOLs that were part of the company's network or referred by other interviewees.

To gather quantitative primary data, webpage A/B tests were also performed. The test consisted in creating webpages as part of the company's main website. These landing pages were distributed through mailing campaigns to a subset of the company's content subscribers, and the reactions of the recipients were analysed to understand which topic elicited more interest by having a higher click rate or direct replies. The webpages were nearly identical except for the keywords that defined each of the tested segments, for example, for encapsulation in droplets, the keywords used were "single-cell encapsulation", "cell encapsulation", and "high throughput screening". For the encapsulation in droplets segment, each webpage was also randomly distributed to an equivalent number of people, divided into "microfluidicists" and "non-microfluidicists". The auction price ranges of the keywords were directly extracted from the Google Adwords platform by selecting the desired geographic region (Europe, North America and Asia).

### 2.2.3. Market sizing and Financial Analysis

The markets of interest were quantified by the number of publications per year on the Google Scholar search engine for the year of 2021. Every Google Scholar search returns, in principle, results corresponding to the sum of scholarly publications of the searched keyword, including journal and conference papers, theses, dissertations, abstracts, technical reports, and pre-prints from a wide range of journals, university repositories, and professional societies. By carefully choosing keywords and using search tools, namely the designation of the publication date, the size of specific fields of research over time can be estimated based on the occurrence of publications within a particular date range. The keywords were chosen based on potential market segments that could be explored for each application. The combination of a particular keyword in quotation marks followed by the keyword "microfluidics" gives the number of publications that contains the word microfluidics in that specific field. Comparing it to the total number of publications of that keyword shows the relevance of microfluidics in a particular area. Thus, the microfluidics relevance was calculated as a percentage of the number of publications mentioning microfluidics in a certain keyword, for example, "'single-cell analysis' + microfluidics" (2,630 published papers in 2021), over the total number of publications for that keyword, for example, "single-cell analysis" (12,400 published papers in 2021, microfluidics relevance of 21%).

Market value sizing was conducted for each of the research themes investigated. The total addressable market (TAM; meaning the size of the largest possible market) figures and growth estimates were obtained from reports of market analysis' companies. The serviceable available market (SAM; meaning the part of the market that fits the product being offered, i.e., biology-related applications) of each market of interest was found by estimating the number of potential customers as a function of the Google Scholar publication results in each biology field that were relevant to microfluidics. The serviceable obtainable market (SOM; meaning the proportion of the SAM that could realistically be captured, factoring in competition) was estimated by multiplying the SAM by the calculated market penetration rate of the company in relation to its competitors.

Key assumptions were made to perform the market sizing and financial analysis. It was assumed that Google Scholar search results provided a representative indication of the biology research market size and trends. It must be noted that while the keyword selection search operators were used to limit the inclusion of irrelevant results in the Google Scholar searches,

keyword searches undoubtedly retrieve results that are unrelated to the intended search. It was assumed that irrelevant results would represent a small minority of overall search results. Thus, market evaluation through Google Scholar accurately depicts the quantity and trends of biology-related publications with some margin of error. Market value sizing estimates (i.e., SAM and SOM) were obtained based on the following assumptions: (i) a biology lab group generating a microfluidics-relevant publication is a potential customer; (ii) the average biology PI generates two publications per year (based on scientific publishing data from Italy<sup>5</sup>), and a single PI represents one possible customer; (iii) the average market penetration rate for the company, when compared to its competitors based on number of publications, is 10%; (iv) an expected product development cost is approximately 100,000 EUR per year (estimated internally).

## **2.3. Results and Discussion**

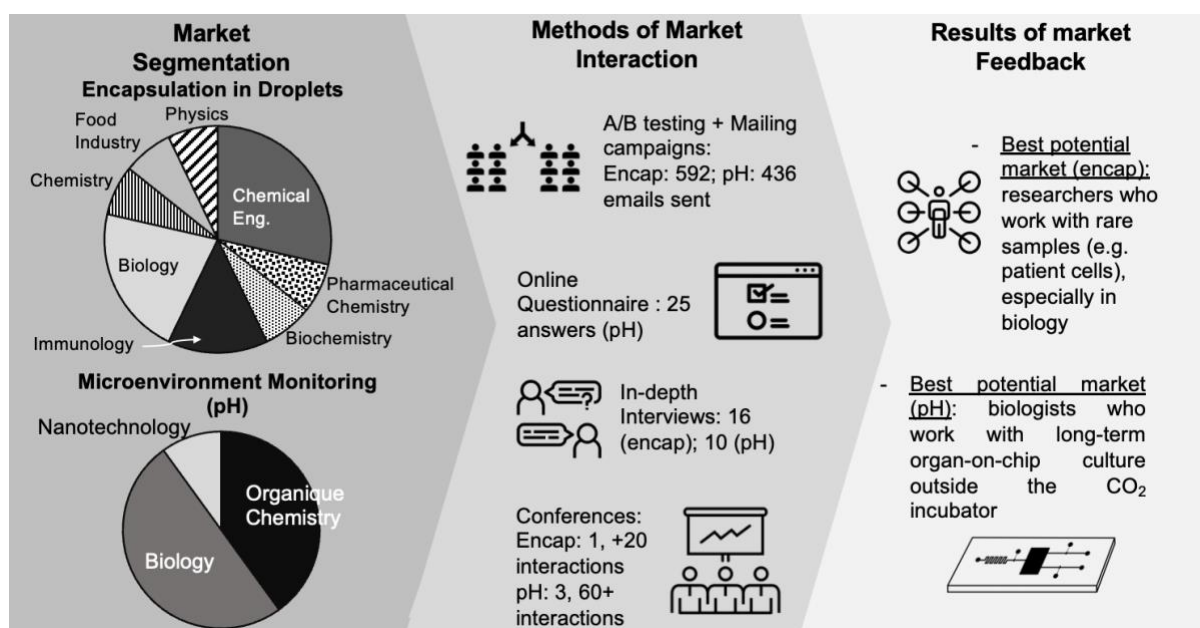
### **2.3.1. Overview of the market assessment**

In the frame of an industrial PhD, the identification and understanding of current challenges in the field of interest is paramount, so that developed solutions can be widely applicable to the broadest community of users in the future. To this end, information was collected from KOLs and stakeholders in the fields of encapsulation in droplets and microenvironment monitoring of microfluidic cell culture to establish technical specifications of the microfluidic system at every level (i.e. chip, connectors, flow, tubing, parameters, etc.) and to identify standards in the field to ensure compliance, reproducibility, and implementation of innovations.

Each of these fields had a different market approach. The market assessment of the encapsulation-in-droplets field can be considered a "technology push", as the goal was to find the best niche for a predefined product. The predefined product was envisioned as a "starter pack", *i.e.* an assembly of the company's instruments and the reagents to perform encapsulation in droplets considering the broadest of applications, so it could be refined with input from the market. The product was built upon an internal knowledge base that can be exploited in commercial terms, enlarging the company's offering and fitting well with the overall market strategy of a "technology push". On the other hand, the field of microenvironment monitoring for microfluidic cell culture was a "market pull" since an increased interest in microfluidic solutions was identified internally, and a market assessment was devised to

determine the technical specifications of a potential product before any development work was carried out.

Regardless of the approach, the market assessment followed a similar process (Figure 2.1), differing mainly on the content, i.e. the questions asked at each stage. Firstly, each field was divided into segments based on applications, which were used to define the profile of users to be contacted. Then, several ways of interacting and gathering data from potential users were applied.



**Figure 2.1.** Summary of market assessment process for the fields of interest. The market was segmented into applications, which were used to define the user profile. Researchers who fit the profile were contacted through different channels. The analysis of the gathered data was compiled, and the most suitable market was suggested.

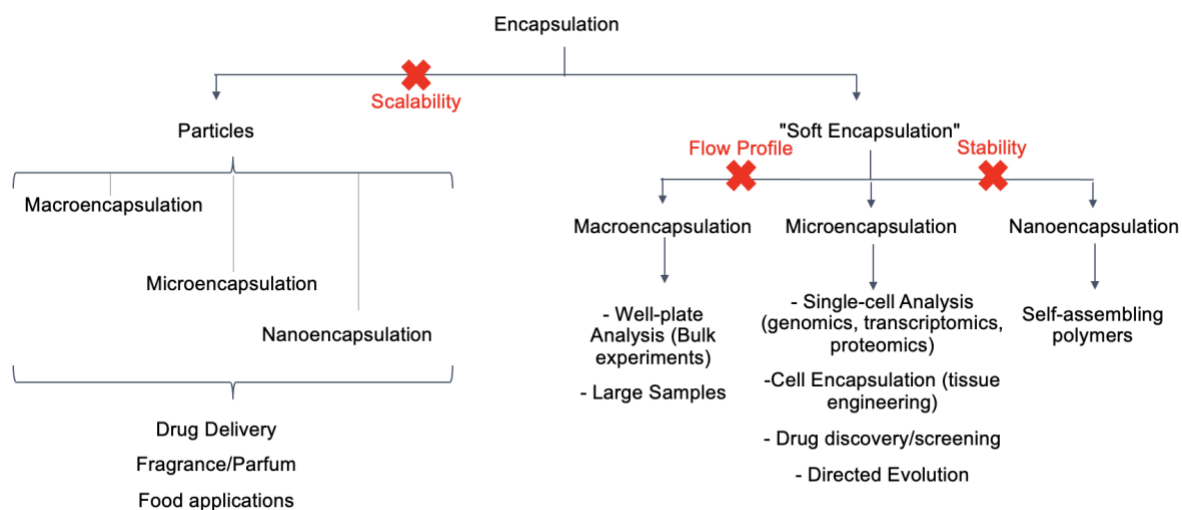
The A/B testing and the mailing campaigns aimed at understanding which keywords elicited more interest from users and the goal was to attain a larger audience than feasible with in-person interactions. Based on the answers, researchers were contacted to take part in in-depth interviews, which explored their application and day-to-day work in detail, assessing the limitations of current setups and considering improvements. During the course of the market assessments, several conferences were attended to enlarge the number of interactions in an efficient manner, which were followed up by interviews when pertinent. In the case of the microenvironmental monitoring of microfluidic cell cultures, an online questionnaire was created, specifically focusing on the determination of technical needs. This questionnaire was widely used in the conferences.

The analysis of the gathered information showed that users most likely to need an "encapsulation-in-droplets" product are those who work with rare or limited samples and are not yet working with microfluidics. For the microenvironment monitoring field, the users would be researchers who culture organ-on-chips for extended periods outside a CO<sub>2</sub> incubator, performing live cell imaging, for example. These points will be elaborated on in the following sections.

## **2.3.2. Investigation of market demand for Encapsulation in Droplets**

### **2.3.2.1. Market Segmentation of applications**

The main goal of this market study was to determine the market interest in an "encapsulation-in-droplets" product, identifying the most strategic niche to focus marketing efforts. To gather relevant market insight, questionnaires were used to guide the in-person interactions at the "Innovation in Encapsulation" conference, London, 2019, and later at in-depth online interviews. About 20 people were contacted during the "Innovation in Encapsulation" conference, and those interactions allowed clarification of the market segmentation (Figure 2.2). Using the gathered information, the encapsulation market was divided into two main segments: particles, i.e. solid or hard-shell structures, such as microparticles; and "soft-encapsulation", i.e. soft structures, such as droplets, vesicles, polymersomes, double emulsions, etc. Each of these segments could be subsequently divided based on the size of the structure, i.e. in the macro, micro or nanometre ranges, which relates intrinsically to the final application.



**Figure 2.2.** Segmentation of the encapsulation market. The encapsulation market was broadly divided into hard and soft encapsulation. The "hard encapsulation" refers to solid particles while the "soft encapsulation" can be interpreted as fluid structures. These segments were further divided by size, defining the application. Red "X"s indicate segments that do not fit the envisioned product.

The production of solid particles usually requires a post-production step<sup>6</sup>. Given the "starter pack" nature of the product, this market segment was considered too complex as an initial go-to-market strategy. Moreover, most applications of solid particles, such as drug delivery<sup>7</sup>, food applications<sup>8</sup> and the fragrance industry<sup>9</sup>, are concerned with the scalability of the equipment<sup>10,11</sup> as they are developed to reach industrial production. Thus, the most suitable market segment for an initial market niche would be to focus on soft structures, *i.e.* single emulsions or water-in-oil-in-water/oil-in-water-in-oil droplets. Microfluidics is better suited to produce compartments in the micrometre range<sup>6</sup> due to the dimensions of the chip. It is challenging to replicate the improved control of laminar flow in the macrometre range, usually implicating highly viscous solutions<sup>12</sup>. Nanometre particles have been produced with droplet microfluidics, but nanoemulsions are thermodynamically unstable and require large energetic input to during preparation<sup>6</sup>. Thus, the best market entry strategy based on the analysis was to focus on researchers working with soft structures in the micrometre range. Considering the applications uncovered through the direct interactions and a literature review to expand the breadth of related areas, the most prominent applications were single-cell analysis<sup>13–15</sup>, drug delivery<sup>16–18</sup>, tissue engineering<sup>17,19–21</sup>, drug discovery/screening<sup>22–24</sup> and directed evolution<sup>25–28</sup>, considered as high-throughput assays.



### 2.3.2.2. Financial Analysis for Risk Assessment

To better understand which of the segments would provide the best return on investment, a financial analysis was performed based on predefined assumptions (Table 2.1). The price was estimated based on the company's catalogue; the market penetration was calculated based on a comparison between publications containing the company's equipment and that of competitors; and the average biology PI generates 2 publications per year (based on scientific publishing data from Italy<sup>5</sup>). For the competitors' landscape, two analyses were made. The first considered the direct competitors of the company, i.e. companies that work with pressure-driven flow control, comparing the total number of publications, with provided a market penetration of 30%. However, that considers only a portion of the market, as there are other ways to control flow, such as mechanically-driven flow control, e.g. syringe pumps, peristaltic pumps, etc<sup>29</sup>. Thus, the second analysis compared the market penetration to a broader set of competitors, resulting in a 10% assumption. Considering the product as a "starter pack", i.e. aimed at users that are not microfluidics specialists, the niche is likely to be found in this broader market, so 10% was used in the calculations.

The market size was calculated based on the total number of publications (excluding citations and patents) for a given keyword, e.g. "single-cell analysis", in a determined period, e.g. full year of 2021 (Table 2.2). The total number of publications was divided by the number of papers published by a PI per year, resulting in the total number of potential clients, e.g. of the 12,400 publications on "single-cell analysis" in 2021, 6,200 came from different labs (assuming that each PI published 2 papers per year). Then, the number of potential clients that might use microfluidics was calculated using the microfluidics relevance for that particular keyword. The microfluidics relevance was calculated by dividing the number of publications citing microfluidics in a particular keyword by the total number of publications of that keyword, and it indicates how many laboratories used microfluidics in that field that year. For example, in 2021, 1,315 labs published an article talking about single-cell analysis and microfluidics. From those research groups, the ones likely to buy from our company were calculated based on the market penetration defined above, resulting in 131.5 potential clients. Multiplying by the assumed price of the product, 15,000 €, results in a market size of 1,972,500 € for single-cell analysis. To evaluate if any of the calculated markets is sizeable enough to justify further investment, the costs must be considered. The estimation of costs was based on an internal assessment that included 5,500€ for a full-time employee, 1,800€ for consumables and 1,200€ for administrative costs, all considered monthly, resulting in an annual cost of approximately

100,000€ per year of development. Hence, none of the calculated market sizes would be readily excluded based on the cost assessment alone.

**Table 2.1.** Assumptions for financial analysis of different market segments in soft microencapsulation

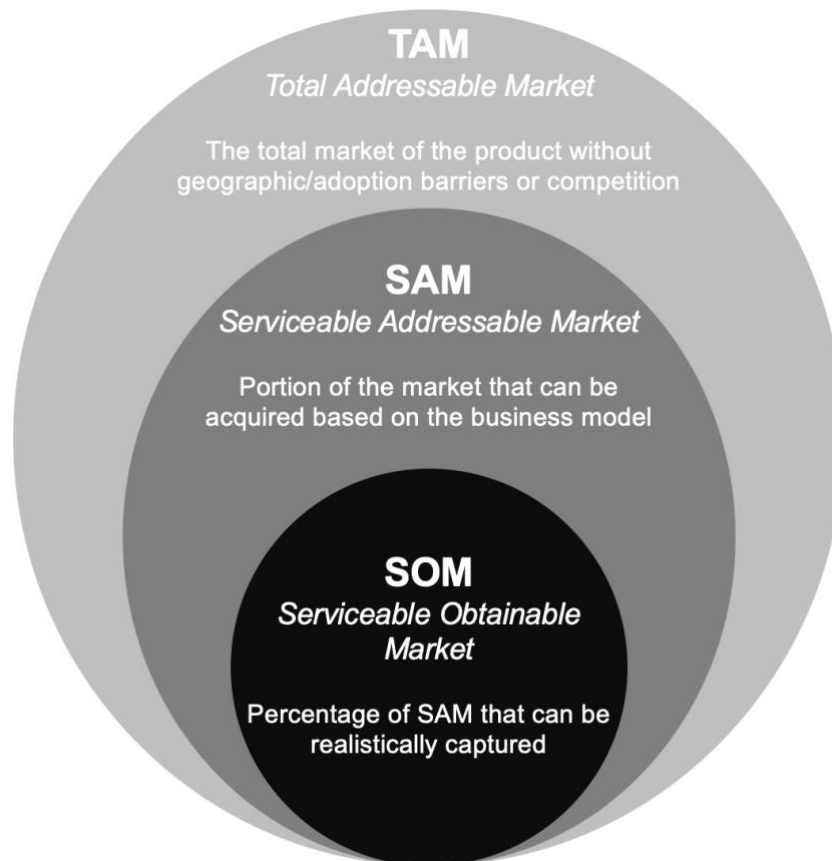
<b>Assumptions</b>	
Pack Price	15,000 €
Market penetration for flow control in microfluidics	30%
Market penetration in microfluidics	10%
Paper production per PI/year	2

**Table 2.2.** Financial analysis of different market segments in soft microencapsulation

<b>Field/Keyword</b>	High Throughput Screening					
	Single-cell analysis	Tissue engineering	Drug Delivery	Drug screening	Drug discovery	Directed Evolution
<b>Year</b>	<b>2021</b>	<b>2021</b>	<b>2021</b>	<b>2021</b>	<b>2021</b>	<b>2021</b>
Number of papers Google Scholar	12,400	37,300	75,100	17,100	59,800	6,480
Number of papers per lab	2	2	2	2	2	2
Total Number of potential clients	6,200	18,650	37,550	8,550	29,900	3,240
Microfluidics relevance (%)	21	19	15	20	9	10
Number of potential clients that might use microfluidics	1,315	3,510	5,632.5	1,670	2,610	3,39.5
Penetration rate in microfluidics (%)	10	10	10	10	10	10
Number of potential clients that might buy from us	131.5	351	563.5	167	261	33.95
Price (€)	15,000	15,000	15,000	15,000	15,000	15,000
<b>Market Size (€)</b>	<b>1,972,500</b>	<b>5,265,000</b>	<b>8,267,273</b>	<b>2,505,000</b>	<b>3,915,000</b>	<b>509,250</b>

Market financial assessments analyse the potential return on investment in a given field. To start, the market must be divided into the total addressable market (TAM), i.e. the total amount of revenue that could be obtained if the company serviced worldwide without competitors and

all users that could potentially purchase the product for any possible application chose to buy it; the Serviceable Available Market (SAM); i.e. the revenue based on the number of clients that could realistically buy the product, could be defined geographically or, in this case, based on the number of publications per PI per year, which gives the number of potential clients that could use microfluidics; and, lastly, the Serviceable Obtainable Market (SOM), i.e. the potential revenue when considering the SAM multiplied by our market penetration, which is the market size of the company for the product in question<sup>30</sup> (Figure 2.3).



**Figure 2.3.** Illustration of the relationship between TAM, SAM and SOM.

The TAM, although unrealistic, provides insight into the relevance of the segment on a global scale, as small TAMs (less than €1B) usually indicate that the SOM will also be small and will not justify investments in product development<sup>31</sup>. Moreover, most market projections of growth are based on the TAM and indicate if the market is expected to expand, typically expressed as the expected Compound Annual Growth Rate (CAGR) (Table 2.3). The TAM is usually found in market reports issued by specialised consultancy firms. Here, instead of searching for a TAM that would encompass all the markets segments, such as "Microfluidic encapsulation", the TAM for each potential market segment was individually defined. This approach was used because the "starter pack" nature of the product implies that people not yet familiar with microfluidics can become potential clients. Thus, each of these TAMs considers every

researcher performing single-cell analysis, drug delivery or direct evolution, for example, that could become a microfluidics user. Using an umbrella term, such as Microencapsulation, would be too broad and consider industrial applications, which are out of scope and would skew the market size, making it look much larger than it is. On the other hand, Microfluidic Encapsulation would be too narrow and not consider the possibility of new users. Although speculative, these data points contribute to a better assessment of the investment risk. Thus, a market with a large TAM that is expected to grow in the next five years, combined with a sizable SOM that is larger than the expected product investment, has a lower risk than a small TAM or a large TAM that is not expected to grow<sup>32</sup>, because it might indicate a consolidated market with high barriers to entry<sup>33</sup>. "Direct evolution" presented the smallest market size. Still, it has a sizable TAM (2.54B€) and a financially relevant CAGR of 11.6%, so it could be a future market to be explored after the product was consolidated by launching in a market that would provide a better return on investment in the short-term. "Drug delivery" and "drug discovery" have both large TAMs (1,175B€ and 52.64B€), that are growing at promising yearly rates (12% and 8.3%), and could provide a fast return on investment, however, further analysis is necessary to understand the competitive landscape and other barriers to entry. "Single-cell analysis" (2.15B€; 15%) and "drug screening" (5.18B€, 16.8%) showed similar TAMs and growth rates, but the SOM of drug screening is slightly larger, indicating a larger penetration of microfluidics in the field and potentially a lower barrier of entry. "Tissue engineering" (22.28€; 18.5%) stands out with its large TAM and largest growth rate, and one of the largest SOMs as well.

**Table 2.3.** Market Sizing for different market segments in soft microencapsulation

Field/Keyword	Single-cell analysis	Tissue engineering	Drug Delivery	Drug screening	Drug discovery	Directed Evolution
<b>TAM</b> (Total Addressable Market; 2020)* (B€)	2.15 <sup>34</sup>	22.28 <sup>35</sup>	1,175 <sup>36</sup>	5.18 <sup>37</sup>	52.64 <sup>38</sup>	2.54 <sup>39</sup>
<b>Expected Compound Annual Growth Rate</b> (CAGR) (%)	15	18.50	12	16.8	8.3	11.6
<b>SAM</b> (Serviceable Available Market) (€)	19,725,000	52,650,000	82,672,733	25,050,000	39,150,000	5,092,500
<b>SOM</b> (Serviceable Obtainable Market)(€)	1,972,500	5,265,000	8,267,273	2,505,000	3,915,000	509,250

\*Currency converted to Euros (1 USD = 0.977279 EUR, 05.08.2022)

### 2.3.2.3. Market acceptance and barriers to entry

Most modern marketing strategies rely heavily on online paid publicity<sup>40</sup>. Briefly, advertisers auction for a keyword on search engines, such as Google, Yahoo, Baidu, etc. Since the number of advertisements that can be shown to a user for that particular keyword is limited, the price of the bid influences the position in which the advertiser will be displayed on the ranking and the likelihood of being seen and clicked by the user. This consequently influences the likelihood of the user buying from that advertiser<sup>41</sup>. Internet advertising has become a multibillion dollar industry, with American companies spending over US\$ 54.7 billion in 2019 on advertisements targeted to match keywords potentially searched by users<sup>42</sup>. As competition has increased, searching for the best keywords, *i.e.* reaching the right audience at the lowest auction price, has become a crucial go-to-market strategy<sup>42</sup>. A successful go-to-market strategy has a precise and well-defined audience and communication plan to breach the first barriers to entry. It does not limit the market of a particular product to that first niche, it only finds which market niche offers the best cost-benefit ratio with regards to marketing efforts and return on investment. The price ranges for the auction of the selected keywords was analysed and found to be similar (from 0.24 to 3.96€) for all keywords except for "Single-cell analysis" and "directed evolution", which were considerable higher (from 2.30 to 10.83€) (Table 2.4). Special attention should be given to the return on investment of the "single-cell analysis" campaigns, as it is the most expensive keyword and one of the smallest markets. The high-throughput segments could be concurrently explored, but the communication strategy would have to be different. In this case, it is necessary to evaluate the extra marketing effort to decide if these segments should be postponed to a later stage of the product life cycle.

**Table 2.4.** Paid advertisement price ranges for selected keywords

Keyword	Average Number of monthly searches	Competition	Auction price for top of the page (minimum to maximum range)
Single-cell Analysis	1,000	Average	2.30 - 10.83€
Tissue Engineering	8,100	Low	0.51 - 2.62€
Drug Delivery	3,600	Average	0.29 - 3.96€
Drug Screening	8,100	Average	1.27 - 3.39€
Drug Discovery	6,600	Low	0.24 - 3.36€
Directed Evolution	1,900	Low	2.43 - 9.14€

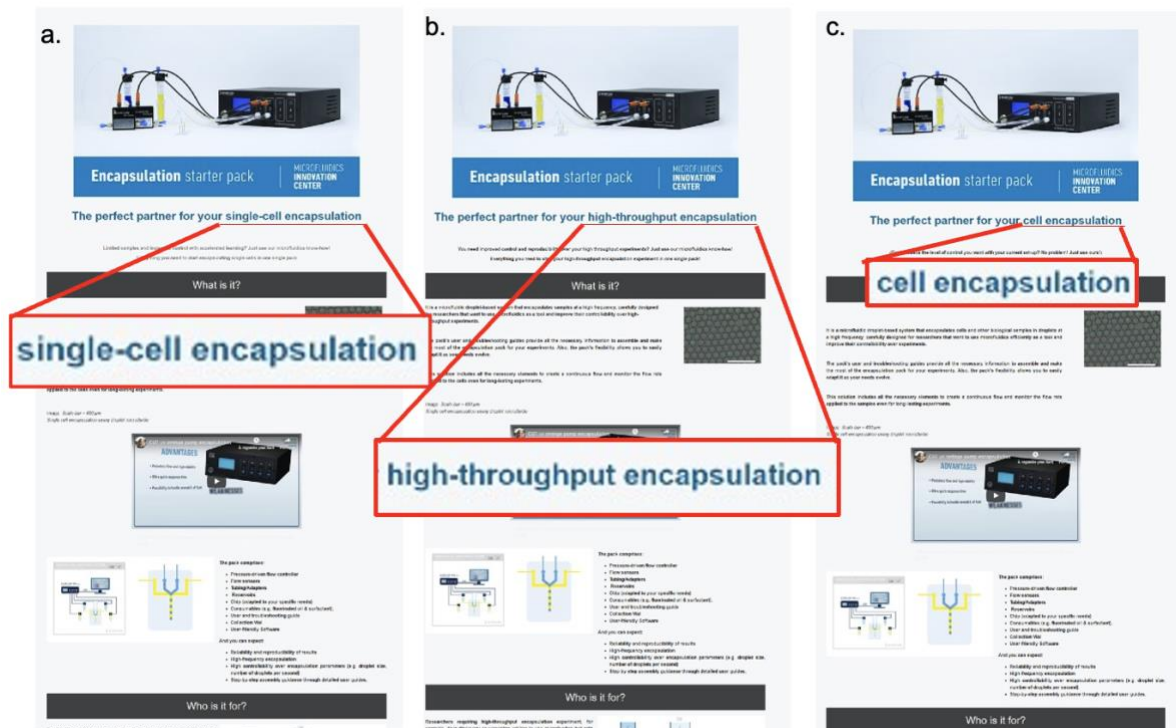
## **2.3.2.4. Feedback analysis of potential users**

### **2.3.2.4.1. Main Target Audience**

To better differentiate between market niches in order to focus marketing efforts once the product is ready, a feedback analysis of potential users was carried out. As mentioned, the financial analysis provided insight into the risk assessment of each segment, but it is also necessary to understand the market acceptance and interest from the point of view of end-users, to gauge the barriers to entry. A/B webpage testing is a great quantitative complement to the qualitative data brought by interviews and one-on-one interactions at conferences. It also provides more information than questionnaires because they require users to demonstrate interest by taking an action, for example, subscribing to a newsletter or asking for a quote, a more direct, less biased, tangible measurement of interest<sup>43</sup>. Also, it differs from paid advertisement in the sense that the audience is defined in advance and it is expected to react to a trigger instead of actively taking the initiative. For example, paid advertisement relies on the fact that users will actively type a particular keyword on the search bar of a search engine, that is why understanding what keywords define your audience is crucial to optimise results.

A/B testing sends email campaigns to a defined audience and required the receivers to act upon the content of that email, giving more flexibility to test which keywords generated more interest. The test consisted of creating three almost-identical landing pages, differentiated only by the keywords for each chosen market segment (Figure 2.4) and emailing them to a selected audience. The chosen keywords were "single-cell encapsulation", "cell encapsulation" and "high-throughput encapsulation". Here, keywords were adapted to include "encapsulation" to better define the offering in the eyes of the audience and avoid eliciting erroneous responses from researchers interested in the "analysis" part. "Cell encapsulation" replaced "tissue engineering" to narrow the field to encapsulation-related topics as droplets encapsulating groups of cells can be used in the organoids field<sup>44-46</sup>. These keywords best reflected the majority of the applications explored in the financial analysis. The webpages were sent to equivalent numbers of two defined audiences, "microfluidicists", people who had already worked with microfluidics, and "non-microfluidicists", people who had minimal experience with microfluidics. The goal was two-fold. First, to better understand from the financial analysis which market segments elicited the most interest from researchers, *i.e.* if there was a significant difference between the segments, then choosing the most appropriate keywords could considerably optimise marketing campaigns; second, to understand if the proposed

product was more appealing to researchers already familiar with microfluidics or to researchers new to microfluidics.



**Figure 2.4.** A/B testing of the landing pages. Representative images of each landing page, highlighting in red the intended market segment: **a.** single-cell encapsulation; **b.** high-throughput screening; **c.** cell encapsulation. (see Appendix for larger version).

The mailing campaigns had similar and above-average open rates, the percentage of people that opened the email over the total sent (31.9% for non-microfluidicists and 34.3% for microfluidicists, market average of 21.33%<sup>47</sup>), but low click-to-open rates, the percentage of people that clicked the link in the email from the ones that opened it (4.9% and 5%, respectively) compared to the market average (10.5%<sup>48</sup>). There was no substantial difference in click rate between market segments in either group (Table 2.5). However, non-microfluidicists demonstrated a clear interest in the solution by replying directly to the email asking for more information/quotes (3.4% and 0.5%, respectively). From these results, the solution was 4x more appealing (8 responses vs 2 responses) to people without previous experience with microfluidics, which is aligned with the intended application of the product as a "starter pack", but the best market segment to target remained inconclusive from this analysis.

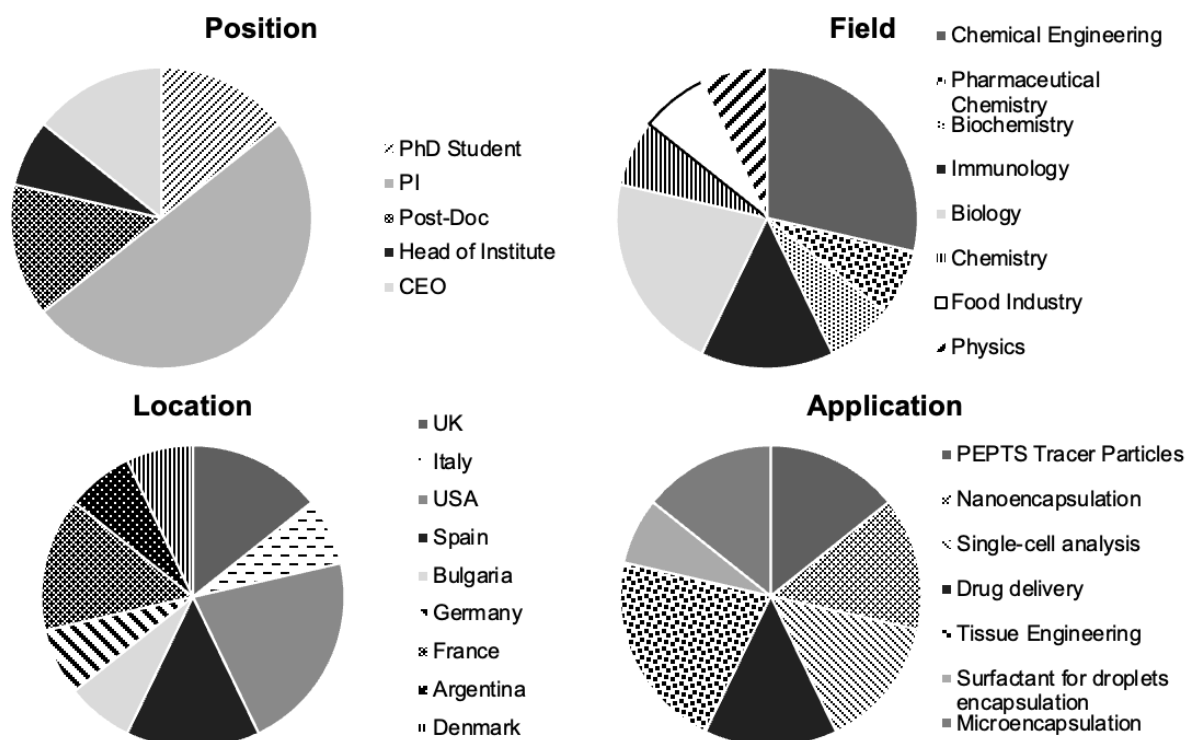
**Table 2.5.** Summary of results of the A/B testing of the webpages.

<b>Landing Page</b>	<b>Open Rate (opened/sent) % (SD)</b>	<b>Click-to-Open Rate (clicked/opened) % (SD)</b>	<b>Number of Direct Responses</b>
<b>Non-microfluidics (average for 235 emails)</b>	<b>31.9</b>	<b>4.9</b>	<b>8 (3.4%)</b>
Single-cell (78 emails)	35.6	4.1	1
Cell (78 emails)	37.7	6.5	4
High-throughput (79 emails)	27.6	3.9	3
<b>Microfluidics (average for 357 emails sent)</b>	<b>34.2</b>	<b>5</b>	<b>2 (0.5%)</b>
Single-cell (119 emails)	27.4	2.7	0
Cell (119 emails)	37.5	5.4	0
High-throughput (119 emails)	39.5	7	2

#### **2.3.2.4.2. Main Limitations and Needs**

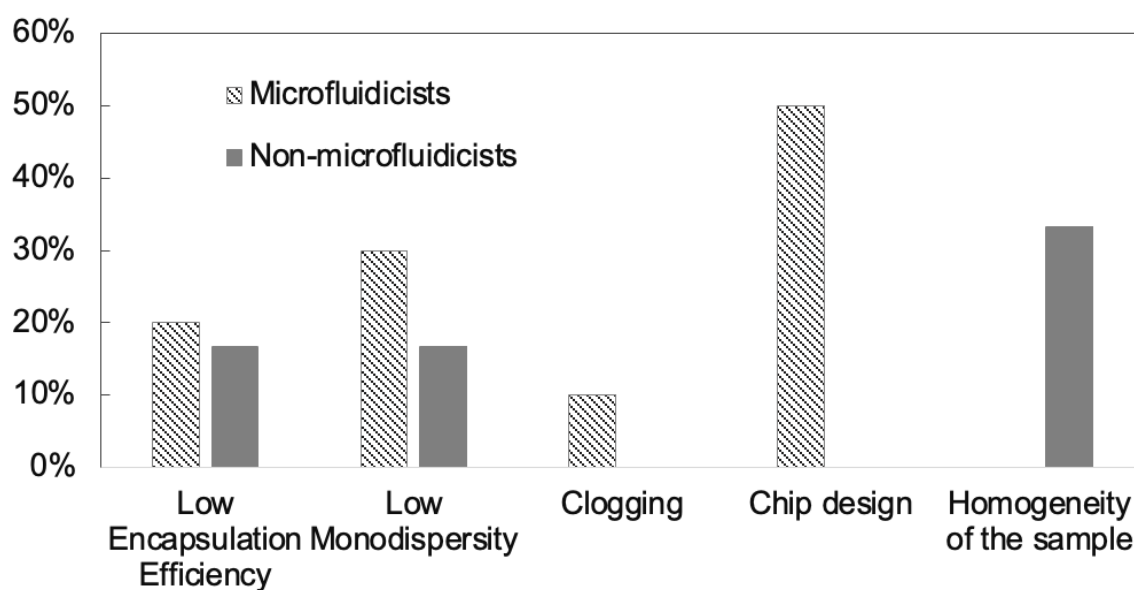
Concurrent with in-person interactions and the insights provided by the financial analysis and A/B testing, 16 in-depth interviews were conducted to better understand the needs of end-users. The interviews covered a range of fields and applications, mainly in the academic sector, as well as different locations, to ensure a broad and unbiased view of the market (Figure 2.5).





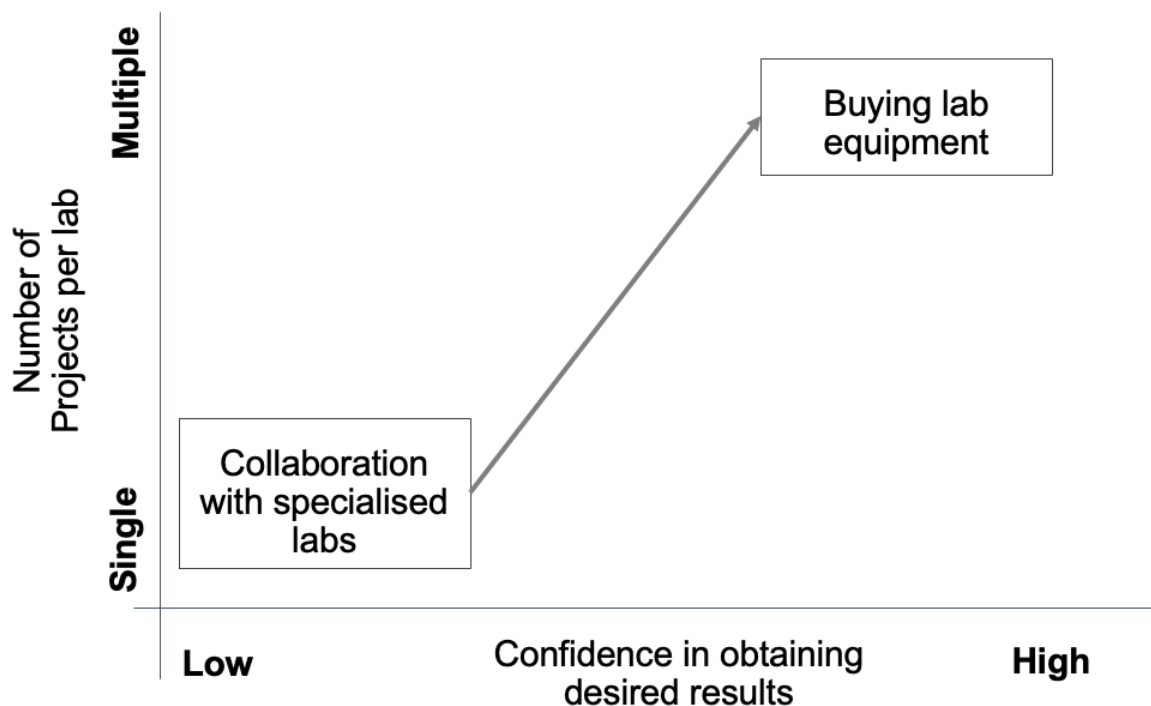
**Figure 2.5.** Profile of interviewees divided by position, location, field and application. Most interviewees were academics, mainly from European institutions. The researchers represented a wide variety of fields and applications.

Following the rationale of the A/B testing, the interviewees were classified as microfluidicists and non-microfluidicists. The challenges reported by each group reflected their familiarity with the technology (Figure 2.6). Microfluidicists reported many challenges related to the chip design and their application (50% of respondents), which were out of the scope of the intended product. Problems with low encapsulation efficiency (20%) and monodispersity of the droplets (30%) and clogging (10%) were also commonly cited. Non-microfluidicists also reported challenges with low encapsulation efficiency (16.7%) and monodispersity (16.7%) of the current methods being employed, and 33% were concerned with the homogeneity of the sample, *i.e.* avoiding the precipitation of cells during the encapsulation process. The product was envisioned to address precisely the low encapsulation and monodispersity problems, while remaining flexible to be used with any chip design. Clogging is related to the size of the channels and the characteristics of the chemical solutions. Although not necessarily related to the components of product, best practices to avoid clogging can be included in the user-guide. The design of the chip is highly related to the application and many are custom-made, designed and fabricated in the lab itself to serve the purpose of the research, not aligned with the company's long term objectives.



**Figure 2.6.** Summary of the challenges reported by microfluidicists and non-microfluidicists during interviews.

The interviews also allowed the understanding of the decision-making process of researchers interested in working with microfluidics. Analysis showed that if the level of confidence in achieving the desired results by the researcher themselves, and the number of projects in their lab involving microfluidics are low, researchers usually collaborate with microfluidics laboratories. If there are multiple projects and the level of confidence is high, then researchers move towards buying a solution such as the one envisioned for this market study (Figure 2.7).



**Figure 2.7.** Decision-making process to work with microfluidics. When the level of confidence and the number of projects using microfluidics is low, researchers tend to collaborate with microfluidic laboratories. If microfluidics gain relevance among the lab's projects and the level of confidence increases, researchers consider buying microfluidic equipment to become autonomous.

The majority of interviewees indicated that, for researchers outside the field of microfluidics, there are two main learning curves that need to be overcome in order to achieve the intended results: learning how to use microfluidics, e.g. understanding exactly what setup they would need, assembling the equipment, understanding the relationships between pressure, flow, and resistance, etc; and learning how to perform encapsulation with microfluidics, e.g. defining the best solutions to use, achieving the right size and dispersity of droplets, avoiding coalescence, etc. Users reported that their level of confidence is closely related to where in this process they judge themselves to be. During the interviews, the need for training and access to detailed material was often cited among non-microfluidicists, highlighting the overall low level of confidence and high barrier to adoption within this public. Some non-microfluidicists mentioned that the setup of the product seemed complex and would rather have something more automated, calling the product an "engineer's approach". Microfluidicists, on the other hand, found the product too simple. They appreciated the flexibility allowed by the "engineer's approach" but would rather have more complex components within the offer. These insights

are in agreement with the behaviour seen on the A/B test, in which microfluidicists demonstrated substantially less interest in the product.

Besides the learning curves, another significant barrier to adoption is changing from a known system, even if not ideal, to a new and unfamiliar one. Researchers demonstrated that they would prefer to continue to work with a suboptimal system with known limitations but reproducible outcomes than to change to a new product with unknown ones, unless the learning curve was decreased by extensive training and support. Interestingly, the interviews clarified that the quantity of cells (single or several cells per droplets) was not a relevant factor, as had been hypothesised for the A/B testing. What mattered most for researchers was the origin of these cells, because the audience that seemed to be more inclined to buy the product was dealing with rare or limited samples, e.g. primary cells (directly derived from patients<sup>49</sup>). Primary cells are used for "single-cell analysis"<sup>50-52</sup> and "tissue engineering"<sup>53,54</sup>, so both keywords could be applicable.

### **2.3.2.4.3. Main Existing Products**

A market study also helps to identify where the biggest added advantages of a product can come from, with regards to what is already available. To review a competitors' landscape, one should consider more than the direct competition, *i.e.* products that perform the same function; because users can employ substitutes to solve the same problem, *i.e.* they can adapt something else to fulfil the same function<sup>55</sup>. When considering droplet microfluidics, the most common substitutes are traditional bulk experiments used to prepare emulsions (Table 2.6). These protocols produce polydisperse emulsions with low encapsulation efficiency<sup>56,57</sup>, but are tried and tested and accessible to most labs. When the limitations of these methods outweigh their advantages, researchers might start considering acquiring a more suitable product. For example, 10x Genomics is one of the most well-known suppliers of biology-oriented droplet applications, focusing on single-cell encapsulation and DNA sequencing. Their instruments are benchtop machines that work in a "black-box" manner; put simply, the researcher inserts the sample, presses a button and receives the readings. The convenience comes with a hefty price of over 100,000€ for some of the equipment, including for consumables that can cost up to 3,000€ per pack, as confirmed by one of the interviewees. Also, researchers have no flexibility and are bound to a single supplier.

At the other end of the spectrum, direct competitors of Elvesys, microfluidics companies such as Fluigent, offer an assembly of instruments, such as pressure-driven flow controllers, flow

sensors, reagents, a microfluidic chip, tubing, caps and connectors and a user-friendly assembly guide. This modular package comprises everything needed to perform encapsulation in droplets and has the advantage of being highly adaptable to different applications. Also, it is much more accessible in terms of price, around 15,000€, and does not bind the researcher, as they can use the microfluidics devices, reagents and other parts of their choice. However, assembling a microfluidics setup for the first time can be daunting. Also, increased flexibility might also mean increased troubleshooting time until the system is fully functional. Although in-person training is offered to some extent in the market, it is usually expensive and on-demand. Alternative ways of filling this gap may offer opportunities for differentiation.

**Table 2.6.** Competitors' and substitutes' landscape

	Competitor	Main Application	Plug-and-Play or modular	Encap. Effic.	Droplet Size ( $\mu\text{m}$ ; CV%)	Virtual Support	In-person Training	Price Range (€)
Elvesys	Product	Soft microencapsulation	Modular	~100%	10 to 80* (<3%)	Yes	Possible	15,000
	Bulk Experiments	Cell encapsulation	-	~30%	Polydisperse	No	-	
Direct	Dolomite	Cell and drug encapsulation	Modular	~100%	12 to 65 (5%)	Yes	Yes	£9,500
	Fluigent	Microparticles, single cell analysis	Modular		60 to 120 (2%)	Yes	-	15,000
Biology-focused	Nisco	Drug release and discovery	Modular	-	20 to 2,000	-		
	Micropore	(Single) Cell encapsulation	Modular	-	10 to 1,000 (11%)	Yes	Yes	
	PreciGenome	Cell encapsulation	Plug-and-Play	up to 90%	60(0.1-5%)	Yes	Yes (for free)	
	Emultech	Pharma/Health	Plug-and-Play with consumables	up to 100%	1-100 (1%)	-	-	

10x Genomic	Health	Plug-and-Play	-	-	Yes		100,000
-------------	--------	---------------	---	---	-----	--	---------

CV = coefficient of variation

\* more sizes available upon request

As mentioned previously, "technology push" approaches are usually employed for disruptive technologies, which is not necessarily the case here. However, innovation is not bound to come from technological advancements, it can arise from the way things are done. A clear example is how Netflix forced Blockbuster out of business by offering the same service in a more convenient manner<sup>58</sup>. This market study showed that biology users willing to venture into microfluidics have a clear demand for substantial support material and in-person training so their perceived level of confidence increases enough to justify the purchase. Thus, the go-to-market strategy to reach the segment with the lowest barrier to entry for this product would be to target researchers that are not familiar with microfluidics and work with limited or rare samples, building a communication plan around how our product can help them make the most of their sample by confining it in minute droplets with a high level of control. This audience could be reached through the "single-cell analysis" and "tissue engineering" keywords explored earlier. Both keywords offer market sizes that offset product development costs and could be jointly employed, as researchers working with primary cells are only a subset of both. "Tissue engineering" is a particularly relevant market segment to consider because it has a high volume of searches on a monthly basis, a large TAM, CAGR and SOM and low auction prices. From this analysis, the product that would best fulfil this audience needs would be a package containing the necessary instruments and reagents to perform biology-related encapsulation, i.e. with biocompatible material, with a detailed and user-friendly assembly and troubleshooting guide, in an offering comprising in-person training and extensive customer support.

### **2.3.3. Determination of technical needs for microenvironment monitoring in microfluidic cell culture**

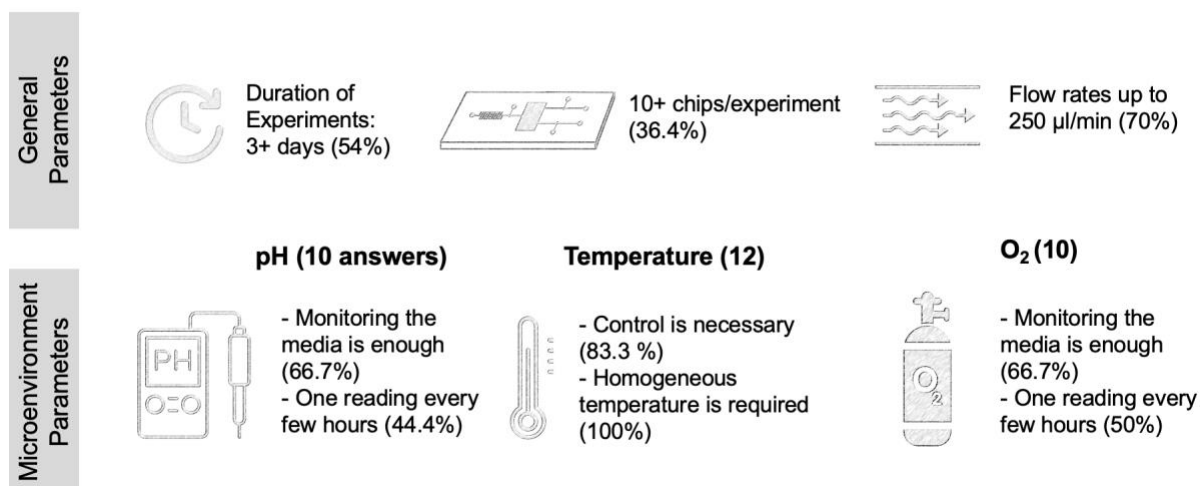
In contrast to the "technology push" approach of the encapsulation-in-droplets product, microenvironment monitoring in microfluidic cell culture was identified as a "market pull", an identified market need that requires technological innovation<sup>4</sup>. In this case, the first step after

identifying a market need is to comprehend the current state-of-the-art, which provides the background for understanding the needs driving the rising interest<sup>59</sup>. Microfluidic cell culture is the process of adding fluid flow to cells in culture, typically on a microfluidic chip, with the aim of more closely mimicking the physiological environment of cells *in vivo*. It adds mechanical stimulus and other physical and chemical dynamics crucially missing in static cell cultures, the models most commonly used for drug testing or metabolism studies<sup>60</sup>. In order to have a better picture of the state-of-the-art as well as to define the parameters which are truly relevant for the large majority of researchers, a questionnaire was devised. To streamline data gathering, microfluidic cell culture was divided into general and microenvironmental parameters. Broadly, these were experimental and microfluidic-related parameters, such as the flow rates used; and microenvironment parameters, such as pH, temperature and O<sub>2</sub>, relevant to cell culture and a broad range of applications. This questionnaire was mainly used during conferences in one-to-one interactions, as the company refrained from mass online distribution to avoid unwanted competitor attention at this early stage.

### **2.3.3.1. Main technical needs**

Questionnaire responses came from KOLs in the field and were sufficient to understand key aspects to guide the following research. It was clear that more than half of respondents were performing long-term microfluidic cell culture (3+ days; 54%), and a substantial number were using as many chips as possible to ensure reproducibility of findings (10+ chips per experiment; 36.4%). 70% of respondents were using flow rates from 10 to 250 µl/min (Figure 2.8), although a substantial number were using very low flow rates (35%, <10 µl/min) (numbers go over 100% because respondents could choose more than one answer for this question). The second part of the questionnaire allowed respondents to choose the parameters that mattered the most in terms of microenvironment monitoring. pH and O<sub>2</sub> were chosen by 10 of the 25 respondents, who indicated that these parameters do not require active control to be kept at acceptable ranges (66.7% for both pH and O<sub>2</sub>), but need to be monitored fairly constantly (44.4% for pH; 50% for O<sub>2</sub>). Temperature, on the other hand, needed to be closely controlled (83.3%) and temperature gradients were not acceptable (100%), according to 12 of the 25 respondents.

## Online Questionnaire – Main Insights (25 answers)

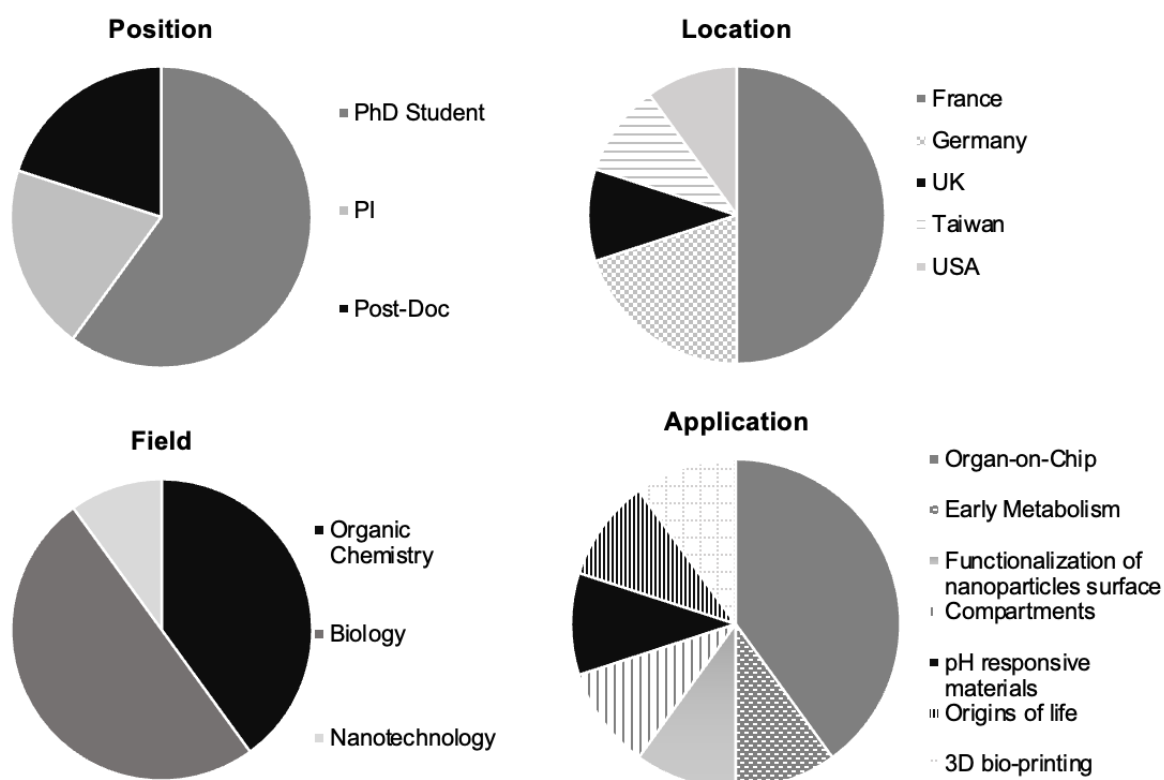


**Figure 2.8.** Results of the questionnaire. The general parameters indicated that microfluidic cell culture is performed for at least 3 days, several chips are used simultaneously and flow rates do not surpass 250 µl/min. The microenvironment parameters indicated that pH and O<sub>2</sub> monitoring every few hours is sufficient, but temperature needs to be tightly controlled.

From the ensemble of the respondents of the questionnaire and researchers contacted at conferences, 10 were willing to be interviewed so data could be refined. The interviewees came from academia, mainly from European institutions. Their fields were organic chemistry, biology and nanotechnology with a wide range of applications (Figure 2.9). The most advanced in terms of microenvironment monitoring were researchers working in the organ-on-chip field. Interestingly, among the cell biologists, most (66%) had developed their own systems to be placed inside the CO<sub>2</sub> incubator for long-term microfluidic cell culture. Only two of interviewees were using commercial systems, one which was also placed inside the incubator and another that reproduced the ideal conditions as a benchtop product. For long-term live cell imaging, most labs were equipped with microscope stage incubators that kept the temperature and CO<sub>2</sub> concentration constant. One of the groups had developed two different systems to be used according to the planned analysis, i.e. one "for the bench" to be left inside the incubator and another, more portable, for when the chips needed to be transported to the microscope. In other cases, chips needed to be disconnected and reconnected to the system, elevating risks of contamination and of introducing air bubbles; besides exposing cells to uncontrolled shear stress caused by manual handling, disrupting cellular microenvironment. Most groups (66%) also had their own chip designs, optimised for their applications and fabricated in-house, and



they cultured several chips at a time to have triplicates of different conditions in parallel (up to 12 chips).



**Figure 2.9.** Profile of interviewees according to position, location, field and application. All interviewees were academic, mainly from European universities and working with organic chemistry, biology or nanotechnology, in a wide range of applications.

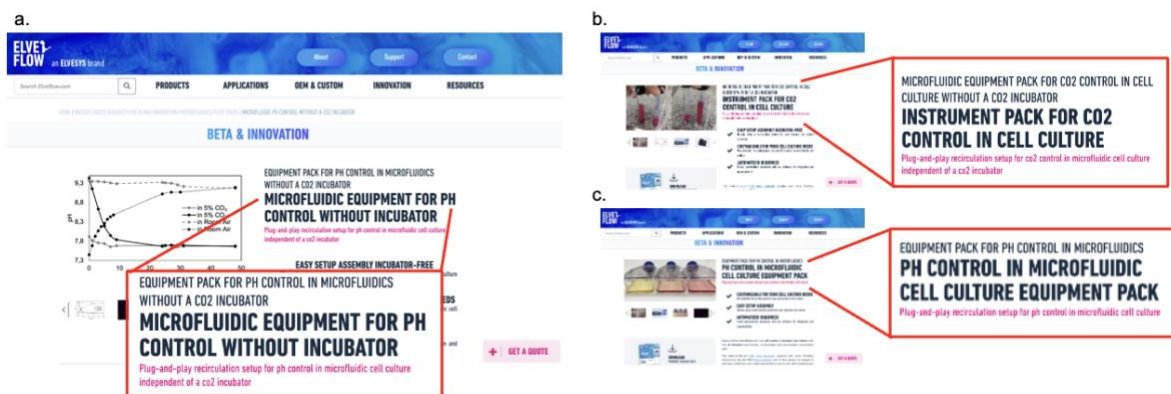
The interviews brought forth several important points to consider when designing a new product. First, researchers heavily rely on the CO<sub>2</sub> incubator to maintain the microenvironment parameters of microfluidic cell culture and they usually assemble their microfluidic systems in-house to be placed inside the incubator without extra monitoring. This workflow posed several challenges to the optimal performance of experiments, other than the risk of contamination and inserting air bubbles previously mentioned. For example, researchers generally did not know or consider the gas permeability of their microfluidic components, apart from the chip, to ensure proper pH buffering of media with CO<sub>2</sub>. Moreover, these in-house assembled systems illustrate one of the main current problems in the field of organ-on-chip: the lack of standardisation. It is understandable that the chip needs to be application-specific in order to promote the best possible features for cell development, however if the entire microfluidic system and parameters are also customised, the results are often not comparable to other systems,

hindering research reproducibility<sup>61</sup>. This difficulty in comparing their results to literature was expressed by respondents.

Existing commercial solutions presented important shortcomings, justifying the limited adoption. For example, the system that was placed inside the incubator could only culture one chip at a time. Also, it required disconnecting and reconnecting the chip to be able to image it on the microscope, risking contamination, air bubbles and shear stress as mentioned. The autonomous system could culture multiple chips in parallel, but it was chip-specific, compromising the flexibility of the researchers and tying them to the brand. Commercial solutions were also used to perform long-term imaging analyses outside the incubator, such as microscope stage top incubators or microscopes with incubation chambers. Main limitations in this case were price, ranging from 10,000€ to 15,000€ for stage top incubators<sup>62</sup> to over 100,000€ for microscope incubation chambers. Furthermore, some of them were not well-adapted to microfluidics<sup>63</sup>.

### **2.3.3.2. Refining technical parameters for off-chip pH monitoring**

To strengthen the findings of the questionnaire and interviews, it was necessary to complement the information with quantitative data without risking exposing the project to competitors. Thus, the microfluidic cell culture parameters were decoupled to be researched individually, with pH becoming the main focus of the following data gathering initiatives. Similar to the "encapsulation-in-droplets" market study, an A/B test, called "pilot packs" on the website, was performed for pH in cell culture. The chosen keywords were "pH control without incubator"; "CO<sub>2</sub> control without incubator"; and "pH control for microfluidic cell culture" as a control (Figure 2.10). In a "market pull" strategy, the market starts being much better defined than in "technology push" approaches, since a demand was identified from a particular group of people<sup>59</sup>. This was reinforced by the interviews that showed the organ-on-chip field as the most likely to require an incremental innovation. Thus, instead of trying to identify the niche and the audience, as it was the case for the previous market study, the goal of this A/B testing was to understand if researchers working with cell culture placed more value on pH or CO<sub>2</sub> as a parameter, and if they were interested in solutions that were independent of the CO<sub>2</sub> incubator. The choice of the word "control" instead of "monitoring" as suggested by the questionnaire was to avoid conflict with other webpages on the company's website. The proposed solutions on the webpages showed schematics with an off-chip sensing solution.



**Figure 2.10.** A/B testing of pH in microfluidic cell culture. Three similar webpages were created to test if researchers valued pH more than CO<sub>2</sub> as a cell culture parameter and if they were interested in being independent of the CO<sub>2</sub> incubator for their experiments.

There were two streams of data coming from the pilot packs: the page views from people actively searching online for similar keywords, and a mailing campaign directed to 436 researchers in the field of organ-on-chip (Table 2.7). The keyword "pH" was more prevalent regardless of the source, with higher number of page views (51 and 40 against 27 for CO<sub>2</sub>) or click rate on the emails (10% and 16% against 6% for CO<sub>2</sub>). This was corroborated by the longer average time on page (4:18 and 6:14 min against 0:35 min for CO<sub>2</sub>), the direct replies to the emails (1.3% and 2%, against 0 replies for CO<sub>2</sub>) and the higher bounce rate for the CO<sub>2</sub> page (93.75%), i.e. percentage of users that left the website after visiting only that page. The "pH without incubator" page caused less visitors to bounce from the website than the "pH control cell culture" (69.44% against 82.35%), showing that pH control without the incubator elicited interest from researchers. Page exits, i.e. percentage of users that left the website through that particular page after visiting other pages from the website, was similar for both pH pages (76.47% and 77.5%, respectively) and lower for CO<sub>2</sub> (62.96%). This is in accordance with the bounce rates, since a higher bounce rate means that visitors were less willing to explore the website because they did not find the content relevant from the page they started the visit<sup>64</sup>. On a side note, the open rates were above average compared to market standards<sup>47</sup> but were not used to differentiate respondents because they are linked to the subject of the email, which was the same for the three pilot packs.

These results highlight the fact that researchers think in terms of pH when considering cell culture parameters, although it is an indirect measure of the concentration of CO<sub>2</sub><sup>65</sup>. Thus, when designing a product, having a pH sensor instead of a CO<sub>2</sub> sensor would more appealing

to them. When considering the second hypothesis, of the willingness of being independent of the CO<sub>2</sub> incubator, the "pH control cell culture" group demonstrated more interest than the other two, confirming what was indicated by the interviews. The click rate of the emails containing pH control without a CO<sub>2</sub> incubator was smaller when compared with only pH control (10% to 16%). The same was true for direct replies, although the difference was smaller (1.3 % to 2%). This behaviour is consistent with an evolving field in which some researchers start to be limited by the tried and tested and want to move towards better fitted instruments while the majority has not reached this stage yet.

**Table 2.7.** Results of pilot packs on the website and of the email campaign

<b>Pilot Pack Pages</b>	<b>pH without incubator</b>	<b>CO<sub>2</sub> control cell culture</b>	<b>pH control cell culture</b>
Pageviews	51	27	40
Unique pageviews	45	23	38
Avg. time on page (min)	4:18	0:35	6:14
Bounce rate (%)	69.44	93.75	82.35
Page exit (%)	76.47	62.96	77.5
<b>Email Campaign</b>	<b>pH without incubator</b>	<b>CO<sub>2</sub> control cell culture</b>	<b>pH control cell culture</b>
# of Recipients	145	145	146
Open Rate (%)	31%	41%	38%
Click Rate (%)	10%	6%	16%
Direct Reply (%)	1.3%	0	2%

### 2.3.3.3. Main existing solutions

A closer look into microfluidic pH monitoring for cell culture depicted several commercially available solutions in a variety of prices (Table 2.8), giving this particular parameter a potential market of its own. pH can be detected electrochemically, by the potential difference of a measuring and a reference electrode<sup>66</sup>, or optically, by detecting fluorescence of dyes in the sensing material or in the solution<sup>67</sup>. Both approaches have limitations, for example, electrochemical sensors require a reference electrode and frequent calibration<sup>68</sup>, while optical

sensors forgo the reference electrode and usually come pre-calibrated, but have limited pH ranges<sup>69</sup> and are susceptible to photobleaching<sup>67</sup>. The use of flow-through cells, placed inline in the microfluidic circuit, allows the monitoring of the microenvironment of the cell culture regardless of the chip design and without the need to integrate the sensor into the chip, considerably simplifying the task<sup>70</sup>. However, most of the commercially-available flow cells for inline measurement have dead volumes that are too large for microfluidics.

Large dead volumes result in high flow rates (over 500  $\mu\text{l}/\text{min}$ ) to ensure that the liquid is exchanged; this way, the measurements are representative of the system and not of a small portion of the fluid that was trapped inside the flow cell. As seen from the questionnaire, researchers working with microfluidic cell culture employ lower flow rates (up to 250  $\mu\text{l}/\text{min}$ ). The only two that present small enough dead volumes that would work with microfluidics, BVT and Sensorex, offer electrochemical sensors, which require calibration. Performing calibration at the start of each experiment can seriously compromise the sterility of the system, as most calibrating solutions are not sterile, a crucial factor for any biological research. This gap has forced researchers to develop their own solutions, contributing for the lack of standardisation and reproducibility mentioned previously and providing a clear market need. Moreover, the availability of "Original Equipment Manufacturer" (OEM) versions is important when considering integrating a pH sensor to the other parameters of the microfluidic cell culture and would weigh on the selection of a supplier in the long-term.

**Table 2.8.** The landscape of competitors in the microfluidic pH monitoring market

Benchmark	Type of Measurement	pH range	OEM	Flow Cell Dead Volume	Price (approx.) (€)
Presens	Optical	5.5 - 8.5 (plugs)	Yes	Large (+500 $\mu\text{l}$ )	4,000
Pyroscience	Optical	5-7; 4-6; 7-9	Yes	Large (+500 $\mu\text{l}$ )	3,000
Microsens	Electrochemical	0-14	Yes	N/A	1,000
IST	Electrochemical	0-14	Yes	N/A	2,000
BVT	Electrochemical	0-14	Yes	Small (5 $\mu\text{l}$ )	1,000
Unisense	Electrochemical	0-14	No	Large (+500 $\mu\text{l}$ )	9,000
Sensorex	Electrochemical	0-14	No	Small (50 $\mu\text{l}$ )	750

### 2.3.3.4. Financial Analysis for Risk Assessment

Similar to the "encapsulation-in-droplets" market study, assumptions were made in order to analyse the potential return on investment of a standalone microfluidic pH monitoring solution (Table 2.9). The chosen price is an average of the products on the market, and the remaining assumptions are the same as for the previous financial analysis in Section 2.3.2.2. As mentioned previously, in a "market pull" strategy, the market starts better defined than in a "technology push"<sup>59</sup>. Nevertheless it is always beneficial to narrow the audience down, so marketing efforts are better employed. Thus, the financial analysis aimed to understand which keywords would be more interesting to pursue for online marketing efforts, as the chosen keywords were a reflection of the actual publications, filtered by their microfluidics relevance and the company's market penetration (Table 2.10).

**Table 2.9.** Assumptions for financial analysis of different market segments in pH monitoring for microfluidic cell culture

Assumptions	
Price (Euro)	3,000 €
Elveflow Market penetration for flow control in microfluidics	30%
Elveflow Market penetration in microfluidics	10%
Paper production per PI/year	2

**Table 2.10.** Financial analysis of different market segments in pH monitoring for microfluidic cell culture

Field/Keyword	pH cell culture	pH cell perfusion	pH microfluidics cell culture	pH dynamic cell culture	pH organ on chip
Year	2021	2021	2021	2021	2021
Number of papers Google Scholar	59,000	25,600	7,560	30,700	10,200
Number of papers per lab	2	2	2	2	2
Total Number of potential clients	29,500	12,800	3,780	15,350	5,100

Microfluidics relevance (%)	11	11	11	14	41
Number of potential clients that might use microfluidics	3,225	1,410	413	2,170	2,115
Elveflow penetration rate in microfluidics (%)	10	10	10	10	10
Number of potential clients that might buy from us	322.5	141	41.3	217	211.5
Price (€)	3,000	3,000	3,000	3,000	3,000
Market Size (€)	967,500	423,000	123,971	651,000	634,500

The most promising keyword were "pH cell culture" and "pH organ on chip". The former has the largest SOM (967,500€), backed by a large TAM (9.18€) and a promising CAGR (10.6%). The latter also has a sizeable SOM (634,500€) with a large TAMs (52.75B€), impressive CAGR of 37.6% (Table 2.11). "pH dynamic cell culture" also has a large SOM, however growth rate and, especially, the TAM are considerably smaller (9.4% and 611M€), indicating a potentially larger risk and lower returns.

**Table 2.11.** Market Sizing for different market segments in pH monitoring of microfluidic cell cultures

Field/Keyword	pH cell culture	pH cell perfusion	pH microfluidics cell culture	pH dynamic cell culture	pH organ on chip
<b>TAM (Total Addressable Market); 2021* (€)</b>	9.18B <sup>71</sup>	1.17B <sup>72</sup>	1.36B (2020) <sup>73</sup>	611M <sup>74</sup>	52.75B <sup>75</sup>
<b>Compound annual growth rate (CAGR); forecasted (%)</b>	10.6	5.2	6.9	9.4	37.6
<b>SAM (Serviceable Market) (€)</b>	9,675,000	4,230,000	1,239,712	6,510,000	6,345,000
<b>SOM (Serviceable Obtainable Market) (€)</b>	967,500	423,000	123,971	651,000	634,500

\*Currency converted to Euros (1 USD = 0.977279 EUR, 05.08.2022)

The keywords used for the financial analysis were specified by "pH" to provide a more realistic analysis of the potential return on investment for a microenvironment monitoring solution.

However, in terms of marketing, the broader keywords (without "pH") give a better sense of the auction price and the reach of the advertisement (Table 2.12). All keywords ranged from approximately 1 to 7€, except "cell culture" that was considerably cheaper (0.16 to 2.48€).

**Table 2.12. Paid advertisement price ranges for selected keywords**

Keyword	Average Number of monthly searches	Competition	Auction price for top of the page (minimum to maximum range)
Cell culture	14,800	Low	0.16 - 2.48€
Cell perfusion	50	Low	1.24 - 6.86€
Microfluidic cell culture	140	Low	1.50 - 5.73€
Dynamic cell culture	20	Low	-
Organ on chip	4,400	Low	0.95 - 5.90€

Combining all explored data points indicated that the most promising go-to-market strategy for a product focused on microenvironment monitoring for microfluidic cell culture should target researchers working with organ-on-chip who require extended periods of time outside the CO<sub>2</sub> incubator and who do not yet have a microscope incubator chamber. For a "market push" strategy, most of the product investment is still upcoming, so considering the feasibility of the product is much more acute. The estimated yearly cost for product development was approximately 100,000€. All analysed segments provide market sizes larger than the estimated cost. "pH microfluidics cell culture" was the lowest one (123,971€), thus it should not be used in a marketing strategy in isolation, as it might not offset the development costs. Given that auction prices are in similar ranges, the chosen keywords can be used in a combined strategy to reach the market. The product technical specifications should satisfy the needs of researchers that culture cells in microfluidic systems outside the CO<sub>2</sub> incubator for extended periods of time, such as constant temperature and several chips in parallel. In particular, it should provide ways to monitor the microenvironment of the cell culture, such as the pH, that are compatible with microfluidics, i.e., flow cells that have small dead volumes and allow low flow rates. Fulfilling these needs will allow researchers to reach another level of resolution, contributing to the evolution of the OoC field.

## 2.4. Conclusions and Outlook



The extensive market studies of the two microfluidic tools proposed for biological applications have allowed answering the questions posed at the introduction, mainly the size of the markets, existing solutions, current user needs and the perceived value of microfluidics to the target audiences. In the case of the encapsulation-in-droplets study, which consisted of a "technology push" strategy, biologists saw value in microfluidics as a tool to gather more in-depth information of their biological samples. Whether researchers are willing to buy equipment or partner with a microfluidics laboratory depends on their level of confidence in obtaining reproducible results. The competition can be divided into microfluidic companies with modular solutions for biology and biology companies with microfluidic-adapted tools. The main limitations of the former is the "engineering approach" that renders the products intimidating and the learning curves too high. For the latter, the hefty price decreases accessibility. The competitors' analysis highlighted that to differentiate the product from existing solutions, the competitive advantage should come from the offering instead of relying solely on the technology, by combining microfluidic equipment with extensive customer support and in-person training. The market sizes range from 200,000 € to 3,000,000 € in potential yearly revenues depending on the chosen go-to-market strategy. Insights from the interactions with KOLs and potential end-users strongly indicate that the target audience should be biologists dealing with rare or limited samples.

For the "market pull" strategy of the microenvironment monitoring for microfluidic cell culture, there was indeed a demonstrated interest in better monitoring the parameters without integrating sensors into the chip. Considering the ensemble of the parameters or pH in isolation, several solutions were identified. Most researchers developed their own systems that would often make use of existing equipment, such as the CO<sub>2</sub> incubator to keep microenvironmental parameters in check. However, this approach brought with it several workflow limitations, such as disconnecting and reconnecting the chip through the experiment. Considering the entire system, commercially available solutions were expensive and often not well-adapted to microfluidics. Moreover, some were chip-specific or allowed the handling of a single chip at a time. As a fast evolving area of research, this plethora of solutions also poses problems for the standardisation of the field, and consequently, affects the reproducibility of results across research groups. As expected of a "market pull" strategy, there is a clear demand for products that can address these limitations, with market sizes of ranging from 120,000 to 900,000 €, when considering the monitoring of pH alone. The recommended go-to-market strategy for the ensemble of the microenvironment parameters is to focus on researchers culturing organ-on-chips that require extended periods outside the CO<sub>2</sub> incubator and do not possess microscope incubation chambers. With the impressive forecasted CAGR of 37.6% for organ-on-chip field, it is an opportunity worth pursuing.

## 2.5. References

1. Veugelers, R. *et al.* The Impact of Horizon 2020 on Innovation in Europe. *Intereconomics* **50**, 4–30 (2015).
2. Čučković, N. & Vučković, V. EU R&D funding as a way of incentivizing innovation of SMEs: A review of impacts. *Croat. Econ. Surv.* **20**, 97–127 (2019).
3. McGivern, Y. The practice of market research : an introduction. 548 (2009).
4. Brem, A. & Voigt, K. I. Integration of market pull and technology push in the corporate front end and innovation management-Insights from the German software industry. *Technovation* **29**, 351–367 (2009).
5. D'Angelo, C. A. & Abramo, G. Publication rates in 192 research fields of the hard sciences. *Proc. ISSI 2015 Istanbul 15th Int. Soc. Sci. Inf. Conf.* 909–919 (2015).
6. Liu, Z., Fontana, F., Python, A., Hirvonen, J. T. & Santos, H. A. Microfluidics for Production of Particles: Mechanism, Methodology, and Applications. *Small* **16**, 1–24 (2020).
7. Gao, Y., Chang, M. W., Ahmad, Z. & Li, J. S. Magnetic-responsive microparticles with customized porosity for drug delivery. *RSC Adv.* **6**, 88157–88167 (2016).
8. Sáez-Orviz, S., Camilleri, P., Marcet, I., Rendueles, M. & Díaz, M. Microencapsulation of calcium lactobionate for protection from microorganisms in a solid phase food. *Biochem. Eng. J.* **150**, 107281 (2019).
9. Perinelli, D. R., Palmieri, G. F., Cespi, M. & Bonacucina, G. Encapsulation of Flavours and Fragrances into Polymeric Capsules and Cyclodextrins Inclusion Complexes: An Update. *Molecules* **25**, (2020).
10. Vinner, G. K., Richards, K., Leppanen, M., Sagona, A. P. & Malik, D. J. Microencapsulation of enteric bacteriophages in a pH-Responsive solid oral dosage formulation using a scalable membrane emulsification process. *Pharmaceutics* **11**, (2019).
11. Schoubben, A., Blasi, P., Giovagnoli, S., Ricci, M. & Rossi, C. Simple and scalable method for peptide inhalable powder production. *Eur. J. Pharm. Sci.* **39**, 53–58 (2010).
12. Chen, R. Y. Flow in the Entrance Region at Low Reynolds Numbers. *J. Fluids Eng.* **95**, 153–158 (1973).
13. Moon, H. S. *et al.* Inertial-ordering-assisted droplet microfluidics for high-throughput single-cell RNA-sequencing. *Lab Chip* **18**, 775–784 (2018).
14. Huebner, A. *et al.* Quantitative detection of protein expression in single cells using droplet microfluidics. *Chem. Commun.* **0**, 1218–1220 (2007).

15. Segaliny, A. I. *et al.* Functional TCR T cell screening using single-cell droplet microfluidics. *Lab Chip* **18**, 3733–3749 (2018).
16. Zhang, H., Liu, Y., Wang, J., Shao, C. & Zhao, Y. Tofu-inspired microcarriers from droplet microfluidics for drug delivery. *Sci. China Chem. 2018 621* **62**, 87–94 (2018).
17. Liu, Y. *et al.* Microfluidic generation of egg-derived protein microcarriers for 3D cell culture and drug delivery. *Sci. Bull.* **62**, 1283–1290 (2017).
18. Pessi, J. *et al.* Microfluidics-assisted engineering of polymeric microcapsules with high encapsulation efficiency for protein drug delivery. *Int. J. Pharm.* **472**, 82–87 (2014).
19. Shao, C., Liu, Y., Chi, J., Ye, F. & Zhao, Y. Hierarchically Inverse Opal Porous Scaffolds from Droplet Microfluidics for Biomimetic 3D Cell Co-Culture. *Engineering* **7**, 1778–1785 (2021).
20. Wang, Y., Zhao, L., Tian, C., Ma, C. & Wang, J. Geometrically controlled preparation of various cell aggregates by droplet-based microfluidics. *Anal. Methods* **7**, 10040–10051 (2015).
21. Siltanen, C. *et al.* Microfluidic fabrication of bioactive microgels for rapid formation and enhanced differentiation of stem cell spheroids. *Acta Biomater.* **34**, 125–132 (2016).
22. Courtney, M. *et al.* Droplet Microfluidic System with On-Demand Trapping and Releasing of Droplet for Drug Screening Applications. *Anal. Chem.* **89**, 910–915 (2017).
23. Au, S. H., Chamberlain, M. D., Mahesh, S., Sefton, M. V. & Wheeler, A. R. Hepatic organoids for microfluidic drug screening. *Lab Chip* **14**, 3290–3299 (2014).
24. Maurya, R. *et al.* Microfluidics device for drug discovery, screening and delivery. *Prog. Mol. Biol. Transl. Sci.* **187**, 335–346 (2021).
25. Fallah-Araghi, A., Baret, J. C., Ryckelynck, M. & Griffiths, A. D. A completely in vitro ultrahigh-throughput droplet-based microfluidic screening system for protein engineering and directed evolution. *Lab Chip* **12**, 882–891 (2012).
26. Sjostrom, S. L. *et al.* High-throughput screening for industrial enzyme production hosts by droplet microfluidics. *Lab Chip* **14**, 806–813 (2014).
27. Holstein, J. M., Gylstorff, C. & Hollfelder, F. Cell-free Directed Evolution of a Protease in Microdroplets at Ultrahigh Throughput. *ACS Synth. Biol.* **10**, 252–257 (2021).
28. Zinchenko, A. *et al.* One in a million: Flow cytometric sorting of single cell-lysate assays in monodisperse picolitre double emulsion droplets for directed evolution. *Anal. Chem.* **86**, 2526–2533 (2014).
29. Byun, C. K., Abi-Samra, K., Cho, Y. K. & Takayama, S. Pumps for microfluidic cell culture. *Electrophoresis* **35**, 245–257 (2014).
30. Denault, J.-F. The Handbook of Marketing Strategy for Life Sciences Companies : Formulating the Roadmap You Need to Navigate the Market. *Handb. Mark. Strateg. Life Sci. Co.* (2018). doi:10.4324/9781351235303

31. The VC Factory. TAM SAM SOM Explained From The Investor's Point Of View » The VC Factory. Available at: <https://thevcfactory.com/tam-sam-som/>. (Accessed: 2nd August 2022)
32. York, J. M. Archives of Business Administration and Management Putting Lean Startup into Perspective: A Novel Approach for Discovering and Developing a Successful Business Model. *Arch Bus Adm Manag ABAM-104* **2**, 3–5 (2018).
33. Gaynor, M. & Haas-Wilson, D. Change, Consolidation, and Competition in Health Care Markets Changing Health Care Markets. *JEP ja28 J. Econ. Perspect.* **13**, 141–164 (1999).
34. Grand View Research. Single-cell Analysis Market. (2022). Available at: <https://www.grandviewresearch.com/industry-analysis/single-cell-analysis-market>. (Accessed: 16th July 2022)
35. Globe NewsWire. Global Tissue Engineering Market 2022. *Market Reports World* (2022). Available at: <https://www.globenewswire.com/en/news-release/2022/01/19/2369074/0/en/Global-Tissue-Engineering-Market-2022-Size-Share-Growth-Rate-Latest-Trends-Development-Plans-New-Opportunities-CAGR-of-18-5-Business-Challenges-Key-Players-Revenue-and-Forecast-Res.html>. (Accessed: 16th July 2022)
36. Business Wire. Global Drug Delivery Market Research Report (2021 to 2027). Available at: <https://www.businesswire.com/news/home/20220221005371/en/Global-Drug-Delivery-Market-Research-Report-2021-to-2027---Featuring-3M-AbbVie-and-Genmab-Among-Others---ResearchAndMarkets.com>. (Accessed: 16th July 2022)
37. Business Wire. Global Drug Screening Market Report 2022: Analytical Instruments Segment to Dominate the Drug Screening Products Market 2021-2026. (2022). Available at: <https://www.businesswire.com/news/home/20220221005153/en/Global-Drug-Screening-Market-Report-2022-Analytical-Instruments-Segment-to-Dominate-the-Drug-Screening-Products-Market-2021-2026---ResearchAndMarkets.com>. (Accessed: 16th July 2022)
38. MarketWatch. Drug Discovery Market is set to experience a significant growth rate 2021-2030. Available at: <https://www.marketwatch.com/press-release/drug-discovery-market-is-set-to-experience-a-significant-growth-rate-2021-2030-2022-04-19>. (Accessed: 16th July 2022)
39. Globe NewsWire. Global Protein Engineering market. (2022). Available at: <https://www.globenewswire.com/en/news-release/2022/04/07/2418621/0/en/Global-Protein-Engineering-market-is-projected-to-reach-at-a-market-value-of-US-9-785-6-Million-by-2031-Visiongain-Research-Inc.html>. (Accessed: 16th July 2022)
40. Taylor, Z. W. & Bicak, I. Buying search, buying students: how elite U.S. institutions

- employ paid search to practice academic capitalism online. *J. Mark. High. Educ.* **30**, 271–296 (2020).
41. Edelman, B. *et al.* Internet Advertising and the Generalized Second-Price Auction: Selling Billions of Dollars Worth of Keywords. *Am. Econ. Rev.* **97**, 242–259 (2007).
  42. Symitsi, E., Markellos, R. N. & Mantrala, M. K. Keyword portfolio optimization in paid search advertising. *Eur. J. Oper. Res.* **303**, 767–778 (2022).
  43. Maurya, A. *Running Lean - Iterate from Plan A to a Plan that works.* (O'Reilly Media, 2012).
  44. Demirci, U. & Montesano, G. Cell encapsulating droplet vitrification. *Lab Chip* **7**, 1428–1433 (2007).
  45. Nicodemus, G. D. & Bryant, S. J. Cell Encapsulation in Biodegradable Hydrogels for Tissue Engineering Applications. <https://home.liebertpub.com/teb> **14**, 149–165 (2008).
  46. Kang, A. R., Park, J. S., Ju, J., Jeong, G. S. & Lee, S. H. Cell encapsulation via microtechnologies. *Biomaterials* **35**, 2651–2663 (2014).
  47. Mailchimp. Comparaisons et statistiques de marketing par e-mail par secteur. Available at: <https://mailchimp.com/fr/resources/email-marketing-benchmarks/>. (Accessed: 17th July 2022)
  48. Campaign Monitor. What are good open rates, CTRs, & CTORs for email campaigns? (2021). Available at: <https://www.campaignmonitor.com/resources/knowledge-base/what-are-good-email-metrics/#:~:text=In 2021%2C the average click,average between 14-17%25.> (Accessed: 3rd August 2022)
  49. Berthier, E., Surfus, J., Verbsky, J., Huttenlocher, A. & Beebe, D. An arrayed high-content chemotaxis assay for patient diagnosis. *Integr. Biol.* **2**, 630–638 (2010).
  50. Bradley, T., Ferrari, G., Haynes, B. F., Margolis, D. M. & Browne, E. P. Single-Cell Analysis of Quiescent HIV Infection Reveals Host Transcriptional Profiles that Regulate Proviral Latency. *Cell Rep.* **25**, 107-117.e3 (2018).
  51. Lindström, S. & Andersson-Svahn, H. Overview of single-cell analyses: microdevices and applications. *Lab Chip* **10**, 3363–3372 (2010).
  52. Love, K. R., Bagh, S., Choi, J. & Love, J. C. Microtools for single-cell analysis in biopharmaceutical development and manufacturing. *Trends Biotechnol.* **31**, 280–286 (2013).
  53. Auxenfans, C. *et al.* Porous matrix and primary-cell culture: a shared concept for skin and cornea tissue engineering. *Pathol. Biol. (Paris)*. **57**, 290–298 (2008).
  54. Palakkan, A. A., Hay, D. C., Pr, A. K., Tv, K. & Ross, J. A. Liver tissue engineering and cell sources: issues and challenges. *Liver Int.* **33**, 666–676 (2013).
  55. Nobel., C. Clay Christensen's Milkshake Marketing - HBS Working Knowledge. *Harvard Business Review* (2011). Available at: <https://hbswk.hbs.edu/item/clay-christensens->

- milkshake-marketing. (Accessed: 6th August 2022)
56. Lu, W. C. & Ellington, A. D. In vitro selection of proteins via emulsion compartments. *Methods* **60**, 75–80 (2013).
  57. Lim, S. W. & Abate, A. R. Ultrahigh-throughput sorting of microfluidic drops with flow cytometry. *Lab Chip* **13**, 4563–4572 (2013).
  58. Shih, W. & Kaufman, S. Netflix in 2011. *Harvard Bus. Sch. Case* **615-0**, (2014).
  59. Walsh, S. T., Kirchhoff, B. A. & Newbert, S. Differentiating market strategies for disruptive technologies. *IEEE Trans. Eng. Manag.* **49**, 341–351 (2002).
  60. Coluccio, M. L. *et al.* Microfluidic platforms for cell cultures and investigations. *Microelectron. Eng.* **208**, 14–28 (2019).
  61. Mastrangeli, M. & van den Eijnden-van Raaij, J. Organs-on-chip: The way forward. *Stem Cell Reports* **16**, 2037–2043 (2021).
  62. Pauly, N., Madigan, T., Koesser, K., Meuler, B. & Campagnola, P. *Microscope Cell Culture Incubator*. (2020).
  63. Charwat, V. *et al.* Potential and limitations of microscopy and Raman spectroscopy for live-cell analysis of 3D cell cultures. *J. Biotechnol.* **205**, 70–81 (2015).
  64. Google Analytics. Bounce rate. Available at: <https://support.google.com/analytics/answer/1009409?hl=en>. (Accessed: 7th August 2022)
  65. Salis, A. & Monduzzi, M. Not only pH. Specific buffer effects in biological systems. *Curr. Opin. Colloid Interface Sci.* **23**, 1–9 (2016).
  66. Ghoneim, M. T. *et al.* Recent Progress in Electrochemical pH-Sensing Materials and Configurations for Biomedical Applications. *Chemical Reviews* **119**, 5248–5297 (2019).
  67. Wencel, D., Abel, T. & Mcdonagh, C. Optical Chemical pH Sensors. *Anal. Chem.* **86**, 15–29 (2014).
  68. Privett, B. J., Shin, J. H. & Schoenfisch, M. H. Electrochemical Sensors. *Anal. Chem.* **80**, 4 (2008).
  69. Lin, J. Recent development and applications of optical and fiber-optic pH sensors. *TrAC - Trends Anal. Chem.* **19**, 541–552 (2000).
  70. Fuchs, S. *et al.* In-line analysis of organ-on-chip systems with sensors: Integration, fabrication, challenges, and potential. *ACS Biomater. Sci. Eng.* **7**, 2926–2948 (2021).
  71. Globe NewsWire. Global Cell Culture Consumables and Equipment Market (2021 to 2030). (2022). Available at: <https://www.globenewswire.com/en/news-release/2021/11/10/2331270/28124/en/Global-Cell-Culture-Consumables-and-Equipment-Market-2021-to-2030-Featuring-Becton-Dickinson-Corning-and-Eppendorf-Among-Others.html>. (Accessed: 16th July 2022)
  72. Biospace. Perfusion System Market Size to Worth Around USD 1.89 Billion by 2030.

- Available at: <https://www.biospace.com/article/perfusion-system-market-size-to-worth-around-usd-1-89-billion-by-2030/>. (Accessed: 16th July 2022)
73. Grand View Research. Global Single-cell Analysis Market Size Report, 2021-2028. Available at: <https://www.grandviewresearch.com/industry-analysis/single-cell-analysis-market>. (Accessed: 16th July 2022)
74. Research and Markets. Global Perfusion Bioreactor Market Research Report 2022 (Status and Outlook). (2022). Available at: <https://www.researchandmarkets.com/reports/5620594/global-perfusion-bioreactor-market-research>. (Accessed: 16th July 2022)
75. Globe NewsWire. Global Organ On Chip Market Estimated to Garner Noteworthy. Available at: <https://www.globenewswire.com/en/news-release/2021/07/19/2264909/0/en/Global-Organ-On-Chip-Market-Estimated-to-Garner-Noteworthy-Revenue-of-6-97-654-30-Million-by-2028-at-a-CAGR-of-37-60-from-2021-2028-Exclusive-Report-180-Pages-By-Research-Dive.html>. (Accessed: 16th July 2022)

# CHAPTER 3.

## MICROFLUIDIC-BASED MICROCOMPARTMENTS: PRODUCTION AND ENCAPSULATION

“If patience was not so easily tested, then it would hardly be a virtue. . .”

— Amor Towles, *A Gentleman in Moscow*

### ABSTRACT

---

The field of microfluidic production of complex compartments is recent, without a well-established protocol for the production of giant unilamellar vesicles (GUVs), or other hierarchical structures such as multivesicular vesicles (MVs). In microfluidics, these compartments are usually templated from double emulsions (DEs), in which the intermediate oil layer is eliminated, leaving behind the lipid bilayer. Market insights have shown that biologists are interested in using microfluidics as a tool to advance their research, but most methods for microfluidic microcompartment production and encapsulation require specialised equipment and know-how, rendering it inaccessible for non-specialists. This Chapter aims to produce microcompartments with varying levels of complexity to encapsulate compounds of interest in non-specialist settings, i.e. without the need of a cleanroom and using standard photolithography and soft lithography techniques. Single and double emulsions encapsulating various compounds of interest were successfully produced by adapting microfluidic devices to standard laboratory techniques. Design 2 was the best in producing stable double emulsions, allowing for the encapsulation of different compounds of interest, such as calcein and phenol red.

---



## *Contributions*

---

Part of this chapter has been published

C. B. Giuliano, N. Cvjetan, J. Ayache, P. Walde, *ChemSystemsChem* 2021, 3, e2000049.

The experimental work was performed by Camila Betterelli Giuliano. Audrey Nsamela and Jesús Manuel Antúnez Domínguez (Elvesys) developed the Python script. Writing of this chapter was done by Camila Betterelli Giuliano. Revision was done by Camila Betterelli Giuliano, Dr Lisa Muiznieks (Elvesys) and Prof. Joseph Moran (University of Strasbourg).

---

## *Chapter Specific Acknowledgements*

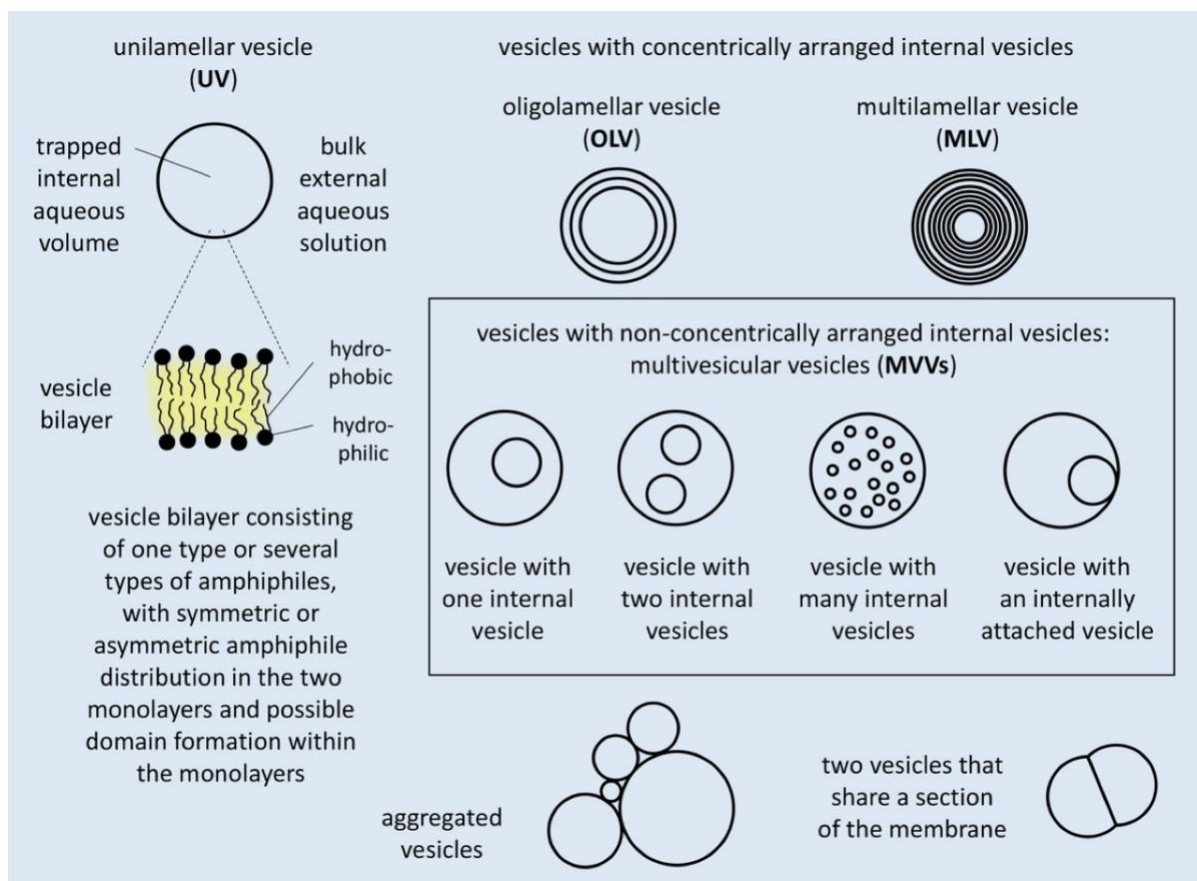
---

The authors would like to thank Prof. Peter Walde and his group at ETH Zurich for the meaningful discussion and collaboration that culminated in the publication. We would also like to thank Dr. Siddharth Deshpande and Dr. Tom Robinson for insightful discussions and the latter, for kindly providing his chips.

---

## 3.1. Introduction

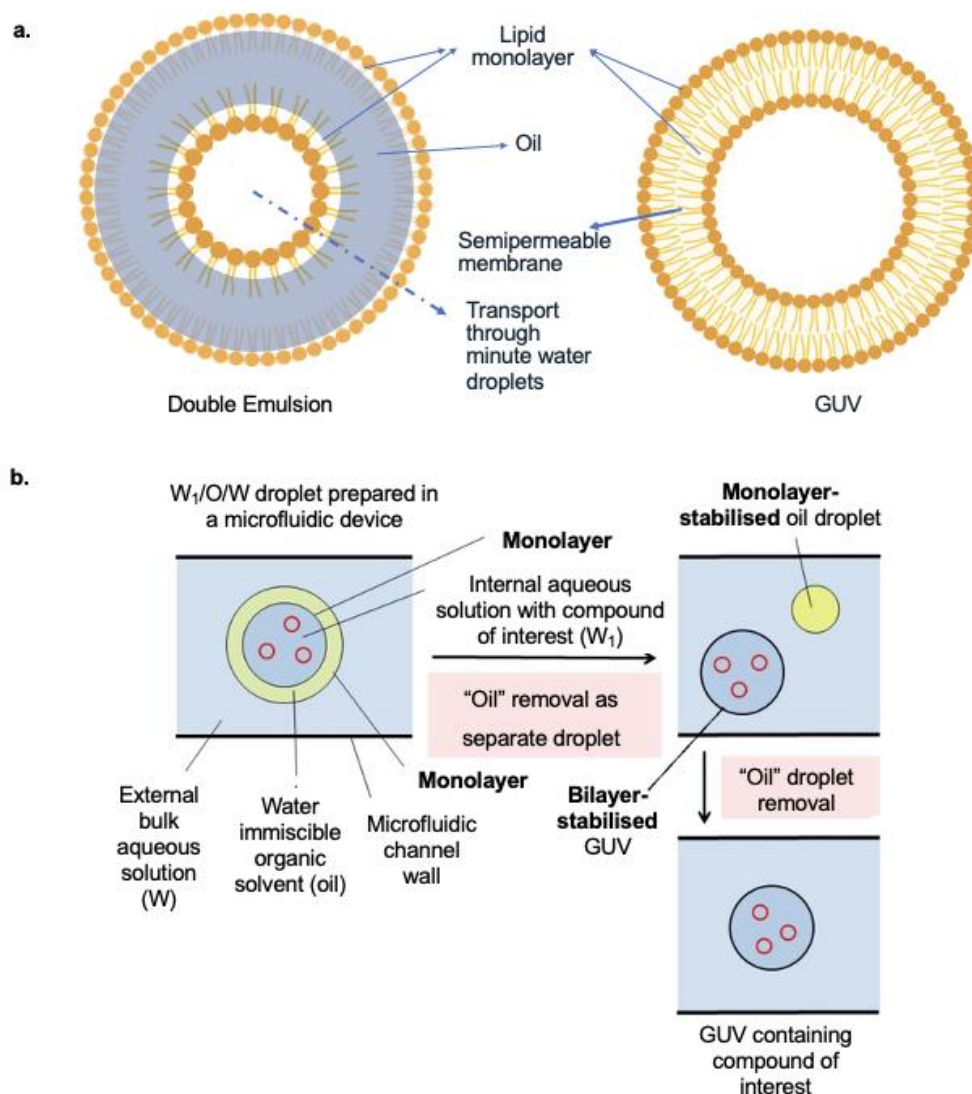
Vesicles are unique types of three-dimensional polymolecular compartments<sup>1-4</sup>, that either exist in biological systems as “biological vesicles” (e.g. intracellular transport vesicles<sup>5</sup> or extracellular vesicles<sup>6-8</sup>), or that form *in vitro* in an aqueous medium in different sizes and morphologies upon dispersing vesicle-forming amphiphiles under suitable conditions<sup>3,9-17</sup>. In the latter case, the vesicles are artificially made by using either naturally occurring or synthetic bilayer-forming amphiphiles. They often are called “artificial vesicles”<sup>4</sup>, but in most cases just “vesicles”. Vesicles from naturally occurring bilayer-forming lipids, e.g. the phosphatidylcholines present in egg yolk, often are called “lipid vesicles” or “liposomes”<sup>11,12,17</sup>. In each type of vesicle, a self-closed boundary (also called vesicle membrane, or bilayer) constituted by the amphiphiles, possibly together with other membrane-embedded molecules, separates an internal trapped aqueous volume from the external bulk aqueous solution. In addition to this membrane, internal boundaries may also exist, as in the case of oligo- or multilamellar vesicles, OLVs and MLVs, where a few or many internal self-closed membranes are concentrically arranged, onion-like. It is only the outermost membrane that is in direct contact with the bulk aqueous solution. A vesicle containing non-concentrically arranged smaller internal vesicles is called “multivesicular vesicle (MVV)”<sup>12,18</sup> or “vesosome”,<sup>19</sup> (Figure 3.1). Vesicles with only one lamella, *i.e.* one bilayer, are unilamellar vesicles (UVs). UVs are usually differentiated by size: SUVs (small or sonicated UVs, ~30-50 nm), LUVs (large UVs ~50-500 nm), and GUVs (giant UVs, >500 nm).



**Figure 3.1.** Simplified cross-sectional representation of different types of spherical vesicles dispersed in a bulk aqueous solution. Large enough vesicles may host one or more internal (inner) vesicles. If they are concentrically arranged, the vesicles are oligo- or multilamellar, OLVs or MLV. Vesicles with non-concentrically arranged internal vesicles are called multivesicular vesicles, MVVs. Sometimes, the internal vesicles may adhere to the outermost boundary. Aggregated vesicles - or vesicle colonies<sup>20</sup> – are vesicles that stick together without undergoing fusion. Vesicles that share a part of their boundary with another vesicle are also known as “multicompartment vesicles”<sup>21</sup>.

GUVs are obtained from W/O/W droplets, i.e. double emulsions (DEs), through the removal of the oil. The main difference between DEs and GUVs is the presence of a layer of oil between the lipid monolayers in DEs, affecting the membrane permeability (Figure 3.2.a). Lipid bilayers are permeable to water and certain ions, such as  $H^+$ <sup>22</sup>, whereas double emulsions are expected to be impermeable due to the immiscibility of the phases, although transport *via* minute water droplets has been reported and characterised<sup>23</sup>. The micrometre-sized W/O/W droplets are obtained by a microfluidic device with a specially designed chip, e.g. double junction (Figure 1.12). Moreover, the removal of the oil and the formation of GUVs may occur within the microchannels of the chip with the inclusion of additional chip features, such as a

long post-junction channel (described below)<sup>24,25</sup>. Depending on the experimental conditions, the chemical structure of the amphiphiles, and the type of oil used, the oil might be released from the W/O/W droplet spontaneously within the microchannels so that one GUV and a separated oil droplet are obtained from each initially created W/O/W droplet (Figure 3.2.b.)<sup>24,25</sup>. These initial W/O/W droplets are obtained on the chip through the stepwise, controlled assembly of two aqueous solutions and the oil containing suitable amphiphiles<sup>24,25</sup>. If the inner aqueous solution ( $W_1$ ) for forming the  $W_1$ /O/W droplets is replaced by an aqueous dispersion of vesicles, uniform MVVs will be obtained in a continuous and reproducible way as long as the microfluidic device is in operation.

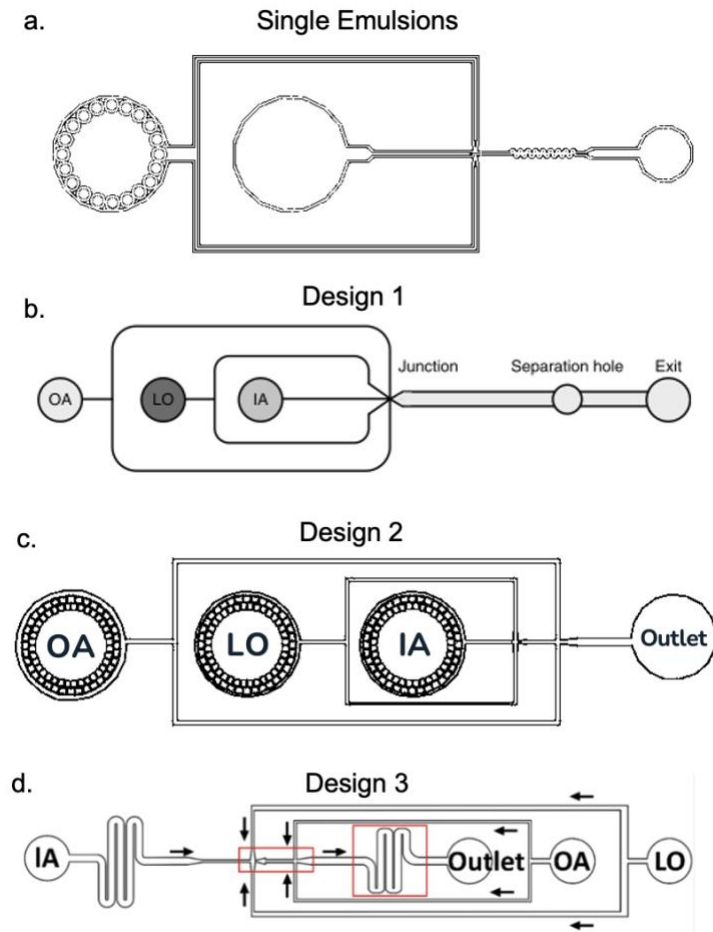


**Figure 3.2.** DE-templated GUVs. **a.** The main difference between DEs and GUVs is the presence of oil in the membrane that affects permeability. **b.** Process of producing GUVs templated from DEs in microfluidic channels.

As seen in Chapter 2, biologists are demonstrating interest in using microfluidics as a tool to advance their research. Consequently, the biocompatibility of components becomes an important factor to consider. In the case of microfluidic-based compartments, such as single emulsions, DEs and GUVs, the biocompatibility of the oil is the main point to consider. HFE7500 and 1-octanol are two well-known biocompatible oils that have been employed in droplet microfluidics<sup>24,26</sup>. Octanol, in particular, has gained relevance as the intermediate phase of DE-templated GUVs because the difference in size between the octanol molecule (8 carbons long) and the lipid molecules (for example, 18 carbons long for 1,2-dioleoyl-sn-glycero-3-phosphocholine, DOPC) thermodynamically favours a molecular rearrangement that forces the octanol out from in between the lipids<sup>24,27</sup>. This process is facilitated by shear stress with the walls of the microfluidic channels.

As an emerging field, microfluidic-based microcompartment production has no well-established protocol, although several methods have been published, with differences in the composition of the solutions<sup>28–33</sup>, surface coating strategies<sup>34,35</sup>, the geometry of the channels<sup>24,36–38</sup>, and, for vesicle production, different oil removal procedures<sup>33,39–41</sup>.

This Chapter investigated the production of microcompartments, beginning with published designs (Figure 3.3). Single emulsions were produced with a flow-focusing chip with a short post-junction channel equipped with a serpentine, developed in-house (Figure 3.3.a.). Design 1<sup>24</sup> (Figure 3.3.b.) and Design 3<sup>38</sup> (Figure 3.3.d.) are two available chip geometries developed so the shear stress applied to the DEs promotes on-chip dewetting of octanol to form GUVs. The shear stress is a result of the contact with the walls of the post-junction channel (due to the short height of Design 1, 11  $\mu\text{m}$ ; and constrictions at the turns of the serpentine, Design 3). Design 2 is an available double-junction chip for producing double emulsions, with the possibility of oil removal off-chip<sup>42</sup> (Figure 3.3.c.). In the respective publications, Design 1 was fabricated using e-beam lithography, a technique that offers high resolution but requires highly specialised equipment<sup>43,44</sup>, know-how and a cleanroom, and Designs 2 and 3 were fabricated with photolithography and soft lithography, also in cleanrooms. Building on the market insights of Chapter 2, this Chapter aims to produce microcompartments with varying levels of complexity to encapsulate compounds of interest in non-specialist settings, i.e. without the need of a cleanroom and using standard photolithography and soft lithography techniques.



**Figure 3.3.** Published designs used for microcompartment production. **a.** Single emulsions flow-focusing chip. **b.** Design 1. Six-way junction with long post-junction channel published by Deshpande et al.<sup>24</sup> to produce DE-templated GUVs with on-chip octanol wetting. **c.** Design 2. Double flow-focusing junction published by Teh et al.<sup>42</sup> to produce DEs. Off-chip dewetting is possible. **d.** Design 3. Double flow-focusing junction with serpentine of Yandrapalli et al.<sup>38</sup> to produce DE-templated GUVs with on-chip dewetting of octanol

## 3.2. Materials and Method

### 3.2.1. Microfluidic chip fabrication

Photomasks of single emulsion chip and Designs 1 and 2 (CAD/Art Services, Inc, USA) were reproduced in AutoCad (Autodesk, Inc., USA) from the respective publications (in-house design for single emulsions). Design 1.2 was adapted in-house in AutoCad from Design 1, and photomasks were similarly produced. Chips were produced from the photomasks by standard photolithography<sup>45</sup> and soft lithography techniques<sup>46</sup>, as described below. Chips from Design 3 (without surface treatment) were kindly provided by Dr Tom Robinson's group (MaxSynBio, MPI, Potsdam, Germany).

#### 3.2.1.1. SU-8 Mold fabrication

Briefly, SU-8 (SU-8 2010, 2050 and 3010; Microchem Inc., USA) was spin-coated (APT, Germany) on top of silicon wafers (Siebert Wafers, Germany). The wafers were then baked to solidify the photoresist (pre-exposure baking) and exposed to UV light (Hamamatsu Photonics K.K., Japan) through photomasks containing the desired design. The silicon wafer was developed (SU-8 developer solution, Microchem Inc., USA) to eliminate the excess of photoresist and hard-baked. Different SU-8 resins were used to fabricate chips with different heights (Table 3.1). To improve adherence and resolution of the smallest channels, a 2- $\mu$ m layer of SU-8 2002 (Microchem Inc., USA) was spin-coated before SU-8 3010.

**Table 3.1.** Protocols according to the SU-8 resin and desired height of the channels.

SU-8	2002	2025	2050	3010
Desired height	2 $\mu$ m	25 $\mu$ m	25 $\mu$ m	11 $\mu$ m
Spinning details	30s 3000 rpm 1000 rpm/s	Step 1: 5s 400 rpm 300 rpm/s  Step 2:	Step 1: 5s 400 rpm 300 rpm/s  Step 2:	Step 1: 5s 500 rpm 300 rpm/s  Step 2:

		30s 4000 rpm 300 rpm/s	30s 4500 rpm 300 rpm/s	30s 2000 rpm 300 rpm/s
Pre-exposure bake	1 min at 95°C	5 min at 95°C	3 min at 65°C 5 min at 95°C	1 min at 65°C 7,5 min at 95°C
Exposure (required energy, lamp power, time)	154 mJ/cm <sup>2</sup> 35 mW/cm <sup>2</sup> 4s (UV-Kub 2, Kloé, France)	150 mJ/cm <sup>2</sup> 18,4 mW/cm <sup>2</sup> 9s	155 mJ/cm <sup>2</sup> 18,7 mW/cm <sup>2</sup> 8,3s	200 mJ/cm <sup>2</sup> 15,4 mW/cm <sup>2</sup> 13s
Post- exposure bake	1 min at 95°C	1 min at 65°C 5 min at 95°C	1 min at 65°C 5 min at 95°C	1 min at 65°C 3 min at 95°C
Development	N/A	4 min	5 min	5 min
Hard bake	N/A	30 min at 150°C	30 min at 150°C	30 in at 150°C

### 3.2.1.2. PDMS Chip fabrication

PDMS was mixed with the curing agent (10:1; ref.: Sylgard 184, Dow Corning, Midland, MI, USA), degassed in a desiccator (30 min) and poured over the silicon wafers. The chips were cured at 85°C overnight then cut and carefully separated from the molds. Inlets and outlets were punched with biopsy punches ( $\varnothing=1$  mm or 4mm) and chips were bonded onto PDMS covered glass slides with air plasma treatment (2 min, Harrick Plasma, USA). The glass slides were spin-coated in advance (10s at 500 rpm and 40s at 1000 rpm) with PDMS mixed with the curing agent (10:1) and cured to solidification (1h at 80°C).

### 3.2.2. Channel Characterisation

First, the top view of the chip was imaged with an upright microscope (built in-house from 5x objective). Then, the height of the channels was characterised by cutting and imaging cross-



sections of the chips with the same microscope. The dimensions were calculated based on the scaling of the images, and image analysis was made with the software Fiji.

### **3.2.3. Single Emulsion Formation**

An in-house developed flow-focusing junction PDMS chip was coated with Aquapel (Autoserv, Germany) to increase the surface hydrophobicity. Briefly, Aquapel was flushed into the channels. Then, HFE7500 oil (Novec7500, 3 M) was flushed into the channels to avoid the crystallisation of Aquapel inside the chip. Filtered water and fluorinated oil with 2% surfactant (ref. DG-DSO-20, Droplet Genomics, Lithuania) were placed in 15 mL Falcon tubes and connected to the chip with PTFE tubing. The fluids were flushed into the chip by a pressure-driven flow controller (OB1, Elveflow, France), and the droplet formation was visualised with an upright microscope (built in-house from 5x objective). Videos and images were made with a high-speed camera (ref. PL-D725CU, Pixelink, Canada).

### **3.2.4. Encapsulation in single emulsions**

Single emulsions were produced as described above. The inner solution was replaced by an aqueous solution with 0.1 mM Rhodamine B (ref. R6626, Sigma Aldrich, France ) or a solution of Dulbecco's Modified Eagle Medium (DMEM, ref. P04-04510, Panbiotech, Germany; supplemented with 10% foetal bovine serum, FBS, ref. 8500-P131704, Panbiotech, Germany; and 1% Penicillin-Streptomycin PS, ref. P06-07100, Panbiotech, Germany) with HeLa cells ( $1 \times 10^5$  or  $1 \times 10^6$  cells/mL) prepared with 15% Optiprep (ref. 07820, StemCell, Norway) to prevent the cells from precipitating. Videos and images were gathered with an upright microscope (built in-house from 5x objective) and a high-speed camera (ref. PL-D725CU, Pixelink, Canada). Droplets containing cells were manually counted with the Fiji software.

### **3.2.5. Double Emulsions Production**

#### **3.2.5.1. Solution Preparation**

Solutions were prepared based on Deshpande *et al.*<sup>27</sup> and Yandrapalli *et al.*<sup>38</sup>.

1. Hydrophilic surface treatment solutions:

- a. **Design 1 and 2:** PVA (1% w/v and 2.5% w/v; 87-90% hydrolysed, average MW 31,000-50,000; ref. 363073, Sigma Aldrich, France) solution was prepared in filtered water (stirring at 85°C, 1.5h at 500 rpm) and filtered (0.22 µm). The solution was stored and used for as long as it remained clear and free of aggregates.
  - b. **Design 3:** three solutions were prepared: a 2% (w/v) PDADMAC (Poly(diallyldimethylammonium) chloride, ref. 409022, Sigma Aldrich, France) in filtered water; 5% (w/v) PSS (Polysodium 4-styrenesulfonate, ref. 243051, Sigma Aldrich, France) in filtered water; and a 1:2 solution of HCl:H<sub>2</sub>O<sub>2</sub> (HCl, 37%, ref. 258148, Sigma Aldrich, France; H<sub>2</sub>O<sub>2</sub>, 30%, ref. H1009, Sigma Aldrich, France). The latter was prepared right before use.
2. Inner Aqueous (IA) Solution: a 15% (v/v) solution of glycerol (ref. 453751-CER, Carlo Erba, Dutscher) in filtered water was prepared. The solution was stored at room temperature and used for as long as there were no aggregates.
3. Outer Aqueous (OA) Solution: a 15% (v/v) of glycerol (ref. 453751-CER, Carlo Erba, Dutscher) and 5% (v/v) of P188 (and 0.5% (v/v) P188; 10% (w/vol) solution, ref. P5556, Sigma Aldrich, France) solution in filtered water was prepared. The solution was stored at room temperature and used for as long as there were no aggregates.
4. Lipid Stock Solution: a 10% (w/v) DOPC (1,2-dioleoyl-sn-glycero-3-phosphocholine, chloroform, ref. 850375C, Sigma Aldrich, France) in ethanol (ref. 4146012-CER, Carlo Erba, Dutscher, France) solution was prepared. The respective amount of DOPC in chloroform (ref. 1024451000, Emsure, Germany) was dispensed with a glass syringe (ref. 074345, Hamilton, Dutscher, France) into a round bottom flask. The chloroform was evaporated under a gentle stream of nitrogen (ref. GAL110350, Core Equipment, Prosynergie, France) to form a lipid film at the bottom of the flask. The flask was put under partial vacuum in a desiccator for at least two hours to ensure evaporation of chloroform. Ethanol was added to form a 10% (w/vol) solution, and the flask was closed with parafilm. The lipids were dissolved in the ethanol. The DOPC stock solution was sealed in a glass container under nitrogen and stored (-20°C).

5. Lipid-oil (LO) Solution: a DOPC solution in 1-octanol (anhydrous,  $\geq 99\%$ , ref. 297887, Sigma Aldrich, France) was prepared from the lipid stock solution in the desired concentrations (2.54 mM; 5 mM; 6.5 mM and 7.3 mM). This solution was prepared right before use. 0.1 mM (v/v) Dil (ref. 42364, Sigma Aldrich, France) was added as specified.
  
6. Density Gradient: IA solutions containing 100 mM and 300 mM sucrose (ref. 1906, Condalab, Spain) and 15% (v/v) glycerol and OA solutions containing 100mM and 300 mM glucose (ref. D9434, Sigma Aldrich, France), 15% (v/v) glycerol and 0.5% (v/v) P188 were prepared to form density gradients between the DEs and the external solution.
  
7. Inner Solutions - encapsulation and membrane permeability Assays: IA solutions containing Phenol Red (0.32 mg/l, ref. 114529, Sigma Aldrich, France), or calcein (0.3 mM, ref. C0004, TCI, Japan) in water were prepared for the encapsulation and membrane permeability assays.

### **3.2.5.2. Surface Coating**

The surface coating treatment was design-specific. The treatment was performed at least a day after bonding to ensure that PDMS had recovered its hydrophobic properties.

For Designs 1 and 2, a PVA solution (1% (v/v) or 2.5% (v/v)) was flushed from the outer aqueous (OA) solution inlet to the outlet for 3 to 5 minutes, using a pressure-driven flow controller (OB1, Elveflow, France), while pressurised air blocked the inner (IA) and oil (LO) channels. To remove the PVA from the chip, the pressure of the air channels was increased to 2000 mbar, and vacuum was applied in the OA inlet and outlet channels at -1000 mbar (vacuum pump (Thomas, USA)). Once empty, the chip was placed at 120°C for at least 15 minutes.

For Design 3, the outlet was used to flush the solutions into the chip, while the OA channel was connected to a vacuum pump (-50 mbar). HCl:H<sub>2</sub>O<sub>2</sub> (1:2, 30s) was vacuumed into the

chip to render the surface negatively charged and rinsed with filtered water (30s). Positively charged polymeric solution (2 wt.% Poly(diallyldimethylammonium) chloride, PDADMAC) was vacuumed into the chip (2 min) to form positively-charged layers and rinsed with filtered water (30s). Then, the negatively charged polymeric solution (5 wt.% Polysodium 4-styrenesulfonate, PSS) was vacuumed (2 min) into the chip and rinsed with filtered water (30s), finishing the hydrophilic coating of the post-junction channel. Finally, the chip was left to dry (30 min) before use.

### **3.2.5.3. Double Emulsion Production**

The outer aqueous (OA) solution was flushed into the chip, followed by the lipid-oil (LO) solution and then the inner aqueous (IA) solution by connecting the reservoirs to the chip by the respective pieces of tubing. Then, the pressures were increased until double emulsions started to form. The double emulsions were collected into an Eppendorf tube or a 0.4  $\mu$ -Slide I Luer chip (ref. 80176, Ibidi, Germany) connected with a piece of tubing to the outlet of the production chip. Image analysis was performed using the image software Fiji and a Python script developed in-house for automated droplet counting and sizing. All fluorescent images were collected with an inverted AxioVert A1 microscope (Carl Zeiss, Germany) using filters (green: ex/em 470/525 nm), and respective camera (AxioCam 202 mono).

In this work, encapsulation efficiency was defined as the percent of DEs produced compared to the total number of DEs expected in a given time, i.e. encapsulation of an inner water phase inside an intermediate oil phase. The expected total number of DEs assumed an ideal scenario in which production was perfect and 100% of the inner solution was encapsulated inside an oil droplet, calculated as the number of DEs per frame X 200 frames. The actual number of produced DEs accounted for common defects of production which led to the escape of the inner solution to the outer solution, calculated as the total number of DEs summed for 200 frames. The production rate was calculated using 200-frame videos of DEs exiting the chip junction captured with a high-speed camera (Pixelink, ref. PL-D725CU). The total number of produced DEs in a given video was counted manually with the software ImageJ and adjusted to give the production in Hertz (double emulsions per second).

#### **3.2.5.4. Off-chip dewetting**

Double emulsions were produced with Design 2 and collected in an observation chamber (0.4  $\mu$ -Slide I Luer chip, ref. 80176, Ibidi, Germany). DEs were imaged through time with an inverted AxioVert A1 microscope (Carl Zeiss, Germany) and camera (AxioCam 202 mono). The thickness of the membrane was manually measured with Fiji software.

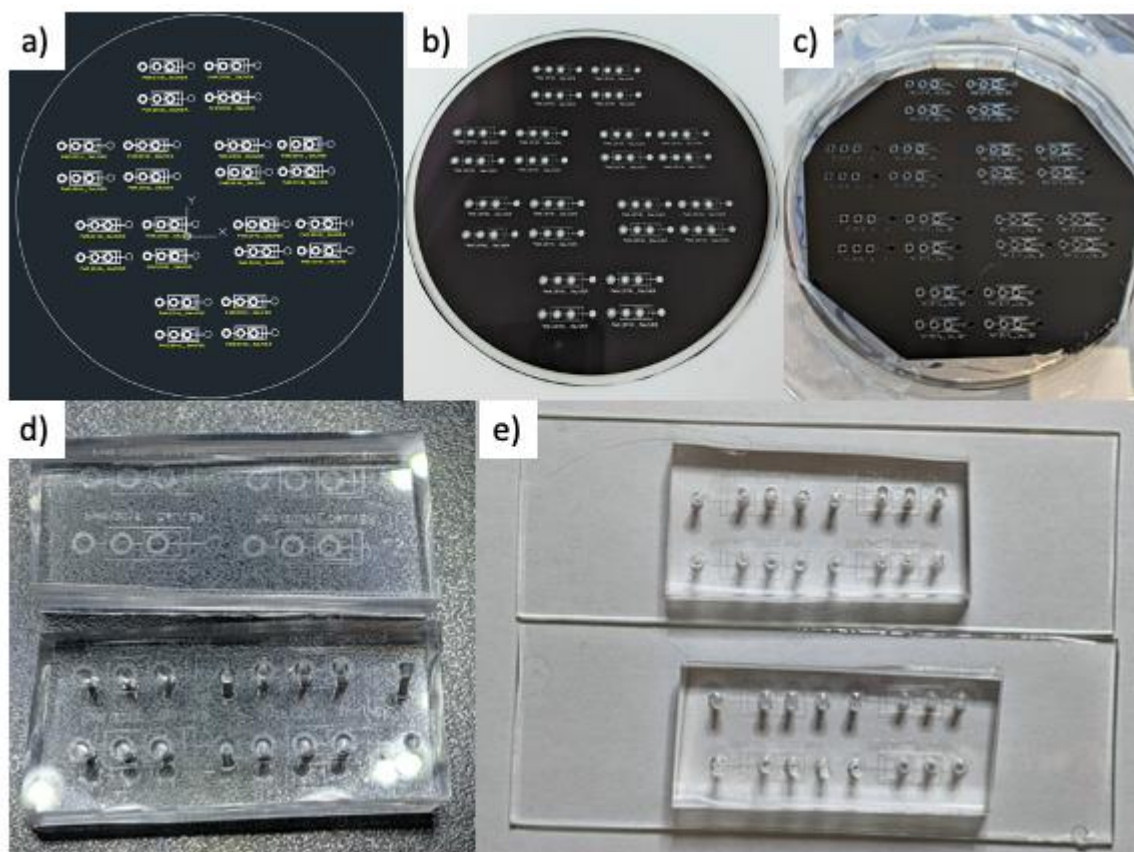
#### **3.2.5.5. Membrane Permeability Assay**

Double emulsions were produced from Designs 2 and 3. For Design 2, the inner solution was replaced with a solution containing Phenol Red (0.32 mg/l) in 15% (v/v) glycerol. The DEs were placed on a glass slide, and an equal volume of 1M NaOH (ref.: 480717000, Carlo Erba, Dutscher, France) or 1M NaCl (ref. S5150, Sigma Aldrich, France) was added on top of them. Images were taken with an upright microscope (built in-house from 5x objective) and a high-speed camera (ref. Pixelink, ref. PL-D725CU, Canada).

### **3.3. Results and Discussion**

#### **3.3.1. Microfluidic chip fabrication**

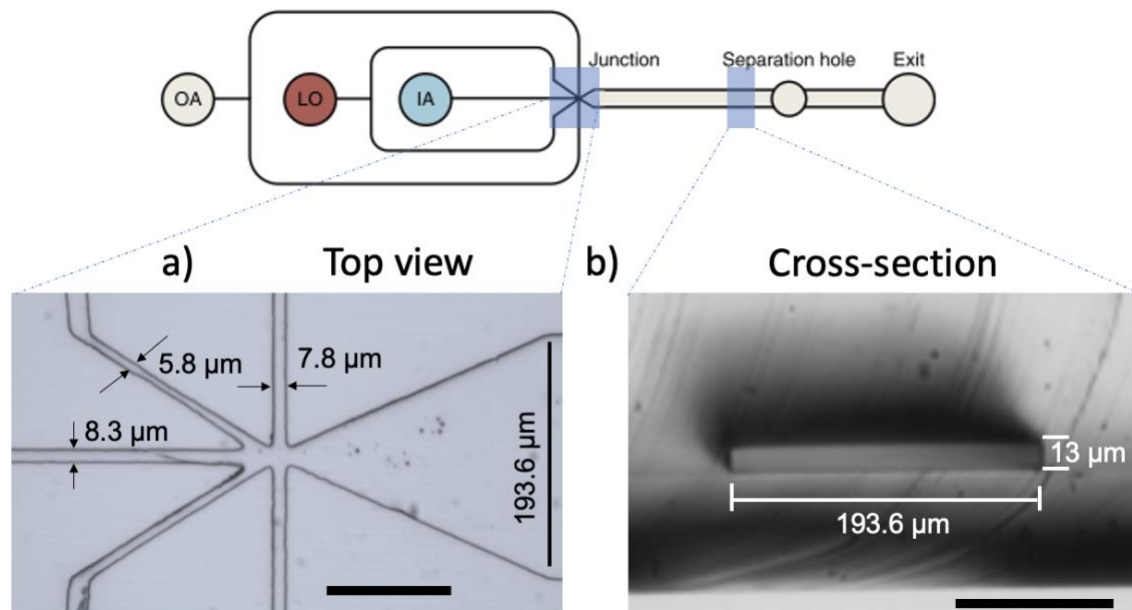
PDMS chips were fabricated with standard soft lithography techniques<sup>46</sup> without the use of a cleanroom. Briefly, photomasks were printed from the published designs and used to produce SU-8 molds. PDMS was poured on top of the molds and cured overnight at 85°C. Then, the chips were cut from the mold, punched and bound to PDMS-covered glass slides with plasma treatment (Figure 3.4).



**Figure 3.4.** Microfluidic chip fabrication steps. **a.** Photomask reproduced on AutoCad; **b.** Printed photomask; **c.** SU-8 mold; **d.** PDMS chips separated from the mold highlighting the channels imprinted into the polymer (upper chip), and punched inlet and outlet holes (lower chip). For design 2, each chip had four independent devices; **e.** PDMS chips bonded to PDMS-covered glass slides.

### 3.3.1.1. Channel characterisation

To characterise the fabrication process and demonstrate consistency between chips, some chips were randomly selected to be characterised. The chips were visualised under the microscope, and images were taken from the top and cross-sections of the channels (Figure 3.5). As an example, for a chip with 13  $\mu\text{m}$  in height, the channels of the junction of Design 1 ranged from 5.8 (LO) to 8.3 (IA)  $\mu\text{m}$  and the post-junction channel was 193.6  $\mu\text{m}$ , as expected based on the mask (Table 3.2).



**Figure 3.5.** Schematic of Design 1 and representative inserts of PDMS chips. **a.** Top view of the junction. **b.** Cross-section of the post-junction channel. Scale bar, 100  $\mu\text{m}$ .

Soft lithography has a lower resolution than e-beam lithography, but it is considerably more accessible regarding equipment and know-how<sup>43,44</sup>. It also does not require a cleanroom. Indeed, the goal of this work was to lower the barriers to the adoption of microfluidic encapsulation tools, consistent with an encapsulation "starter pack" for non-specialists. Consequently, the achievable resolution in soft lithography was 13  $\mu\text{m}$  in height for Design 1 (Table 3.2). The dimension of the LO channel was increased on the photomask to stay within the SU-8 resolution. The SU-8 2050 is indicated for channel heights of around 20  $\mu\text{m}$ , and it has a >10:1 aspect ratio resolution, so the dimensions were around 6% larger than desired for the smaller channels. SU-8 3010 is indicated for channel heights of around 10  $\mu\text{m}$ , and it has a resolution of >5:1 aspect ratio, resulting in the desired dimensions (the measurements are an indirect assessment of the SU-8 mold, made with PDMS chips that are cured overnight at 80°C, explaining the small differences in size). Both chip sizes (25  $\mu\text{m}$ -chip and 13  $\mu\text{m}$ -chip) were used in the following experiments. Designs 2 and 3 have heights of 50  $\mu\text{m}$  and larger features, easily attainable with soft lithography.

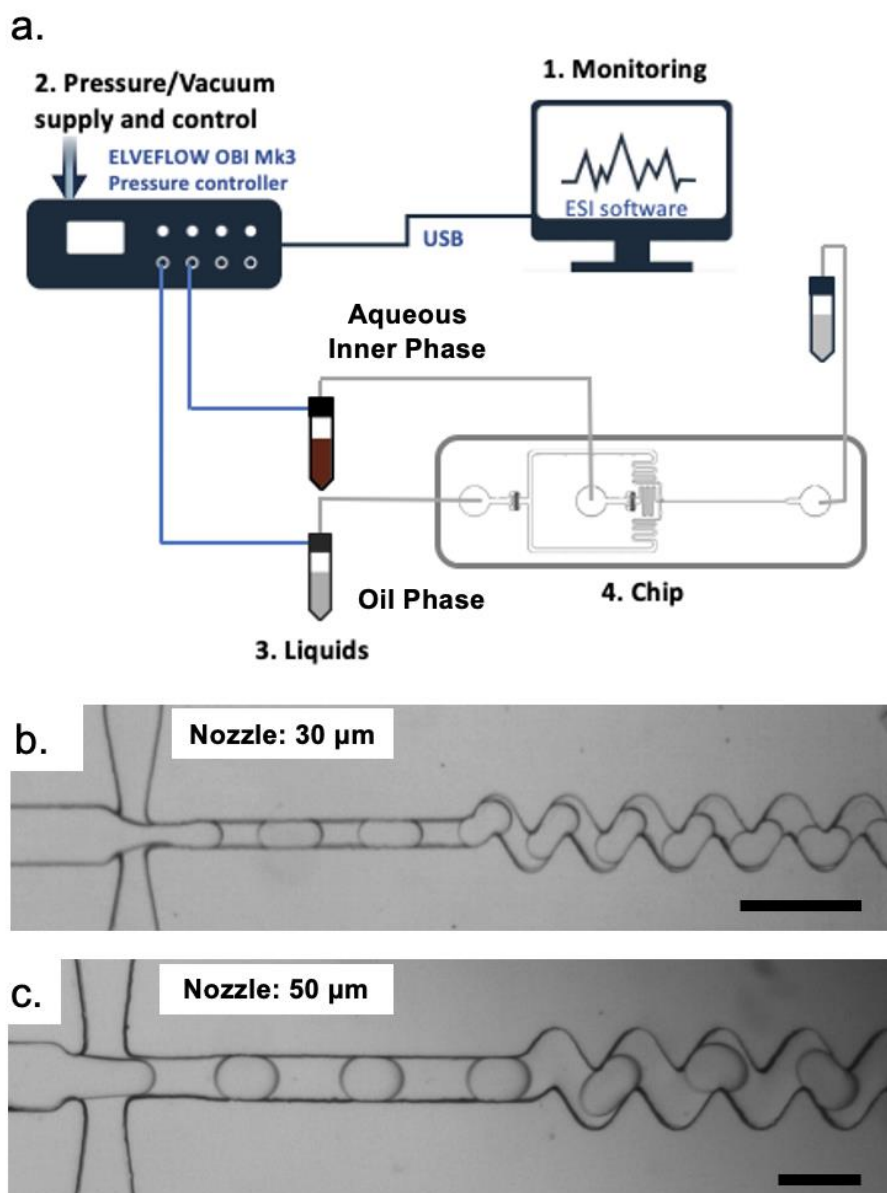
**Table 3.2.** The widths and heights obtained from different SU-8 resins compared to the desired measures.

	<i>Design 1<sup>27</sup></i>	<i>Photomask (adapted from Design 1)</i>	SU-8 2050	SU-8 3010
IA Junction ( $\mu\text{m}$ )	10	10	14.4	8.3
LO Junction ( $\mu\text{m}$ )	5.4	8	11.9	5.8
OA Junction ( $\mu\text{m}$ )	10	10	16.9	7.8
Post-Junction ( $\mu\text{m}$ )	200	200	197.6	193.6
Height ( $\mu\text{m}$ )	11		25	13.1

### 3.3.2. Single-emulsion production

Microfluidic production of single emulsions was performed as a positive control for production and encapsulation in complex microcompartments. The size of the nozzle is one of the main factors impacting the final size of droplets. For this reason, PDMS chips with different nozzle sizes (30 and 50  $\mu\text{m}$ ) were investigated. The devices were surface treated with Aquapel prior to use to increase the hydrophobicity of the surface. The fluids were driven from the reservoirs to the chip by a pressure-driven flow controller (Figure 3.6.a.). Water-in-oil single emulsions were successfully produced with fluorinated oil (HFE7500, 2% of surfactant) and water in different sizes (Figure 3.6.b.).



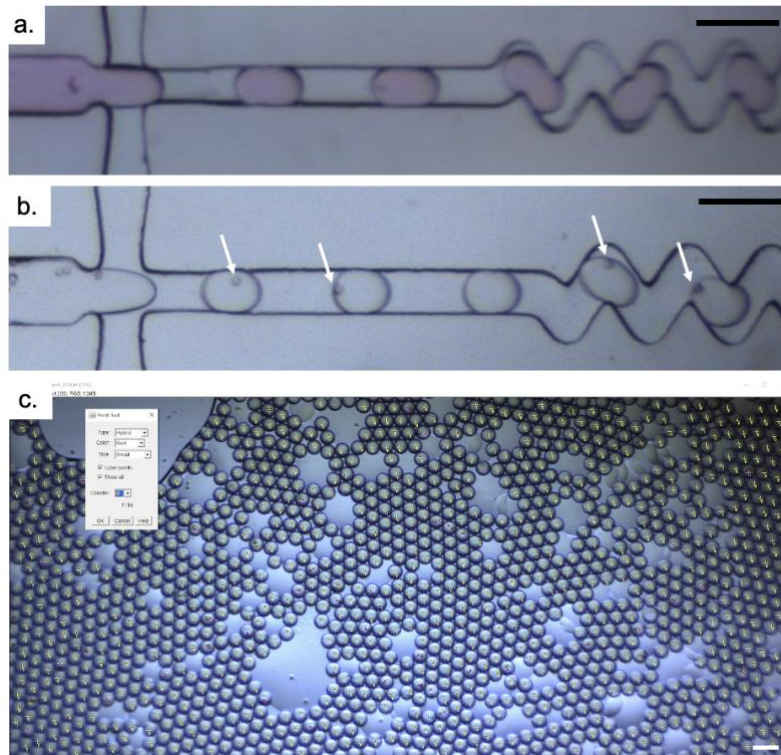


**Figure 3.6.** Microfluidic single emulsion production **a.** Schematic of microfluidic setup for single emulsion production. **b. and c.** Representative images of single emulsion production in PDMS chips with different nozzle sizes (b. 30  $\mu\text{m}$ ; c. 50  $\mu\text{m}$ ). Scale bar, 100  $\mu\text{m}$ .

### 3.3.2.1. Encapsulation in single emulsions

As a step toward the production of complex compartments encapsulating compounds of interest, encapsulation in single emulsions was performed. The inner solution was replaced with a solution containing the compound of interest. Rhodamine B (0.1 mM), a hydrophilic dye, was successfully encapsulated in single emulsions produced with a PDMS chip (nozzle, 50

$\mu\text{m}$ , Figure 3.7.a.) The encapsulation of single HeLa cells was also performed (Figure 3.7.b.). To investigate the efficiency of single-cell encapsulation, the droplets were manually counted (Figure 3.7.c.) for different cell concentrations. The quantity of cells and how well dispersed they are in solution affect the encapsulation efficiency of single cells. If a solution has a large number of cells that are well dispersed and do not clump together, the number of single cells encapsulated in droplets will be higher. Cells were kept in suspension with the addition of a buoyancy agent, Optiprep<sup>47</sup>.



**Figure 3.7.** Encapsulation in single emulsions. **a.** Encapsulation of Rhodamine B in water-in-oil single emulsions. **b.** Encapsulation of single cells (white arrows) in W/O single emulsions. **c.** Representative image of manual analysis of single-cell encapsulation in Fiji software. Nozzle, 50  $\mu\text{m}$ . Scale bar, 100  $\mu\text{m}$ .

The impact of cell quantity can be seen by the difference in percentage of single cells encapsulated for each concentration (Table 3.3). For the concentration of  $1 \times 10^5$  cells/ml, only 1.89% of droplets contained a single cell, with most being empty. For  $1 \times 10^6$  cells/ml, 5.53% of droplets had a single cell encapsulated, which is comparable to the 12.2% reported by Liu *et al.*<sup>47</sup> for a concentration twice as high.

**Table 3.3.** Numbers of cells encapsulated per droplet for different cell concentrations.

<b>Concentration cells/mL</b>	<b>Droplets (total)</b>	<b>Droplets with one cell</b>	<b>Droplets with 2 cells</b>	<b>Droplets with &gt;2</b>	<b>Percentage single cells</b>	<b>Percentage cells &gt;2</b>
1x10 <sup>5</sup>	4678	102	14	13	1.89%	0.59%
1x10 <sup>6</sup>	5413	315	53	19	5.53%	1.33%
Poisson distribution (based on concentration 2x10 <sup>6</sup> )					12.2%	0.9%

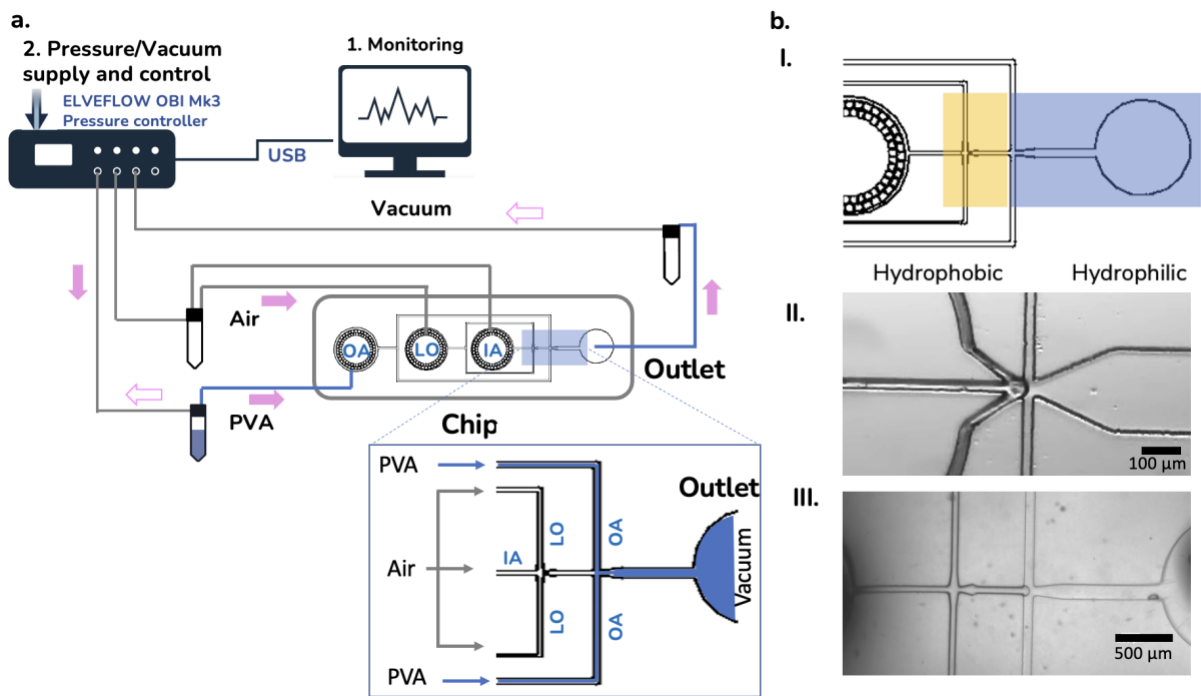
### **3.3.3. Double Emulsion Production**

#### **3.3.3.1. Surface Coating**

A major part of a successful double emulsion production relies on surface interactions. Thus, the surface treatment is a crucial part of the process. To form W/O/W double emulsions, the first junction needs to be hydrophobic, so the oil wets the channel walls and forms water-in-oil droplets. The second junction needs to be hydrophilic, so the outer aqueous solution wets the channel walls and forms water-in-oil-in-water droplets. If the inner aqueous phase wets the walls of the channel after the first junction, it will not be encapsulated inside the oil droplet at the second junction. Likewise, double emulsion stability will be compromised if the oil wets the channel walls after the second junction.

#### **a. Design 1 and 2**

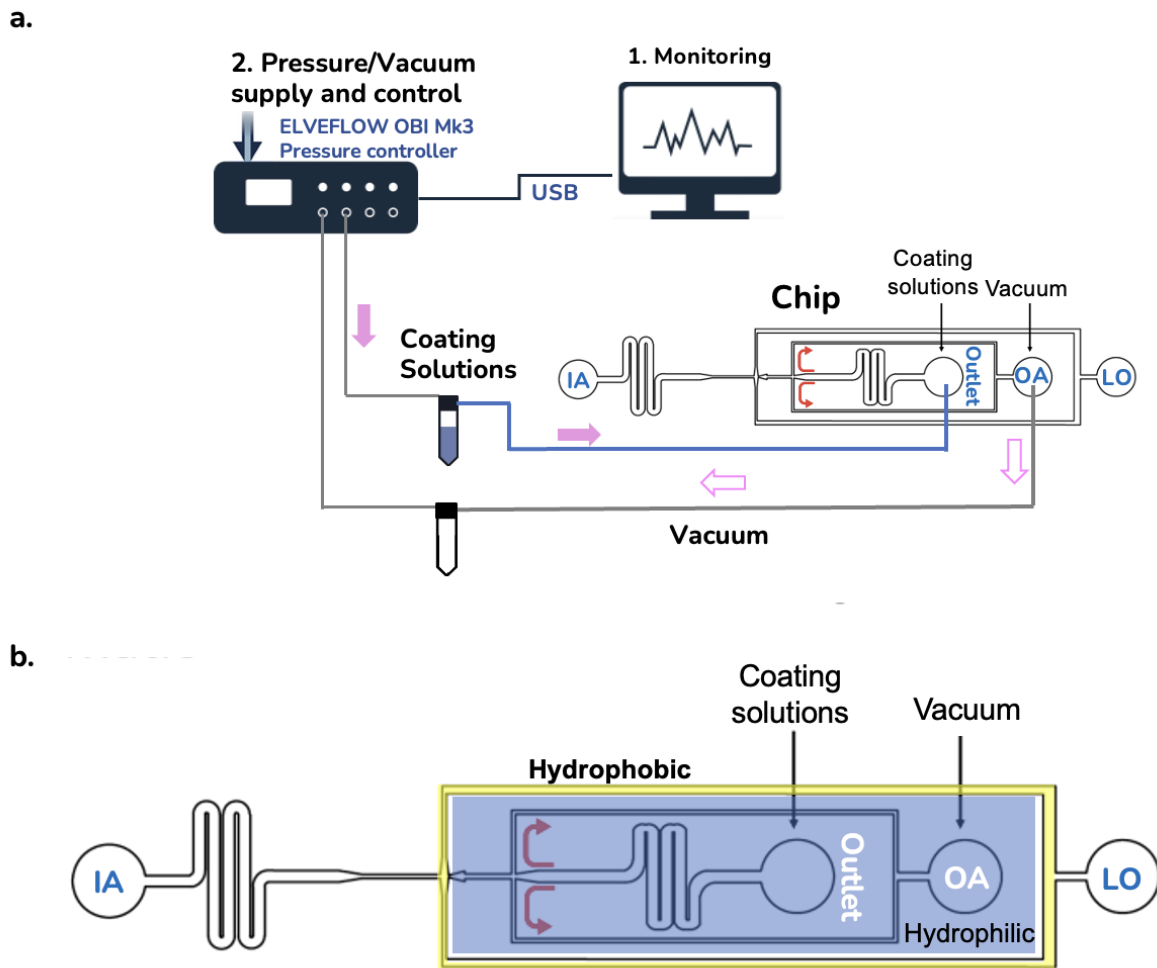
PDMS is hydrophobic, so PVA was used to turn the post-junction channel of Designs 1 and 2 hydrophilic. In order to avoid PVA entering channels that should remain hydrophobic, positive air pressure was applied in the inner and intermediate channels forming an air/liquid interface right at the junction, while vacuum was applied at the outlet (Figure 3.8.a.).



**Figure 3.8. a.** Schematic of the coating setup. Inset details air/liquid interface at the junction. **b.i.** Schematic of the different surface properties required at the junction to produce double emulsions. **b.ii. and iii.** Representative images of surface coating treatment in Designs 1 and 2.

### b. Design 3

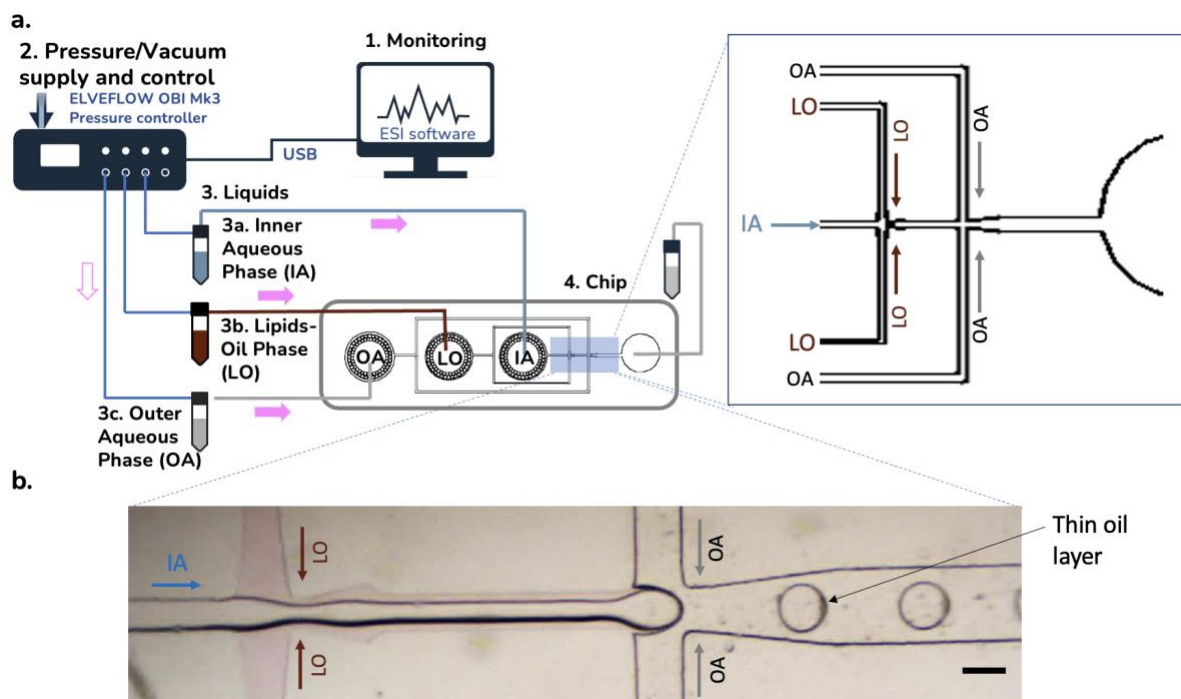
Chips of Design 3 were received untreated because the hydrophilic coating decreases with time. Hence, surface treatment was performed prior to use. Chips were successfully coated with a positive layer of PDADMAC followed by a negative layer of PSS. Vacuum was used to drive the solutions from the "outlet" to the "OA" inlet, maintaining the "IA" and the "LO" channels hydrophobic (Figure 3.9).



**Figure 3.9.** Schematic of surface coating for Design 3. **a.** Microfluidic setup. Solutions entered through the outlet and were directed to the OA channel with vacuum, without the need to block the other channels. **b.** Illustration of different surface properties of the channels after coating. Schematic reproduced from Yandrapalli et al.<sup>38</sup>

### 3.3.3.2. Microfluidic Setup

The microfluidic setup for double emulsion production consisted of a pressure-driven flow controller and the reservoirs connected to the inlets of the chip with pieces of PTFE tubing (Figure 3.10.a.). Double emulsions had a thin layer of oil as the intermediate phase (Figure 3.10.b.) and were collected at the outlet of the chip. The setup was equivalent to all chip designs used.

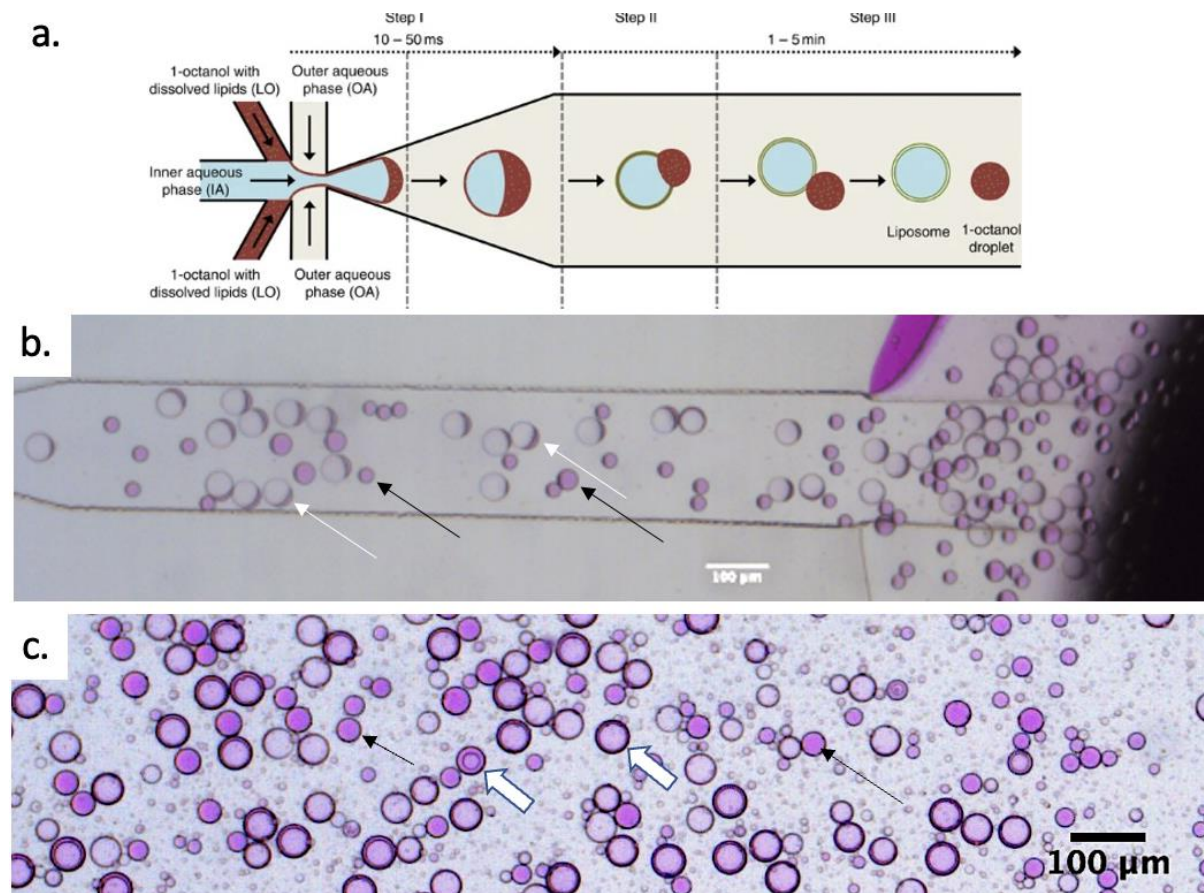


**Figure 3.10. a.** Schematic of the microfluidic setup for double emulsion production. The chip had three inlets that were connected to the reservoirs with the inner aqueous (IA) solution, lipid-oil (LO) solution and outer aqueous (OA) solution, which were in turn connected to the pressure-driven flow controller. Double emulsions were produced at the junction and collected at the outlet. The inset details the flow of liquids at the junction. The schematic uses Design 2 as an example, but the setup is equivalent for all designs. **b.** Representative image of double emulsions being produced at the junction. The oil phase was stained with Dil (a lipid-specific dye), and the arrow highlights the thin oil layer, which forms a small half-moon at the edge of the double emulsion.

### 3.3.3.3. DE production with Design 1

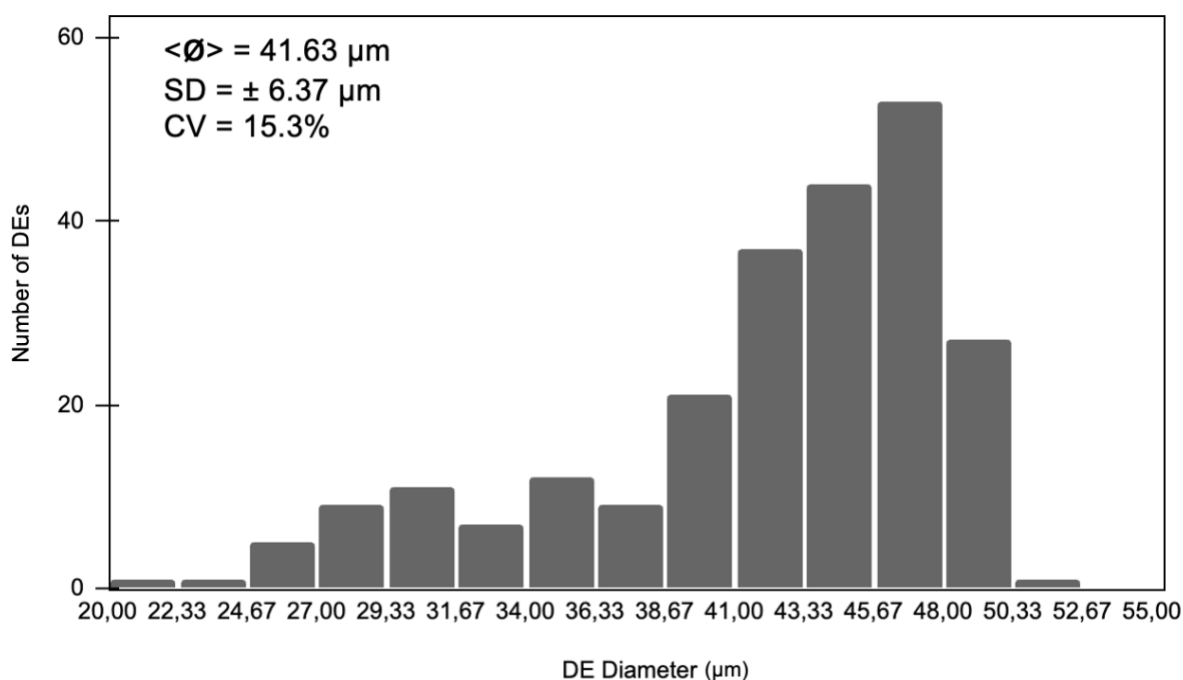
Designs 1 and 3 were based on the same chemical properties and interactions between octanol and amphiphiles, with aqueous and oil solutions having the same compositions in varying concentrations. Design 2 has also been used with solutions of similar composition<sup>48</sup>. Thus, to improve comparability between results, the solutions of Design 1 were the initial solutions of this work, i.e. the inner aqueous solution (IA) was 15% (v/v) glycerol in water; the outer aqueous (OA) solution was 15% (v/v) glycerol and 5% P188 in water; and the lipid-oil (LO) solution was 2.54 mM of DOPC in octanol.

Double emulsions were successfully produced with Design 1 (Figure 3.11). When the LO solutions were stained with Dil, a lipid-specific dye, the presence of octanol was distinguishable in the form of discrete pink half-moons in the intermediate phase of DEs at the outlet of the chip (white arrows, Figure 3.11.b.) and as a clear pink circle around the light pink droplets after collection (white arrows, Figure 3.11.c.). The dark pink droplets were octanol droplets formed due to instability during production that caused DEs to burst prematurely (black arrows, Figure 3.11.b. and c.). The main difference between DEs and GUVs is the presence of oil between the lipid monolayers. The absence of the intermediate steps of the dewetting as DEs travelled down the post-junction channel combined with the clear presence of octanol, visible by eye due to the lipid-specific dye (Figure 3.11.a., steps II. And III.) indicated that the microcompartments collected from Design 1 were DEs.



**Figure 3.11.** Double emulsions production with Design 1. **a.** Schematic of the production and dewetting of the octanol expected of Design 1. **b.** DEs reaching the outlet of Design 1 (IA: 15% glycerol; LO: 5mM DOPC in octanol and 0.1 mM Dil; OA: 15% glycerol and 0.5% P188). The pink half-moons (white arrows) indicate the presence of octanol in the membrane. The smaller pink droplets (black arrows) are octanol droplets formed by the bursting of DEs earlier in the channel. **c.** Collected double emulsions on a glass slide (white arrows, DEs; black arrows, octanol droplets).

Double emulsions produced in a 25- $\mu\text{m}$  high chip were 41.6  $\mu\text{m}$  in diameter ( $\pm 6.37$   $\mu\text{m}$  SD, total number of DEs = 239) (Figure 3.12). Although DE production was continuous, it presented instabilities that resulted in a large coefficient of variation (15.3%, CV). Monodisperse DE populations have CV of approximately 5%<sup>49,50</sup>.



**Figure 3.12.** Size distribution of DEs produced with Design 1. The average diameter of DEs produced in the 25- $\mu\text{m}$  high chip was 41.63  $\mu\text{m}$  ( $\pm 6.37$   $\mu\text{m}$  SD), resulting in a polydisperse population (CV=15.3%).

DEs did not turn into GUVs as the octanol layer did not dewet from the intermediate layer, despite their compression between the top and bottom walls of the post-junction channel. This was most likely due to the DEs not spending enough time in the post-junction channel (i.e. flow rate was too high in the channel) due to the high pressures required to achieve microfluidic DE production in the soft lithography-made chips (Table 3.4). For the 25  $\mu\text{m}$ -chip, pressure values were around 4 times higher and, for the 13  $\mu\text{m}$ -chip, from 8 to 12 times higher than for chips produced with e-beam lithography and associated flow circuit<sup>27</sup>. The substantial increase in pressure in the 13  $\mu\text{m}$ -chip is consistent with increased resistance caused by the smaller dimensions. The pressure in the LO channel was particularly high, probably due to the observed accumulation of lipid molecules at the turns right before the junction, narrowing the channel even further.



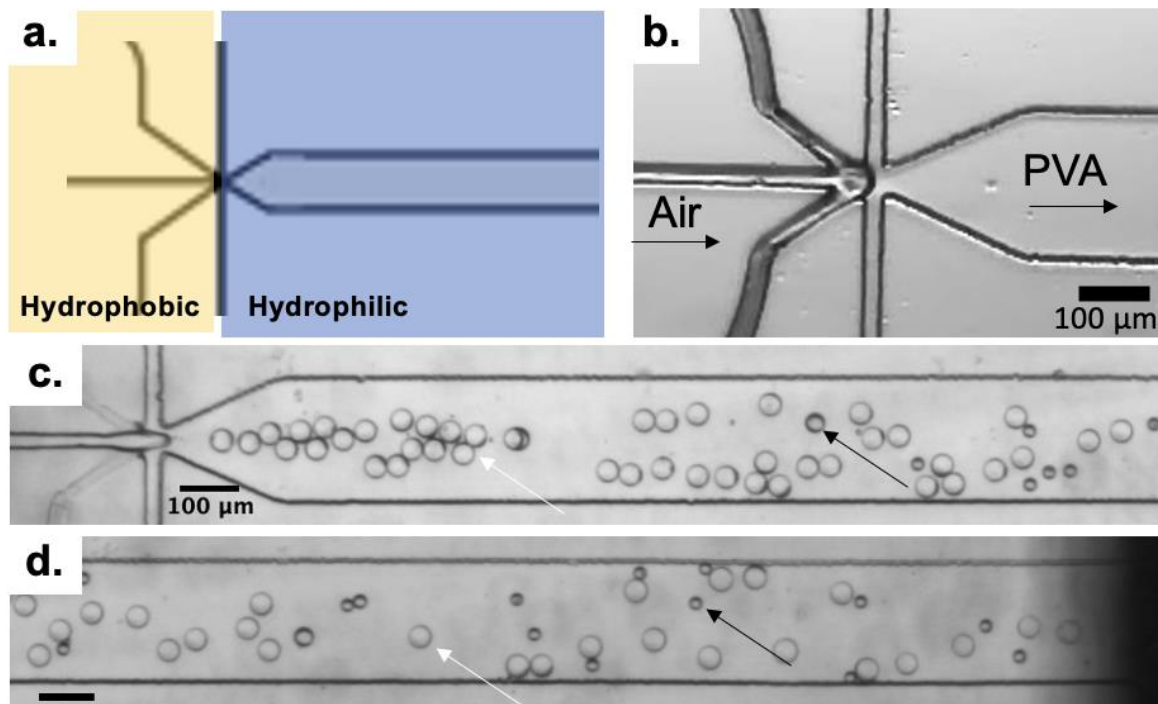
**Table 3.4.** Comparison between the pressures used in the published e-beam lithography chip and the 25  $\mu\text{m}$ -high and 13  $\mu\text{m}$ -high soft lithography-made chips.

		E-beam lithography <sup>27</sup>	Soft lithography – 25 $\mu\text{m}$ -chip	Soft lithography – 13 $\mu\text{m}$ -chip
Pressure (mbar)	Range	Three inlets: 50 to 150	IA: 200 to 300 LO: 200 to 400 OA: 200 to 600	IA: 400 LO: 2000 OA: 500

One of the goals of using this design was to investigate the formation of DEs as a complex microcompartment for encapsulation. Based on market needs of non-specialist settings and the results above, several modifications were performed and are described below, namely: I. Surface treatment; II. IA/OA composition; III. LO composition; IV. Physical Parameters.

## I. Surface Treatment

Two concentrations of PVA were tested (2.5% and 1% (w/v)) for the surface coating treatment. The quality of the coating was assessed in two ways: first, observation of a clear air/PVA interface during the coating procedure without PVA entering the hydrophobic channels (Figure 3.13.b.), followed by the observation of DE production at the junction, was confirmation that the junction was adequately coated (Figure 3.13.c.); second, the lack of octanol attachment and accumulation on the walls of the post-junction channel indicated that the channel was hydrophilic (Figure 3.13.d.).



**Figure 3.13.** Surface treatment of Design 1. **a.** Schematic of the coating properties required at the junction. **b.** Representative image of how the required properties were attained. **c. and d.** Representative images of well coated (2.5% PVA; 25  $\mu\text{m}$ -chip) junction (c.) and post-junction channel (d.), highlighting double emulsions (white arrows) and octanol droplets (black arrows).

2.5% (v/v) PVA worked well for the 25  $\mu\text{m}$ -chip (Figure 3.13.c. and d.), but it was found to clog the smallest channels of the 13  $\mu\text{m}$ -chip. It was then replaced by 1% (v/v) PVA without negatively affecting the coating quality (Table 3.5).

**Table 3.5.** Results of varying surfactant concentration in double emulsion production

Variables	Design 1		
Height ( $\mu\text{m}$ )	25	X	X
Coating	2,5% PVA	X	
	1% PVA		X
Results	DEs	X	X

## II. Inner Solution (IA) and Outer Solution (OA) compositions

Surfactant concentrations (5% and 0.5%) were tested in the OA. The concentration of 5% of P188 was found to make pinching the DEs difficult. It gives an "elastic" behaviour to the LO, making it stretch far from the junction before being pinched, affecting the droplets' stability and monodispersity. Then, P188 was reduced to 0.5% (v/v) and this concentration proved to be sufficient to produce stable double emulsions (Table 3.6), being kept henceforth.

Next, a density gradient was tested. The goal was to make the double emulsions sink to the bottom of the channel and collection vial by making them denser than the outer solution. This would increase the shear stress with the floor of the channel while DEs were still inside the chip and promote dewetting on the collection vial by forcing the octanol, which has a lower density, to detach and float to the surface. Thus, 100mM sucrose was added to the IA and 100 mM glucose was added to the OA (Table 3.6). However, the production was not stable enough to obtain DEs.

**Table 3.6.** Results of varying the composition of the inner and outer phases in double emulsion production. Controls use the standard solutions stated previously.

Variables	Design 1				
Height (µm)	13				X
	25	X	X	X	
Inner Aqueous Solution	15% Glycerol	X	X		X
	15% glycerol + 100mM Sucrose			X	
Outer Aqueous Solution	15% Glycerol + 5% P188	X			X
	15% Glycerol + 0.5% P188		X		
	15% Glycerol + 0.5% P188 + 100mM Glucose			X	
Results	DEs	-	X	-	-

### III. Lipid-Oil (LO) Solution composition

One of the interesting potential outcomes of using this chip was to investigate the formation of GUVs templated from DEs. The decrease in the pluronic surfactant was aligned with the market trend and literature review that pointed toward more biocompatible systems. In the same light, several concentrations of lipids were tested to investigate whether an increase in lipid concentration (from 2.54 mM to 5 mM, 6.5 mM and 7.3 mM) combined with the decrease in P188 (from 5% to 0.5%) would lead to octanol dewetting (Table 3.7). DEs were successfully produced with all concentrations of lipid except the highest (7.3mM) in the 25  $\mu\text{m}$ -chip, but no dewetting was observed. Based on the rationale presented in the publication of Design 3<sup>38</sup>, the concentration of 6.5 mM DOPC was chosen for the follow-up experiments.

**Table 3.7.** Results of varying lipid concentrations in double emulsion production

Variables	Design 1					
Height ( $\mu\text{m}$ )	25	X	X	X	X	
	13					X
Lipid-Oil Phase	2.54mM DOPC in octanol	X				X
	5mM DOPC in octanol		X			
	6.5mM DOPC in octanol			X		
	7.3mM DOPC in octanol				X	
Results	DEs	X	X	X	-	-
	GUVs	-	-	-	-	-

Next, the presence or absence of Dil, a lipid-specific dye, was tested. The goal was to test if the stain affected the stability of the double emulsions or prevented dewetting. With or without Dil, DEs were produced and collected in the 25  $\mu\text{m}$ -chip, but no dewetting was observed, indicating the presence of Dil had a negligible effect (Table 3.8).

**Table 3.8.** Results of addition of lipid-specific dye, Dil, to the intermediate phase in double emulsion production

<b>Variables</b>	<b>Design 1</b>			
<b>Height (<math>\mu\text{m}</math>)</b>	<b>25</b>	X	X	
	<b>13</b>			X
<b>Stain</b>	<b>Dil</b>		X	
<b>Results</b>	<b>DEs</b>	X	X	-
	<b>GUVs</b>	-	-	-

#### IV. Physical Parameters

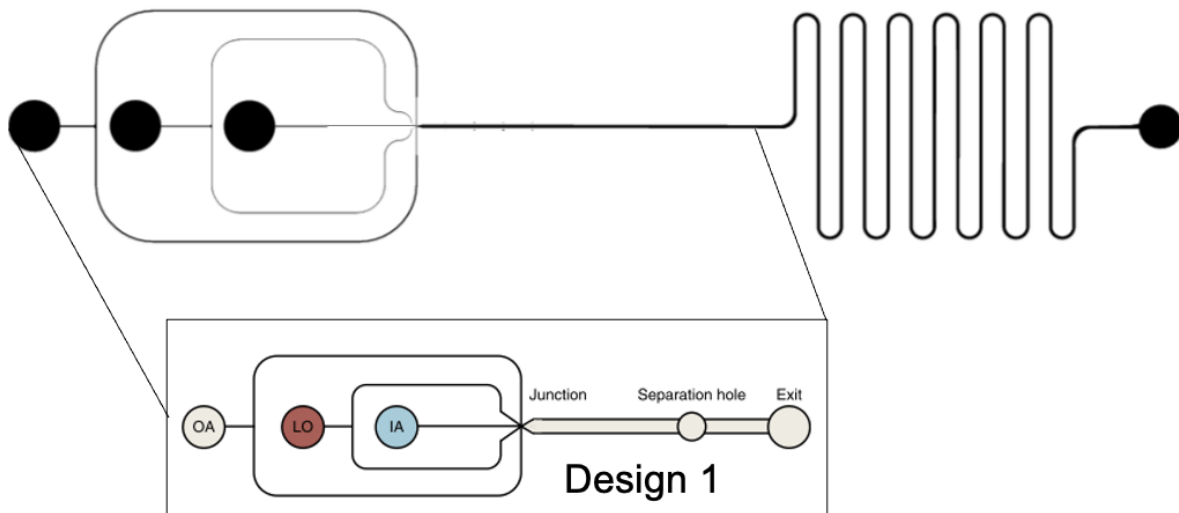
Besides requiring high pressures to be formed, it was observed that in some cases DE production was stable at the junction, but DEs would burst before reaching the outlet. To investigate the role of resistance in the system, two diameters of the outlet were tested (1 mm and 4 mm). DEs were only successfully produced and collected with the 4 mm outlet diameter and the 25  $\mu\text{m}$ -chip (Table 3.9), suggesting that a higher resistance of the system (1 mm outlet) was negatively affecting DE stabilisation during and after production.

**Table 3.9.** Results of changing the resistance of the system in double emulsion production

<b>Variables</b>	<b>Design 1</b>				
<b>Height (<math>\mu\text{m}</math>)</b>	<b>25</b>	X	X		
	<b>13</b>			X	X
<b>Outlet</b>	<b>1mm</b>	X		X	
	<b>4mm</b>		X		X
<b>Results</b>	<b>Stable DEs</b>	-	X	-	-

The lower resistance of the 4 mm outlet allowed stable production and collection of DEs, but the pressures remained high. Consequently, DEs did not have enough time inside the post-junction channel for the octanol to dewet. To compensate, the length of the post-junction channel was modified. A serpentine (100 or 200  $\mu\text{m}$  in width) was added to the end of the chip (Figure 3.14).

## Design 1.2



**Figure 3.14.** Design 1.2 was adapted from Design 1 (inset) to improve the dewetting of the octanol by allowing the DEs to stay longer in contact with the post-junction channel.

SU-8 2050 and 2025 have the same resolution ( $>10:1$  aspect ratio) but are indicated for different channel heights (40 and 20  $\mu\text{m}$ , respectively). The chips produced with SU-8 2050 had larger widths than the photomask (IA: 50%; LO: 25%; OA: 10%) and a height of 35.8  $\mu\text{m}$ , consistent with the properties of the photoresist. Chips produced with SU-8 2025 also had larger widths for IA and LO (IA: 78.5%; LO: 28.75%) and a smaller width for OA (13% smaller). The height was consistent with the resolution of the photoresist (27.3  $\mu\text{m}$ ). In both cases, the serpentine was 7% larger than the photomask dimensions. SU-8 3010 has a better resolution ( $>5:1$  aspect ratio) and is intended for smaller heights (around 10  $\mu\text{m}$ ), resulting in chips with smaller channels (IA: -24%; LO: -37%; OA: -61%; serpentine: -3%). The smallest achievable height was 13  $\mu\text{m}$ , as the soft lithography chips from Design 1 (Table 3.10). To remain comparable to the previous experiments, chips with heights of 25  $\mu\text{m}$  and 13  $\mu\text{m}$  were investigated.

**Table 3.10.** The widths and heights obtained from different SU-8 resins compared to the desired measures.

<b>Channels</b>	<b>Design 1<sup>27</sup></b>	<b>Design 1.2. Photomask 100 (adapted from Design 1)</b>	<b>Design 1.2. Photomask 200 (adapted from Design 1)</b>	<b>SU-8 2050 (Photomask 100)</b>	<b>SU-8 2025 (Photomask 100)</b>	<b>SU-8 3010 (Photomask 200)</b>
IA Junction ( $\mu\text{m}$ )	10	10	10	15	17.4	7.6
LO Junction ( $\mu\text{m}$ )	5.4	8	8	10	10.3	5.1
OA Junction ( $\mu\text{m}$ )	10	10	10	11	8.7	3.9
Post-Junction ( $\mu\text{m}$ )	200	100	200	100.2	97.4	194.4
Height ( $\mu\text{m}$ )	11	-	-	35.8	27.3	13.1
Serpentine ( $\mu\text{m}$ )	-	100	200	107.2	107	194

The new design proved difficult to surface treat, as PVA attached to the turns of the serpentine, rendering it impossible to clear the channels after treatment. Thus, it was not possible to achieve a uniform coating. For 25  $\mu\text{m}$ -chips, the post-junction channel was easier to coat; however, higher pressures were required to cover the full extent of the serpentine while preventing PVA from staying attached to the walls. Consequently, it was harder to properly coat the junction, as the larger dimensions decreased the resistance, and PVA invaded the hydrophobic areas. Only the 13  $\mu\text{m}$ -chips had properly coated junctions and were tested. The post-junction channels had remnants of PVA near the turns due to the capillarity effects of the small channel combined with the viscosity of the coating solution, but they were not blocked. Hence, the post-junction channel was hydrophilic, allowing tests to be performed (Table 3.11).

**Table 3.11.** Results of varying surface treatment concentration in the double emulsion production in Design 1.2.

<b>Variables</b>	<b>Design 1.2.</b>		
<b>Height (um)</b>	<b>13</b>	X	X
<b>Coating</b>	<b>2,5% PVA</b>	X	
	<b>1% PVA</b>		X
<b>Inner Aqueous Solution</b>	<b>15% Glycerol</b>	X	X
<b>Lipid-Oil Phase</b>	<b>2,54 mM DOPC in octanol</b>	X	X
<b>Outer Aqueous Solution</b>	<b>15% Glycerol + 0,5% P188</b>	X	X
<b>Outlet</b>	<b>4mm</b>	X	X
<b>Results</b>	<b>Stable DEs</b>	-	-
	<b>GUVs</b>	-	-

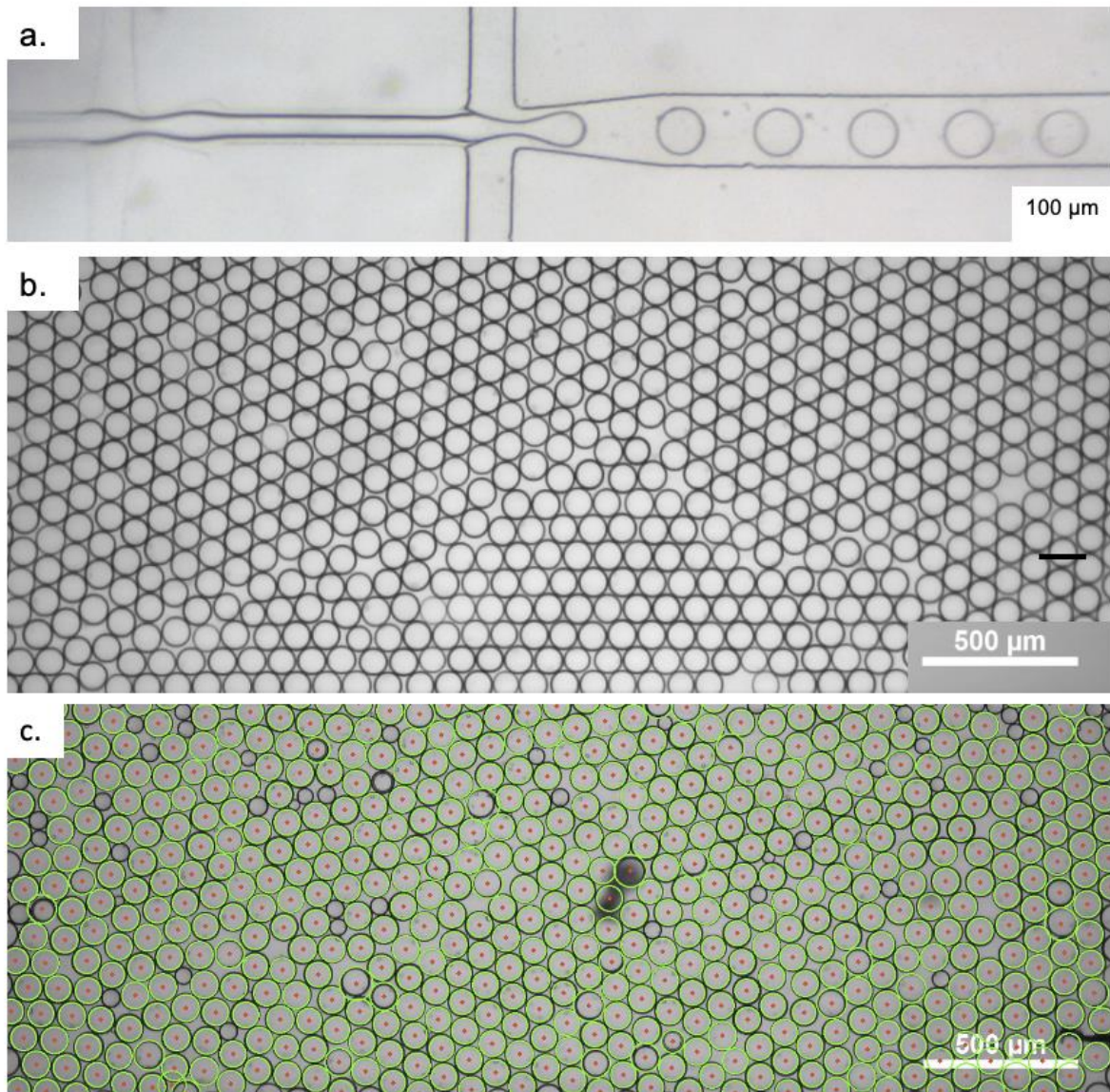
Given the difficulty in coating the device, the only difference between the two tested chips was the coating solution concentration. The remnants of the PVA solution along the serpentine likely caused instabilities at the junction because the stable production of double emulsions was not achieved.

### 3.3.3.4. DE production with Design 2

Given the challenges of producing complex compartments using Design 1, a different chip was investigated. Design 2<sup>42</sup> is intended mainly for the production of DEs, as its post-junction channel is too short to allow dewetting to take place (GUVs must be templated from DEs using further steps off-chip). Following results from previous design, the standard solutions were defined as IA: 15% (v/v) glycerol in water; LO: 6.5mM DOPC in octanol; and OA: 15% (v/v) glycerol and 0.5% P188. The double-junction design provided increased control over the fluids (pressures ranging from 25 to 35 mbar for the IA; 35 to 45 mbar for the LO; and 70 mbar for the OA solution). The solutions were driven to the first junction, where the IA solution was enveloped by the LO solution, and then to the second junction, where the OA solution pinched the DEs with a very thin layer of oil (Figure 3.15.a.). Large numbers of monodisperse thin-oil shell DEs were produced and collected (Figure 3.15.b). The oil shell was about 2.6  $\mu\text{m}$  in thickness ( $\pm 0.7 \mu\text{m}$ ,  $n=195$  DEs), representing about 5.9% of the total radius and 16% of the total volume of the double emulsion<sup>47</sup>. The size and number of DEs were automatically



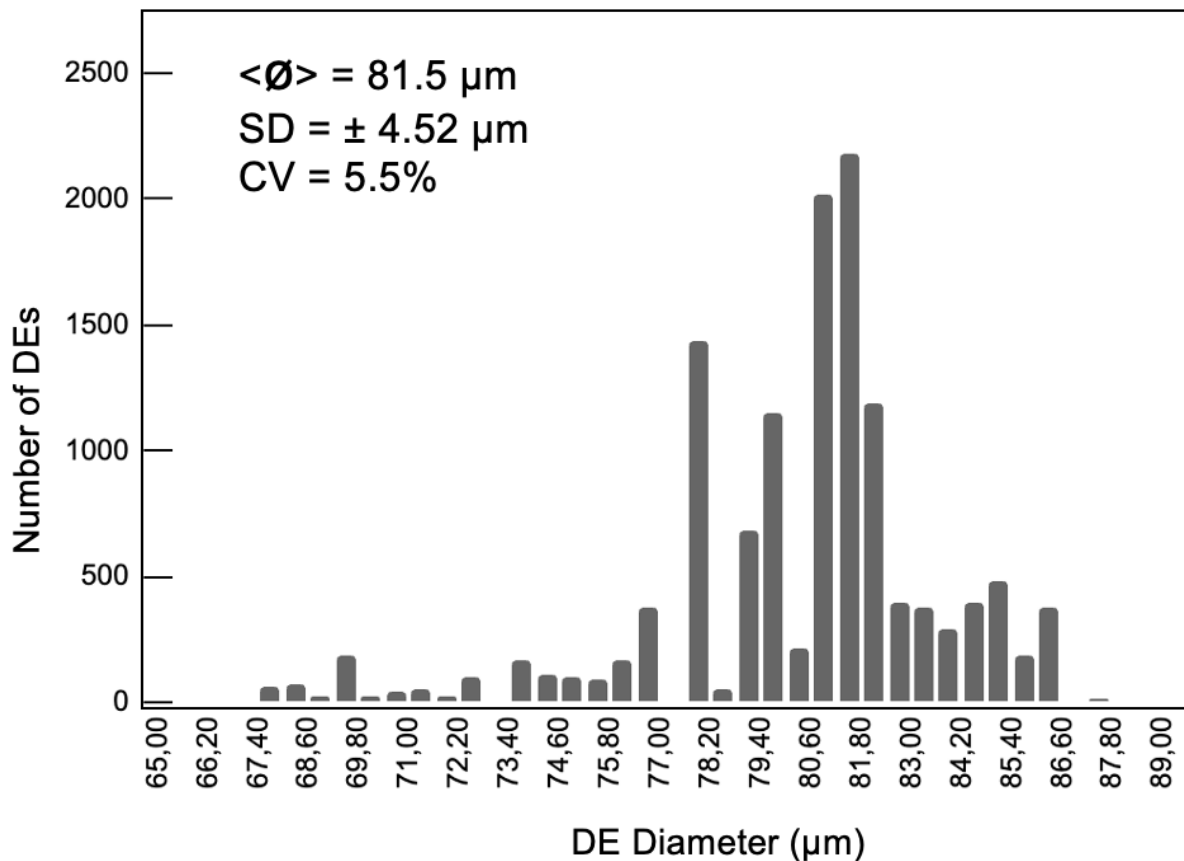
calculated by a Python script developed in-house. This script readily differentiated between DEs and oil droplets (Figure 3.15.c.).



**Figure 3.15.** Double emulsion production with Design 2. **a.** at the junction (IA: 15% glycerol; LO: 6.5 mM DOPC in octanol; OA: 15% glycerol and 0.5% P188). **b.** Representative image of the collected DEs. Double emulsions were approximately 80 μm in diameter (SD ±4.52 μm). **c.** Representative image of the Python script output, highlighting the efficacy in excluding the oil droplets from the analysis.

The production rate of DEs was 233 Hz which translates to more than 800,000 DEs per hour. DE diameter was 81.5 μm (±4.52 μm SD; total number of DEs =14,750) (Figure 3.16), resulting in a CV of 5.5%, a considerable improvement from Design 1 (CV = 15.3%). Besides the size of the nozzle, the ratio between the pressures directly impacts the size of DEs. The pressure on the inner channel determines how much of the inner phase occupies the lumen, the

pressure on the intermediate channel determines the thickness of the membrane, and the pressure on the outer channel determines how quickly the droplets are pinched, i.e. a faster pinching results in smaller droplets. There is a fine balance between these three forces, and any change in mid-production can affect the overall CV of that batch.



**Figure 3.16.** Microfluidic DEs size characterisation. Size distribution of DEs diameters in  $\mu\text{m}$  ( $\langle \phi \rangle = 81.5 \mu\text{m}$ ,  $\pm 4.53 \mu\text{m}$ ; total number of DEs = 14,750). CV, coefficient of variation

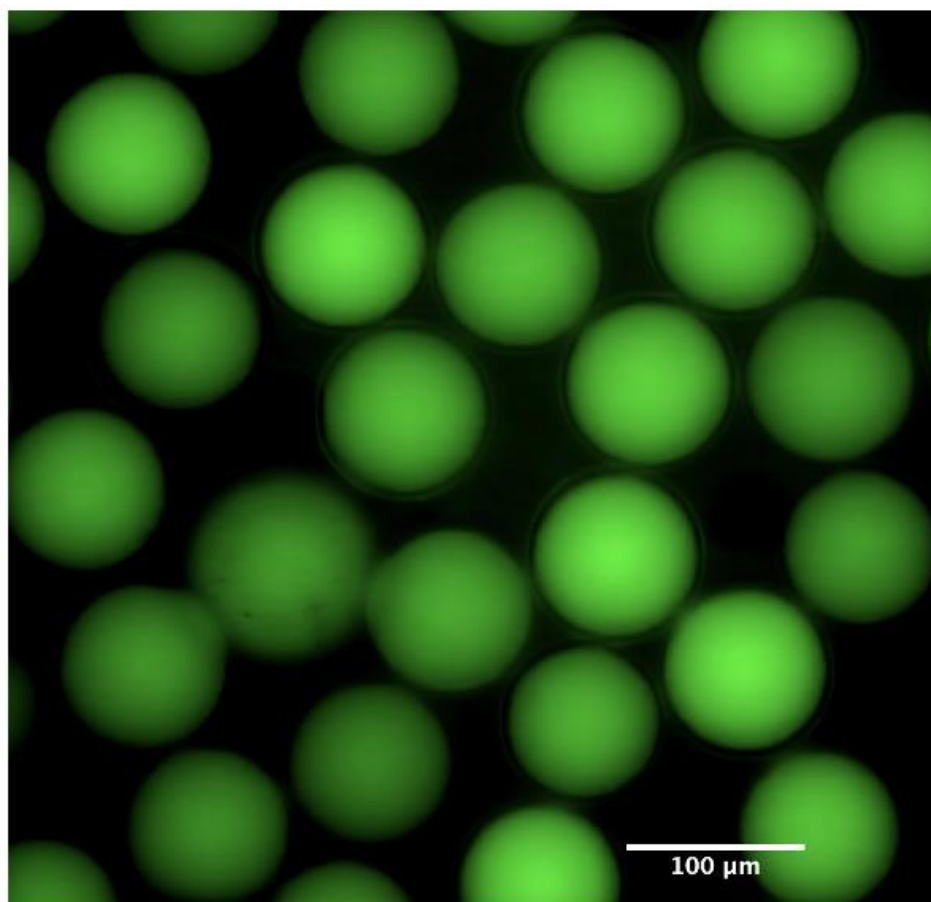
The stable production of double emulsions was successfully achieved in all tested conditions (Table 3.12). All devices had 50- $\mu\text{m}$  high channels with  $\phi = 1\text{mm}$  outlets and were coated with 2.5% PVA. As with Design 1, different concentrations of DOPC were tested for improved stability, with 6.5 mM being selected based on the literature<sup>38</sup>. The surfactant concentration in the OA, P188, was also tested with the same goal. Consistent with Design 1, the standard concentration of 5% made pinching more difficult, so the concentration of 0.5% was kept for the following experiments. In certain cases, the lipid-specific Dil was added to stain the

intermediate phase. The increased flexibility and reproducibility of Design 2 allowed the production and collection of DEs using only pure water as the IA and OA, decreasing the number of required additives for stability and considerably improving the biocompatibility of the formulation.

**Table 3.12.** Summary of tested variables and respective results of Design 2.

<b>Variables</b>	<b>Design 2</b>							
<b>Height (µm)</b>	<b>50</b>	X	X	X	X	X	X	X
<b>Coating</b>	<b>2.5% PVA</b>	X	X	X	X	X	X	X
<b>Inner Aqueous Solution</b>	<b>15% Glycerol</b>	X	X	X				X
	<b>H2O</b>				X			
	<b>Phenol Red</b>					X		
	<b>Calcein</b>						X	
<b>Lipid-Oil Phase</b>	<b>2.54mM DOPC in octanol</b>	X						
	<b>5mM DOPC in octanol</b>		X					
	<b>6.5mM DOPC in octanol</b>			X	X	X	X	X
<b>Outer Aqueous Solution</b>	<b>15% Glycerol + 0.5% P188</b>	X	X	X		X	X	
	<b>15% Glycerol + 5% P188</b>							X
	<b>H2O</b>				X			
<b>Stain</b>	<b>Dil</b>	-	-	-	-	-	X	-
<b>Outlet</b>								
	<b>1mm</b>	X	X	X	X	X	X	X
<b>Results</b>	<b>Stable DEs</b>	X	X	X	X	X	X	X

The reproducible production of DEs allowed the encapsulation of compounds of interest. Thus, the encapsulation of (0.3mM) calcein (Figure 3.17) and (0.32mg/ml) phenol red (Figure 3.18) was performed.



**Figure 3.17.** Encapsulation of calcein (0.3mM) in DEs produced with Design 2 (green: ex/em 470/525 nm).

The encapsulation efficiency of unloaded double emulsions, i.e. 15% glycerol in water, and loaded, i.e. calcein, is comparable (88%), although the production rate for DEs loaded with calcein was about 39% of that of the control (Table 3.13).

**Table 3.13.** Encapsulation efficiencies and production rates of unloaded DEs and loaded DEs

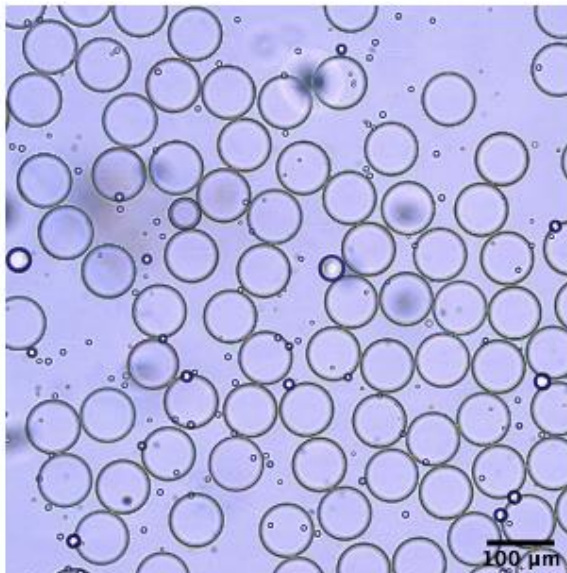
	Control	Calcein
Encapsulation Efficiency	88.13%	88.03%
Production Rate (DEs/s)	232.7	90.5

### a. Membrane Permeability Assay

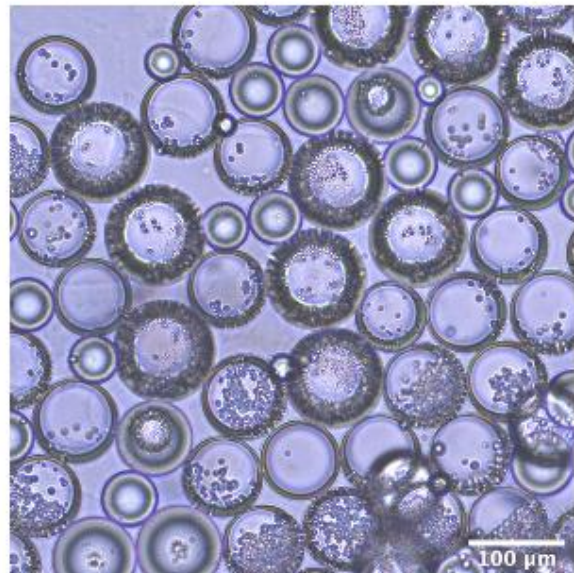
Previous reports have shown that the oil, when in small quantities, can organise in domains in the membrane<sup>51</sup>. In other words, the octanol could be arranged in domains between patches

of lipid bilayer instead of all around the surface area, affecting the membrane's permeability. A permeability assay was performed to clarify the distribution of oil in the membrane. DEs encapsulating Phenol Red were exposed to 1M NaOH. If the oil was uniformly distributed around the membrane, it was expected that water from inside the DEs would try to move across the membrane due to the osmotic gradient. If octanol were arranged in domains,  $H^+$  ions would leave the inner aqueous phase through the lipid bilayer patches due to the pH gradient caused by the  $OH^-$ , increasing the pH inside the DE and changing the colour of Phenol Red (Figure 3.18.a.). Once exposed to 1M NaOH, the intermediate phase of DEs was seen to swell and form minute droplets at the interface of the phases (Figure 3.18.b.). This behaviour was characterised as the formation of a multisome<sup>52</sup>, suggesting that the octanol was uniformly distributed in the membrane.

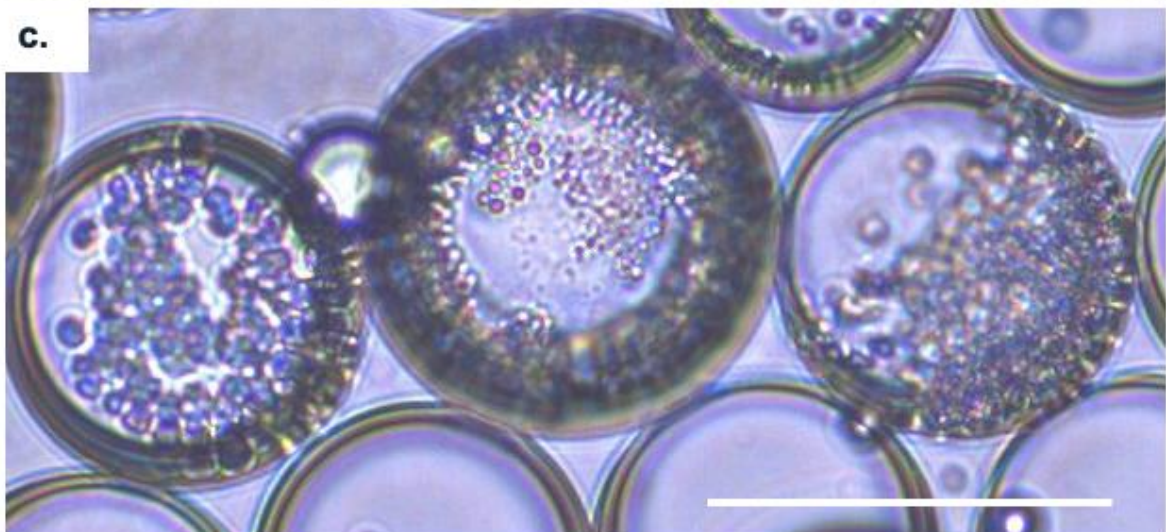
**a.** Before addition of 1M NaOH



**b.** After addition of 1M NaOH



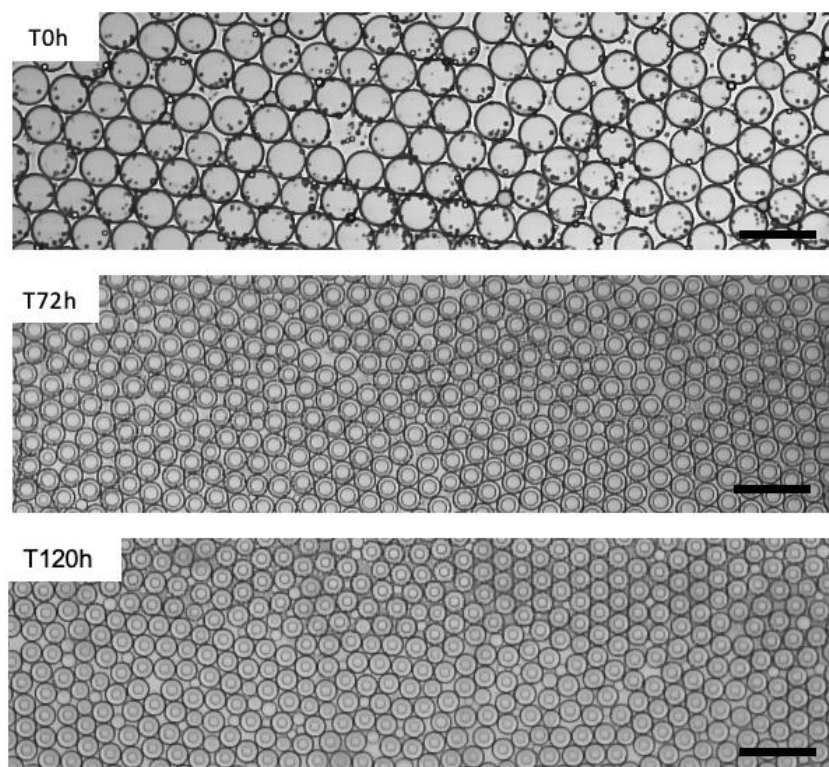
**c.**



**Figure 3.18.** Membrane Permeability Assay **a.** DEs before and after **(b.)** addition of 1M NaOH. **c.** Expanded view of DEs after exposure. Scale bar, 100  $\mu\text{m}$ .

## b. Off-chip dewetting

Following the successful and reproducible production of DEs and the probing of membrane permeability, the next step was investigating the possibility of off-chip octanol dewetting for the formation of GUVs. Based on a report that observed off-chip dewetting of octanol in the collection vial<sup>38</sup>, the off-chip dewetting was designed to take advantage of the partial miscibility of octanol in water<sup>24</sup>. It was expected that the more thermodynamically favoured arrangement of the lipids in bilayers, combined with the partial miscibility of the octanol in water, would promote a slow dewetting with the thinning of the membrane, similar to that seen for oleic acid and ethanol<sup>42</sup>. Here, DEs were collected into an observation chamber filled with the outer solution and observed for 120h. The membrane thickness increased over time, while the volume of the inner phase decreased (Figure 3.19). Immediately after production ( $t=0\text{h}$ ), the intermediate phase was 2.6  $\mu\text{m}$  in thickness ( $\pm 0.7 \mu\text{m}$  SD,  $n=195$  DEs) and, after 5 days, the thickness of the intermediate phase showed a 4-fold increase ( $12.11 \pm 1.4 \mu\text{m}$ , SD). The DE mean external radius decreased 36% in the observed period.

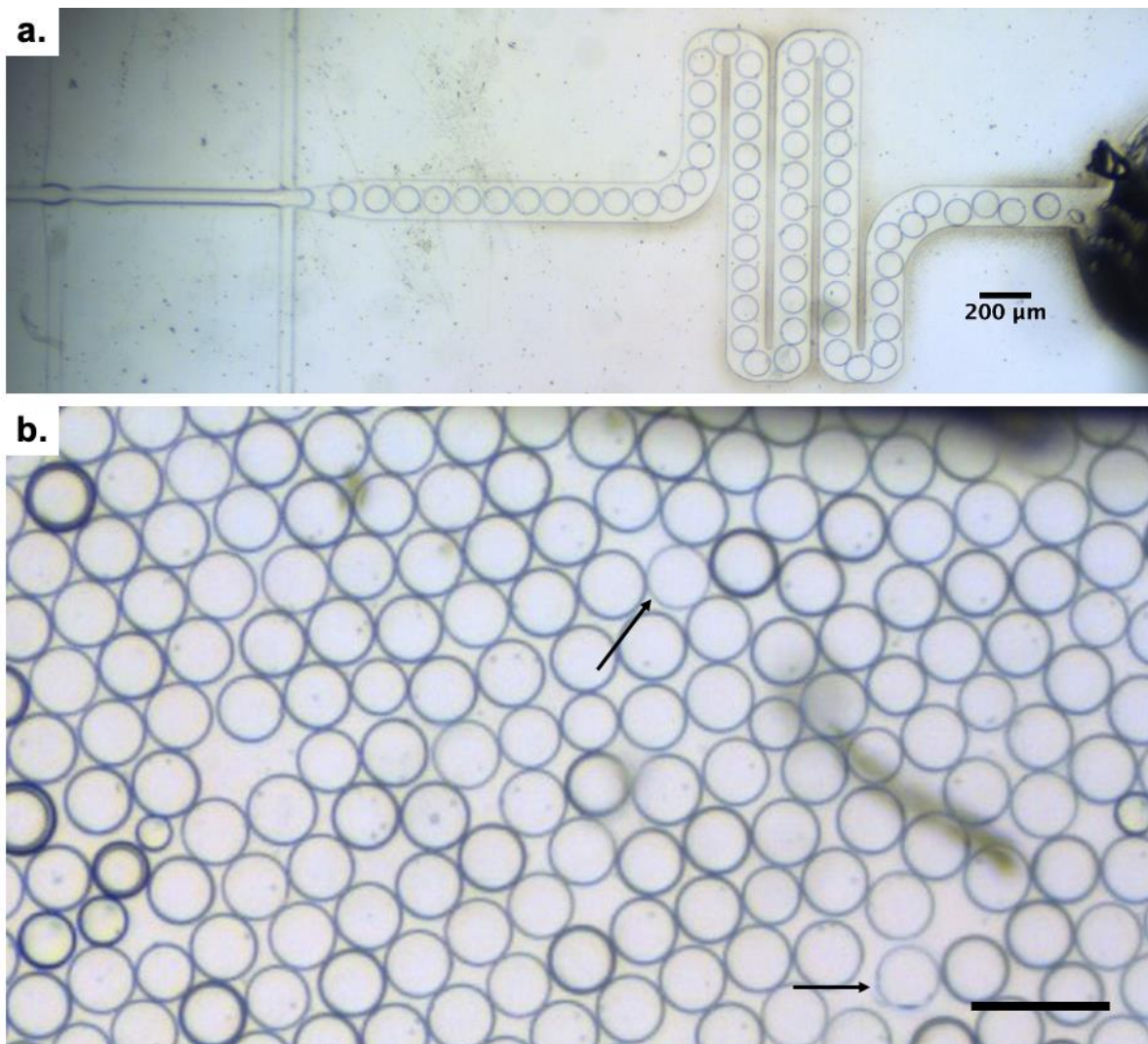


**Figure 3.19.** Off-chip octanol dewetting assay. DEs were placed in an observation chamber surrounded by the outer phase. The intermediate phase was seen to increase substantially in thickness while DE sizes decreased.

This swelling is likely to be a result of a diffusion-based migration of water molecules from the inner phase into the membrane due to the partial miscibility of octanol in water. However, it does not characterise dewetting, or the formation of GUVs, as the octanol molecules remained in between the lipid molecules, preventing the formation of the lipid bilayer. The decrease in size of the inner phase, and overall DE, is likely due to the transport across the membrane.

### **3.3.3.5. DE production with Design 3**

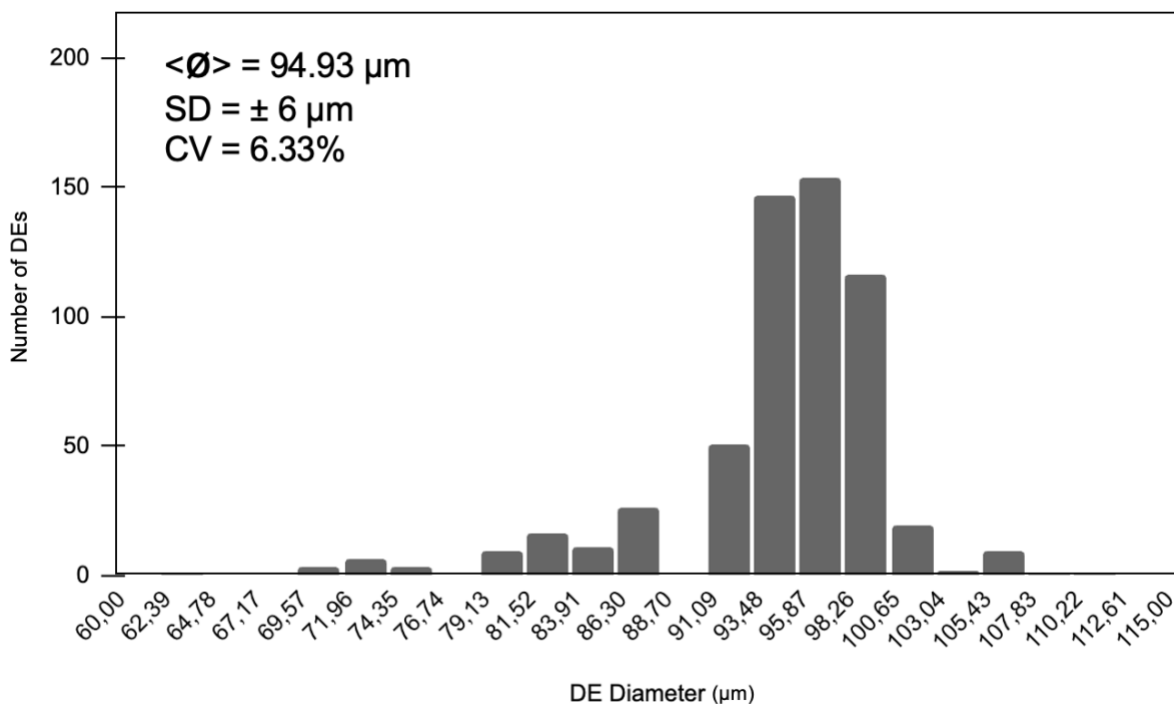
The increased level of control over the fluids provided by the double junction considerably improved DE production and reproducibility of Design 2 over Design 1. However, it did not allow on-chip dewetting to form GUVs. A third chip design combining elements of improved DE production and a serpentine to promote on-chip dewetting of octanol (Design 3) was then tested<sup>38</sup>. These microfluidic devices were kindly provided by Dr Tom Robinson's lab (MaxSynBio, MPI, Potsdam, Germany). Here, the solutions of IA, LO, OA were used with the previous modifications (IA: 15% (v/v) glycerol in water; LO: 6.5 mM DOPC in octanol; and OA: 15% (v/v) glycerol and 0.5% P188). The stable production of DEs within acceptable pressure ranges (IA: 30 to 50 mbar; LO: 40 to 50 mbar; and OA: 30 to 60 mbar) was successfully achieved (Figure 3.20).



**Figure 3.20.** Double emulsion production with Design 3. **a.** at the junction (IA: 15% glycerol; LO: 6.5mM DOPC in octanol; OA: 15% glycerol and 0.5% P188). **b.** Representative image of the collected DEs. Black arrows indicate DEs with thinner membrane. Scale bar, 200 μm.

DEs produced with Design 3 were larger ( $94.95 \mu\text{m}$ ,  $\pm 6 \mu\text{m}$  SD, 575 DEs; Design 1:  $41.6 \mu\text{m}$ ,  $\pm 6.3 \mu\text{m}$ ; Design 2:  $81.5 \mu\text{m}$ ,  $\pm 4.52 \mu\text{m}$ ) than DEs produced with Design 2 (with comparable nozzle dimensions) as expected as the highest OA pressure used was 60 mbar, and pressure directly impacts the size (Figure 3.21). The populations were nearly monodisperse (6.33, CV). However, no evidence of dewetting was seen, even if several DEs appeared to have very thin membranes (Figure 3.20.b., black arrows).





**Figure 3.21.** Size distribution of DEs produced with Design 3.

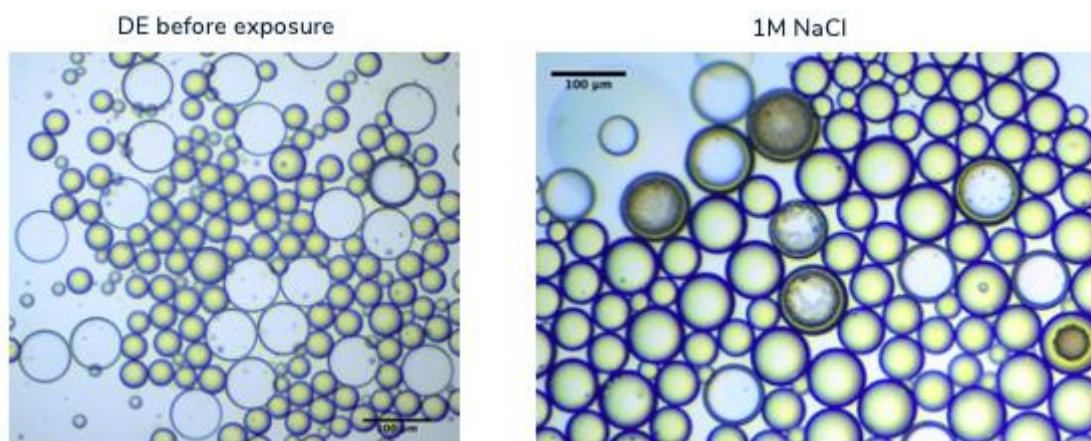
To compare with Design 2, pure water was employed as the inner and outer solutions. However, while DEs were successfully produced with the standard solutions (IA: 15% (v/v) glycerol in water; LO: 6.5 mM DOPC in octanol; and OA: 15% (v/v) glycerol and 0.5% P188), the production was unsuccessful with water as the IA and OA phases (Table 3.14).

**Table 3.14.** Summary of tested variables and respective results of Design 3.

Variables	Design 3		
Height (μm)	50	X	X
Coating	PDMMAC/PSS	X	X
Inner Aqueous Solution	15% Glycerol	X	
	H2O		X
Lipid-Oil Phase	6.5mM DOPC in octanol	X	X
Outer Aqueous Solution	15% Glycerol + 0.5% P188	X	
	H2O		X
Outlet	0.7mm	X	X
Results	Stable DEs	X	-

## a. Membrane Permeability Assay

As no dewetting was observed, a membrane permeability assay was performed to test for the presence of octanol in the membrane. The assay followed the same principle of the one performed in Design 2 (Section 3.3.3.4.a.): upon creating an osmotic gradient in the outer phase, the formation of multisomes would be seen if octanol was uniformly distributed. If no change was seen, further experiments would be required to determine if octanol was absent or organised in domains. Thus, DEs were exposed to 1 M NaCl (Figure 3.22). The swelling of the octanol layer and formation of minute water droplets was clearly seen at the interface after exposure, indicating the presence of uniformly distributed octanol in the membrane of DEs produced by Design 3.



**Figure 3.22.** Membrane permeability assay. Before and after images of DEs exposed to 1M NaCl. The swelling of the intermediate phase and the formation of minute water droplets indicated that octanol was uniformly distributed around the membrane.

## 3.4. Discussion

### 3.4.1. DEs were successfully produced in non-specialist settings

Although the modified chemical and physical properties were described as separated variables for clarity, they are, in fact, interdependent; one of the reasons why double emulsions are considered one of the most challenging compartments to produce<sup>53</sup>. Double emulsions were only successfully produced and collected from the ensemble of tested variables in four

instances using Design 1 (Table 3.5, Table 3.6, Table 3.7, Table 3.8). Although stable DEs were produced, the production presented instabilities that affected the size distribution and the CV (15.3%) of the collected populations. These instabilities were likely related to the high pressures required to achieve DE production and the accumulation of lipids in the corners of the LO channel. These experiments were all made in the 25  $\mu\text{m}$ -high chip, with the IA containing only 15% (w/v) glycerol, OA, 15% glycerol and 0.5% P188, with a range of amphiphile concentrations. These chips were punched with the large outlet (4 mm), and the decrease in overall resistance proved beneficial. Moreover, DEs were stably made in the presence or absence of Dil, indicating that the dye did not interfere with the arrangement of the lipids.

Monodisperse (CV, 5.5%) DEs in large quantities (233 Hz) were produced in a reproducible manner with Design 2. Chips were produced with standard photolithography and soft lithography techniques without a cleanroom, suitable for non-specialists. Several solution compositions were employed with success, including pure water, aligned with the current trend toward additive-free formulations and the market insights into biocompatibility. Compounds of interest were also readily encapsulated (calcein, encap. effic. 88%).

Design 3 substantially improved the experimental handling. The simple rearrangement of the positions between inlets and the outlet considerably facilitated the surface coating treatment, forgoing the need to use positive pressure to block the hydrophobic channels and significantly decreasing the chances of rendering the chip unusable. The addition of the serpentine in the IA channel improved flow stability with a clear impact on the easiness of achieving DE production, requiring less time to adjust the pressure balance. The main limitation of this design is the propensity for clogging. The constrictions at the turns make it easier for unwanted particles to remain blocked, disrupting the post-junction channel, bursting the DEs before collection and destabilising the flow at the junction. The instabilities require pressure adjustments that cause variations in size, resulting in quasi-monodisperse population (CV, 6.3%).

### **3.4.2. No dewetting was observed**

In none of these cases, however, did the dewetting process occur, so no GUVs were produced. As previously noted, Bao *et al.*<sup>54</sup> successfully triggered the dewetting of DEs in 25- $\mu\text{m}$  high chips adapted from Design 1 at high production rates. The authors used a very high concentration of lipids (19 mM) to achieve it. As other authors<sup>38,48,55,56</sup> achieved the same

outcome with considerably lower concentrations, it was decided not to pursue this approach. The higher pressures required to achieve DE production substantially reduced the time that the DEs spent inside the channels (from 5-8 minutes to just seconds)<sup>27</sup>, justifying the addition of the serpentine at the end of the post-junction channel. A similar approach was employed previously using an external serpentine device to flow the DEs in and promote dewetting<sup>56</sup>. However, they also reported that the process was not efficient, with several GUVs being collected with a prominent octanol droplet attached, so dewetting was not complete. Here, the goal was to produce double emulsions with the same high pressures but give them enough time inside the chip to dewet. Other authors continue to report challenges with the dewetting of the octanol and have resorted to extra post-production steps, such as osmotic gradients<sup>41</sup>, or modifications in the solution compositions, such as higher lipid concentrations<sup>54,57</sup>, to promote or trigger the process.

For Design 1, the fabrication method and chip dimensions were the main differences between the published protocol and the experiments performed in this work. The authors used e-beam lithography to produce the molds, instead of photolithography, which confers a higher level of precision to the chips<sup>43,44,58</sup>, differing in achievable resolution and the "sharpness" of the edges. This difference in geometry may be a sufficient barrier to octanol dewetting and liposome formation. The sharper edges might have promoted better pinching of the double emulsions and enhanced the stability of the production, allowing for lower pressures to be applied. Nevertheless, e-beam lithography requires highly specialised equipment, rendering it inaccessible for non-specialists. Considering the market interest of non-specialists in encapsulation-in-droplet, achieving stable complex microcompartment production with more accessible techniques, such as soft lithography, is paramount.

The main drawback of Design 2 is the need to perform off-chip dewetting when the desired outcome is to produce GUVs. Teh *et al.*<sup>42</sup> reported in 2011 a solvent-extraction method to produce liposomes templated from double emulsions. The principle of liposome formation relied on the high solubility of oleic acid in ethanol. The oleic acid slowly left the intermediate phase of the DE by dissolving into the ethanol, which in turn evaporated and left the oleic acid floating on top of the outer phase. This process lasted 15 hours. Krafft *et al.*<sup>41</sup> successfully reproduced the protocol and promoted the dewetting by osmotic gradient instead of dilution in ethanol, as ethanol might be harmful to encapsulated molecules, hindering the biocompatibility of the protocol. Here, a new off-chip method was explored, based on the partial miscibility of octanol in water<sup>59</sup> and a reported off-chip dewetting of octanol<sup>38</sup>. Instead of dewetting, the membrane thickness increased 4-fold in the observed period (120h), possibly due to the migration of water molecules from the inner aqueous phase.

The substantial decrease in pluronic surfactant and the increase in lipid concentration characterised the DEs produced in this work as lipid-stabilised DEs, *i.e.* the main stabilising surfactant is a naturally occurring amphiphile, a phospholipid. Lipid-stabilised DEs present the same transport characteristics as other types of DEs, as lipids are also surfactants. The transport happens *via* minute aqueous droplets, surrounded by surfactant molecules. The amphiphilic nature of the surfactants allows the water droplets to cross the oil membrane<sup>23,60</sup>. However, when lipid-stabilised DEs are exposed to osmotic pressure, this behaviour is exacerbated. As the water tries to leave the inner droplet to compensate for the osmotic gradient in the exterior, it forms water droplets surrounded by lipid bilayers that remain at the DE interface with the outer solution. These complex structures are called multisomes<sup>52,53,61</sup> and were used to understand that octanol is uniformly distributed around the membrane. Overall, Design 2 demonstrated to be an excellent method to reproducibly produce and encapsulate compounds of interest in complex microcompartments, such as double emulsions, with high encapsulation efficiency.

The forces governing the dewetting of octanol for the membrane of GUV templated DEs are not yet clear. Shear stress and osmotic gradients have been used to trigger a process that is said to be spontaneous<sup>24,38,54</sup>. Further work should focus on characterising this process. Meanwhile, current strategies, such as the serpentine to increase shear stress and time in contact with channel walls, seem promising.

### **3.5. Conclusion and Outlook**

Microcompartments of varying levels of complexity, *i.e.* single and double emulsions, were successfully produced with several designs in non-specialist settings, *i.e.* standard photolithography and soft lithography techniques without a cleanroom. Design 1 was modified to be better aligned with the market insights from Chapter 2. Double emulsions were produced but populations were polydisperse due to instabilities at the junction. Dewetting of the octanol did not occur because DEs did not stay sufficient time inside the post-junction channel. Design 2 was the best for the production of double emulsions, providing great flexibility in the composition of the solutions and allowing reproducible encapsulation of different compounds of interest. However, the dewetting has to be triggered off-chip, adding an extra step of complexity. Design 3 is based on a combination of Designs 1 and 2. It uses the chemical parameters of Design 1, with adjustments, and a modified version of the Design 2 geometry. It was the fastest to achieve double emulsion production within expected pressure ranges, and

the geometry modifications improved the surface coating treatment and flow stability. The dewetting was expected to happen on-chip, although it was not observed. Further work would benefit from a better understanding of the underlying forces governing the dewetting of octanol from lipid membranes. This work renders the production of complex compartments, and especially the encapsulation of compounds of interest, more accessible, aligned with the "starter pack" approach of the product in Chapter 2. The microcompartments produced here can be used in several biological applications, such as for single-cell analysis or drug delivery systems, as will be explored in Chapter 4.

### 3.6. References

1. Fendler, J. H. *Membrane Mimetic Chemistry*. Wiley, New York (1982).
2. Ringsdorf, H., Schlarb, B. & Venzmer, J. Molecular Architecture and Function of Polymeric Oriented Systems: Models for the Study of Organization, Surface Recognition, and Dynamics of Biomembranes. *Angew. Chemie Int. Ed. English* **27**, 113–158 (1988).
3. Walde, P., Cosentino, K., Engel, H. & Stano, P. Giant Vesicles: Preparations and Applications. *ChemBioChem* **11**, 848–865 (2010).
4. Walde, P., Umakoshi, H., Stano, P. & Mavelli, F. Emergent properties arising from the assembly of amphiphiles. Artificial vesicle membranes as reaction promoters and regulators. *Chem. Commun.* **50**, 10177–10197 (2014).
5. Rothman, J. E. & Wieland, F. T. Protein Sorting by Transport Vesicles. *Science (80-. )*. **272**, 227–234 (1996).
6. Vlassov, A. V., Magdaleno, S., Setterquist, R. & Conrad, R. Exosomes: Current knowledge of their composition, biological functions, and diagnostic and therapeutic potentials. *Biochim. Biophys. Acta - Gen. Subj.* **1820**, 940–948 (2012).
7. Colombo, M., Raposo, G. & Théry, C. Biogenesis, Secretion, and Intercellular Interactions of Exosomes and Other Extracellular Vesicles. <http://dx.doi.org/10.1146/annurev-cellbio-101512-122326> **30**, 255–289 (2014).
8. Gill, S., Catchpole, R. & Forterre, P. Extracellular membrane vesicles in the three domains of life and beyond. *FEMS Microbiol. Rev.* **43**, 273–303 (2019).
9. Szoka, F. & Papahadjopoulos, D. *Comparative properties and methods of preparation of lipid vesicles (liposomes)*. *Annual review of biophysics and bioengineering* **9**, (1980).
10. Lasch, J., Weissig, V. & Brandl, M. *Liposomes: a practical approach*. Oxford University Press (2003).
11. Walde, P. & Ichikawa, S. Enzymes inside lipid vesicles: preparation, reactivity and applications. *Biomol. Eng.* **18**, 143–177 (2001).
12. Walde, P. *Encyclopedia of Nanoscience and Nanotechnology*. (American Scientific Publishers, 2004).
13. Lichtenberg, D. & Barenholz, Y. *Methods in Biochemical Analysis*. (Wiley, 1988).
14. Laouini, A. *et al.* Preparation, Characterization and Applications of Liposomes: State of the Art. *J. Colloid Sci. Biotechnol.* **1**, 147–168 (2012).
15. Patil, Y. P. & Jadhav, S. Novel methods for liposome preparation. *Chemistry and Physics of Lipids* **177**, 8–18 (2014).
16. Dimova, R., Stano, P., Marques, C. M. & Walde, P. *The giant vesicle book*. (CRC Press, Taylor & Francis Group, 2020).
17. Lasic, D. D. *Liposomes: from physics to applications*. (Elsevier, 1993).

18. Spector, M. S., Zasadzinski, J. A. & Sankaram, M. B. Topology of multivesicular liposomes, a model biliquid foam. *Langmuir* **12**, 4704–4708 (1996).
19. Walker, S. A., Kennedy, M. T. & Zasadzinski, J. A. Encapsulation of bilayer vesicles by self-assembly. *Nature* **387**, 61–64 (1997).
20. Carrara, P., Stano, P. & Luisi, P. L. Giant Vesicles “Colonies”: A Model for Primitive Cell Communities. *ChemBioChem* **13**, 1497–1502 (2012).
21. Elani, Y., Law, R. V. & Ces, O. Vesicle-based artificial cells as chemical microreactors with spatially segregated reaction pathways. *Nat. Commun.* **2014** *5*, 1–5 (2014).
22. Deamer, D. W. & Bramhall, J. Permeability of lipid bilayers to water and ionic solutes. *Chem. Phys. Lipids* **40**, 167–188 (1986).
23. Etienne, G., Vian, A., Biočanin, M., Deplancke, B. & Amstad, E. Cross-talk between emulsion drops: How are hydrophilic reagents transported across oil phases? *Lab Chip* **18**, 3903–3912 (2018).
24. Deshpande, S., Caspi, Y., Meijering, A. E. C. & Dekker, C. Octanol-assisted liposome assembly on chip. *Nat. Commun.* **7**, 1–9 (2016).
25. Deng, N. N., Yelleswarapu, M. & Huck, W. T. S. Monodisperse Uni- and Multicompartment Liposomes. *J. Am. Chem. Soc.* **138**, 7584–7591 (2016).
26. Prastowo, A., Feuerborn, A., Cook, P. R. & Walsh, E. J. Biocompatibility of fluids for multiphase drops-in-drops microfluidics. *Biomed. Microdevices* **18**, 1–9 (2016).
27. Deshpande, S. & Dekker, C. On-chip microfluidic production of cell-sized liposomes. *Nat. Protoc.* **13**, 856–874 (2018).
28. Trantidou, T., Elani, Y. & Ces, O. Microfluidic generation of double emulsions as multiphase compartmentalised cell-like systems. *IET Conf. Publ.* **2016**, (2016).
29. Petit, J., Polenz, I., Baret, J. C., Herminghaus, S. & Bäümchen, O. Vesicles-on-a-chip: A universal microfluidic platform for the assembly of liposomes and polymersomes. *Eur. Phys. J. E* **39**, 1–6 (2016).
30. Sander, J. S., Isa, L., Rühls, P. A., Fischer, P. & Studart, A. R. Stabilization mechanism of double emulsions made by microfluidics. *Soft Matter* **8**, 11471–11477 (2012).
31. Aditya, N. P. *et al.* Co-delivery of hydrophobic curcumin and hydrophilic catechin by a water-in-oil-in-water double emulsion. *Food Chem.* **173**, 7–13 (2015).
32. Kong, L. *et al.* Lipid-Stabilized Double Emulsions Generated in Planar Microfluidic Devices. *Langmuir* **36**, 2349–2356 (2020).
33. Lussier, F. *et al.* pH-Triggered Assembly of Endomembrane Multicompartment in Synthetic Cells. *ACS Synth. Biol.* **11**, 366–382 (2022).
34. Bauer, W. A. C., Fischlechner, M., Abell, C. & Huck, W. T. S. Hydrophilic PDMS microchannels for high-throughput formation of oil-in-water microdroplets and water-in-oil-in-water double emulsions. *Lab Chip* **10**, 1814–1819 (2010).
35. Trantidou, T., Elani, Y., Parsons, E. & Ces, O. Hydrophilic surface modification of pdms for droplet microfluidics using a simple, quick, and robust method via pva deposition. *Microsystems Nanoeng.* **3**, (2017).
36. Wang, W., Zhang, M.-J. & Chu, L.-Y. Microfluidic approach for encapsulation via double emulsions. *Curr. Opin. Pharmacol.* **18**, 35–41 (2014).
37. Utada, A. S. *et al.* Monodisperse double emulsions generated from a microcapillary device. *Science (80-. )*. **308**, 537–541 (2005).
38. Yandrapalli, N., Petit, J., Bäümchen, O. & Robinson, T. Surfactant-free production of biomimetic giant unilamellar vesicles using PDMS-based microfluidics. *Commun. Chem.* **2021** *4*, 1–10 (2021).
39. Liu, L. *et al.* Preparation of monodisperse calcium alginate microcapsules via internal gelation in microfluidic-generated double emulsions. *J. Colloid Interface Sci.* **404**, 85–90 (2013).
40. Wang, W. *et al.* Hole-shell microparticles from controllably evolved double emulsions. *Angew. Chemie - Int. Ed.* **52**, 8084–8087 (2013).
41. Krafft, D. *et al.* Compartments for Synthetic Cells: Osmotically Assisted Separation of Oil from Double Emulsions in a Microfluidic Chip. *ChemBioChem* **20**, 2604–2608 (2019).
42. Teh, S. Y., Khnouf, R., Fan, H. & Lee, A. P. Stable, biocompatible lipid vesicle

- generation by solvent extraction-based droplet microfluidics. *Biomicrofluidics* **5**, (2011).
43. Rogers, J. A. & Nuzzo, R. G. Recent progress in soft lithography. *Mater. Today* **8**, 50–56 (2005).
  44. Martinez-Duarte, R., Turon Teixidor, G., Mukherjee, P., Kang, Q. & Madou, M. J. Perspectives of Micro and Nanofabrication of Carbon for Electrochemical and Microfluidic Applications. in *Microfluidics and Microfabrication* (ed. Chakraborty, S.) 181–263 (Springer Science + Business Media, LLC, 2010). doi:10.1007/978-1-4419-1543-6
  45. Burklund, A., Tadimety, A., Nie, Y., Hao, N. & Zhang, J. X. J. *Advances in diagnostic microfluidics. Advances in Clinical Chemistry* **95**, (Elsevier Inc., 2020).
  46. Whitesides, G. M., Ostuni, E., Takayama, S., Jiang, X. & Ingber, D. E. Soft Lithography in Biology and Biochemistry. *Annu. Rev. Biomed. Eng.* **3**, 335–373 (2001).
  47. Liu, H., Li, M., Wang, Y., Piper, J. & Jiang, L. Improving Single-Cell Encapsulation Efficiency and Reliability through Neutral Buoyancy of Suspension. *Micromachines* **11**, 94 (2020).
  48. Love, C. *et al.* Reversible pH-Responsive Coacervate Formation in Lipid Vesicles Activates Dormant Enzymatic Reactions. *Angew. Chemie* **132**, 6006–6013 (2020).
  49. Takeuchi, S., Garstecki, P., Weibel, D. B. & Whitesides, G. M. An Axisymmetric Flow-Focusing Microfluidic Device. *Adv. Mater.* **17**, 1067–1072 (2005).
  50. Chang, F.-C. *et al.* A monolithically three-dimensional flow-focusing device for formation of single/double emulsions in closed/open microfluidic systems. *J. Micromechanics Microengineering* **16**, 2336 (2006).
  51. Richmond, D. L. *et al.* Forming giant vesicles with controlled membrane composition, asymmetry, and contents. *Proc. Natl. Acad. Sci. U. S. A.* **108**, 9431–9436 (2011).
  52. Czekalska, M. A. *et al.* One-Step Generation of Multisomes from Lipid-Stabilized Double Emulsions. *ACS Appl. Mater. Interfaces* **13**, 6739–6747 (2021).
  53. Trantidou, T., Regoutz, A., Voon, X. N., Payne, D. J. & Ces, O. A “cleanroom-free” and scalable manufacturing technology for the microfluidic generation of lipid-stabilized droplets and cell-sized multisomes. *Sensors Actuators B Chem.* **267**, 34–41 (2018).
  54. Peng Bao *et al.* Production of giant unilamellar vesicles and encapsulation of lyotropic nematic liquid crystals. *Soft Matter* **17**, 2234–2241 (2021).
  55. Gonzales, D. T. Building synthetic multicellular systems from the bottom-up. (2022).
  56. Dolder, N. The Challenges of Measuring Membrane Protein Function in Giant Unilamellar Vesicles. (University of Bern, 2021).
  57. Gonzales, D. T., Yandrapalli, N., Robinson, T., Zechner, C. & Tang, T.-Y. D. Cell-Free Gene Expression Dynamics in Synthetic Cell Populations. *Cite This ACS Synth. Biol* **2022**, 205–215 (2022).
  58. Ziaie, B., Baldi, A., Lei, M., Gu, Y. & Siegel, R. A. Hard and soft micromachining for BioMEMS: Review of techniques and examples of applications in microfluidics and drug delivery. *Adv. Drug Deliv. Rev.* **56**, 145–172 (2004).
  59. PubChem Compound Database. 1-Octanol - Hazardous Substances Data Bank. Available at: <https://pubchem.ncbi.nlm.nih.gov/compound/957#section=Solubility>. (Accessed: 30th June 2022)
  60. Cheng, J. *et al.* Transport of ions through the oil phase of W1/O/W2 double emulsions. *J. Colloid Interface Sci.* **305**, 175–182 (2007).
  61. Yuval Elani, I. Solvas, X. C., B. Edel, J., V. Law, R. & Oscar Ces. Microfluidic generation of encapsulated droplet interface bilayer networks (multisomes) and their use as cell-like reactors. *Chem. Commun.* **52**, 5961–5964 (2016).



## CHAPTER 4.

# PRODUCTION AND STABILITY OF DOUBLE EMULSIONS FOR ORAL DRUG DELIVERY

“Fortitudine vincimus — By endurance we conquer.”

— Alfred Lansing, Endurance: Shackleton's Incredible Voyage

### Abstract

---

Double emulsions (DEs) are water-in-oil-in-water (or oil-in-water-in-oil) droplets with the potential to deliver combinatory therapies due to their ability to co-localise hydrophilic and hydrophobic molecules in the same carrier. However, DEs are thermodynamically unstable and only kinetically trapped. Extending this transitory state, rendering DEs more stable, would widen the possibilities of real-world applications, yet characterisation of their stability in physiologically-relevant conditions is lacking. In this work, we used microfluidics to produce lipid-stabilised DEs with reproducible monodispersity and high encapsulation efficiency. We investigated DE stability under a range of physicochemical parameters such as temperature, pH and mechanical stimulus.

Stability through time was inversely proportional to temperature. DEs were significantly stable up to 8 days at 4 °C, 5 days at RT and 2 days at 37 °C. When encapsulating cargo, DE stability decreased significantly. When exposed to a pH change, unloaded DEs were only significantly unstable at the extremes (pH 1 and 13), largely outside physiological ranges. When exposed to flow, unloaded DEs behaved similarly regardless of the mechanical stimulus applied, with approximately 70% remaining after 100 flow cycles of 10s. These results indicate that lipid-stabilised DEs produced via microfluidics could be tailored to endure physiologically-relevant conditions and act as carriers for drug delivery. Special attention should be given to the composition of the solutions, e.g. osmolarity ratio between inner and outer solutions, and the interaction of the molecules, e.g. carrier and cargo, involved in the final formulation.

---

## *Contributions*

---

Part of this chapter has been published

Betterelli Giuliano C, Moran J, Ayache J and Muiznieks L. *Stability characterization of microfluidics lipid-stabilized double emulsions under physiologically-relevant conditions* [version 1; peer review: 1 approved with reservations]. *Open Res Europe* 2022, **2**:103 (<https://doi.org/10.12688/openreseurope.14766.1>)

The experimental work was performed by Camila Betterelli Giuliano. Writing of this chapter was done by Camila Betterelli Giuliano. Revision was done by Camila Betterelli Giuliano, Dr. Lisa Muiznieks (Elvesys) and Prof. Joseph Moran (Univ. Strasbourg).

---

## 4.1. Introduction

Double emulsions (DEs) are water-in-oil-in-water (W/O/W) or oil-in-water-in-oil (O/W/O) droplets frequently used in the food industry to fabricate low-fat products and improve nutrient and flavour delivery.<sup>1</sup> However, historically speaking, most interest derived from DEs has come from the pharmaceutical industry.<sup>1,2</sup> They have been studied as drug delivery systems<sup>3–5</sup>, blood substitutes<sup>6,7</sup>, and vaccines<sup>8,9</sup>, with one of the earliest reported applications in the late 1960s, which aimed to enhance the absorption of insulin in the intestine<sup>10</sup>. DEs are usually produced in a two-step process: two immiscible solutions are mixed, forming an emulsion that is, in turn, vigorously stirred in a third solution of similar properties as the inner phase. The rotation speed of each step allows for some control over the size and number of inner droplets within the outer droplet. However, resulting populations tend to be polydisperse and vary widely in encapsulation efficiency, ranging from 10 to 98%<sup>2,11–18</sup>. Polydispersity has been shown to affect the release profile of drugs encapsulated in microparticles<sup>19</sup>, while reproducible encapsulation efficiency, specifically the homogeneous concentration of drug inside each DE, is crucial for well-controlled release kinetics and therapeutic benefit<sup>20</sup>. Thus, these current constraints hinder more widespread commercial use of DEs.

Microfluidics is well poised to address these limitations. The microfluidic production of single, double, and multiple emulsions has been reported<sup>21,22</sup>, demonstrating highly monodisperse populations and encapsulation efficiencies of nearly 100%<sup>23</sup>. Still, complex setups, e.g. cleanroom microfabrication and microfluidic glass capillaries<sup>21,24,25</sup>, have created a barrier to wider use in multiple applications. As the technology has matured over the last decade, an increasing number of reports show the successful production of DEs in microfluidic polydimethylsiloxane (PDMS) chips, which are cheap and simple enough to fabricate and assemble<sup>26–29</sup>.

One key characteristic of DEs, driving the recent interest in the field, is their ability to co-localise and co-transport, in a single carrier, molecules of opposing properties<sup>30–34</sup>, such as hydrophobic and hydrophilic drugs, for example, the synergistic anticancer drugs paclitaxel and doxorubicin<sup>34</sup>. As a consequence, they are promising delivery systems for combinatory therapies. However, it remains that DEs are characteristically metastable structures, i.e. thermodynamically unstable<sup>29,35–37</sup>. DEs are kinetically trapped in a transitory local energy minimum state that can move towards the global minimum at a given disturbance. Thus, they are prone to bursting, due to the coalescence of the inner phase with the outer phase, forming

an O/W droplet<sup>35,37,38</sup>. In order to take advantage of their drug co-localisation properties, increasing the time that they remain in this transitory state is a critical issue.

Most DEs are stabilised with surfactants, usually block copolymers<sup>26,37,39–42</sup>, that arrange themselves at the interfaces, and other additives that increase the viscosity of the aqueous solutions<sup>40,43</sup>. Recent works in the field of artificial-cell like systems, which studies the origins of life and the molecular dynamics of the modern cell membrane<sup>44</sup>, have focused on double emulsions with more biomimetic compositions, replacing synthetic surfactants and additives with molecules that could be found in the regular cellular constitution, such as lipids<sup>25,28,29,45–47</sup>. The exploration of these lipid-stabilised double emulsions as drug delivery systems is very recent, but promising<sup>25</sup>. Besides their more biologically-relevant composition, the presence of lipids confers several advantages. They allow the formation of multisomes, a network of smaller water droplets inside an oil droplet, that can be used as a multi-compartmentalised delivery system<sup>25</sup>, and potentially enhance intestinal absorption<sup>48</sup>. Furthermore, it has been shown that lipids play an important role in the absorption of hydrophobic drugs<sup>49,50</sup>, enhancing their bioavailability<sup>51</sup>. In 2002, the Food and Drug Administration (FDA) issued the "Food-effect Bioavailability and Fed Bioequivalence" guidance, in which it recommended high-fat meals when taking hydrophobic drugs to improve drug absorption due to the effect of fats on the gastrointestinal tract physiology, to maximise drug transfer to the systemic circulation<sup>48</sup>. At least five pharmaceutical products that take advantage of these characteristics have been approved for commercial use (Intralipid®, 1975; Cleviprex®, 2008; Perikabiven®, 2014; Smoflipid®, 2016; Cinvanti®, 2018)<sup>52</sup>. They consist of single emulsions stabilised by lipids, encapsulating only one drug (i.e. not combinatory therapies), and are indicated for nutritional purposes, the treatment of acute and delayed nausea and vomiting, and reduction of blood pressure. To date, no DE formulations have reached clinical stages.

A reason for the lack of commercial exploitation resides in the fact that DEs are one of the most challenging types of droplets to generate<sup>46</sup>. Almost every variable from formulation composition to production parameters can affect their stability. Also, a robust characterisation of their stability, especially under physiologically-relevant parameters, is lacking. In this work, we investigate the stability of lipid-stabilised DEs described in Chapter 3, made by microfluidics in PDMS chips fabricated under basic laboratory conditions (no cleanroom), for the generation of reproducible monodisperse populations. We characterised their stability when exposed to various stresses representing physiological conditions relevant to DE-based therapeutics, such as temperature, pH and mechanical stress. Finally, we encapsulated representative cargo in the intermediate and inner phases to assess how these additions affect the stability.

The gained insights contribute to the growing body of knowledge that can advance the use of DEs in commercial applications.

## 4.2. Materials and Methods

### 4.2.1. Microfluidic Production of Double Emulsions

PDMS chips (Design 2) received a surface treatment with PVA solution (2.5% (w/v)) as described in Chapter 3. Inner aqueous phase (IA), lipid-oil intermediate phase (LO) and outer aqueous phase (OA) solutions were prepared, described in Chapter 3 (DOPC (6.5 mM) in the intermediate solution<sup>29</sup> and P188 (0.5%) in the outer solution) (Table 4.1).

**Table 4.1.** Composition of the solutions used in the Temperature Assays

	4°C	RT	RT-Dil	RT-LUVs	37°C
<b>IA</b>	15% (v/v) glycerol in water	15% (v/v) glycerol in water	15% (v/v) glycerol in water	0.2mM POPC LUVs, 0,1 Mm Dil and 15% (v/v) glycerol in water	15% (v/v) glycerol in water
<b>LO</b>	6.5mM DOPC in octanol	6.5mM DOPC in octanol	6.5mM DOPC and 0.1mM Dil in octanol	6.5mM DOPC in octanol	6.5mM DOPC in octanol
<b>OA</b>	15% (v/v) glycerol and 0.5% P188 in water	15% (v/v) glycerol and 0.5% P188 in water	15% (v/v) glycerol and 0.5% P188 in water	15% (v/v) glycerol and 0.5% P188 in water	15% (v/v) glycerol and 0.5% P188 in water

The solutions were driven into the chip with a pressure-driven flow controller (OB1, Elveflow, France). The pressure ranges for each solution were: IA = 25 to 35 mbar; LO = 35 to 45 mbar; OA = 70 mbar. The pressure of the OA was kept constant throughout experiments for comparable production rates.

## 4.2.2. Image Analysis

DEs were collected into a  $\mu$ -Slide I Luer channel slide (height=0.4mm, Ibidi, ref. 80176) attached to the exit of the production chip via a short piece of tubing. For size distribution, encapsulation, and temperature assay analyses, images were taken with an inverted AxioVert A1 microscope (Carl Zeiss, Germany) and camera (AxioCam 202 mono). For pH and flow assay analyses, an upright microscope (built in-house from 5x objective), and high-speed camera (Pixelink, ref. PL-D725CU) were used. Image analysis was performed using the image software Fiji and a Python script developed in-house for automated droplet counting and sizing. The parameters of the script were adjusted to better fit the change in size over time and were verified manually through representative images. Data are reported as the mean percentage of counted DEs  $\pm$  SD or SEM as specified. Statistical analysis was performed using a Student's T-Test, two-sample assuming unequal variances. Production rates and encapsulation efficiencies were done as described in Chapter 3.

## 4.2.3. Encapsulation of compounds of interest

### 4.2.3.1. Production of Large Unilamellar Vesicles (LUVs)

In collaboration with Prof. Peter Walde's group at ETH Zurich, Large Unilamellar Vesicles (LUVs) were produced by the standard extrusion method<sup>53</sup>. Briefly, 20 mM of POPC diluted in chloroform was added to a round bottom flask and placed under nitrogen overnight for the complete evaporation of chloroform. The dried lipid film was resuspended in 15% (v/v) glycerol in water. The solution was frozen and thawed 10 times with liquid nitrogen to form vesicles. Finally, the vesicles were extruded first through 200nm and then through 100nm polycarbonate membranes, 10 times each. The size and dispersity of the vesicles were measured with Dynamic Light Scattering (DSL). The solution was kept at 4°C and used for as long as there was no aggregation.

### **4.2.3.2. Encapsulation in Double Emulsions**

For encapsulation assays, the inner solution was replaced with a solution containing 100-nm diameter POPC large unilamellar vesicles (LUVs) (0.2 mM; DiI, 0.1 mM, inner phase) in glycerol (15% (v/v)). The experiments were performed with a hypertonic inner phase (higher concentration of solute in the inner phase than in the outer phase).

All fluorescent images were collected with an inverted AxioVert A1 microscope (Carl Zeiss, Germany) using filters (red: ex/em 546/572-640 nm), and respective camera (AxioCam 202 mono).

### **4.2.4. Stability Assays**

#### **4.2.4.1. DE temperature stability over time**

DEs were generated at room temperature (RT) and collected in an Ibidi  $\mu$ -Slide Luer (0.4 mm height) chip. Then, DEs were placed at the respective temperatures (4 °C; room temperature (22 °C, RT); 37 °C) and imaged as described above at defined time points. The chip was imaged in its entirety each time and DEs were counted and measured using a Python script, as described above. Data are presented as the percentage of DEs remaining normalised to the maximum value ( $n \geq 3$ ).

#### **4.2.4.2. DE pH stability**

DEs were pipetted on a clean glass slide and imaged as described above. Aqueous solutions with pH between 1-13 were prepared by adding 1 M HCl or 1 M NaOH to a solution of water and phenol red until the desired pH was reached. Then, an equivalent volume of each solution was gently pipetted into the standing droplet. DEs were imaged 10 minutes after exposure at RT. DEs were counted using the Python script (described above). Data are presented as percent DEs remaining after exposure compared to before exposure  $\pm$  SD;  $n \geq 5$ .

#### 4.2.4.3. Stability of unloaded and loaded DEs at different mechanical stress conditions

Different flow regimens (14, 20 and 30 mbar) were applied with pressure using an autonomous recirculation system (Cobalt, Elveflow, France) that allowed double emulsions to flow back and forth in the field of view for 100 cycles of 10 seconds (i.e. 5 s forward flow, 5 s backward flow) through an Ibidi u-Slide Luer (0.4 mm height) chip at RT. Videos were captured and the number of DEs from the most populated frame was counted for every 10 cycles.

The experiment was performed with unloaded DEs and with LUV-loaded DEs (0.2 mM POPC; stained with Dil, 0.1 mM). Chips under static conditions were used as controls. Images before and after flow were collected and analysed as described above.

The pressures were converted into estimations of flow rates (ml/min) using an online calculator (Elveflow, France, Table 4.2)<sup>54</sup>.

**Table 4.2.** Pressures and corresponding flow rates used to test the stability of the double emulsions under flow

Pressure (mbar)	Flow rate (ml/min)
14	0.5
20	1
30	2

### 4.3. Results

#### 4.3.1. Microfluidics as a highly suitable method for reproducible DE production

DEs with diameters in the micrometre range are well-suited for oral administration and have been reported for both pharmaceutical<sup>4</sup> and food<sup>61</sup> applications. Monodispersity is particularly crucial for drug delivery systems, because it improves reproducibility and provides increased control over encapsulation, allowing for a more homogeneous distribution of cargo<sup>24,62</sup>.



The standard two-step emulsification production method results in considerably large size distributions, e.g. from 1 to 100  $\mu\text{m}$ <sup>63</sup> or 1 to 500  $\mu\text{m}$ <sup>61</sup>. Attempts to improve the monodispersity of two-step emulsification samples usually include extra post-production steps (i.e. extrusion through polycarbonate membranes<sup>15</sup> or a multi-purification step<sup>64</sup>) which adds complexity and may limit the flexibility of the formulation. The DEs presented in this work, as demonstrated in Chapter 3, highlight the advantage of microfluidics in producing monodisperse double emulsions with a simple setup, without any post-production step, with high encapsulation efficiencies, directly in the targeted size for oral drug delivery systems.

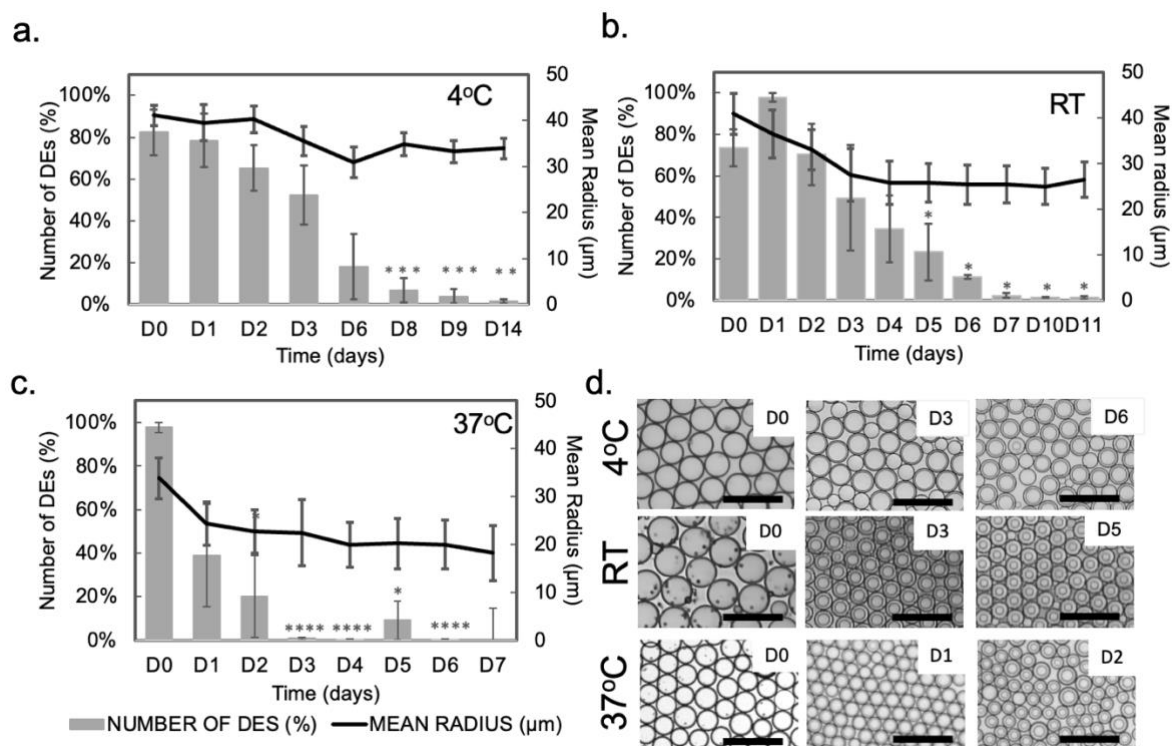
### **4.3.2. Stability Assays**

Stability is the key issue for the practical application of DEs. Emulsions larger than 0.1  $\mu\text{m}$  are only kinetically stable, breaking or coalescing over time<sup>37,55</sup>. To investigate a potential future application as a combinatory drug delivery system, the stability of lipid-stabilised DEs was tested in different physiologically-relevant conditions, being exposed to ranges of temperature, pH and mechanical stress.

### **4.3.3. DE stability at different temperatures over time**

Temperature plays an important role in meta-stable states by potentially providing the necessary energy required for the molecular assembly to leave the transient equilibrium (local energy minimum) and move towards a lower energy state<sup>55</sup>. Temperatures were chosen according to their relevance to the lifecycle of a DE therapeutic: from physiological body temperature, 37°C, to temperatures relevant to handling and storage, RT and 4°C, respectively. Lipid-stabilised double emulsions were exposed to 4°C, RT and 37°C for a minimum of 7 days, and the number of DEs and mean radius were measured (Figure 4.1). The highest number of DEs in a given day (i.e. D0 for 4°C and 37°C and D1 for RT in Figure 4.1) was used as the maximum value to normalise the data as a percent. At 4°C, there was a trend towards a loss of DEs over time, but a significant reduction in numbers (92%) was observed by day 8 compared to day 0. At RT, the loss of DEs presented a similar profile, with a significant reduction (68%) at day 5 compared to day 0, demonstrating a positive effect of colder temperatures in prolonging the transient meta-state, as expected. DEs were considerably less

resistant to warmer temperatures, with a steep decrease (79%) in numbers and statistical difference from day 2 onwards at 37°C.

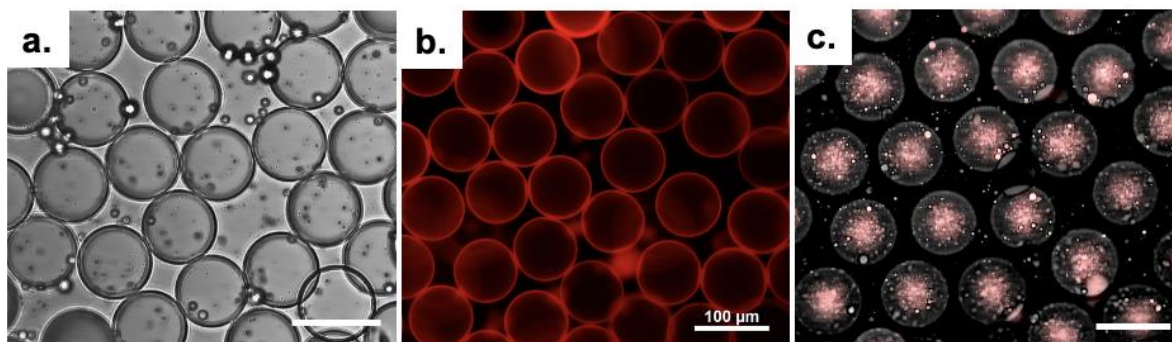


**Figure 4.1.** Stability and morphological changes of unloaded DEs at different temperatures. a-c. Percentage of maximum value over time (left y-axis); Thick line shows DE radius (μm), +/- SD (right y-axis). **a.** DEs held at 4°C (n=4, total number of DEs at D0=16,357 DEs, +/- SEM); **b.** RT (n=3, 72,245 DEs, +/- SEM); and **c.** 37°C (n=4, 119,051 DEs, +/- SEM); **d.** Representative images at different time points highlighting the swelling of the intermediate phase; scale bars: 200 μm; Statistical significance from D0 (Student T-test): p<0.05 (\*); p<0.01(\*\*); p<0.005 (\*\*\*) ; p<0,001 (\*\*\*\*).

Radius at D0 was 41 μm for DEs placed at 4 °C, 40 μm for RT and 34 μm for 37 °C. At each temperature, the mean external radius decreased (17%, 36% and 48%, respectively) throughout the testing period (Figure 4.1.d). Also, DEs showed a clear increase in the thickness of the intermediate layer over time, in which the oil shell thickness increased from 5.98% of the outer droplet radius to 24.63% (4°C, D6; average thickness, 8.4±1.7 μm), 50.07% (RT, D5; 12.11±1.4 μm) and 37.75% (37°C, D2; 7.6±1.9 μm).

#### 4.3.4. Encapsulation of compounds of interest and stability of loaded DEs over time

To investigate the effect of locally encapsulated cargo on DE stability, one of the key advantages of DEs as delivery systems, a cargo was added to the inner and intermediate phase solutions (Figure 4.2). Dil, a lipid-specific fluorescent dye that locates just below the lipid-water interface<sup>56</sup>, was used as a hydrophobic cargo, and LUVs were used as hydrophilic cargo. In both cases, loaded DEs were successfully produced. Encapsulation efficiency was over 80% (Dil, n=5; LUVs, n=4).



**Figure 4.2.** Encapsulation of cargo in DEs. **a.** DEs, no cargo, bright field; **b.** DEs loaded with Dil (lipid specific, intermediate phase, red fluorescent filter); **c.** DEs loaded with POPC LUVs pre-stained with Dil (inner phase; red fluorescent filter). Scale 100 µm.

Commonly, encapsulation in double emulsions produced with microfluidics is done with isotonic solutions<sup>29,40,57</sup>, but there are reports of two-step emulsification methods using a hypertonic inner phase due to the higher stability of the resulting DEs<sup>58,59</sup>. Aiming to explore this characteristic and provide more flexibility to the final formulation of the outer solution for an oral drug delivery system, the DEs were loaded in the inner phase with a hypertonic solution (i.e. LUVs). In all cases, encapsulation was successful, with the exception of the highest concentration of POPC LUVs (2mM) (Table 4.3), which caused a disruptive osmotic unbalance and hindered stable DE production.

**Table 4.3.** Results of varying POPC LUV concentrations in double emulsion production

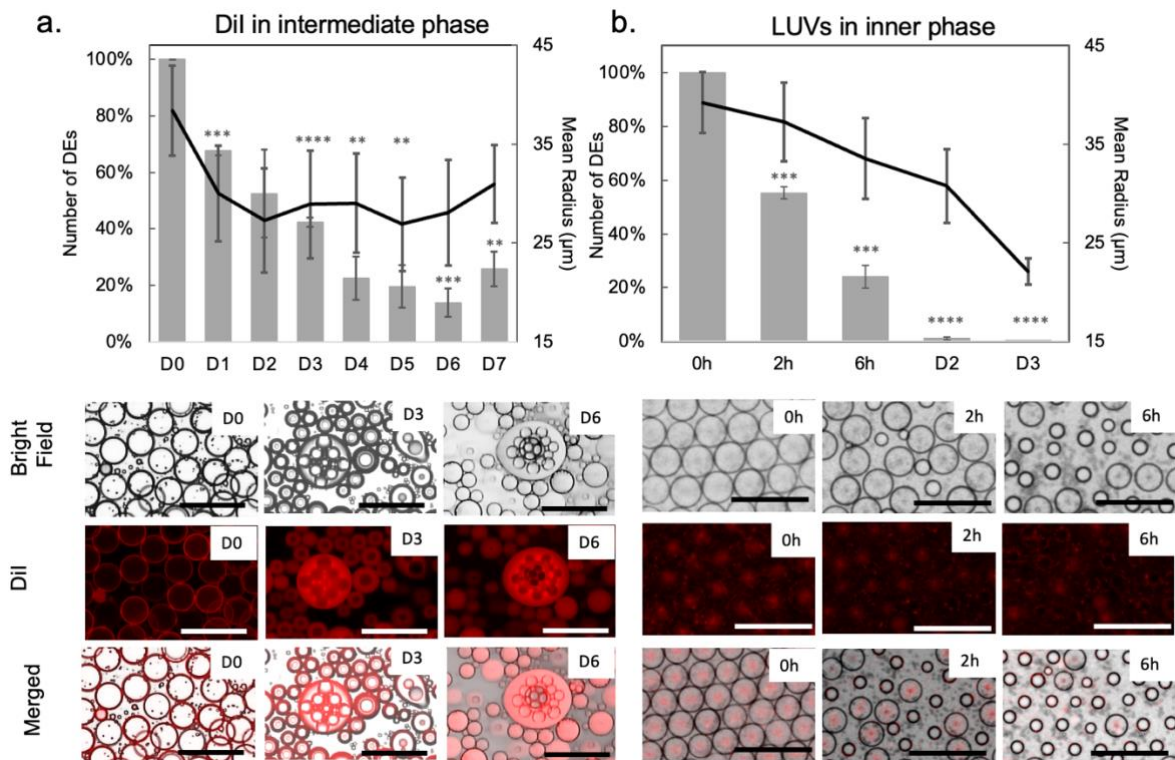
Variable	Description	POPC LUV Concentration (mM)		
		0.02	0.2	2
Coating	2.5% PVA	X	X	X
Inner Aqueous Solution (IA)	LUVs	X	X	X
Lipid-Oil Phase (LO)	6.5mM DOPC in octanol	X	X	X
Outer Aqueous Solution (OA)	15% Glycerol + 0.5% P188	X	X	X
Stain	Dil in inner phase	X	X	X
Outlet	1mm	X	X	X
Results	Stable Double Emulsions	X	X	-

The encapsulation efficiency (as defined in Chapter 3) of unloaded double emulsions, i.e. 15% glycerol in water, and loaded, i.e. POPC LUVs, is comparable (88.13% and 90.63%, respectively) (Table 4.4).

**Table 4.4.** Encapsulation efficiencies and production rates of unloaded and loaded DEs.

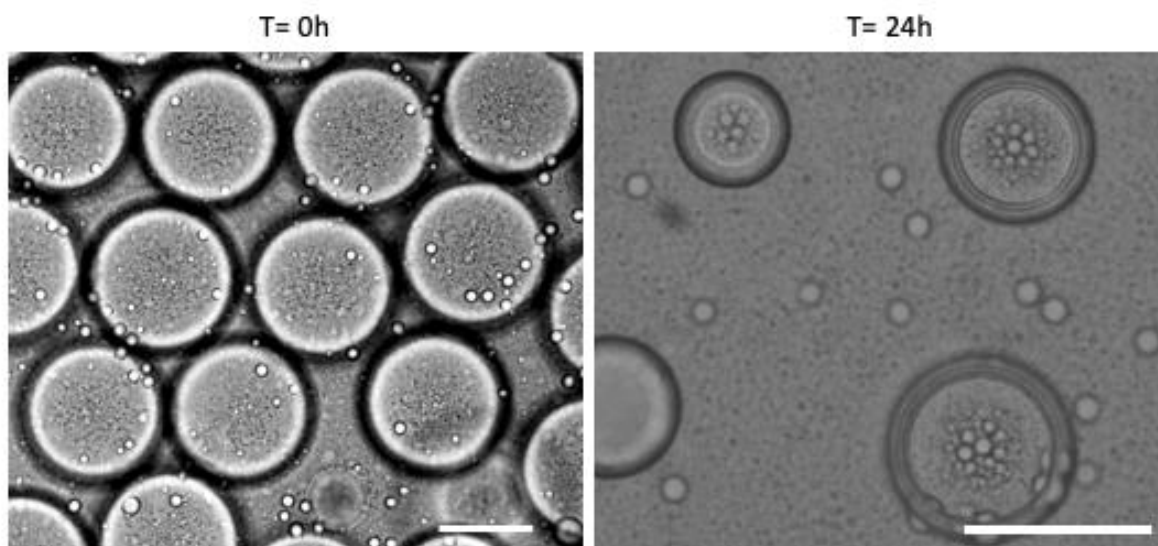
	Control	POPC LUVs
Encapsulation Efficiency	88.13%	90.63%
Production Rate (DEs/s)	232.7	233.3

Encapsulation of cargo affected the post-production stability of DEs. When loaded with a hydrophobic cargo, there was a significant decrease (32%) in DE numbers by day 1 at RT (Figure 4.3.a), showing less stability than for unloaded DEs. Decreased DE stability was further observed as coalescence of the intermediate phase, resulting in complex structures with multiple water droplets inside a large droplet of octanol (shown stained in red). The change in morphology is also seen in the mean radius data (Figure 4.3.a), showing a decrease (25%) in radius up to D3. The formation of larger multi-inner droplet structures due to the coalescence of the intermediate phase caused the average radius to remain around 30  $\mu\text{m}$  until D7, although most DEs that had not coalesced had burst by that time point.



**Figure 4.3.** Stability of loaded DEs over time at RT. **a.** Encapsulation of hydrophobic cargo in the intermediate phase. The percentage of remaining DEs carrying Dil in the intermediate phase and the average size, in  $\mu\text{m}$ , observed through time at RT ( $n=3$ ; total number of DEs at D0=37,492, +/-SEM; normalised to the maximum value). **b.** Encapsulation of 100nm LUVs (0,02mM POPC) in the inner phase ( $n=3$ ; 10,863 DEs; +/-SEM). Insets show representative fluorescence (filter: ex 546 nm/em 572nm) and bright field images of DEs at the indicated time points. Black line, radius ( $\mu\text{m}$ ), +/- SD. Scale bar, 200  $\mu\text{m}$ . Statistical significance from D0 (Student T-test):  $p<0.05$  (\*);  $p<0.01$ (\*\*);  $p<0.005$  (\*\*\*) ;  $p<0,001$  (\*\*\*\*).

Similarly, the addition of LUVs also affected post-production DE stability. The first 2 hours after production revealed a significant decrease (45%) in numbers, and most DEs had burst by D2 (Figure 4.3.b.). Based on the concentration of POPC (0.02 mM), it was estimated that each DE carries around 40.000 LUVs in the lumen. An important point to consider is the stability of the cargo itself. In the experiments performed at room temperature, besides the increased instability of the DEs, the LUVs presented morphological changes (Figure 4.4). At  $t=0\text{h}$ , it was possible to see small black dots well dispersed in the lumen of the DEs. After 24h, there were large white droplets agglomerated in the middle of the inner phase, suggesting that LUVs do not remain stable at room temperature.

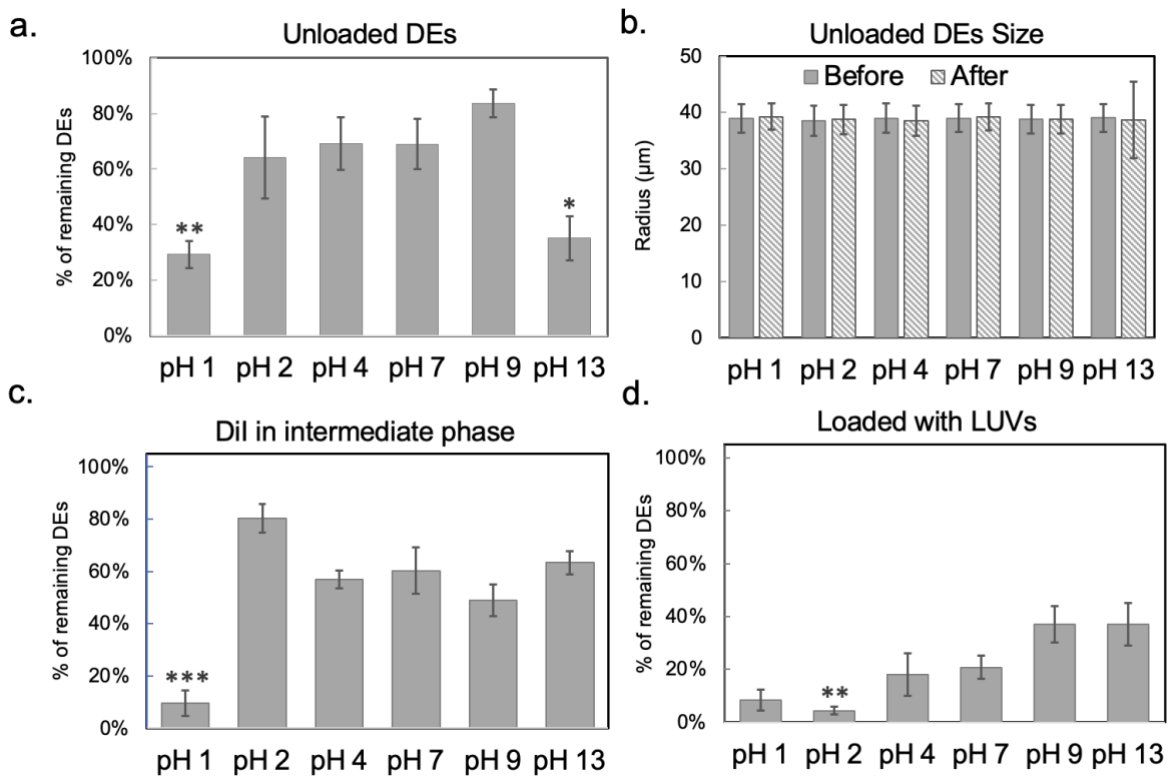


**Figure 4.4.** Morphological alterations of LUVs inside DEs in 24h. Scale bar, 50  $\mu\text{m}$ .

This contrasts with LUV stability in colder temperatures. DSL measurements made of POPC LUVs in 15% glycerol after the extrusion process indicated that the mean diameter of the vesicles was 106.9 nm (PI: 0.048). The same batch of POPC LUVs, kept at 4°C for 12 months, was measured and the results showed that the mean diameter was 106 nm (PI: 0.015).

#### 4.3.5. DE stability at different pH ranges

Another important parameter when considering an oral drug delivery system is pH<sup>60</sup>. DEs were exposed to a range of pH from 1 to 13, either unloaded or loaded with hydrophobic or hydrophilic cargos (Dil or LUVs, respectively) and their numbers were assessed at t=0 (before) and t=10 minutes after exposure. For unloaded DEs, 56% of DEs remained intact after exposure to pH 7. Also, there was only a significant reduction at the extremes (pH=1, 48%, and pH 13, 38%) when compared to pH 7 (Figure 4.5.a). The size was also not affected (Figure 4.5.b). A similar profile was demonstrated for DEs loaded with Dil (Figure 4.5.c), with only pH 1 significantly different (81% reduction) from pH 7. LUV-loaded DEs were considerably less stable, with 13-60% reduction across different pH (not significantly different from pH 7), and 79% reduction at pH 2 (significantly different from pH 7, Figure 4.5.d).

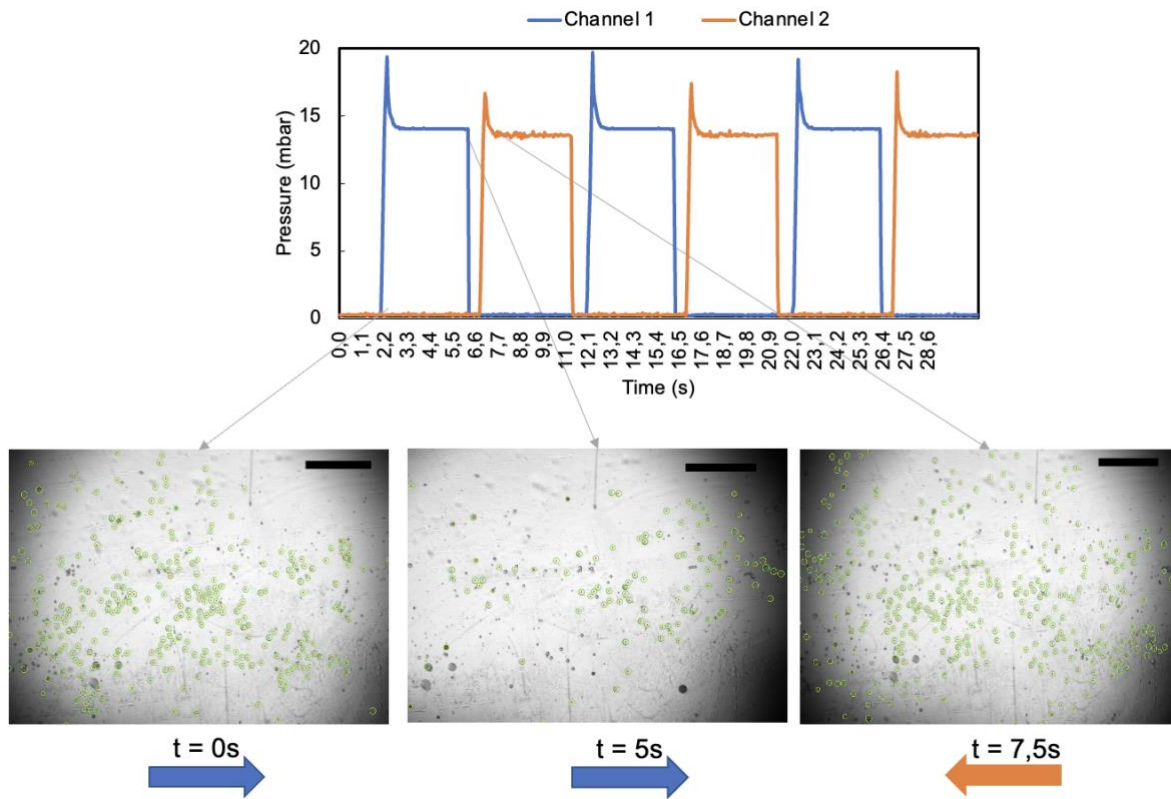


**Figure 4.5.** DE stability to different pH ranges. **a.** Percentage of remaining DEs after 10 min exposure to respective pH +/- SEM (pH 1, n=5, total number of DEs before exposure = 3,402; pH 2, n=5, 4,746 DEs; pH 4, n=5, 4,645 DEs; pH 7, n=10, 13,802 DEs; pH 9, n=5, 4,850 DEs; pH 13, n=5, 3,989 DEs). **b.** Radius of DEs before and after exposure to respective pH +/- SEM. **c.** Percentage of remaining Dil-loaded DEs after 10 min (pH 1, n=5, 3,402 DEs; pH 2, n=5, 4,746 DEs; pH 4, n=5, 4,645 DEs; pH 7, n=5, 6,248 DEs; pH 9, n=5, 4,850 DEs; pH 13, n=5, 3,989 DEs). **d.** Percentage of remaining LUVs-loaded DEs after 10 min (pH 1, n=5, 3,402 DEs; pH 2, n=5, 4,746 DEs; pH 4, n=5, 4,645 DEs; pH 7, n=5, 6,248 DEs; pH 9, n=5, 4,850 DEs; pH 13, n=5, 3,989 DEs). In each panel, statistical significance from pH 7 is indicated (Student T-test):  $p < 0.05$  (\*);  $p < 0.01$  (\*\*);  $p < 0.005$  (\*\*\*) ;  $p < 0.001$  (\*\*\*\*).

#### 4.3.6. Stability of unloaded and loaded DEs under mechanical stimulus

The effect of flow and mechanical forces is relevant for applications involving the gastrointestinal tract due to its peristaltic properties. Mechanical stress is also known to affect the transition from a meta-stable to a thermodynamically stable state<sup>55</sup>. For this reason, DEs

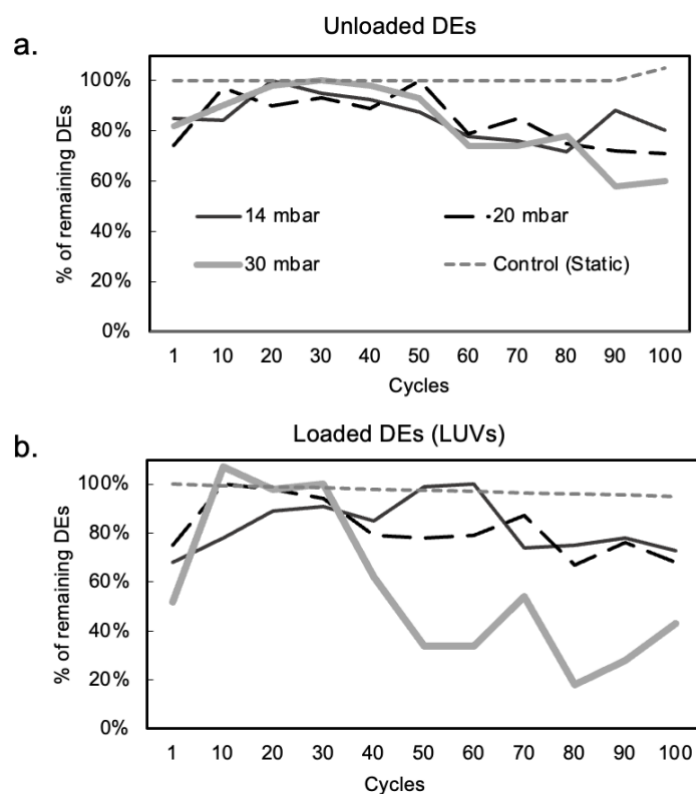
were subjected to mechanical forces caused by a stop-flow regimen made by back-and-forth cycles with an abrupt change in direction at the edges (Figure 4.6).



**Figure 4.6.** Flow profile of the stop-flow regimen for mechanical stimulus. DEs were driven back and forth in a 400- $\mu\text{m}$  high chip for 100 cycles of 10s.

The estimated flow rates were calculated for each pressure: 14 mbar = 0.5 ml/min; 20 mbar = 1 ml/min; 30 mbar = 2 ml/min<sup>54</sup>. For up to 50 back and forth cycles, DE numbers remained similar to starting values, then numbers decreased about 30% for each of the 3 applied pressures by the 100th cycle (Figure 4.7.a). DEs loaded with LUVs presented a similar behaviour for 14 mbar and 20 mbar, but were considerably more sensitive to the pressure of 30 mbar, with only around 35% of the initial number of DEs remaining by the last cycle.





**Figure 4.7.** Stability of unloaded and loaded DEs at different flow conditions. Percentage of remaining double emulsions over the highest number of DEs per cycle of 10 seconds, **a.** unloaded or **b.** loaded with 0.2mM POPC LUVs.

## 4.4. Discussion

### 4.4.1. Environmental conditions affect loaded and unloaded DEs differently

As a potential oral drug delivery system, DEs will be subjected to environmental conditions, including different pH and flow regimens of the gastrointestinal tract. For example, the pH of saliva is between 6.3 and 7.6<sup>61</sup>; the stomach pH is 2 or lower; and the intestine pH varies from 6.6 to 8<sup>62</sup>.

As DEs are less dense than the outer solution and float, they could not easily be trapped to enable the exchange of the pH solution via continuous flow. Thus, pH was adjusted by the addition of a droplet of pH solution to a droplet of DEs. While carefully done, this provided a

disruptive physical force to the DEs on the slide. Even unloaded DEs responded to this force by losing about 30% of their number at pH 7. Their reduction in number was not a consequence of doubling the volume, as all volumes were small enough that the entire content was counted in each case.

Unloaded DEs were stable across physiological pH, with increased sensitivity to the extremes. On one hand, an optimisation of the formulation, such as using a different surfactant<sup>63</sup> or higher concentration of glycerol in the inner phase<sup>64</sup>, might improve stability at lower pH so DEs are better equipped to pass through the acidic environment of the stomach. However, the instability to specific pH observed here could be leveraged as a trigger for localised drug delivery<sup>65,66</sup>.

Loaded DEs behaved differently depending on the location and type of the cargo. When loaded with Dil in the intermediate phase, DEs were more resistant to high pH than unloaded DEs, suggesting that the properties of the cargo can be leveraged to improve stability at higher pH. On the other hand, DEs loaded with LUVs were considerably more sensitive to the increased disturbance of the addition of the pH solution and to the range of pH as well, losing more than 60% of initial numbers in all cases. Interestingly, LUV-loaded DEs presented no significant difference from pH 7 at high pH, similarly to Dil-loaded DEs, although they were more sensitive to low pH than the two other cases. These results show that this formulation is particularly sensitive to low pH, which can be accentuated by the presence of the cargo. Therefore, further optimisation is needed in order to render this particular formulation apt to withstand the conditions it would face as an oral drug delivery system.

Oral drug delivery systems are subjected to the fluid flow and mechanical forces of the gastrointestinal tract. The recirculation experiments were designed to reproduce, to some extent, the environment and respective forces that would be applied to and/or felt by DEs. Here, DEs were not subjected to direct shear stress because the height of the channel was approximately 4-fold larger than the diameter of the DEs, so they could flow freely with the fluid, as is expected to happen in the body. The dimensions of the GI tract are orders of magnitude larger than the size of the DEs, so they are not expected to be constricted or to experience direct shear stress on the surface<sup>67</sup>. However, DEs are expected to experience mechanical stress as they flow along the tract, such as drops, stops, turns and turbulence<sup>67</sup>. To reproduce this in microfluidics, we introduced a sudden change in the direction of flow, so the DEs would feel as if they were hitting a wall. The chosen pressures, and consequently, the flow rates, are in the same order of magnitude as the lowest flow rates of the GI (2 to 3.6 ml/min in the duodenum and jejunum<sup>68</sup>).

It is not surprising that highest forces produced the biggest disruption, as LUV-loaded DEs were consistently more sensitive than the other two formulations in all tested conditions in this work. More interestingly, LUV-loaded DEs handled the two lower pressures as well as unloaded DEs, suggesting that they might withstand these external stresses as oral drug delivery systems once the formulation is optimised. In that light, it is important to consider the properties of the cargo and osmotic ratio of inner and outer solutions early in the design, so that DEs are tailored to best fulfil the intended final application.

#### **4.4.2. Cargo has considerable effect on long-term DE stability**

The required stability for DEs to be used as oral drug delivery systems is largely dependent on the final application, however their actual stability depends on the cargo. For perspective, the Pfizer-BioNTech mRNA vaccine (a lipid nanoparticle, not a DE) is stable for up to 5 days at 2-8 °C and only 2 h to 6 h at room temperature<sup>69</sup>. Stability of our unloaded DEs lay within this time span at fridge-based storage conditions (8 days, 4°C) and presented substantial resistance to size change or aggregation at conditions favourable to distribution and administration of a therapeutic (5 days, RT). However, when loaded with cargo, the time spans at RT were significantly reduced (Dil, 1 day; LUVs, 2h), demonstrating the large impact of cargo on DE stability. As exemplified by the Pfizer-BioNtech case, these time spans could still be feasible for real-world applications, although they call for complex distribution chains.

The decrease in size and swelling of the intermediate phase are expected to play an important role in the release profile of encapsulated compounds. This impact is demonstrated by studies that varied the shell thickness of core-shell microparticles, templated from double emulsions. Microparticles with thicker shells had a slower release of compounds present in the inner phase<sup>33,70</sup>. However, the release rate across lipid/octanol shells and the release profile when the thickness increases over time, as seen here, are less well known. The swelling of the intermediate phase is likely due to the partial miscibility of octanol in water (0.54 g/L)<sup>71</sup>. Octanol has recently gained relevance as a suitable intermediate phase when paired with lipids to form GUVs after dewetting from double emulsions templates<sup>29,40,72,73</sup>. In our work, the octanol in the intermediate layer was compatible with DE use as an oral drug delivery. Therefore, production conditions for the octanol dewetting, such as a given lipid concentration<sup>74</sup> and external stress<sup>40,57</sup>, were not necessary.

It is expected that further tuning of each solution and the properties of the lipid monolayer will improve DE stability, to broaden the range of potential applications. For example, different concentrations of lipids (e.g. 4% compared to 8% of phospholipids) have been shown to improve the long-term stability of DEs by maintaining their size and morphology constant for up to 30 days at 4°C<sup>75</sup>, or different concentrations/combinations of surfactants<sup>9,35,76</sup>. On a pioneering work, Ficheux *et al.*,<sup>35</sup> demonstrated that by changing the concentration of the hydrophilic surfactant, the stability of the double emulsions could be varied from a few minutes to months. Another approach is to use DEs as a template for other types of compartments, such as giant unilamellar vesicles<sup>29,40,72–74</sup>, gels<sup>77–79</sup> or microparticles<sup>33,36,51</sup>, although this increases the complexity of the process, since one or more post-production steps are required.

#### **4.4.3. Localisation and properties of cargo are important parameters for DE drug delivery**

It is becoming well accepted that cargo plays a huge role in physical properties and stability of encapsulated therapeutics, including micro- and nano- formulations<sup>80,81</sup>. This applies also to DEs, in particular because they can disrupt or enhance the overall stability of the metastable system<sup>82</sup>. In the case of Dil as the hydrophobic cargo, DE stability was affected in terms of morphological changes, i.e. coalescence of the intermediate phase.

There are various factors that can be at play. The arrangement of the hydrophobic cargo between the lipid molecules or monolayers can affect the behaviour of the membrane. Dil, for example, is located slightly below the water interface with a lipid monolayer, with the long alkyl tails parallel to the lipid molecules. Detailed studies about the location and arrangement of Dil in lipid membranes have shown that the presence of Dil increases the order around the lipid molecules, suggesting a stabilising effect<sup>56,83</sup>. This effect might have played a role in avoiding the simple bursting of the DEs and promoting coalescence due to a decrease in the surface tension.

The encapsulation of LUVs in the inner phase caused a drastic decrease in the long-term stability, reducing it from days to hours. The main reason for this might be the hypertonic inner phase. Works using a hypertonic inner phase in two-step emulsification also reported a thicker oil layer around the hypertonic DEs, while microfluidics allows for a higher degree of control

and thus, the possibility of combining a hypertonic inner phase with a very thin oil layer. The very thin oil layer is also expected to increase stability because it hinders transport across the oil layer<sup>37,84,85</sup>, however the combination of both might have been detrimental. Nevertheless, the LUV-loaded DEs had stability equivalent to that of the Pfizer-BioNtech vaccine at RT, which indicates a potential for application as an oral drug delivery system. Besides, the production of hypertonic DEs opens the possibility to use osmotic triggers for regional release of drugs<sup>86</sup>. Further work should explore the ratio of hypertonicity between inner and outer solutions and its effect on the long-term stability of DEs.

## 4.5. Conclusion

Lipid-stabilised DEs were successfully produced via microfluidics in PDMS chips, fabricated without the need of a cleanroom. DEs were monodisperse and allowed for the encapsulation of molecules of different properties in specific compartments. The stability through time was inversely proportional to temperature. When encapsulating a compound of interest the long term stability at RT decreased substantially from several days to hours. This behaviour highlights the importance of considering the properties of cargo early on in the formulation.

When exposed to pH, unloaded DEs were only significantly unstable at the extremes (pH 1 and 13) which are outside the physiological ranges. DiI-loaded and LUV-loaded DEs were more sensitive to acidic pH, although LUV-loaded DEs were overall more unstable to the stress than the other experimental conditions. When exposed to mechanical stress, LUV-loaded DEs behaved similarly to unloaded DEs at the lower pressures and were more sensitive to higher pressures. This indicates that the high instability to the pH conditions might be linked to the osmotic unbalance more than the mechanical stress caused by the experimental setup.

Together, these results suggest that lipid-stabilised DEs produced via microfluidics could be tailored to endure physiologically-relevant conditions and act as carriers for oral drug delivery. Further work should focus on the combined effect of different stresses on DE stability, e.g. combined effect of temperature and pH, since these conditions do not happen in isolation in real settings. Also, similar to other drug delivery systems, the cargo in DEs carriers should be actively considered as an integral part of the formulation design for better outcomes. Thus, special attention should be given to the composition and interplay of solutions and molecules involved in the final formulation from the start.

## 4.6. References

1. Muschiolik, G. & Dickinson, E. Double Emulsions Relevant to Food Systems: Preparation, Stability, and Applications. *Compr. Rev. Food Sci. Food Saf.* **16**, 532–555 (2017).
2. Ding, S., Serra, C. A., Vandamme, T. F., Yu, W. & Anton, N. Double emulsions prepared by two-step emulsification: History, state-of-the-art and perspective. *J. Control. Release* **295**, 31–49 (2019).
3. Sengupta, S. *et al.* Temporal targeting of tumour cells and neovasculature with a nanoscale delivery system. *Nature* **436**, 568–572 (2005).
4. Qi, X., Wang, L. & Zhu, J. Water-in-oil-in-water double emulsions: An excellent delivery system for improving the oral bioavailability of pidotimod in rats. *J. Pharm. Sci.* **100**, 2203–2211 (2011).
5. Yang, Y. Y., Chung, T. S. & Ping Ng, N. Morphology, drug distribution, and in vitro release profiles of biodegradable polymeric microspheres containing protein fabricated by double-emulsion solvent extraction/evaporation method. *Biomaterials* **22**, 231–241 (2001).
6. Lu, M. *et al.* Preparation, characterization and in vivo investigation of blood-compatible hemoglobin-loaded nanoparticles as oxygen carriers. *Colloids Surfaces B Biointerfaces* **139**, 171–179 (2016).
7. Yu, W. P. & Chang, T. M. . Submicron Polymer Membrane Hemoglobin Nanocapsules as Potential blood substitutes: Preparation and Characterization. *Artif. Cells, Blood Substitutes Immob. Biotech.* **24**, 169–183 (1996).
8. Verma, R. & Jaiswal, T. N. Protection, humoral and cell-mediated immune responses in calves immunized with multiple emulsion haemorrhagic septicaemia vaccine. *Vaccine* **15**, 1254–1260 (1997).
9. Liao, J. J., Hook, S., Prestidge, C. A. & Barnes, T. J. A lipid based multi-compartmental system: Liposomes-in-double emulsion for oral vaccine delivery. *Eur. J. Pharm. Biopharm.* **97**, 15–21 (2015).
10. Engel, R. H., Riggi, S. J. & Fahrenbach, M. J. Insulin: Intestinal Absorption as Water-in-Oil-in-Water Emulsions. *Nature* **219**, 856–857 (1968).
11. Matsumoto, S., Kita, Y. & Yonezawa, D. An attempt at preparing water-in-oil-in-water multiple-phase emulsions. *J. Colloid Interface Sci.* **57**, 353–361 (1976).
12. Frenkel, M., Shwartz, R. & Garti, N. Multiple Emulsions. I. stability, inversion, apparent and weighted HLB. *J. Colloid Interface Sci.* **94**, 174–178 (1983).
13. Garti, N. & Remon, G. F. Relationship between nature of vegetable oil, emulsifier and the stability of w/o emulsion. *Int. J. Food Sci. Technol.* **19**, 711–717 (1984).
14. Omotosho, J. A., Law, T. K., Whateley, A. T. & Florence, A. T. The stabilization of w/o/w emulsions by interfacial interaction between albumin and non-ionic surfactants. *Colloids and Surfaces* **20**, 133–144 (1986).
15. Kawashima, Y., Hino, T., Takeuchi, H., Niwa, T. & Horibe, K. Shear-induced phase inversion and size control of water/oil/water emulsion droplets with porous membrane. *J. Colloid Interface Sci.* **145**, 512–523 (1991).
16. Kim, C. K. *et al.* Preparation and characterization of cytarabine-loaded W/O/W multiple emulsions. *Int. J. Pharm.* **124**, 61–67 (1995).
17. Okochi, H. & Nakano, M. Preparation and evaluation of w/o/w type emulsions containing vancomycin. *Adv. Drug Deliv. Rev.* **45**, 5–26 (2000).
18. Benichou, A., Aserin, A. & Garti, N. Double emulsions stabilized by new molecular recognition hybrids of natural polymers. *Polym. Adv. Technol.* **13**, 1019–1031 (2002).
19. Berchane, N. S., Carson, K. H., Rice-Ficht, A. C. & Andrews, M. J. Effect of mean diameter and polydispersity of PLG microspheres on drug release: Experiment and theory. *Int. J. Pharm.* **337**, 118–126 (2007).
20. Kita, K. & Dittrich, C. Drug delivery vehicles with improved encapsulation efficiency: Taking advantage of specific drug-carrier interactions. *Expert Opin. Drug Deliv.* **8**, 329–

- 342 (2011).
21. Chu, L. Y., Utada, A. S., Shah, R. K., Kim, J. W. & Weitz, D. A. Controllable monodisperse multiple emulsions. *Angew. Chemie - Int. Ed.* **46**, 8970–8974 (2007).
  22. Shah, R. K. *et al.* Designer emulsions using microfluidics. *Mater. Today* **11**, 18–27 (2008).
  23. Tumarkin, E. *et al.* High-throughput combinatorial cell co-culture using microfluidics. *Integr. Biol.* **3**, 653–662 (2011).
  24. Utada, A. S. *et al.* Monodisperse double emulsions generated from a microcapillary device. *Science (80-. )*. **308**, 537–541 (2005).
  25. Czekalska, M. A. *et al.* One-Step Generation of Multisomes from Lipid-Stabilized Double Emulsions. *ACS Appl. Mater. Interfaces* **13**, 6739–6747 (2021).
  26. Petit, J., Polenz, I., Baret, J. C., Herminghaus, S. & Baumchen, O. Vesicles-on-a-chip: A universal microfluidic platform for the assembly of liposomes and polymersomes. *Eur. Phys. J. E* **39**, (2016).
  27. Trantidou, T., Dekker, L., Polizzi, K., Ces, O. & Elani, Y. Functionalizing cell-mimetic giant vesicles with encapsulated bacterial biosensors. *Interface Focus* **8**, (2018).
  28. Kong, L. *et al.* Lipid-Stabilized Double Emulsions Generated in Planar Microfluidic Devices. *Langmuir* **36**, 2349–2356 (2020).
  29. Yandrapalli, N., Petit, J., Baumchen, O. & Robinson, T. Surfactant-free production of biomimetic giant unilamellar vesicles using PDMS-based microfluidics. *Commun. Chem.* **2021 41 4**, 1–10 (2021).
  30. Aditya, N. P. *et al.* Co-delivery of hydrophobic curcumin and hydrophilic catechin by a water-in-oil-in-water double emulsion. *Food Chem.* **173**, 7–13 (2015).
  31. Choi, C. H., Weitz, D. A. & Lee, C. S. One Step Formation of Controllable Complex Emulsions: From Functional Particles to Simultaneous Encapsulation of Hydrophilic and Hydrophobic Agents into Desired Position. *Adv. Mater.* **25**, 2536–2541 (2013).
  32. Bazylińska, U. Rationally designed double emulsion process for co-encapsulation of hybrid cargo in stealth nanocarriers. *Colloids Surfaces A Physicochem. Eng. Asp.* **532**, 476–482 (2017).
  33. Li, Y. *et al.* Composite core-shell microparticles from microfluidics for synergistic drug delivery. *Sci. China Mater.* **60**, 543–553 (2017).
  34. Windbergs, M., Zhao, Y., Heyman, J. & Weitz, D. A. Biodegradable core-shell carriers for simultaneous encapsulation of synergistic actives. *J. Am. Chem. Soc.* **135**, 7933–7937 (2013).
  35. Ficheux, M. F., Bonakdar, L., Leal-Calderon, F. & Bibette, J. Some stability criteria for double emulsions. *Langmuir* **14**, 2702–2706 (1998).
  36. Tu, F. & Lee, D. Controlling the stability and size of double-emulsion-templated poly(lactic-co-glycolic) acid microcapsules. *Langmuir* **28**, 9944–9952 (2012).
  37. Zhao, C. X., Chen, D., Hui, Y., Weitz, D. A. & Middelberg, A. P. J. Controlled Generation of Ultrathin-Shell Double Emulsions and Studies on Their Stability. *ChemPhysChem* **18**, 1393–1399 (2017).
  38. Leister, N. & Karbstein, H. P. Evaluating the stability of double emulsions— A review of the measurement techniques for the systematic investigation of instability mechanisms. *Colloids and Interfaces* **4**, 8 (2020).
  39. Kanouni, M., Rosano, H. L. & Naouli, N. Preparation of a stable double emulsion (W1/O/W2): Role of the interfacial films on the stability of the system. *Adv. Colloid Interface Sci.* **99**, 229–254 (2002).
  40. Deshpande, S., Caspi, Y., Meijering, A. E. C. & Dekker, C. Octanol-assisted liposome assembly on chip. *Nat. Commun.* **7**, 1–9 (2016).
  41. Okushima, S., Nisisako, T., Torii, T. & Higuchi, T. Controlled Production of Monodisperse Double Emulsions by Two-Step Droplet Breakup in Microfluidic Devices. *Langmuir* **20**, 9905–9908 (2004).
  42. Yang, J. *et al.* Effect of temperature, pH, and ionic strength on the structure and physical stability of double emulsions prepared with starch. *LWT* **141**, (2021).
  43. Deng, N. N., Yelleswarapu, M. & Huck, W. T. S. Monodisperse Uni- and

- Multicompartment Liposomes. *J. Am. Chem. Soc.* **138**, 7584–7591 (2016).
44. Martino, C. & deMello, A. J. Droplet-based microfluidics for artificial cell generation: a brief review. *Interface Focus* **6**, (2016).
  45. Torbensen, K., Baroud, C. N., Ristori, S. & Abou-Hassan, A. Tip Streaming of a Lipid-Stabilized Double Emulsion Generated in a Microfluidic Channel. *Langmuir* **37**, 7442–7448 (2021).
  46. Trantidou, T., Regoutz, A., Voon, X. N., Payne, D. J. & Ces, O. A “cleanroom-free” and scalable manufacturing technology for the microfluidic generation of lipid-stabilized droplets and cell-sized multisomes. *Sensors Actuators B Chem.* **267**, 34–41 (2018).
  47. Ilaria Clemente *et al.* Exploring the water/oil/water interface of phospholipid stabilized double emulsions by micro-focusing synchrotron SAXS. *RSC Adv.* **9**, 33429–33435 (2019).
  48. Pandey, V. & Kohli, S. *Lipids and surfactants: The inside story of lipid-based drug delivery systems. Critical Reviews in Therapeutic Drug Carrier Systems* **35**, (2018).
  49. Hunt, J. N. & Knox, M. T. A relation between the chain length of fatty acids and the slowing of gastric emptying. *J. Physiol.* **194**, 327 (1968).
  50. Khan, S. *et al.* Nanostructured lipid carriers: An emerging platform for improving oral bioavailability of lipophilic drugs. *Int. J. Pharm. Investig.* **5**, 182 (2015).
  51. Weng, T. *et al.* The role of lipid-based nano delivery systems on oral bioavailability enhancement of fenofibrate, a BCS II drug: Comparison with fast-release formulations. *J. Nanobiotechnology* **12**, 1–8 (2014).
  52. Zhong, H., Chan, G., Hu, Y., Hu, H. & Ouyang, D. A comprehensive map of FDA-approved pharmaceutical products. *Pharmaceutics* **10**, 1–19 (2018).
  53. Hope, M. J., Bally, M. B., Webb, G. & Cullis, P. R. Production of large unilamellar vesicles by a rapid extrusion procedure. Characterization of size distribution, trapped volume and ability to maintain a membrane potential. *BBA - Biomembr.* **812**, 55–65 (1985).
  54. Elveflow. Microfluidic calculator - Elveflow. Available at: <https://www.elveflow.com/microfluidic-calculator/>. (Accessed: 30th June 2022)
  55. Kornyshev, Y. Short Communication A Model for Metastable States. *J. Non-Equilib. Thermodyn.* **18**, 353–358 (1993).
  56. Gullapalli, R. R., Demirel, M. C. & Butler, P. J. Molecular dynamics simulations of DiI-C18(3) in a DPPC lipid bilayer. *Phys. Chem. Chem. Phys.* **10**, 3548–3560 (2008).
  57. Krafft, D. *et al.* Compartments for Synthetic Cells: Osmotically Assisted Separation of Oil from Double Emulsions in a Microfluidic Chip. *ChemBioChem* **20**, 2604–2608 (2019).
  58. Kawashima, Y., Hino, T., Takeuchi, H. & Niwa, T. Stabilization of Water/Oil/Water Multiple Emulsion with Hypertonic Inner Aqueous Phase. *Chem. Pharm. Bull.* **40**, 1240–1246 (1992).
  59. Hino, T., Kawashima, Y. & Shimabayashi, S. Basic study for stabilization of w/o/w emulsion and its application to transcatheter arterial embolization therapy. *Adv. Drug Deliv. Rev.* **45**, 27–45 (2000).
  60. Liu, L., Yao, W. D., Rao, Y. F., Lu, X. Y. & Gao, J. Q. pH-Responsive carriers for oral drug delivery: challenges and opportunities of current platforms. <https://doi.org/10.1080/10717544.2017.1279238> **24**, 569–581 (2017).
  61. Baliga, S., Muglikar, S. & Kale, R. Salivary pH: A diagnostic biomarker. *J. Indian Soc. Periodontol.* **17**, 461 (2013).
  62. Pfeiffer, J. K. *Innate host barriers to viral trafficking and population diversity. Lessons learned from poliovirus. Advances in Virus Research* **77**, (Elsevier Inc., 2010).
  63. Pimentel-González, D. J., Campos-Montiel, R. G., Lobato-Calleros, C., Pedroza-Islas, R. & Vernon-Carter, E. J. Encapsulation of *Lactobacillus rhamnosus* in double emulsions formulated with sweet whey as emulsifier and survival in simulated gastrointestinal conditions. *Food Res. Int.* **42**, 292–297 (2009).
  64. van der Ark, K. C. H. *et al.* Encapsulation of the therapeutic microbe *Akkermansia muciniphila* in a double emulsion enhances survival in simulated gastric conditions. *Food Res. Int.* **102**, 372–379 (2017).



65. Malik, B., Gupta, R. K., Rath, G. & Goyal, A. K. Development of pH responsive novel emulsion adjuvant for oral immunization and in vivo evaluation. *Eur. J. Pharm. Biopharm.* **87**, 589–597 (2014).
66. Cardenas-Bailon, F., Osorio-Revilla, G. & Gallardo-Velazquez, T. Microencapsulation of insulin using a W/O/W double emulsion followed by complex coacervation to provide protection in the gastrointestinal tract. *J. Microencapsul.* **32**, 308–316 (2015).
67. Chen, W., Yan, G., Wang, Z., Jiang, P. & Liu, H. A wireless capsule robot with spiral legs for human intestine. *Int. J. Med. Robot. Comput. Assist. Surg.* **10**, 147–161 (2014).
68. Ho, N. F. H., Merkle, H. P. & William I. Higuchi. Quantitative, mechanistic and physiologically realistic approach to the biopharmaceutical design of oral drug delivery systems. *Drug Dev. Ind. Pharm.* **9**, 1111–1184 (1983).
69. Crommelin, D. J. A., Anchordoquy, T. J., Volkin, D. B., Jiskoot, W. & Mastrobattista, E. Addressing the Cold Reality of mRNA Vaccine Stability. *J. Pharm. Sci.* **110**, 997–1001 (2021).
70. Wu, J. *et al.* Fabrication and characterization of monodisperse PLGA-alginate core-shell microspheres with monodisperse size and homogeneous shells for controlled drug release. *Acta Biomater.* **9**, 7410–7419 (2013).
71. PubChem Compound Database. 1-Octanol - Hazardous Substances Data Bank. Available at: <https://pubchem.ncbi.nlm.nih.gov/compound/957#section=Solubility>. (Accessed: 30th June 2022)
72. Deshpande, S. & Dekker, C. On-chip microfluidic production of cell-sized liposomes. *Nat. Protoc.* **13**, 856–874 (2018).
73. Love, C. *et al.* Reversible pH-Responsive Coacervate Formation in Lipid Vesicles Activates Dormant Enzymatic Reactions. *Angew. Chemie* **132**, 6006–6013 (2020).
74. Peng Bao *et al.* Production of giant unilamellar vesicles and encapsulation of lyotropic nematic liquid crystals. *Soft Matter* **17**, 2234–2241 (2021).
75. Qi, X., Wang, L., Zhu, J., Hu, Z. & Zhang, J. Self-double-emulsifying drug delivery system (SDEDDS): A new way for oral delivery of drugs with high solubility and low permeability. *Int. J. Pharm.* **409**, 245–251 (2011).
76. Moriano, M. E. & Alamprese, C. Whey Protein Concentrate and Egg White Powder as Structuring Agents of Double Emulsions for Food Applications. *Food Bioprocess Technol.* **13**, 1154–1165 (2020).
77. Liu, L. *et al.* Preparation of monodisperse calcium alginate microcapsules via internal gelation in microfluidic-generated double emulsions. *J. Colloid Interface Sci.* **404**, 85–90 (2013).
78. Flaiz, L. *et al.* Comparison of simple, double and gelled double emulsions as hydroxytyrosol and n-3 fatty acid delivery systems. *Food Chem.* **213**, 49–57 (2016).
79. Delample, M., Da Silva, F. & Leal-Calderon, F. Osmotically driven gelation in double emulsions. *Food Hydrocoll.* **38**, 11–19 (2014).
80. Pilkington, E. H. *et al.* From influenza to COVID-19: Lipid nanoparticle mRNA vaccines at the frontiers of infectious diseases. *Acta Biomater.* **131**, 16–40 (2021).
81. Schoenmaker, L. *et al.* mRNA-lipid nanoparticle COVID-19 vaccines: Structure and stability. *Int. J. Pharm.* **601**, 120586 (2021).
82. O'Grady, D., Barrett, M., Casey, E. & Glennon, B. The effect of mixing on the metastable zone width and nucleation kinetics in the anti-solvent crystallization of benzoic acid. *Chem. Eng. Res. Des.* **85**, 945–952 (2007).
83. Repáková, J., Holopainen, J. M., Karttunen, M. & Vattulainen, I. Influence of Pyrene-Labeling on Fluid Lipid Membranes. *J. Phys. Chem. B* **110**, 15403–15410 (2006).
84. Etienne, G., Vian, A., Biočanin, M., Deplancke, B. & Amstad, E. Cross-talk between emulsion drops: How are hydrophilic reagents transported across oil phases? *Lab Chip* **18**, 3903–3912 (2018).
85. Arriaga, L. R., Amstad, E. & Weitz, D. A. Scalable single-step microfluidic production of single-core double emulsions with ultra-thin shells. *Lab Chip* **15**, 3335–3340 (2015).
86. Zhang, W. *et al.* Osmotic Pressure Triggered Rapid Release of Encapsulated Enzymes with Enhanced Activity. *Adv. Funct. Mater.* **27**, 1700975 (2017).

## CHAPTER 5.

# MONITORING ENVIRONMENTAL PARAMETERS IN MICROFLUIDIC CELL CULTURE

“Henrietta’s cells have now been living outside her body far longer than they ever lived inside it,”

— Rebecca Skloot, *The Immortal Life of Henrietta Lacks*

### ABSTRACT

---

CO<sub>2</sub> incubators are the silent enablers of most advancements in cell biology in modern biological research and health. They keep cells under constant physiological temperature (37 °C), humidity and CO<sub>2</sub> levels to buffer the pH of the media during cell growth. Organ-on-chip (OoC) has gained relevance in recent years for adding complexity to traditional cell culture, better replicating physiological conditions of mechanical stimulus and cell-to-cell interactions. However, OoC still depends substantially on the traditional cell culture infrastructure, such as the CO<sub>2</sub> incubator. Most researchers design microfluidic circuits to be placed inside the CO<sub>2</sub> incubator, using gas permeable chips made of PDMS or other polymers to ensure that the proper levels of CO<sub>2</sub> reach the media. This aspect becomes even more relevant when there is a need to keep the system outside the CO<sub>2</sub> incubator, and little is mentioned about the gas permeability of the other microfluidic components other than the chip. In this light, this work developed a complete microfluidic solution to support the advance of OoC outside the CO<sub>2</sub> incubator. The gas permeability of the flow circuit components was characterised by continuously inline monitoring of the pH of the cell culture due to its tight correlation with the CO<sub>2</sub> content of the media and the metabolic activity of the cells. The measurements were performed with an off-chip, inline 3D-printed flow cell and commercially available pH sensor plug that demonstrated enough sensitivity to differentiate between metabolic cycles in the tested conditions. PTFE was shown to allow the enrichment of the media with CO<sub>2</sub> nearly at the same rate as open vials but to retain CO<sub>2</sub> for much longer periods. Together, the results show proof-of-concept of an inline solution with strong potential to enable the emerging technology of OoC to expand into new applications, opening new avenues of research.

---

## ***Contributions***

---

The main part of this experimental work was performed by Camila Betterelli Giuliano. Based on discussions with Camila, Bibek Raut (Elvesys) designed and 3D-printed the flow cell. Savitashva Shringi (Elvesys) provided the thermalisation chamber prototype. Writing of this chapter was done by Camila Betterelli Giuliano. Revision was done by Camila Betterelli Giuliano, Dr. Lisa Muiznieks (Elvesys) and Prof. Joseph Moran (Univ. Strasbourg).

---

## ***Chapter Specific Acknowledgements***

---

We thank Juan Sandubete (Elvesys) for aiding with the data processing of continuous pH measurements and flow rates and Dr. Adam Anglart (Elvesys) for helping with the gas handling of the colorimetric assays.

---

## 5.1. Introduction

CO<sub>2</sub> incubators are the silent enablers of most advancements in cell biology in modern biological research and health. They keep cells under constant physiological temperature (37 °C), humidity and CO<sub>2</sub> levels to buffer the pH of the media during cell growth<sup>1,2</sup>. Organ-on-chip (OoC) has gained relevance in recent years for adding complexity to traditional cell culture, better replicating physiological conditions of mechanical stimulus and cell-to-cell interactions<sup>3</sup>. However, OoC still depends substantially on the traditional cell culture infrastructure, such as the CO<sub>2</sub> incubator, to maintain appropriate levels of CO<sub>2</sub> and temperature during long-term culturing on-chip<sup>4-6</sup>. One key advantage of these long-term cultures on-chip is the possibility of gathering real-time data at a resolution previously unattainable. Live cells can be continuously imaged on-chip, and metabolic processes can be followed to the single-protein level<sup>7-9</sup>. Nonetheless, CO<sub>2</sub> incubators are usually large pieces of equipment not necessarily located near the data-gathering instruments, such as microscopes. This can create difficulties when the chip needs to be moved from the incubator to the microscope stage at defined time points to gather data or require sophisticated and expensive equipment to maintain the chip on the microscope stage within acceptable conditions<sup>10</sup>. Besides the risk of contamination, mechanical shear stress and the introduction of air bubbles into the system due to the need to disconnect the chip, this duality incubator-microscope also limits continuous monitoring, which can be instrumental for a better understanding of cellular behaviour.

As detailed in Chapter 1, pH is a critical parameter to monitor during long-term microfluidic cell culture. Moreover, it is tightly linked to the atmospheric composition surrounding the system since CO<sub>2</sub> is part of the bicarbonate buffering system, the one favoured in many commonly used cell culture media<sup>11</sup>. As seen in Chapter 2, most researchers design microfluidic circuits to be placed inside the CO<sub>2</sub> incubator, to minimise unknown variables and because accessible alternatives are not available. These circuits employ gas permeable chips made of PDMS or other polymers to ensure the proper levels of CO<sub>2</sub> reach the media. pH monitoring becomes even more relevant when there is a need to keep the system outside the CO<sub>2</sub> incubator, and little is mentioned about the gas permeability of microfluidic components other than the chip<sup>12-14</sup>. PTFE is a commonly used polymer for tubing in microfluidics<sup>15,16</sup>. Commercially named Teflon, it is composed of C-F bonds arranged as [(CF<sub>2</sub>-CF<sub>2</sub>)<sub>n</sub>]. It is an inert and semi-crystalline thermoplastic with a wide range of applications, such as a lubricant and insulant in industrial processes and a coating material for biomedical instruments in health, and protection against acidic corrosion in chemistry<sup>17</sup>. Along with the other chemical and physical properties of PTFE, the gas permeability of PTFE is well-known and can be modulated<sup>18</sup>.

Several publications have used PTFE-based tubing and membranes for gas permeability applications. For example, *De Gregorio et al.*<sup>19</sup> assembled a device for long-term continuous measurement of dissolved CO<sub>2</sub> in groundwater, using a PTFE tube as the entry point of the gas into the system. The CO<sub>2</sub> from the groundwater slowly diffused through the PTFE wall and equilibrated inside the hollow tube, later analysed by an infrared gas analyser. *Tang et al.*<sup>20</sup> developed a similar approach for CO<sub>2</sub> capture, with PTFE purposefully made into a porous membrane. *Ozeki et al.*<sup>21</sup> coated PTFE with diamond-like carbon films to decrease the gas permeability of the polymer to volatile acids and make it more suitable to be used as gaskets, sealing materials and semiconductor devices. *Polyzos et al.*<sup>22</sup> used two different pieces of PTFE tubing to develop a device for the continuous-flow synthesis of carboxylic acids using CO<sub>2</sub> in a gas-liquid reactor. The authors concentrically arranged Teflon AF-2400, gas permeable, within a larger outer diameter PTFE tubing less permeable to gas. The liquid reagent was flushed inside the more permeable PTFE inner tubing, and CO<sub>2</sub> was flushed into the PTFE outer tubing, so it would diffuse into the liquid and trigger the chemical reactions. *Jensen et al.*<sup>23</sup> assembled a similar reactor, but the fluids were in the reverse order, i.e. the gas was flushed inside the inner permeable tubing, and the liquid in the outer shell between the two PTFE outer tubes.

While it is clear that PTFE tubing can be manufactured with different permeabilities to gas, the permeability of the tubing is hardly considered in OoC publications as most systems are placed inside the incubator. As mentioned, most assays investigating the gas permeability of the system focus on the microfluidic chip<sup>24–26</sup>. Even so, works have reported replacing the PTFE tubing with silicone tubing (Tygon) without further explanation of the added benefit<sup>27,28</sup>. Suppliers of microfluidic devices for cell culture, such as Ibidi, already provide information on the gas permeability of the chip based on the fabrication material. Still, the same information is not found on the datasheets of the tubing suppliers<sup>29</sup>. Microfluidics has evolved into a biology field from physics-related applications<sup>30</sup>; thus, the legacy of the components other than the chip has not yet been characterised or updated to best fit biological needs. This knowledge gap becomes more obvious once researchers start to move away from standard biology laboratory practices, such as using the CO<sub>2</sub> incubator, to profit from the full spectrum of possibilities that the OoC technology can offer. Hence, it is important to understand if the standard components of microfluidic setups are suitable for the next level of biological assays or if adjustments are required to ensure the best possible performance.

As noted in Chapter 1, microenvironmental monitoring of cell cultures becomes even more important in microfluidics. The minute volumes accelerate diffusion processes and the laminar

flow promotes the formation of gradients across the short axis of the chip (longitudinal liquid-liquid interfaces are maintained in laminar flows), creating more dynamic and fast-changing environments<sup>31</sup>. Using on-chip sensors provides spatiotemporal resolution, yet it substantially complexifies microfabrication and narrows the window of possibilities regarding chip design. Off-chip solutions allow the system to employ any chip design and are considerably easier to fabricate and assemble, besides being much more cost-effective when the goal is to ensure that microenvironmental parameters are kept within appropriate ranges. Flow-through cells (flow cells) are the most commonly used microfluidic components to house off-chip sensors in line in the microfluidic circuit. They can be placed before and/or after the chip and house several sensors simultaneously<sup>32</sup>. Although commercial solutions exist<sup>33–37</sup>, flow cells are usually custom-made to best fit the intended application. Several have been successfully employed to measure pH in microfluidic cell culture<sup>24,38–40</sup>.

This Chapter focuses on the gas permeability characterisation of the microfluidic cell culture components, namely chip and tubing, through pH and %CO<sub>2</sub> measurements. To understand the effects on cell growth and metabolism, the pH of the microenvironment of cell cultures performed outside the CO<sub>2</sub> incubator was monitored with a commercially available sensor and an in-house 3D-printed flow cell placed in line in two different microfluidic circuits, a simple reservoir-to-waste setup and a more complex miniaturised recirculation system inside a thermalisation chamber prototype. This chapter provides insights into the design of microfluidic cell culture equipment to be employed independently of a CO<sub>2</sub> incubator to enable the emerging technology of OoC to expand into new applications, opening new avenues of research.

## **5.2. Materials and Methods**

### **5.2.1. CO<sub>2</sub> and pH characterisation of media**

#### **5.2.1.1. Colorimetric Assay**

Dulbecco's Modified Eagle Medium (DMEM, ref. P04-04510, Panbiotech, Germany) supplemented with foetal bovine serum (10% FBS, ref. 8500-P131704, Panbiotech, Germany)

and Penicillin-Streptomycin (1% (v/v) P/S, ref. P06-07100, Panbiotech, Germany) was equilibrated to 0% CO<sub>2</sub> in room air for 3 days and then bubbled with the desired concentration of CO<sub>2</sub>. An optical CO<sub>2</sub> sensor (pH sensor plug, ref. 200001368; Presens, Germany) was used to ensure that the correct concentration was attained, and the pH was measured with a standard pH electrode (ref. STARA2115; Thermo Scientific, France, 3-point calibration). With a smartphone camera, pictures were taken of the vials to illustrate the pH scale of phenol red in DMEM. Measurements were done in duplicate.

### **5.2.1.2. DMEM/CO<sub>2</sub> Characterisation: Static conditions**

DMEM was either equilibrated to 0% CO<sub>2</sub> (in room air inside a 37°C bead bath (Precision GP 10, Thermo Scientific)) or 5% CO<sub>2</sub> (inside a CO<sub>2</sub> incubator (HERAcell VIOS 160i, Thermo Scientific)) for 6 days. The initial pH of both conditions was measured with a handheld pH electrode (ref. STARA2115; Thermo Scientific, France, 3-point calibration) to establish the initial pH of both conditions. The vial equilibrated at room air (0% CO<sub>2</sub>) was then placed inside the CO<sub>2</sub> incubator. The inverse was done with the vial equilibrated at 5% CO<sub>2</sub>, and pH measurements were taken at defined intervals. Controls were kept in the same conditions used for equilibration. Three measurements were taken for each time point, the values were averaged, and the standard deviation was calculated. The experiments were done in triplicate.

## **5.2.2. Gas permeability of components**

### **5.2.2.1. Development of 3D printed flow cell**

A flow cell was designed in SolidWorks 2021 (Dassault Systèmes, France). Then, the 3D CAD file was saved in STL format. The STL file was then imported to Chitubox®3D printing Slicing software and sliced at 50 µm-layer heights. The bottom 5-layer curing time was set to 45s, and each layer afterwards was set to 4s. Elegoo Mars 2 Pro (Elegoo, China) 3D printer was used with Elegoo Standard Translucent resin to print the parts. After printing, parts were immersed and cleaned in 99% isopropanol for 5 minutes, followed by post UV curing for 5 minutes.

### **5.2.2.2. Gas permeability of different tubing materials**

Pieces of a defined length of PTFE (OD: 1/16", ref. BL-PTFE-1608-20, Darwin Microfluidics, France), PVA (OD: 1/16", ref. F015229, Fluorotherm, USA) and PVDF (OD: 1/8", ref. F310006, Fluorotherm, USA) were cut (30 cm, PTFE and PVA; 15 cm, PVDF) and filled with media either equilibrated at room air (0% CO<sub>2</sub>) or in the CO<sub>2</sub> incubator (5% CO<sub>2</sub>). The pieces were closed with unions and stoppers and placed at the opposing conditions of the equilibrated media, i.e., pieces containing media at 0% CO<sub>2</sub> were placed inside the CO<sub>2</sub> incubator and pieces containing media at 5% CO<sub>2</sub> were placed inside the bead bath (to keep the temperature constant across conditions). The pH of the media was measured before filling and then after 72h. The pH of the pieces was measured after 72h with the aid of a flow cell (50 µl; ref. FC49K, Sensorex, USA) and the respective pH electrode (flat bottom probe; ref.S450CD/BNC, Sensorex, USA). Three measurements were made for each piece of tubing and the experiments were done in triplicates.

### **5.2.2.3. Gas permeability curve of PTFE in static conditions**

Pieces of PTFE (OD: 1/16") were cut at defined lengths (30cm) and filled with media. Pieces placed in room air (in bead bath at 37°C) were filled with media equilibrated to 5% CO<sub>2</sub> and pieces placed inside the CO<sub>2</sub> incubator were filled with media equilibrated to 0% CO<sub>2</sub>. Different pieces of tubing were prepared for measurements at defined time points. pH measurements were made before the filling of the pieces, with a pH electrode (flat bottom; Sensorex) and then at the defined intervals with the aid of a commercial flow cell (50 µl; ref. FC49K, Sensorex, USA) and respective pH electrode (flat bottom; Sensorex). Each measurement was made three times.

The same experiment was performed with a length of PTFE tubing with a smaller inner diameter (OD: 1/32", ref. DM-PTFE-0803-20, Darwin Microfluidics, France). The pieces were 30 cm long and, due to the minute volume, the measurements were made with a microfluidic-adapted pH sensor (pH sensor plug, ref. 200001368; Presens, Germany) placed inside an in-house developed flow cell. The measurements were made every second for the time required for the reading to stabilise and the plateau was averaged.



#### **5.2.2.4. Gas permeability of the chip in dynamic conditions**

A recirculation system comprising a pressure controller (OB1; Elveflow, France); two 15ml falcon tubes (total volume of the media: 13 ml); two 3/2 valves and MUX-Wire controller (Elveflow, France), a flow sensor (MFS3; Elveflow, France); 40 cm of resistance tubing (OD: 1/16"; ID: 125  $\mu$ m); a microfluidic chip (glass, ref.: 80177, or polymer coverslip, ref. 80176,  $\mu$ -Slide I Luer, height: 0.4mm, Ibidi, Germany), a flow cell and a pH sensor (standard electrode, ref. S450CD/BNC, and commercial flow cell, ref. FC49K, Sensorex, USA; or pH sensor plug, ref. 200001368, Presens, Germany, and 3D-printed flow cell, as specified) was assembled with PTFE tubing (OD: 1/16"; ID: 1/32') and placed inside the CO<sub>2</sub> incubator (total length: 374.5 cm; total volume inside the system: 1.44 ml). Media equilibrated to 0% CO<sub>2</sub> was recirculated for 72h at 10  $\mu$ l/min. pH measurements were made manually with a flat bottom pH electrode and commercial flow cell or continuously with a pH sensor plug and 3D-printed flow cell as specified. Experiments were made in triplicates.

The same system was assembled with PVDF tubing (OD: 1/8"; ID: 1/16"; total length: 214.5 cm; total volume inside the system: 4.25 ml; total volume of media: 13 ml). Media equilibrated to 5% CO<sub>2</sub> was perfused at 5  $\mu$ l/min with the system placed in a bead bath at 37°C for 72h with a gas impermeable chip. The inverse was performed with media equilibrated to 0% CO<sub>2</sub>, with the system placed in the CO<sub>2</sub> incubator and a gas permeable chip. pH measurements were made continuously with the pH sensor plug and flow cell. For the recirculation, the time between reservoir changes was dependent on the flow rate and the volume in the reservoirs, calculated based on the time that would take to almost empty the first reservoir. These experiments were done with 13 ml of volume (approximately 6 ml in the first reservoir; 4 ml in the second, and 3 ml in the microfluidic circuit), which meant that each reservoir was pressurised for 12 hours, leaving enough buffer time and volume to avoid introducing air into the system.

### **5.2.3. Culturing cells outside the CO<sub>2</sub> incubator**

#### **5.2.3.1. Cell Seeding**

HEK293 cells were kept in flasks (25 cm<sup>2</sup>, Thermo Scientific) with 7.5 ml of DMEM (ref. P04-04510, Panbiotech, Germany) supplemented with foetal bovine serum (10% FBS, ref. 8500-

P131704, Panbiotech, Germany) and Penicillin-Streptomycin (1% (v/v) P/S, ref. P06-07100, Panbiotech, Germany) inside the 5% CO<sub>2</sub> incubator at 37°C. For seeding in microfluidic chips, cells were released from the bottom of the flask with trypsin (0.05% in PBS), counted, pelleted, and resuspended at the desired concentration. Then, the chip (glass or polymer coverslip, straight-channel, height: 0.4mm, Ibidi, Germany) was filled with the suspension with a pipette and placed inside the CO<sub>2</sub> incubator overnight for the cells to attach. A solution of collagen type I (25 µg/ml in PBS, 2 h incubation in CO<sub>2</sub> incubator; ref. 354249, Corning, USA) was first used to coat the surface of the gas impermeable chips which have a glass coverslip (ref. 80177, Ibidi, Germany). The chips with the polymer coverslip came coated from the supplier (ref. 80176, Ibidi, Germany).

### **5.2.3.2. Static microfluidic cell culture outside the CO<sub>2</sub> incubator**

Cells were seeded in gas permeable (polymer coverslip, ref. 80176) or gas impermeable (glass coverslip, ref.: 80177, µ-Slide I Luer, height: 0.4mm, Ibidi, Germany) chips as described above and kept outside the CO<sub>2</sub> incubator after attachment overnight. The chips were placed in Petri dishes inside the bead bath at 37°C and surrounded with beads to ensure good temperature transfer. A falcon tube lid full of water was placed inside the Petri dish to prevent evaporation from the microfluidic chamber. The cells were cultured in static conditions with the media changed manually daily.

### **5.2.3.3. Intermittent reservoir-to-waste cell culture outside the CO<sub>2</sub> incubator**

A reservoir-to-waste system was assembled with PTFE (OD:1/16"). The system was composed of an OB1 pressure controller; one 15 ml falcon tube (total volume of the system: 13 ml); an MFS3 flow sensor; 40 cm of resistance tubing (ID: 125 µm); a microfluidic chip (glass or polymer coverslip, straight-channel, height: 0.4mm, Ibidi), a flow cell and a pH sensor (pH sensor plug, Presens; and 3D-printed flow cell). The system was placed in the bead bath at 37°C and used to culture cells in the gas impermeable (glass, 1.2x10<sup>6</sup> cell/ml; cell attachment and incubation, 2 days; n=2) and gas permeable chips (polymer, 2.2x10<sup>6</sup> cell/ml, cell attachment and incubation, 1 day; n=1). The total volume of media of the system was 13 ml, the length of the tubing of the system was 167 cm (total volume: 600 µl) and the flow was intermittent (5 µl/min, 2 min per hour, for 40h). pH measurements were automatically taken

every 5 minutes, and the standard deviation was calculated from the pH values between each flow cycle. Control chips of the respective material were kept in the bead bath and had the media changed once a day manually.

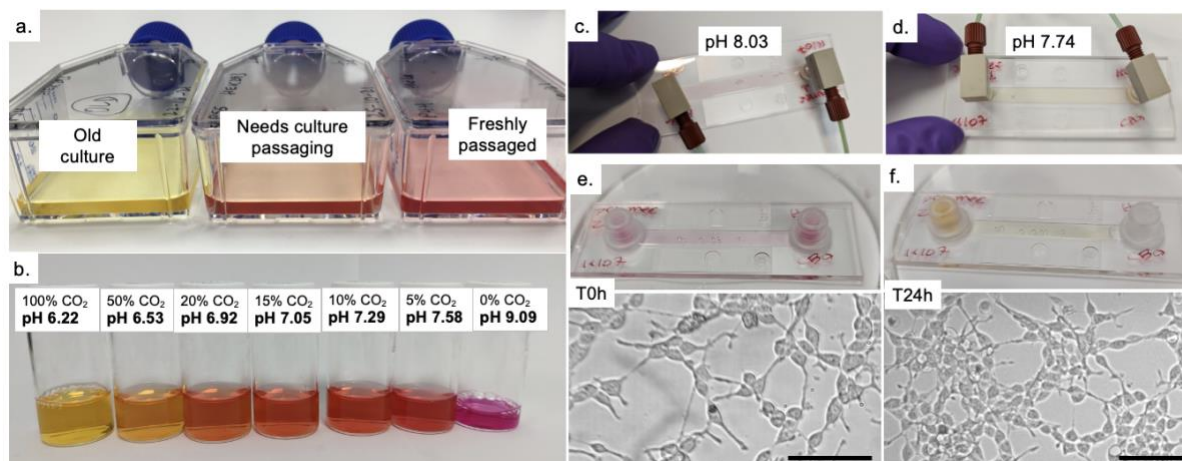
#### **5.2.3.4. Intermittent recirculation cell culture outside the CO<sub>2</sub> incubator**

A miniaturised recirculation setup was assembled with PTFE (OD: 1/32"), placed in a thermalisation chamber prototype kept at 37°C over the microscope stage and used to culture cells in the gas impermeable (glass,  $1.9 \times 10^6$  cell/ml, cell attachment and incubation, 1 day; n=3) and gas permeable chips (polymer,  $2.43 \times 10^6$  cell/ml, cell attachment and incubation, 1 day; n=2). The resistance tubing had the same inner diameter, but a smaller outer diameter (OD: 1/32"), and the flow sensor had no casing. The total volume of media of the system was 4 ml (2 Eppendorf tubes), and the flow was intermittent (5 µl/min, 2 min per hour, for 60h). The length of the tubing was 109 cm (total volume: 77 µl). pH measurements were automatically taken every 5 minutes, and the standard deviation was calculated from pH values between each flow cycle.

## **5.3. Results**

### **5.3.1. The importance of measuring pH in microfluidics**

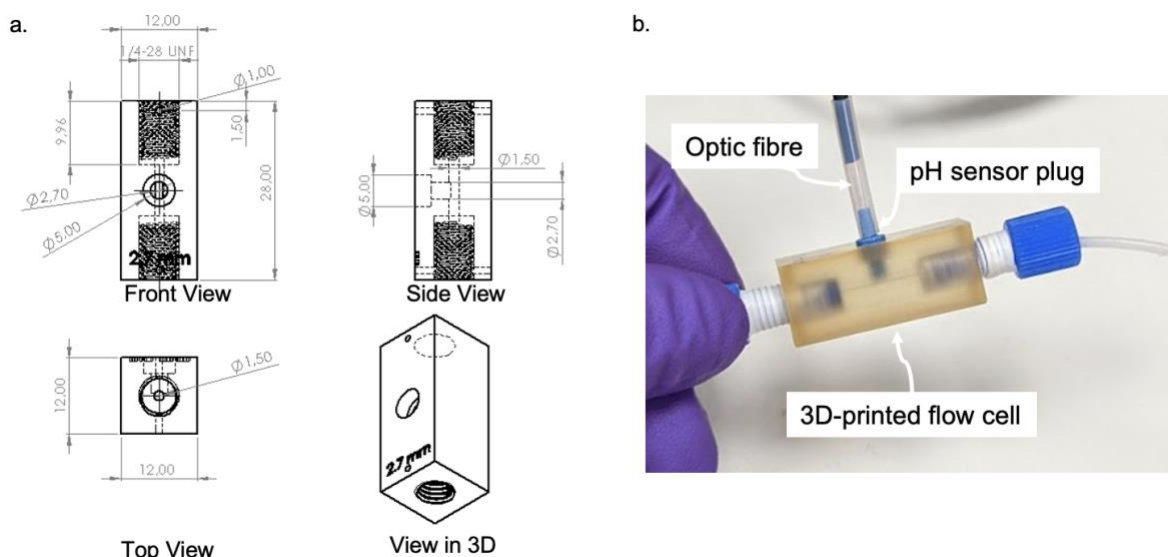
Phenol red is a common pH indicator for cell culture media. It indicates metabolic activity in traditional cell culture and the overall health of stock cultures between passages (Figure 5.1.a). However, a single shade of Phenol red can represent an entire pH point (Figure 5.1.b). Moreover, during microfluidic cell culture, the channel often presents a yellow shade while measuring pH 7.74 (Figure 5.1.c. and d.). When observed under the microscope in this condition, the cells are growing and dividing, with a healthy attached morphology (Figure 5.1.e and f.).



**Figure 5.1.** Phenol Red, as a pH indicator of cell cultures in traditional flasks and microfluidic devices. **a.** Phenol red is a standard pH indicator added to the cell culture media, providing a visual indication of the microenvironment pH and cell culture health. **b.** The same shade of Phenol red presents an entire pH point, outside the tolerated physiological variation range. **c. and d.** Phenol red becomes unreliable once the system is down-scaled to the micrometre range (measured with an off-chip flow cell and pH sensor plug). **e. and f.** Static cell culture on-chip, showing the lack of relationship between the colour of the media and the morphology of the cells. Initial cell concentration:  $2.43 \times 10^6$  cell/ml. Scale bars, 100  $\mu$ m.

### 5.3.2. Design of 3D-printed flow cell

To house the pH sensor plug and allow its placement in line in the microfluidic circuit, a flow cell was designed and 3D-printed (Figure 5.2). The design was optimised to avoid leakage and increased resistance of the system while keeping the internal volume to a minimum.



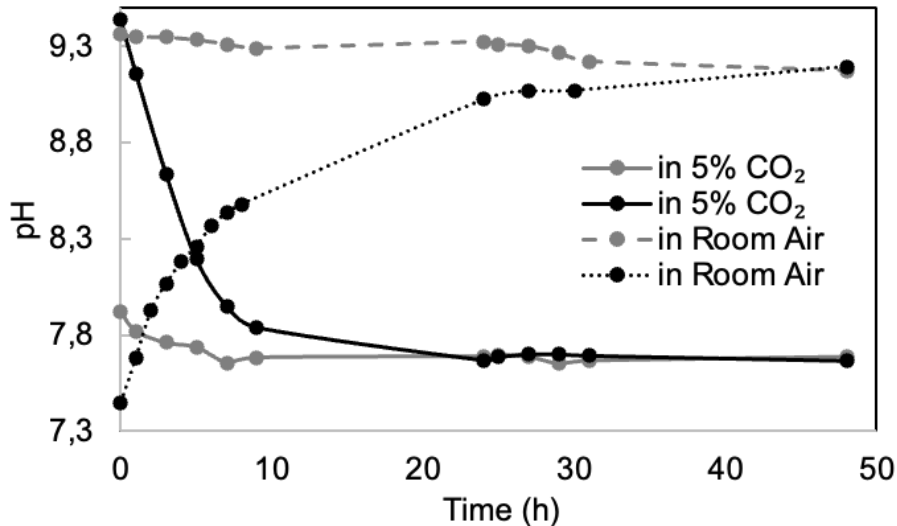
**Figure 5.2.** 3D-printed flow cell to house pH sensor plug. **a.** Schematic of the flow cell design in different angles. **b.** 3D-printed flow cell with sensor and optic fibre, fittings, and tubing of the microfluidic circuit.

The flow cell was designed with a 1.5 mm-diameter through hole with two 1/4-28" threaded port at the ends to fit the microfluidic connectors. In the middle of the flow cell, a 2.7mm-diameter hole was used for inserting the pH sensor plug. 1.5 mm-holes near the end and on the 1/4-28" ports were designed to allow the parts to maintain equilibrium to atmospheric pressure during printing and prevent the build-up of resins near the edge.

### 5.3.3. Characterisation of the effect of CO<sub>2</sub> on DMEM

DMEM is a commonly employed cell culture media that uses the bicarbonate buffering system (NaHCO<sub>3</sub>/CO<sub>2</sub>) to keep the pH at a desirable range for cell growth<sup>41</sup>. To understand the extent to which the microfluidic components, mainly the tubing and the chip, affect this buffering system, i.e., how much CO<sub>2</sub> the materials allow to enter or leave the system, it was important to understand the behaviour of DMEM's pH in different CO<sub>2</sub> concentrations. When exposed to different CO<sub>2</sub> concentrations (room air, 0%; CO<sub>2</sub> incubator, 5%), DMEM's pH varied considerably (black lines, Figure 5.3). When equilibrated to 0% CO<sub>2</sub> (pH 9.3-9.5) and placed inside a 5% CO<sub>2</sub> incubator, medium equilibrated to pH 7.7 within 24 hours, with the 83% of the pH change happening in the first 10 hours (DMEM at 5% CO<sub>2</sub> equilibrates to pH 7.7-7.8<sup>41</sup>). The reverse was also observed. Medium enriched with 5% CO<sub>2</sub> equilibrated to pH 9.3-9.5 when left in room air for at least 24 hours (placed inside the bead bath for comparable

temperature with CO<sub>2</sub> incubator, 37°C), with the 91% of increase also in the first 10 hours. These measurements were performed in static conditions (13 ml, glass vials with unscrewed lids).



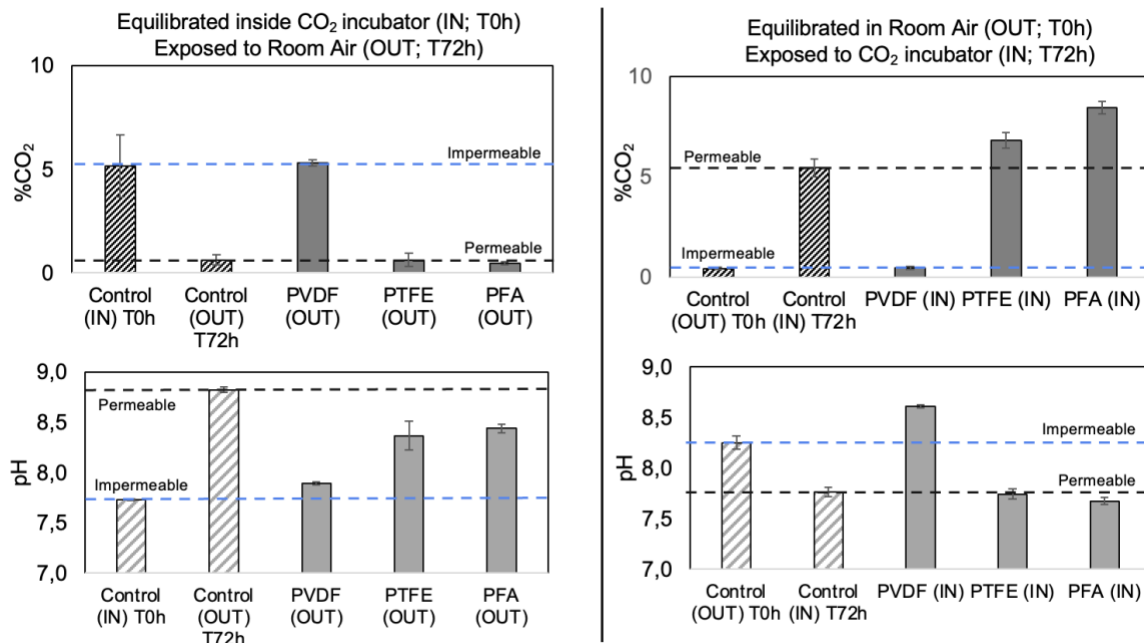
**Figure 5.3.** Characterisation of the pH of DMEM in different atmospheric concentrations of CO<sub>2</sub> (room air, 0%; CO<sub>2</sub> incubator, 5%), in static conditions. When inside the CO<sub>2</sub> incubator, the pH equilibrated to 7.7, if initially higher. When in room air, the pH increased to pH 9.3-9.5 if initially at pH 7.5-7.7. Major changes take place in the first 10 hours of exposure.

## 5.3.4. Gas permeability of microfluidic components

### 5.3.4.1. Gas permeability of Microfluidic tubing

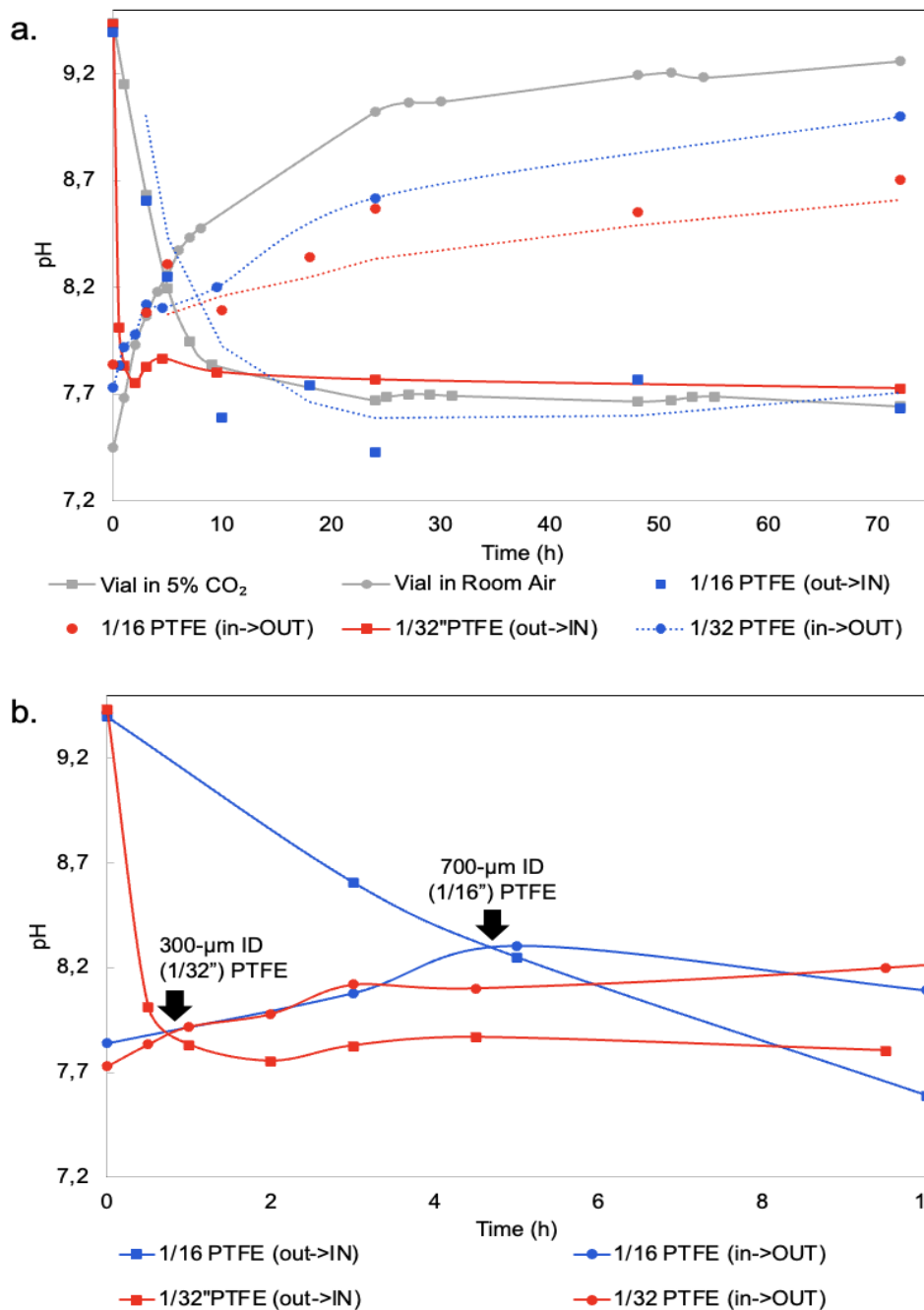
PTFE is the most common material for tubing used in microfluidic systems and is expected to be highly gas-permeable<sup>42</sup>, although the gas permeability can be modulated<sup>18</sup>. Due to the intimate relation between CO<sub>2</sub> and pH, the gas permeability of the microfluidic components was determined. Focusing first on the tubing, the gas permeability of PTFE was compared to two other polymeric materials: Perfluoroalkoxy alkanes (PFA) and Polyvinylidene fluoride (PVDF). PFA is reported to be partially permeable to CO<sub>2</sub>, but to a lesser extent than PTFE<sup>43</sup>. Given that it is optically transparent and as malleable as PTFE, it could be considered a replacement in case the gas permeability of PTFE proved detrimental. PVDF is reported to be nearly impermeable to gas<sup>43</sup>. PTFE showed a considerable permeability to CO<sub>2</sub> (Figure 5.4), i.e., when filled with media equilibrated to pH 7.73 (5% CO<sub>2</sub>) and placed outside (0% CO<sub>2</sub>) the incubator, the pH increased to 8.37 over 72h. Inversely, when filled with media equilibrated to

pH 8.25 and placed inside the incubator (5% CO<sub>2</sub>), the pH dropped to 7.74, in the same period. PFA demonstrated similar behaviour to PTFE, contradicting reports that it would be less gas permeable than PTFE. PVDF demonstrated to be impermeable to CO<sub>2</sub>, as expected, and could be a good choice to keep the gas characteristics of the system unaffected by external conditions; however, it is hard to use due to its rigidity.



**Figure 5.4.** Gas permeability of different polymeric materials. PTFE, PFA and PVDF were filled with media equilibrated to varying concentrations of CO<sub>2</sub> and exposed to conditions that promoted the transport of CO<sub>2</sub> across the tubing wall for 72h. The CO<sub>2</sub> and the pH percentage were measured and compared to vials exposed to the same conditions (control). PTFE and PVA were similarly permeable to CO<sub>2</sub>, while PDVF showed no permeability.

PFA did not confer any advantages in gas permeability compared to PTFE, and PVDF was challenging to use. As PTFE is the standard material for microfluidic circuits, a more in-depth analysis of PTFE gas permeability was required. A time-lapsed analysis of the gas permeability of PTFE with different outer diameters (OD: 1/16", ID: 700 μm; OD: 1/32"; ID: 300 μm) showed that it allowed CO<sub>2</sub> to enter more quickly than it allowed CO<sub>2</sub> to leave the tubing (Figure 5.5). When placed outside the incubator, the pH of the larger tubing (ID: 700 μm) remained 0.6 pH points below the open vials and the smaller tubing (ID: 300 μm), 0.3 pH points, while both diameters reached pH 7.7 when inside the incubator. The larger tubing equilibrated in about 10 h as the open vials, and the smaller tubing, in 2 h. This behaviour can be theoretically explained by Eq.5.1.



**Figure 5.5.** Gas permeability curve of PTFE tubing of different diameters (1/16" OD, ID = 700 µm ID; 1/32" OD, ID = 300 µm). **a.** PTFE showed different permeabilities to CO<sub>2</sub> depending on the direction of the flux compared to open vials filled with media. The pH of the media in both PTFE diameters decreased as quickly as the open vials when placed inside the CO<sub>2</sub> incubator, while it increased slower when placed outside the incubator, remaining approximately 0.6 pH (1/16") and 0.3 (1/32") points lower than the vial for the studied period. **b.** Highlight of the first 10 h. Black arrows point to the crossing of each curve as an indication of the equilibration time. The 1/32" PTFE tubing equilibrated 4 times faster than the 1/16" PTFE tubing.



The equilibration time of a gas-liquid system can be defined by Eq. 5.1<sup>19,44</sup>.

$$t_{eq} = -\ln(0.01) \frac{hV}{k_p A} \quad \text{Eq. 5.1}$$

where  $t_{eq}$  is the equilibrium reached at a certain time, s;  $h$  is the membrane thickness, cm;  $V$  is the volume of the system,  $\text{cm}^3\text{STP}$ ;  $k_p$  is the coefficient of permeability ( $\text{cm}^3 \text{STP cm}^{-1}\text{sec}^{-1}\text{atm}^{-1}$ ), and  $A$  is the surface area,  $\text{cm}^2$ .

Given the known variables of the PTFE permeability curve and the equilibration time for 5%  $\text{CO}_2$  (Table 5.1), it was possible to calculate the coefficient of permeability of these types of tubing and the polymer chip.

**Table 5.1.** Values used to calculate the coefficient of permeability of PTFE tubing

<b>PTFE Experimental Parameters</b>	<b>1/16" PTFE</b>	<b>1/32" PTFE</b>	<b>Polymer Chip Parameters</b>	<b>Polymer Chip</b>
Outer Diameter (cm)	1/16" = 0.1587	1/32"= 0.0793	Height (cm)	0.04
Inner Diameter (cm)	1/32" = 0.0793	0.03	Length (cm)	5
Length (cm)	30	30	Width (cm)	0.5
<b>Calculated Parameters</b>			<b>Calculated Parameters</b>	
Volume of the system (V) ( $\text{cm}^3\text{STP}$ )	0.1154	0.0212	Volume of the system (V) ( $\text{cm}^3\text{STP}$ )	0.1
Surface Area (A) ( $\text{cm}^2$ )	6.61	2.82	Surface Area (A) ( $\text{cm}^2$ )	2.5
Membrane Thickness (h) (cm)	0.0794	0.0493	Membrane Thickness (h) (cm)	0.0170
Equilibration time ( $t_{eq}$ ) (s)	86,400 (24h)	7,200 (2h)	Equilibration time ( $t_{eq}$ ) (s)	432,000 (120h)
<b>Calculated <math>k_p</math> (<math>\text{cm}^3\text{STP.cm}^{-1}.\text{s}^{-1}.\text{atm}^{-1}</math>)</b>	$7.38 \times 10^{-7}$	$2.36 \times 10^{-7}$	<b>Calculated <math>k_p</math> (<math>\text{cm}^3\text{STP.cm}^{-1}.\text{s}^{-1}.\text{atm}^{-1}</math>)</b>	$7.248 \times 10^{-9}$

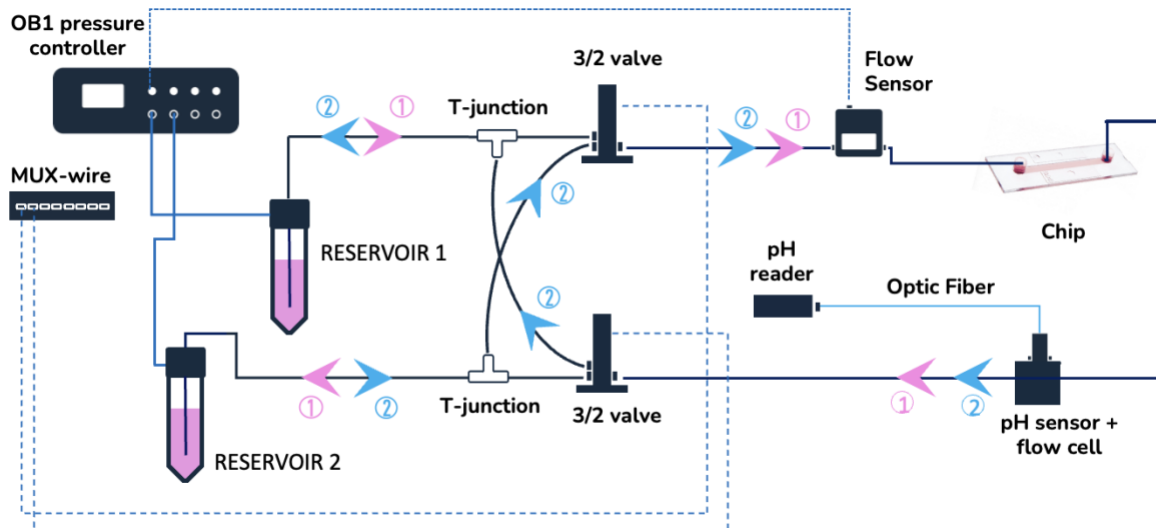
Using the equilibration time for PTFE inside the  $\text{CO}_2$  incubator (24h, 1/16"; 2h, 1/32"; 120h, polymer chip), the coefficient of permeability of 1/16" PTFE tubing was calculated to be

$7.38 \times 10^{-7} \text{ cm}^3\text{STP}\cdot\text{cm}^{-1}\cdot\text{s}^{-1}\cdot\text{atm}^{-1}$ ;  $2.36 \times 10^{-7} \text{ cm}^3\text{STP}\cdot\text{cm}^{-1}\cdot\text{s}^{-1}\cdot\text{atm}^{-1}$  for the 1/32" PTFE; and,  $7.248 \times 10^{-9} \text{ cm}^3\text{STP}\cdot\text{cm}^{-1}\cdot\text{s}^{-1}\cdot\text{atm}^{-1}$  for the polymer chip.

Considering the physical parameters of the tubing in isolation, the surface area of the 1/16" tubing is 134% larger than the one of the 1/32" tubing. The membrane is 61% thicker in the 1/16" tubing than in the 1/32" tubing. A larger surface area is more permissive of gas permeation whereas a thicker membrane hinders it. Taking both parameters in consideration, which are directly correlated to gas permeability, the 1/16" tubing has 73% faster gas permeation than the 1/32" tubing, in accordance to the experimental data.

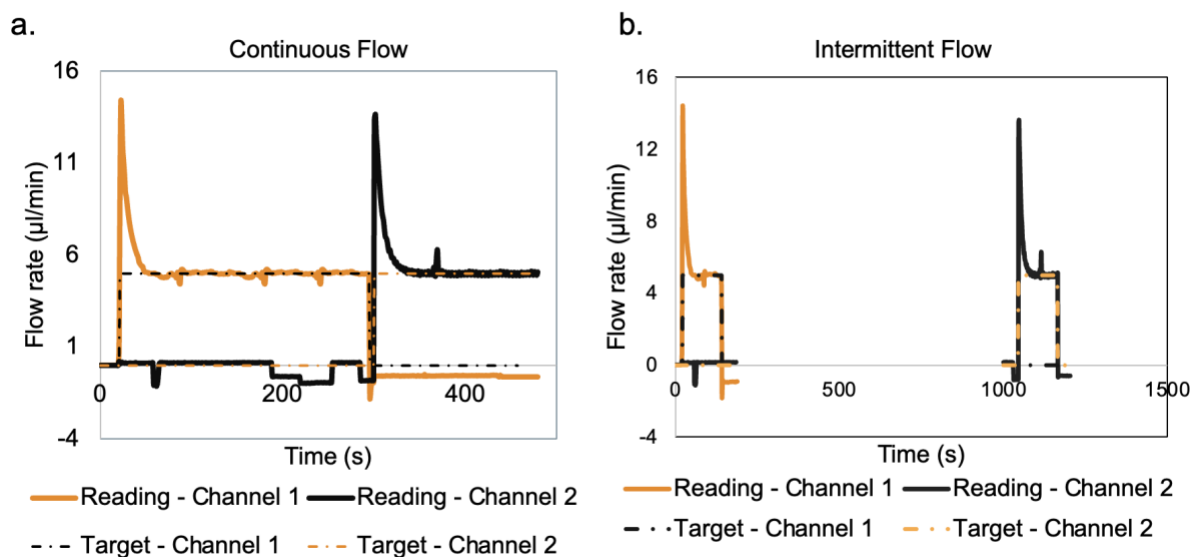
#### **5.3.4.2. Gas permeability of microfluidic chip**

The chip is a crucial component of microfluidic circuits. As microfluidics relevance increases in biological fields, microfluidic devices are becoming better adapted to biology, and the properties of the materials, such as the gas permeability, have started to be incorporated into datasheets<sup>45</sup>. Hence, it is easy to purchase gas permeable or impermeable microfluidic chips; however, as seen with PTFE and PFA, the actual gas permeability is not specified. A microfluidic recirculation circuit was assembled to investigate this characteristic in pertinent conditions (Figure 5.6). Two reservoirs were connected to two 3/2 valves via T-junctions. The T-junctions were interconnected, between the reservoirs and valves, to ensure unidirectional flow. The flow sensor controlled the pressure-driven flow and secured a steady and constant flow rate. A pH sensor and flow cell were placed after the chip outlet to measure the effect of gas permeability. The position was chosen to ensure that measurements of the outlet of the chip were collected, detecting changes that took place inside the chip.



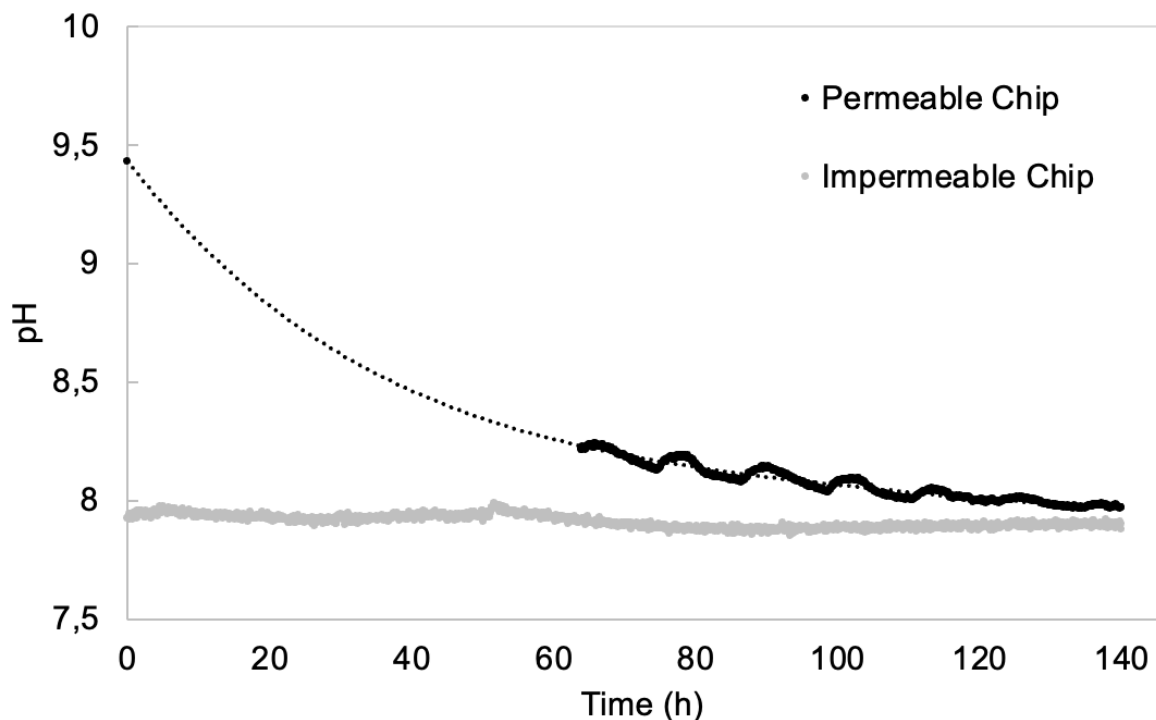
**Figure 5.6.** Schematic of microfluidic recirculation circuit. Two reservoirs were connected to two 3/2 valves via T-junctions. Medium flows from reservoir 1 (pink arrows) through the circuit and collects in reservoir 2. Then, valve positions are switched and medium flows from reservoir 2 (blue arrows) unidirectionally through the chip and collects in reservoir 1. Alternating cycles produce smooth continuous flow.

Two flow profiles were used in the microfluidic experiments (Figure 5.7). Recirculation setups not involving cells used continuous flow at 5  $\mu\text{l}/\text{min}$ . Continuous flow consisted in pressurising one reservoir at a time and maintaining the flow constant at the desired flow rate for a defined period. Once the period ended, this reservoir stopped being pressurised while the pressure started in the second reservoir, re-establishing the flow at the desired rate nearly without interruption (Figure 5.7.a.). Cycles of 12 h of flow from each reservoir were used. In experiments culturing cells, the flow profile was intermittent (Figure 5.7.b.), i.e. 5  $\mu\text{l}/\text{min}$  was flushed on top of the cells for two minutes every hour and the media remained static between each cycle of two minutes. This adjustment was made to prevent exerting excessive shear stress on the cells. In this case, the change between reservoirs happened every 12 hours. These experiments will be detailed in Section 5.3.5.



**Figure 5.7.** Continuous and intermittent flow profiles of recirculation experiments. **a.** Representative profile, switching every 5 minutes. In continuous flow, one of the channels was constantly pressurised, and the flow remained constant until the channel was switched off and the second channel was switched on. **b.** In intermittent flow, the channels were only on for brief periods.

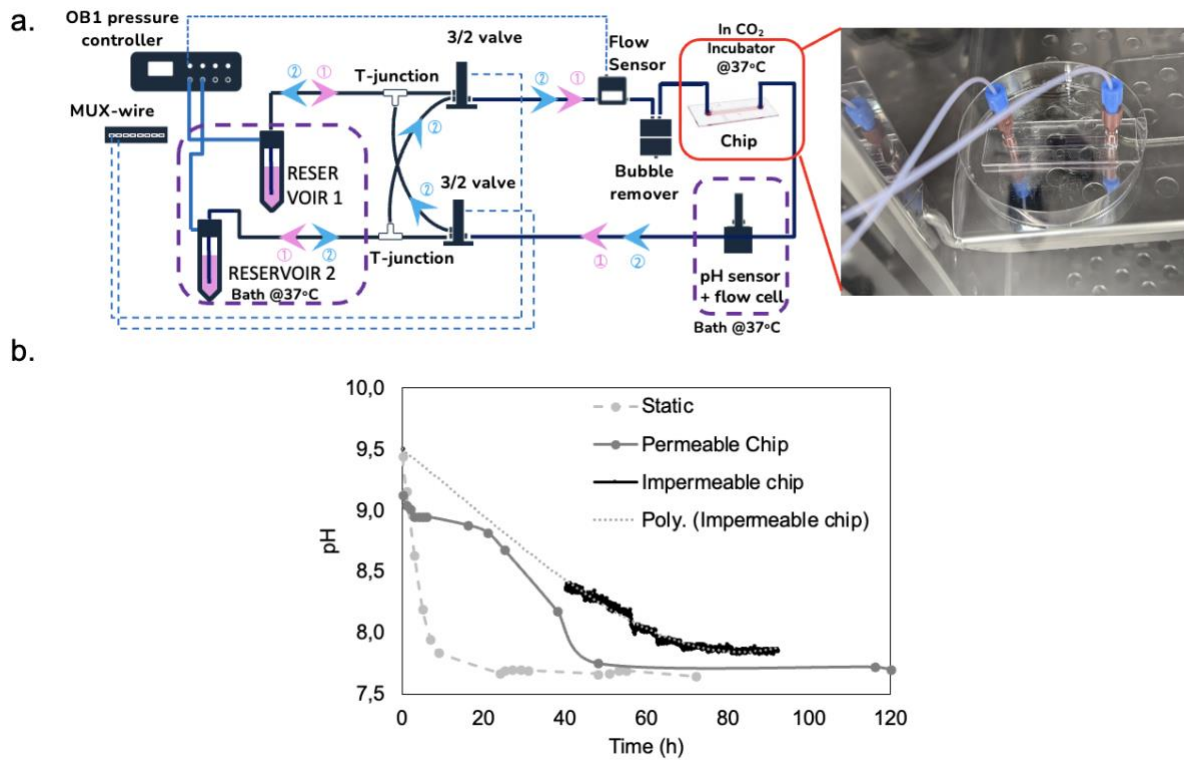
The recirculation was assembled with PVDF tubing and gas permeable (polymer coverslip) and gas impermeable chip (glass coverslip). The gas permeable chip setup was placed inside the  $\text{CO}_2$  incubator and the pH of the medium (initially equilibrated to 0%  $\text{CO}_2$ , pH 9.43) decreased over time (140h) as  $\text{CO}_2$  entered the system through the chip. The microfluidic circuit with the gas impermeable chip was left outside the  $\text{CO}_2$  incubator, inside the bead bath for constant temperature, and the pH was constant for over 140 h (Figure 5.8). Flow cell was leak free, pH sensor measurements were steady and consistent, indicating a suitable pH monitoring solution for OoC.



**Figure 5.8.** Gas permeability of microfluidic devices. A gas impermeable chip was inserted into a recirculation system assembled with gas impermeable tubing, resulting in constant pH due to an absence of external influence from the atmosphere. A gas permeable chip was added to the same recirculation system, and placed inside the CO<sub>2</sub> incubator, showing a decrease in pH due to the CO<sub>2</sub> entry into the system. The trendline is to guide the eye; pH sensor plug pH range: pH 5.5-8.5; initial measurement done with a flat bottom pH electrode

To assess whether the permeability behaviour of the PTFE would be significant to a cell culture microfluidic setup designed to remain outside the CO<sub>2</sub> incubator, the recirculation system was rearranged so the chip and a small portion of the tubing were inserted into the CO<sub>2</sub> incubator (exposed to CO<sub>2</sub>), while the rest of the system remained exposed to room air (Figure 5.9, inset). The goal was to assess whether the gained CO<sub>2</sub> would be lost once the medium left the incubator. To that extent, the pH sensor was placed outside the incubator in the bead bath (Figure 5.9.a.). Compared to the glass vials in static conditions, the decrease in pH of the permeable chip was slow, taking approximately 48 h to reach pH 7.8, while it took approximately 10 h for the media in the vial to reach that value. For the condition with the impermeable chip, the decrease was even slower, taking over 60 h to reach the lowest pH point (Figure 5.9.b.). The relevant point here is that the pH did not equilibrate back to "room air levels", i.e. over pH 8.5, during the studied period of the experiment. The initial pH measurement was 9.5 for the impermeable chip (measured with a flat bottom pH electrode, as

it was outside the range of the pH sensor plug). The average measurement of the reservoirs after 72h was 7.93 (measured with the same pH electrode), illustrating that the tubing inside the incubator was permeable to CO<sub>2</sub> and the gas did not leave the system at the same rate as it entered it.

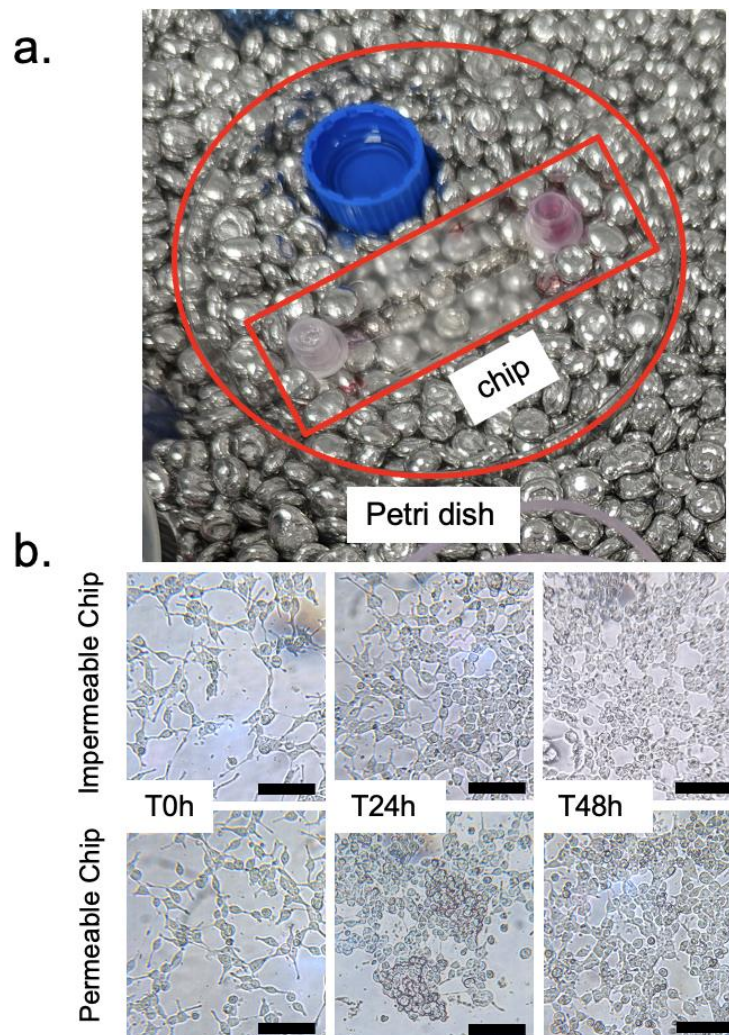


**Figure 5.9.** Gas permeability of PTFE tubing. **a.** Schematic of the recirculation system placed partially inside the CO<sub>2</sub> incubator and partially outside. Inset shows the chip placed inside the CO<sub>2</sub> incubator. **b.** pH measurements of the recirculation experiments. The pH changed slower in the microfluidic system for both conditions (permeable, 48 h, and impermeable chip, 60 h) than in the static conditions (10 h). Static and gas permeable chip measurements were performed with a flat bottom pH electrode inserted into a commercial flow cell; gas impermeable chip measurements were made with a pH sensor plug and a 3D-printed flow cell. The trendline is to guide the eye; pH sensor plug pH range: pH 5.5-8.5; initial measurement done with a flat bottom pH electrode.

## 5.3.5. Culturing cells outside the CO<sub>2</sub> incubator

### 5.3.5.1. Static cell cultures on chip

To evaluate if the chip gas permeability would influence cell survival outside the CO<sub>2</sub> incubator, cells were seeded in gas permeable or impermeable chips and kept outside the CO<sub>2</sub> incubator for 48h (in the bead bath at 37°C), with media changes once a day and images taken at defined time points (Figure 5.10).



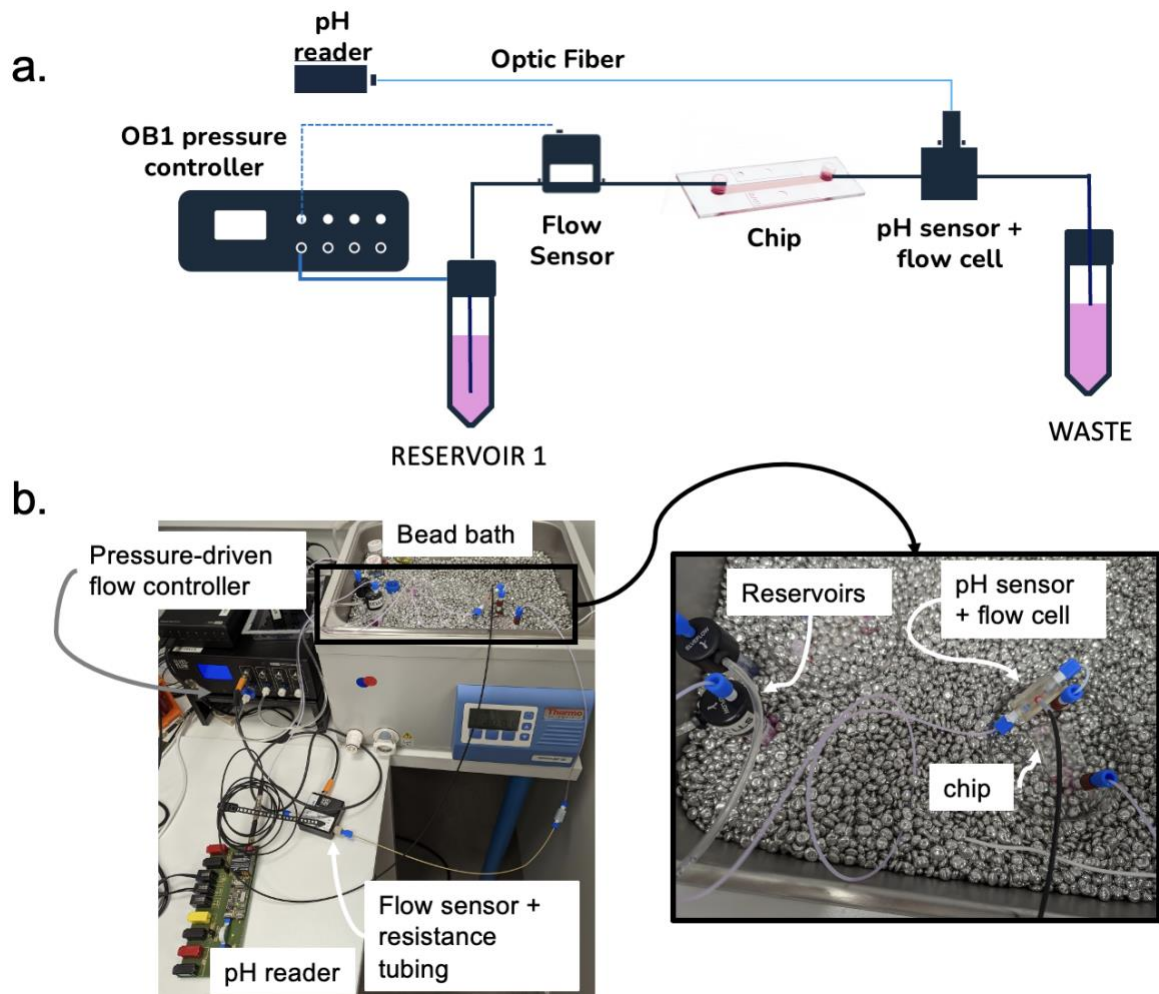
**Figure 5.10.** Static microfluidic cell culture outside the CO<sub>2</sub> incubator. **a.** Microfluidic chip placed inside the bead bath at 37°C. Beads surrounded the chip to ensure good temperature transfer and the blue lid was filled with water to avoid evaporation. **b.** Bright-field images of the cells inside the microfluidic chamber at defined time points. Impermeable chip,  $1.2 \times 10^6$  cells/ml; Permeable chip,  $2.2 \times 10^6$  cells/ml. Scale bars, 100  $\mu\text{m}$ .

## **5.3.5.2. Dynamic cell cultures on chip**

### **5.3.5.2.1. Reservoir-to-waste microfluidic setup**

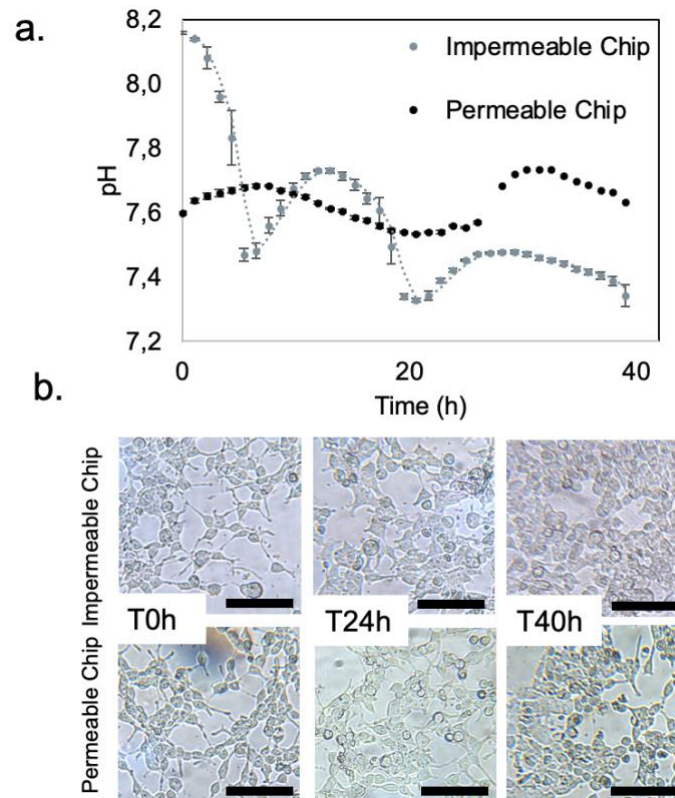
Culturing cells in microfluidics offers an increased resolution in attainable information but is also comprised of a multitude of different parameters. To simplify the interpretation of the results, a reservoir-to-waste microfluidic system was assembled to culture HEK293 cells outside the CO<sub>2</sub> incubator (Figure 5.11). The system components were a pressure-driven flow controller, a flow sensor and resistance tubing (ID: 125 µm), a microfluidic chip, either gas impermeable or permeable, and the pH sensor plug and flow cell, all connected with PTFE tubing (OD: 1/16"). The media was driven from the reservoir to the waste by a pressure-driven flow controller, while the intermittent flow rate was ensured by the flow sensor (5 µl/min, 2 min every hour). This system aimed to validate that the microenvironment monitoring of pH of dynamic cell cultures could be done with an inline sensor and flow cell while also assessing the effect of the permeable tubing on cell viability.





**Figure 5.11.** Reservoir-to-waste microfluidic cell culture. **a.** Schematic of the reservoir-to-waste microfluidic circuit. The media was driven from the reservoir to the waste by a pressure-driven flow controller. The flow sensor ensured the intermittent flow rate at  $5 \mu\text{l}/\text{min}$ . **b.** Images of the system arranged in the bead bath.

The pH data from the cultured cells showed a cyclical wavy profile, consistent with metabolic cycles of HEK293 cell growth (Figure 5.12.a.). Considering that cell concentrations were similar for both chips at the start of the dynamic cell culture ( $2.2 \times 10^6$  cells/ml), the impermeable chip showed more pronounced cycles while the permeable chip presented more uniform cycles. There was no apparent difference between the doubling time of cells in the chips (Figure 5.12.b.) so the difference remains consistent with the gas permeability of the microfluidic devices.

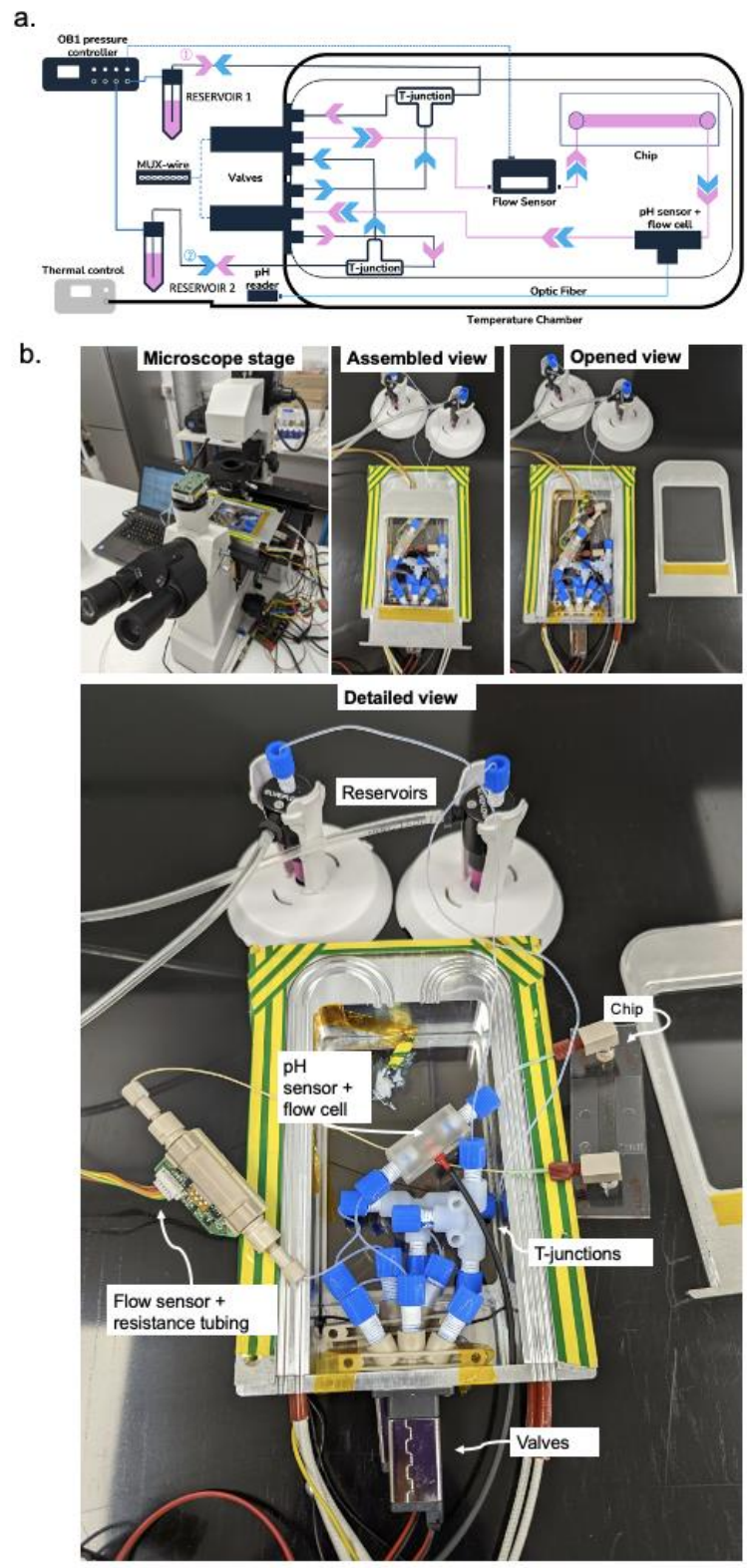


**Figure 5.12.** Reservoir-to-waste microfluidic cell culture. **a.** The pH profiles of HEK293 cells cultured in gas impermeable and permeable chips. The gas impermeable chip demonstrated more pronounced metabolic cell cycles while the permeable chip showed more uniform cycles (the gap in the data is due to a computer malfunction during data acquisition, but the physical experiment was not affected). SDs were calculated from pH values between flow cycles. **b.** Representative images of cell culture of the respective chips. No apparent differences in cell doubling were noted. Impermeable chip,  $1.2 \times 10^6$  cells/ml, 2 days incubation prior to flow; Permeable chip,  $2.2 \times 10^6$  cell/ml, 1 day incubation prior to flow. Scale bar, 100  $\mu$ m.

### 5.3.5.2.2. Recirculation in thermalisation chamber

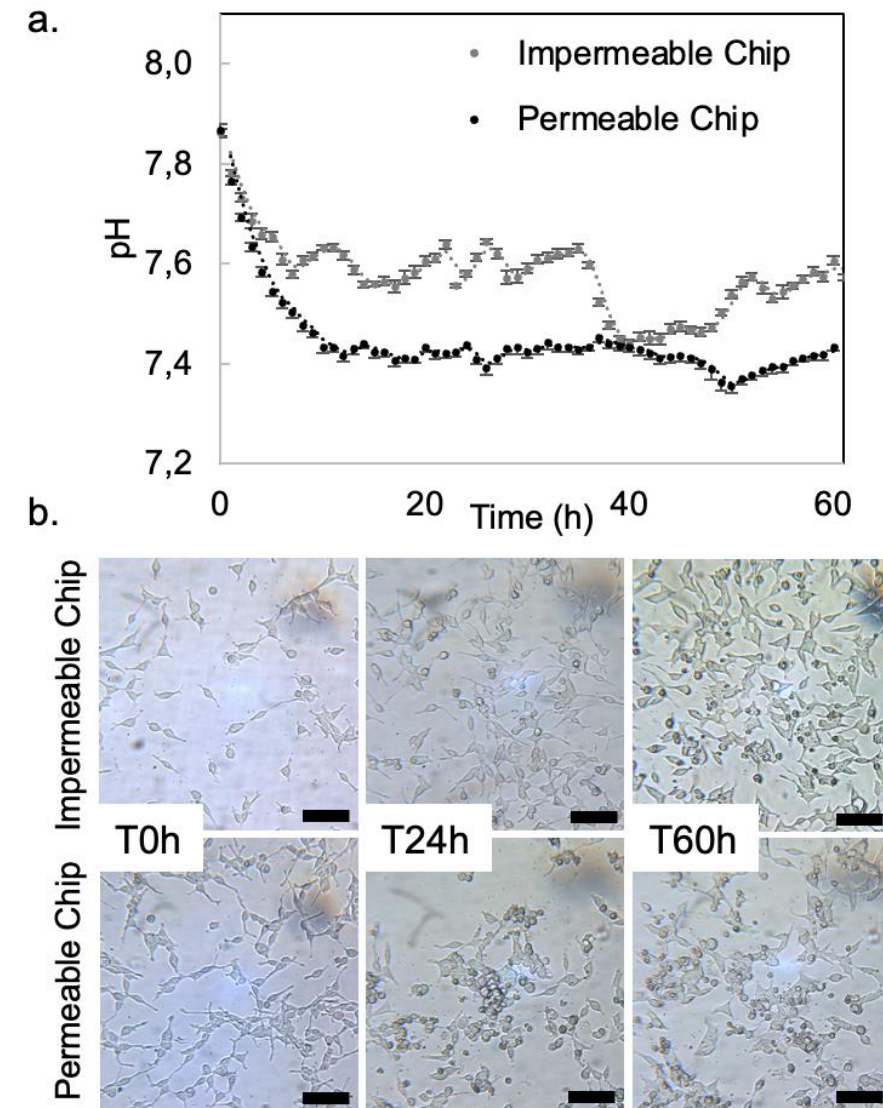
The reductionist approach of the reservoir-to-waste microfluidic cell culture validated the pH measurements for microenvironment monitoring of dynamic cell cultures. However, it overlooked one of the main advantages of microfluidic cell cultures, the enrichment of the media with cell-secreted metabolites, chemical cues responsible for cell-cell interaction<sup>46</sup>. Also, it is not cost-effective as large volumes of media are employed. To investigate the effect of media enrichment and better use of resources, a miniaturised recirculation system was assembled. Due to the intermittent nature of the flow profile and the low flow rate, only 120  $\mu$ l of media passed through the channels every 12 hours. For this reason, the volume of the

system had to be substantially decreased to ensure that the media would be fully exchanged and mixed in the reservoirs. For that, the PTFE tubing with 1/32" inner diameter (~700  $\mu\text{m}$ ) was replaced by the PTFE tubing with 300  $\mu\text{m}$  inner diameter. The total length of the system was decreased to 109 cm (from more than 250 cm in previous recirculation systems), resulting in a total volume of approximately 77  $\mu\text{l}$  (total volume of media, 4 ml; reservoir-to-waste, 13 ml). To keep the temperature constant and to substantially simplify data gathering from images, a thermalisation chamber prototype was employed to house the entire system on top of the microscope stage (Figure 5.13).



**Figure 5.13.** Miniaturised recirculation system inside thermalisation chamber for microscope stage top. **a.** Schematic of the flow path and components of the microfluidic circuit. **b.** Images of the system on the microscope stage; completely assembled and closed (from the top); without the lid (opened view); and a detailed view, highlighting each microfluidic component.

Cells were cultured for 60h in gas permeable or gas impermeable chips with continuous monitoring of the pH with an intermittent flow in the recirculation system. Similarly to the reservoir-to-waste experiments, the gas impermeable chip demonstrated clear pH cycles while the gas permeable chip showed a more uniform and linear tendency (Figure 5.14.a). Cell growth and doubling time remained similar for both conditions (Figure 5.14.b.).



**Figure 5.14.** Microfluidic culture of HEK293 cells in thermalisation chamber with continuous pH monitoring. **a.** pH measurements of gas impermeable and permeable chips during cell culture. Measurements of cells cultured in the impermeable chip showed larger pH variations than those in the gas permeable chip. **b.** Bright-field images of cells during culture at defined time points. Initial cell concentrations: permeable chip:  $2.43 \times 10^6$  cells/ml; impermeable chip:  $1.9 \times 10^6$  cells/ml. Scale bars, 100  $\mu$ m.

## 5.4. Discussion

### 5.4.1. Colorimetric pH assessment is insufficient for microfluidic cell culture

The addition of Phenol Red in cell culture media is a common practice and is often the only source of information that researchers rely on to assess the cell culture pH. It gives sufficient information about the indicative pH of cell cultures in standard flasks (Figure 5.1.a.). Nevertheless, it is not precise, with the same shade representing the spectrum of a full pH point (Figure 5.1.b.). DMEM, for example, comes equilibrated to the right CO<sub>2</sub> concentration for physiological pH (7.4, approx. 8% CO<sub>2</sub><sup>41</sup>). It is inferred that 8% CO<sub>2</sub> fills the open space of the medium bottle to prevent the CO<sub>2</sub> from diffusing away from the liquid, as the medium is at the correct pH when a new bottle is opened.

According to Henry's Law, the solubility of a gas is proportional to its overlying partial pressure; thus the CO<sub>2</sub> remains diluted into the media when the atmosphere over the liquid has a higher CO<sub>2</sub> partial pressure, in a dynamic equilibrium between liquid and gas phases. This equilibrium is dictated by Le Chatelier's Principle, which states that "if a dynamic equilibrium is disturbed by changing the conditions, the position of equilibrium shifts to counteract the change to re-establish an equilibrium". Once the bottle is opened for the first time, the atmosphere inside becomes that of room air. The CO<sub>2</sub> present in the media starts to equilibrate back to room air concentrations (approx. 0%) (Figure 5.3). The rate of this exchange can be explained by the Stagnant Boundary Layer Model. Briefly, it assumes that there is a well-mixed atmosphere over the liquid and a well-mixed solution, separated by a stagnant film, in which transport is controlled by molecular diffusion. The rate of transport is described by Fick's Law, stating that the flux is proportional to the concentration gradient and is defined by the molecular diffusion coefficient specific to the gas and the thickness of the stagnant film<sup>47</sup>. The molar flux of the gas is related to the volume of the liquid<sup>48</sup>; hence as the media is used and the volume decreases inside the bottle, it contains less CO<sub>2</sub> and the more basic the pH becomes. As this process takes time, and a bottle of media can be used over several weeks, the change in colour of the Phenol Red, from dark red to violet, is not obvious.

Researchers rarely check the pH of the media in another way and use it as it comes from the bottle. This practice results in variations that are not accounted for during experiments (Figure

5.12) and might affect the metabolism of the cells in unknown ways. As mentioned in Chapter 1, variations of about  $\pm 0.3$  from physiological pH 7.4 are well-tolerated in traditional cell cultures; however the small volumes enhance the diffusivity in microfluidic cell cultures, exacerbating the negative effects of pH variability<sup>49</sup>. Moreover, Phenol Red ceases to be a sufficient indicator of pH for the naked eye in microfluidic devices (Figure 5.1.c.), as cells present a healthy morphology while the phenol red in the media indicates it is too acidic (Figure 5.1.e. and f.). Hence, a more adequate and reliable manner of measuring pH in microfluidic cell culture is required.

#### **5.4.2. The rate of CO<sub>2</sub> diffusion through PTFE varies according to the parameters of the system**

The close relationship between pH and CO<sub>2</sub> renders the gas permeability of microfluidic components a relevant parameter to determine, especially when considering a system independent of the CO<sub>2</sub> incubator. The gas permeability of PTFE is well-known and can be modulated depending on the application<sup>22,23,50-52</sup>, but the characterisation of the gas permeability of the PTFE tubing normally used in microfluidics had not yet been performed. The equilibration curves of PTFE showed different equilibration times depending on the atmospheric exposure. CO<sub>2</sub> entered the tubing almost as fast as it diffused into media in an open vial, but it diffused out of the tubing at a much slower rate. This behaviour can be theoretically explained by the relationship between the volume, thickness of the wall, surface area and the coefficient of permeability of the system, independently of the CO<sub>2</sub> concentration surrounding it (Eq. 5.1)<sup>19,44</sup>.

Considering these parameters for the PTFE types of tubing employed in the experiments (1/16" and 1/32" OD), the equilibration time decreases with the decrease in volume and wall thickness (from 24 h to 2 h when placed inside the CO<sub>2</sub> incubator; (Figure 5.5). The inverse can also be explained by the same rationale, considering the tubing as the reservoir of CO<sub>2</sub> and the room as the receiver of CO<sub>2</sub>; thus, the volume of the system becomes orders of magnitude larger and the equilibration time increases substantially, explaining why it seemed that the PTFE tubing prevented the diffusion of CO<sub>2</sub> into the atmosphere. In truth, it is only a slower process that was not concluded within the timeframe of the experiments. Therefore, it can be an interesting asset to explore when considering a system independent of the CO<sub>2</sub> incubator, as having the media at the correct pH from the start might suffice to keep the system within acceptable ranges.

### **5.4.3. Off-chip pH sensing flow cell can detect metabolic cycles of cells cultured outside the CO<sub>2</sub> incubator**

CO<sub>2</sub> diffuses slower out of PTFE tubing than into it, but it does diffuse out with time, increasing the pH. Thus, to understand whether the loss of CO<sub>2</sub> would negatively impact cell viability, microfluidic cell cultures were successfully performed outside the CO<sub>2</sub> incubator. Along with the previously discussed importance of pH for cell culture, pH was chosen as the monitoring parameter also due to its dual function: it is an indirect measurement of CO<sub>2</sub> in the media, and it is closely related to cell metabolism, which acidifies the media with the production of CO<sub>2</sub> and acid lactic<sup>53,54</sup>. The commercial pH sensor plug employed in this work detects pH in minute volumes and has a particularly good format for microfluidic circuits but was not adapted for inline flow. The design and development of the 3D-printed flow cell enabled the continuous inline monitoring of pH with the pH sensor plug, a potentially important tool for future research in the OoC area. The most striking difference between cells cultured in permeable and impermeable chips was the amplitude of the pH measurements during cell metabolic cycles. Cells in the impermeable chip showed more pronounced cycles in both experimental setups (reservoir-to-waste and recirculation, Figure 5.12 and Figure 5.14). It was hypothesised that the permeability of the polymer chip created a tempering effect over the measurements due to the gas exchange with the exterior, while the glass chip had an intensified signal due to its impermeability.

Cells metabolise glucose and other nutrients to obtain energy and maintain basic cellular functions. In mammalian cells, this process releases 4 molecules of CO<sub>2</sub>, which is just one of the metabolic processes that have CO<sub>2</sub> as waste<sup>53</sup>. In the permeable chip, the loss of CO<sub>2</sub> through the polymer coverslip increased the pH, which was counterbalanced by the production of CO<sub>2</sub> from regular metabolism, maintaining the pH within physiological levels between perfusion cycles of media in the intermittent flow profile. In the impermeable chip, on the other hand, the pH dropped more significantly as CO<sub>2</sub> remained trapped inside. The excess CO<sub>2</sub> dislocated the equilibrium of the bicarbonate buffering system, favouring the formation of hydrogen carbonate and hydronium and counterbalancing pH drop. The absence of exchange with the surrounding environment made these changes more pronounced, whereas the polymer chip acted as a "lung" releasing CO<sub>2</sub> to the atmosphere, tempering the amplitude. The actual pH values might have been slightly offset by the off-chip nature of the measurements and the intermittent flow, which resulted in long periods for the media to reach the pH sensor



from the chip. Nevertheless, the off-chip pH measurements were intended to monitor the system's microenvironment as a surveillance system to indicate cell death or contamination through significant changes in pH, whereas it actually showed enough resolution to differentiate the metabolic behaviour of the two investigated conditions.

## 5.5. Conclusion and Outlook

As microfluidics moves from being a physicist toolkit to becoming a biological workhorse, it is important not to lose things in translation. Thus, understanding the characteristics of components is of the utmost relevance to realise what can be used and what needs to be adjusted. As seen in Chapter 2, researchers prefer using known and proven methods and equipment, so the characterisation of the standard microfluidic tubing provides essential information to support the continued use of PTFE as a standard material for microfluidic cell culture. For microfluidic cell cultures outside the CO<sub>2</sub> incubator, the CO<sub>2</sub> equilibration time and the timeframe of the cultures must be considered to ensure ideal conditions throughout the experiment.

This work achieved dynamic cell culture outside the CO<sub>2</sub> incubator by placing the PTFE-based microfluidic circuit inside the prototyped thermalisation chamber to maintain the temperature constant, with the added advantage of keeping the system on top of the microscope stage for more straightforward data gathering. Furthermore, the pH of the microfluidic cell culture was monitored with a pH sensor plug inserted into a 3D-printed flow cell. Off-chip solutions for microenvironment monitoring offer great advantages in terms of assembly flexibility, ease of fabrication and cost reduction. However, most criticism is directed at the absence of spatiotemporal resolution in this approach. Here, the off-chip solution demonstrated sufficient resolution to differentiate the metabolic behaviour of the two experimental conditions.

Hence, PTFE-based microfluidic circuits maintain the current status quo regarding materials, and off-chip sensing solutions make data gathering more accessible in terms of fabrication and flexibility. Moreover, they enable long-term culture of cells in a recirculation setting outside the CO<sub>2</sub> incubator with enhanced data gathering capabilities. Together, they are a promising way to simplify microfluidic cell culture and allow researchers to focus their attention on the pressing questions of biology.

## 5.6. References

1. Lavrentieva, A. Essentials in Cell Culture. in *Cell Culture Technology, Learning Materials in Bioscience* (ed. C.. Kasper et al) 23–48 (Springer International Publishing, 2018). doi:10.1007/978-3-319-74854-2\_2
2. Lo, C. M., Keese, C. R. & Giaever, I. pH changes in pulsed CO<sub>2</sub> incubators cause periodic changes in cell morphology. *Experimental Cell Research* **213**, 391–397 (1994).
3. Mastrangeli, M. & van den Eijnden-van Raaij, J. Organs-on-chip: The way forward. *Stem Cell Reports* **16**, 2037–2043 (2021).
4. Azizgolshani, H. *et al.* High-throughput organ-on-chip platform with integrated programmable fluid flow and real-time sensing for complex tissue models in drug development workflows. *Lab Chip* **21**, 1454–1474 (2021).
5. Kim, H. J., Lee, J., Choi, J. H., Bahinski, A. & Ingber, D. E. Co-culture of living microbiome with microengineered human intestinal villi in a gut-on-a-chip microfluidic device. *J. Vis. Exp.* **2016**, 3–9 (2016).
6. Yamada, A. *et al.* Transient microfluidic compartmentalization using actionable microfilaments for biochemical assays, cell culture and organs-on-chip. *Lab Chip* **16**, 4691–4701 (2016).
7. Brown, J. A. *et al.* Metabolic consequences of inflammatory disruption of the blood-brain barrier in an organ-on-chip model of the human neurovascular unit. *J. Neuroinflammation* **13**, 1–17 (2016).
8. Zakharova, M. *et al.* Multiplexed blood–brain barrier organ-on-chip. *Lab Chip* **20**, 3132–3143 (2020).
9. Maoz, B. M. *et al.* A linked organ-on-chip model of the human neurovascular unit reveals the metabolic coupling of endothelial and neuronal cells. *Nat. Biotechnol.* **2018 369** **36**, 865–874 (2018).
10. Pauly, N., Madigan, T., Koesser, K., Meuler, B. & Campagnola, P. *Microscope Cell Culture Incubator*. (2020).
11. Bird, B. R. & Forrester, F. T. *Basic Laboratory Techniques in Cell Culture*. (1981).
12. Gonçalves, I. M. *et al.* Recent trends of biomaterials and biosensors for organ-on-chip platforms. *Bioprinting* **26**, e00202 (2022).
13. Kratz, S. R. A. *et al.* Characterization of four functional biocompatible pressure-sensitive adhesives for rapid prototyping of cell-based lab-on-a-chip and organ-on-a-chip systems. *Sci. Reports* **2019 91** **9**, 1–12 (2019).
14. Bhatia, S. N. & Ingber, D. E. Microfluidic organs-on-chips. *Nat. Biotechnol.* **32**, 760–772 (2014).

15. Roy, E. *et al.* Overview of Materials for Microfluidic Applications. in *Advances in Microfluidics: New Applications in Biology, Energy, and Material Sciences* (ed. Yu, X.-Y.) 335–356 (IntechOpen, 2016). doi:10.5772/60788
16. Elveflow. Microfluidic tubings and sleeves: the basics. Available at: <https://www.elveflow.com/microfluidic-reviews/general-microfluidics/the-basics-of-microfluidic-tubing-sleeves/>. (Accessed: 26th July 2022)
17. Dhanumalayan, E. & Joshi, G. M. Performance properties and applications of polytetrafluoroethylene (PTFE) - a review. *Adv. Compos. Hybrid Mater.* **1**, 247–268 (2018).
18. Gladysz, J. A. & Jurisch, M. Structural, Physical and Chemical Properties of Fluorous Compounds. in *Topics in Current Chemistry* (ed. Horváth, I. T.) **308**, 1–24 (Springer, 2012).
19. De Gregorio, S. *et al.* Long-term continuous monitoring of the dissolved CO<sub>2</sub> performed by using a new device in groundwater of the Mt. Etna (southern Italy). *Water Res.* **45**, 3005–3011 (2011).
20. Tang, H., Zhang, Y., Wang, F., Zhang, H. & Guo, Y. Long-Term Stability of Polytetrafluoroethylene (PTFE) Hollow Fiber Membranes for CO<sub>2</sub> Capture. *Energy and Fuels* **30**, 492–503 (2015).
21. Ozeki, K. *et al.* Gas barrier properties of diamond-like carbon films coated on PTFE. *Appl. Surf. Sci.* **255**, 7286–7290 (2009).
22. Polyzos, A., O'Brien, M., Petersen, T. P., Baxendale, I. R. & Ley, S. V. The Continuous-Flow Synthesis of Carboxylic Acids using CO<sub>2</sub> in a Tube-In-Tube Gas Permeable Membrane Reactor. *Angew. Chemie - Int. Ed.* **50**, 1190–1193 (2011).
23. Yang, L. & Jensen, K. F. Mass transport and reactions in the tube-in-tube reactor. *Org. Process Res. Dev.* **17**, 927–933 (2013).
24. Ali, S., Shaegh, M., De Ferrari, F. & Zhang, Y. S. A microfluidic optical platform for real-time monitoring of pH and oxygen in microfluidic bioreactors and organ-on-chip devices. *Biomicrofluidics* **10**, 044111 (2016).
25. Jalili-Firoozinezhad, S. *et al.* A complex human gut microbiome cultured in an anaerobic intestine-on-a-chip. *Nat. Biomed. Eng.* **3**, 520 (2019).
26. Hasic, S. *et al.* Rapid Prototyping of Multilayer Microphysiological Systems. *ACS Biomater. Sci. Eng.* **7**, 2949–2963 (2021).
27. Huh, D. *et al.* Microfabrication of human organs-on-chips. *Nat. Protoc.* **8**, 2135–2157 (2013).
28. Benam, K. H., Novak, R., Ferrante, T. C., Choe, Y. & Ingber, D. E. Biomimetic smoking robot for in vitro inhalation exposure compatible with microfluidic organ chips. *Nat. Protoc.* **15**, 183–206 (2020).

29. Adtech. PTFE Technical Properties.
30. Convery, N. & Gadegaard, N. 30 years of microfluidics. *Micro Nano Eng.* **2**, 76–91 (2019).
31. Santbergen, M. J. C., van der Zande, M., Bouwmeester, H. & Nielen, M. W. F. Online and in situ analysis of organs-on-a-chip. *TrAC - Trends Anal. Chem.* **115**, 138–146 (2019).
32. Zhang, Y. S. *et al.* Multisensor-integrated organs-on-chips platform for automated and continual in situ monitoring of organoid behaviors. *Proc. Natl. Acad. Sci. U. S. A.* **114**, E2293–E2302 (2017).
33. Krejčí, J. *et al.* The measurement of small flow. *Sensors Actuators, A Phys.* **266**, 308–313 (2017).
34. Strebl, M. G., Bruns, M. P., Schulze, G. & Virtanen, S. Respirometric In Situ Methods for Real-Time Monitoring of Corrosion Rates: Part II. Immersion. *J. Electrochem. Soc.* **168**, 011502 (2021).
35. Ahmerkamp, S. *et al.* The effect of sediment grain properties and porewater flow on microbial abundance and respiration in permeable sediments. *Sci. Reports 2020 101* **10**, 1–12 (2020).
36. Higuera, G. A. *et al.* Supporting data of spatiotemporal proliferation of human stromal cells adjusts to nutrient availability and leads to stanniocalcin-1 expression in vitro and in vivo. *Data Br.* **5**, 84–94 (2015).
37. Illner, S., Hofmann, C., Löb, P. & Kragl, U. A Falling-Film Microreactor for Enzymatic Oxidation of Glucose. *ChemCatChem* **6**, 1748–1754 (2014).
38. Farooqi, H. M. U., Khalid, M. A. U., Kim, K. H., Lee, S. R. & Choi, K. H. Real-time physiological sensor-based liver-on-chip device for monitoring drug toxicity. *J. Micromechanics Microengineering* **30**, (2020).
39. Khalid, M. A. U. *et al.* A lung cancer-on-chip platform with integrated biosensors for physiological monitoring and toxicity assessment. *Biochem. Eng. J.* **155**, 107469 (2020).
40. Wu, M. H., Lin, J. L., Wang, J., Cui, Z. & Cui, Z. Development of high throughput optical sensor array for on-line pH monitoring in micro-scale cell culture environment. *Biomed. Microdevices* **11**, 265–273 (2009).
41. Michl, J., Park, K. C. & Swietach, P. Evidence-based guidelines for controlling pH in mammalian live-cell culture systems. *Commun. Biol.* **2019 21** **2**, 1–12 (2019).
42. Trivedi, V. *et al.* A modular approach for the generation, storage, mixing, and detection of droplet libraries for high throughput screening. *Lab Chip* **10**, 2433–2442 (2010).
43. Adtech. *Fluoropolymers Gas Permeability*.
44. De Gregorio, S., Gurrieri, S. & Valenza, M. A PTFE membrane for the in situ extraction of dissolved gases in natural waters: Theory and applications. *Geochemistry, Geophys.*

- Geosystems* **6**, (2005).
45. Ibidi. *u-Slide Luer Slide Datasheet*. **6.2**, (2020).
  46. Coluccio, M. L. *et al.* Microfluidic platforms for cell cultures and investigations. *Microelectron. Eng.* **208**, 14–28 (2019).
  47. Murray, J. Gas and Gas Permeability. in (University of Washington, 2001).
  48. Clarke, K. G. The oxygen transfer rate and overall volumetric oxygen transfer coefficient. *Bioprocess Eng.* 147–170 (2013). doi:10.1533/9781782421689.147
  49. Lu, C. & Verbridge, S. S. Microfluidic methods for molecular biology. *Microfluid. Methods Mol. Biol.* 1–376 (2016). doi:10.1007/978-3-319-30019-1
  50. Roper, F. G. Some effects of the permeability of P.T.F.E. gas sample loops used in gas chromatography. *J. Chromatogr. Sci.* **9**, 697–699 (1971).
  51. Dobson, J. V. & Taylor, M. J. The permeability of gases through PTFE and other membranes at 25°C. *Electrochim. Acta* **31**, 231–233 (1986).
  52. Park, G. G. *et al.* Effect of PTFE contents in the gas diffusion media on the performance of PEMFC. *J. Power Sources* **131**, 182–187 (2004).
  53. Dashty, M. A quick look at biochemistry: Carbohydrate metabolism. *Clin. Biochem.* **46**, 1339–1352 (2013).
  54. Rabinowitz, J. D. & Enerbäck, S. Lactate: the ugly duckling of energy metabolism HHS Public Access. **2**, 566–571 (2020).

## CHAPTER 6.

### Conclusion and Outlook

“For me, becoming isn’t about arriving somewhere or achieving a certain aim. I see it instead as forward motion, a means of evolving, a way to reach continuously toward a better self. The journey doesn’t end.”  
— Michelle Obama, Becoming

This thesis discussed the role of microfluidics as a tool for biological applications. In the frame of an industrial PhD, these applications were also considered with regard to the potential market interest they could elicit. Chapter 1 provided a general overview of the microfluidic concepts and techniques and the two major biological applications to be explored in order to test the versatility of the technology: oral drug delivery and cell culture. To undertake product development, companies analyse markets and possible returns on investments of potential products. Chapter 2 presented the market analyses of the two main topics of this thesis: encapsulation-in-droplets and microenvironmental monitoring of microfluidic cell cultures. The market studies were carried out in two different approaches, respectively: a technology push, in which the product is already in a later stage of development due to internal technological advancements but the market to be serviced was not pre-defined; and a market pull, in which the product development has not started yet, but there is a clear demand coming from the market. The first market study concluded that the product development should go ahead and target biologists working with rare or limited samples. The main competitive advantage is likely to come from an offering that supports the client, helping researchers increase their level of confidence in obtaining reproducible results with microfluidics rather than from advancements in the technology itself. The second market study also resulted in a positive product investment decision, focusing on researchers that required long-term microfluidic cell culture outside the CO<sub>2</sub> incubator and did not possess a stage-top microscope incubator.

Given the two positive conclusions of the market studies, further research was developed. Chapter 3 produced microcompartments with varying levels of complexity in non-specialist settings. These compartments successfully encapsulated compounds in monodisperse double emulsions with a PDMS chip featuring a double flow-focusing junction and a short post-junction

channel. They are promising tools to advance the fields of single-cell analysis, tissue engineering and drug delivery with enhanced controllability and high throughput. The formation of GUVs by removal of oil proved a challenge. The ability to form biomimetic lipid bilayers is paramount for the field of artificial-cell-like systems. Several reports have investigated in detail the characteristics of the membrane once oil is removed, including whether the presence of residual oil is detrimental to membrane functionality. However the reason for octanol dewetting is still mostly hypothetical. Further work should investigate the underlying forces governing the removal of oil from the membrane, so more control can be provided to the formation of other types of complex microcompartments. In this light, the production of nanocompartments with microfluidics is a fast developing field that holds promise for the health sector, with the production of lipid nanoparticles for drug delivery, for example. Once protocols for micro and nanocompartments are established, scalability is the next challenge hindering microfluidics wider adoption. Integration of parallelised microfluidic devices in highly automated systems will be required to power the next revolution in pharmaceuticals (drug development, testing and production), producing higher quality micro and nanoparticles with economies of scale in a fraction of the footprint.

Chapter 4 explored the reproducibility of the double junction PDMS chip to produce monodisperse and biocompatible double emulsions. These DEs were investigated as oral drug delivery systems due to their ability to co-localise compounds of opposing properties in the same carrier. Compounds of interest were encapsulated in the inner and intermediate phase of the double emulsions, and their stability was tested under physiologically-relevant conditions. The stability of the double emulsions was inversely proportional to temperature, a behaviour exacerbated by the presence of cargo. They were more sensitive to extreme pH, showing acceptable stability in the physiologically-relevant range. Also, double emulsions, loaded or unloaded, showed good stability under mechanical stress intended to mimic that of the gastrointestinal tract. Given their inherent instability, DEs are usually employed only as an intermediate step to template other microcompartments, such as GUVs, polymersomes and core-shell microparticles. Thus, their application as microcompartments themselves is often overlooked. Here, we have demonstrated that the application of double emulsions as oral drug delivery systems seems feasible and promising. Further work should focus on optimising the formulation to a particular combination of synergistic drugs, so properties can be tailored to the desired level of stability, which is linked to the optimal delivery location, i.e. mouth, stomach, intestine, liver, etc. Then, understanding of the behaviour of these carriers under combined stresses becomes essential, as the parameters tested here do not happen in isolation in real settings. Once the optimal formulation is defined, the release profile of DEs should be investigated, followed by the definition of PK/PD in *in vitro* studies. In summary, microfluidics

was shown to be a valuable tool for producing complex compartments that could be employed as oral drug delivery systems in combinatory therapies.

Microfluidics was also shown to confer several advantages to traditional cell culture, specifically, the off-chip monitoring of microenvironment cell culture parameters. With the aid of a flow cell, the continuous and inline tracking of pH was successfully demonstrated in Chapter 5, going as far as detecting metabolic cycles of HEK293 cells. The market study in Chapter 2 noted that researchers tend to adapt equipment they are familiar with for microfluidic cell culture, such as the CO<sub>2</sub> incubator. As the field evolves and the possibilities widen, relying on adaptations to familiar instruments becomes a limiting factor to progress. Thus, new demands, such as long-term live cell imaging, require more suitable solutions. This trend was already remarked in the demonstrated interest for pH monitoring solutions without a CO<sub>2</sub> incubator and is likely to eventually move microfluidic cell culture from the CO<sub>2</sub> incubator to the microscope stage. A slew of young companies have recently started to develop commercial microfluidic solutions tailored to cell biologists, notably, chips and hardware, but many are so far still only designed for one specific application. Thus, envisioning an incubator-independent solution, a miniaturised recirculation system was assembled and successfully cultured live cells for extended periods outside the CO<sub>2</sub> incubator. The gas permeability characterisation of PTFE tubing, the most common material used to connect microfluidic circuits, was performed to assess the effect on the pH of the media. The media inside the tubing was enriched with CO<sub>2</sub> easily, but the gas did not leave at the same rate, proving to be a convenient component for microfluidic cell culture outside the CO<sub>2</sub> incubator. This work is aligned with the efforts as a whole in the field to develop new technologies to launch the creation of market and research opportunities for OoC. The aim is defining a new paradigm for cell models of health, disease and pharmaceutical development based on adding flow to cells in culture. The field is young and increasingly coordinating efforts to establish standards in the technology (protocols and hardware), and education avenues (conferences, training networks, OoC societies) to further advance OoC as the backbone of biotechnology.

Through this work, microfluidics has been shown to be a versatile tool for biological applications as diverse as biocompatible complex compartment fabrication to control and monitoring of long-term cell culture parameters. As a technology that evolved from non-biological domains, such as physics and semiconductors, it is important to ensure that things do not get lost in translation. The biocompatibility of components, from the composition of the solutions used to template double emulsions to the gas permeability of the tubing that connects microfluidic circuits, should not be overlooked. There are still many questions that remain to be answered in this regard, for example: what is the most appropriate flow rate to provide



physiologically-relevant flow to cells? How to avoid clogging and air bubbles? How does O<sub>2</sub> diffuse through microfluidic components, and how does that impact cells? What is the best sterilisation method for a microfluidic circuit? The road seems long, but works like the one presented here build upon the interdisciplinarity of the technology, combining physics, chemistry and biology and its market relevance so that non-specialists can use microfluidics to thrive where they know best, their area of expertise.

# Appendices

# Appendix 1 - Chapter 2. [Encapsulation-in-Droplets] Questionnaire for Experts

## Objectives:

- Understand why people use droplet encapsulation
- Understand their encapsulation set-up
- Understand their limitations

## Hypotheses:

- They use microfluidics because they (or their lab) have previous experience with it
- The set-up is simple (syringe pump or pressure/flow controller, tubing/adapters, chip, surfactant, samples and droplet collector/analyser) and does not vary a lot between applications
- They analyse the droplets on-chip (they don't store them elsewhere and use them later).
- They have to treat their channels for hydrophobicity
- Post-docs or teaching assistants make buying decisions.
- Researchers need to visualise the droplets
- They need to control the environmental parameters, such as temperature, humidity, etc

## Questions

### 1. Warm-up questions:

1. What is your project about?
2. Why did you decide to use droplet encapsulation in your research?
3. Did you work with other forms of encapsulation before? What is different between them and microfluidics?

### 2. Droplet Encapsulation Questions:

4. What are the most important parameters for the droplet encapsulation for you?
5. Could you tell me what do you use on your set-up? How do you know how much tubing you need? How many inlets do you use on your chip?
6. How do you analyse your droplets?

### 3. Admin Questions

7. Where did you buy your equipment from? How did you know what to buy?
8. How is the buying process in your lab?
9. Could you give us a ballpark of the budget you had for the set-up?

### 4. Wishful thinking/ Closing Questions:

10. What is the most difficult thing about your project? And regarding microfluidics?
11. If you had a magic wand, what would you change on your project? And regarding microfluidics/droplet encapsulation?
12. If you could go back in time, what do you wish you had known when you started working with microfluidics?
13. Is there anything that we didn't cover and you think it is important to mention?
14. Would you like to add something?

## **Script**

Hi Dr. XXX,

thank you so much for having the time to talk to us. Just to give you a little bit of background, we are part of Elveflow, the Microfluidics Innovation Centre, which is the Innovation Unit of Elveflow, the equipment manufacturer. And our mission is to understand market needs to develop new products.

We are exploring a new offering for droplets encapsulation and would like to ask you a few questions about it. The questions will last around 30 minutes, and you may feel that they sound strange sometimes, but that's just in order to avoid biasing your answers. So, feel free to ask any questions if you have doubts and, please, feel free to be 100% honest even if it sounds too harsh! If you are interested, we can give you more details about what we are working on after we finished.

[Questions]

Thank you again for your time! It has been incredibly valuable for us. Just as closing remarks, (would you be willing to take part in a beta tester group if we move forward with the product?) could you refer us to anyone that you think might be interested or could provide useful feedback?

Thank you and have a nice day!

Questions for Florine:

- Why did they decide to develop a product for droplet-microfluidics?
- Why they focused on biological applications? What are the market segments?

- How large she estimates the market is?
- Does she see any potential new markets gaining relevance in the near future?
- What does she think an encapsulation starter pack should have
- What is the largest barrier in the market? (What is the most difficult thing about working on this market?)
- Who is her ideal customer profile?

# Appendix 2 - Chapter 2. [Encapsulation-in-Droplets] Questionnaire for Potential Clients

## Objectives:

- Understand their needs regarding encapsulation in their research
- Understand why people think droplet encapsulation can help their research
- Understand the limitations of their current set-up
- Understand their reservations towards microfluidics

## Hypotheses:

- They find microfluidics too complicated to start on their own
- They think microfluidics is too expensive to use compared to traditional methods
- They saw they could use microfluidics in their research in a conference
- They think the set-up is more complicated than it actually is
- They need to analyse the droplets on-chip (they don't store them elsewhere and use them later).
- Researchers need to visualise the droplets
- They have to treat their channels for hydrophobicity
- They need to control the environmental parameters, such as temperature, humidity, etc
- Post-docs or teaching assistants make buying decisions.

## Questions

### 1. Warm-up Questions

1. What is your project about?
2. Why do you need to encapsulate samples?
3. How do you perform your experiments/encapsulation today? How do you analyse it?
4. What are the parameters you need in your encapsulation?

### 2. Droplet Encapsulation Questions

5. Where did you see that droplets encapsulation could be used in your research?
6. What advantages do you think it can provide?
7. What do you think a microfluidics set-up for your experiment would look like?
8. Do you know how they would translate to droplets encapsulation?

### 3. Admin Questions

9. How do you usually buy your equipment? How is the buying process in your lab?
10. Could you give us a ballpark of how much budget you would have for a droplet encapsulation set-up?

#### **4. Wishful thinking/ Closing Questions**

11. What is the most difficult thing about your project?
12. If you had a magic wand, how would you fix it (or what you change on your project)?  
And regarding encapsulation?
13. If you could go back in time, what do you wish you had known when you started working with encapsulation?

#### **Script**

Hi Dr. XXX,

thank you so much for having the time to talk to us. Just to give you a little bit of background, we are part of Elvsys, the Microfluidics Innovation Centre, which is the Innovation Unit of Elveflow, the equipment manufacturer. And our mission is to understand market needs to develop new products.

We are exploring a new offering for droplets encapsulation and would like to ask you a few questions about it. The questions will last around 30 minutes, and you may feel that they sound strange sometimes, but that's just in order to avoid biasing your answers. So, feel free to ask any questions if you have doubts and, please, feel free to be 100% honest even if it sounds too harsh! If you are interested, we can give you more details about what we are working on after we finished.

[Questions]

Thank you again for your time! It has been incredibly valuable for us. Just as closing remarks, would you be willing to take part in a beta tester group if we move forward with the product? (could you refer us to anyone that you think might be interested or could provide useful feedback?)

Thank you and have a nice day!

# Appendix 3 - Chapter 2. [Microenvironment Monitoring] Online Questionnaire

Elvesys is a microfluidic company specialized in flow control systems. We commercialize a range of pressure controllers, flow sensors and valves under the Elveflow brand. This questionnaire aims to identify the bottlenecks encountered by biologists in cell perfusion. Thanks for your time!

**How long do you perfuse for?**

- $\leq 24$  h
- $24 \text{ h} < h \leq 48 \text{ h}$
- $48 \text{ h} < h \leq 72 \text{ h}$
- $> 72 \text{ h}$

**How many chips do you want to perfuse at once?**

- 1
- 2 or 3
- $3 < n < 10$
- $\geq 10$

**What flow rates do you generally use?**

- $\leq 10 \mu\text{L}/\text{min}$
- $10 \mu\text{L}/\text{min} < n \leq 250 \mu\text{L}/\text{min}$
- $250 < n \leq 500 \mu\text{L}/\text{min}$
- $> 500 \mu\text{L}/\text{min}$

**How often do you change or clean your tubing?**

- Never
- After every experiment
- Once in a while
- When contamination occurs
- When clogging occurs

**What size (diameter) of tubing do you generally use for your perfusion experiments? (In inches (mm))**

- 1/32 (0,8)
- 1/16 (1,6)
- 1/8 (3,2)
- 1/4 (6,35)

**How many different media/ buffers do you test?**

- 1
- 2 or 3
- $> 3$

**What is the typical volume of reagent/ drug injected on the cells?**

- $\leq 10 \mu\text{L}$
- $10 \mu\text{L} < n \leq 50 \mu\text{L}$
- $50 < n \leq 100 \mu\text{L}$
- $> 100 \mu\text{L}$

**Do you need to retrieve samples during your experiment?**

- Yes
- No

**How many reagents/ drugs are tested in one experiment?**

- 1
- $1 < n < 5$
- $\geq 5$

**If there are multiple injections, what is the usual time between sequential injections?**

- Seconds
- Minutes
- Hours
- Days

**What is a reasonable time frame between the moment of the injection of reagent/ drug and the moment it reaches the cells?**

- Immediate
- Seconds to minutes

**Do you need to recirculate medium?**

- Yes
- No



What extra features would you need/ like in the perfusion platform? To save time, you can answer just the questions of the features you are interested in.

- pH
- Temperature
- Mechanical stimulus
- O<sub>2</sub>
- CO<sub>2</sub>

Would you be willing to take part in a beta tester group if we move forward with a platform enabling perfusion and dosing? If yes, share your contact details (name, email address, institution/company) with us here!

Email:

Institute:

- By sharing your contact info, you agree that Elvsys will use the information you provide to help design new products.

<p style="text-align: center;"><b>pH MODULE</b></p> <p>How important is knowing the pH? (Not important) 1 - 2 - 3 - 4 - 5 (Very important)</p> <p>Do you need to know the pH near the cells or just of the medium in the reservoir?</p> <ul style="list-style-type: none"> <li>• near the cells (e.g. metabolism studies)</li> <li>• not required but would be useful</li> <li>• just of the medium in the reservoir is sufficient</li> </ul> <p>How often should pH measurements be taken?</p> <ul style="list-style-type: none"> <li>• Continuous monitoring needed</li> <li>• Once every few hours</li> <li>• Once before and once after the experiment is sufficient</li> </ul> <p>I use medium containing a phenol red pH indicator (Never) 1 - 2 - 3 - 4 - 5 (Always)</p> <p>Phenol red colour is acceptable precision for pH monitoring: (Disagree) 1 - 2 - 3 - 4 - 5 (Agree)</p> <p style="text-align: center;">_____</p> <p style="text-align: center;"><b>O<sub>2</sub> MODULE</b></p> <p>How important is knowing the O<sub>2</sub> concentration? (Not important) 1 - 2 - 3 - 4 - 5 (Very important)</p> <p>Do you need to know the O<sub>2</sub> concentration near the cells or just of the medium in the reservoir?</p> <ul style="list-style-type: none"> <li>• near the cells (e.g. metabolism studies)</li> </ul>	<p style="text-align: center;"><b>MECHANICAL STIMULUS MODULE</b></p> <p>Do you know/ measure shear stress in your experiment?</p> <ul style="list-style-type: none"> <li>• Yes</li> <li>• No</li> </ul> <p>If no, would it be useful to know/ measure shear stress?</p> <ul style="list-style-type: none"> <li>• Yes</li> <li>• No</li> </ul> <p>What mechanical forces are most relevant to your cell experiment?</p> <ul style="list-style-type: none"> <li>• Shear stress (eg. blood flow)</li> <li>• Tensile (stretching)</li> <li>• Compression</li> <li>• Radial/ hoop (eg. compliance)</li> <li>• Peristaltic</li> <li>• An elastic/ soft cell substrate would be sufficient</li> </ul> <p>Do you apply an external mechanical stimulus to your cells in culture? What type _____</p> <ul style="list-style-type: none"> <li>• Always</li> <li>• Sometimes</li> <li>• Never</li> </ul> <p style="text-align: center;">_____</p> <p style="text-align: center;"><b>TEMPERATURE CONTROL MODULE</b></p> <p>If you are using a thermal control, are you satisfied with it for your cell culture platform?</p> <ul style="list-style-type: none"> <li>• Yes</li> <li>• No</li> </ul> <p>Could you name the system and specify why you like it or not? _____</p> <p>If you use an oil immersion objective, how important is it for your data gathering?</p>
---	--

- not required but would be useful
- just of the medium in the reservoir is sufficient

**How often should measurements be taken?**

- Continuous monitoring needed
- Once every few hours
- Once before and once after the experiment is sufficient

**Do you need to control the O<sub>2</sub> concentration in the cell medium?**

- Yes
- No, monitoring is sufficient

**Would it be acceptable to add a fluorescent dye to the medium (e.g. PtTFPP)?**

- Yes
- Yes (no contact with cells)
- No

- Dispensable
- Nice to have
- Crucial

**How precise in temperature should your incubator be?**

- $\leq \pm 0.1^\circ\text{C}$
- 0.1 to 1°C
- $\approx 1^\circ\text{C}$

**Would you prefer constant temperature across the chip or would you like to have temperature gradients across the chip?**

- Constant
- Gradient

**CO<sub>2</sub> MODULE**

**What is the percentage of CO<sub>2</sub> you use?**

- < 5%
- 5 %
- > 5%

**What do you use to control CO<sub>2</sub>? (e.g. incubator, microscope...) \_\_\_\_\_**

# Appendix 4 - Chapter 2. [Microenvironment Monitoring] Interview Questionnaire

## Objectives

- Understand how people do long-term cell imaging
- Understand if there are limitations to the current setup
- Understand if people use perfusion to do long-term cell culture. If not, why.

## Hypotheses:

- Most biology labs have the microscope incubator
- The microscope incubator keeps pH and temperature constant, but the media needs to be changed by hand
- It is a very expensive and bulky equipment
- They don't do perfusion because
  - they have not reached this step yet
  - it adds too much complexity/many variables to the experiment
  - cells don't like it

## Questions

### 1. Warm-up questions:

1. What is your project about?

### 2. PPP Questions:

2. How do you perform long-term live-cell imaging?
3. How long do you need to culture your cells for?
4. How many chips do you do at once? Which type of chip do you use? (Commercial, in-house?)
5. What parameters are important to you regarding long-term cell culture? (Temp, pH, O<sub>2</sub>)
6. How do you keep them in acceptable ranges?
7. Can you describe in detail the routine procedure?


### 3. Specific Questions - depending on the application

8. Do you need to add buffers or retrieve samples? if yes, how do you do it?
9. Do you perfuse your cells? If yes, at which flow rate?
10. Do you apply mechanical stress/shear stress on your cells?

#### **4. Wishful thinking/ Closing Questions:**

11. What is the most difficult thing about your project? And regarding the cell culture?
12. If you had a magic wand, what would you change on your project? And regarding cell culture?
13. If you could go back in time, what do you wish you had known about cell culture?
14. Is there anything that we didn't cover that you think is important to mention?
15. Would you like to add something?

# Appendix 5 - Chapter 2. A/B Testing - Single-cell Encapsulation



**Encapsulation starter pack** | MICROFLUIDICS INNOVATION CENTER

## The perfect partner for your single-cell encapsulation

Unlimited samples and increased control with accelerated learning? Just use our microfluidics know-how! Everything you need to start encapsulating single cells in one single pack.

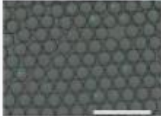
### What is it?

It is a single-cell microfluidic droplet-based system that encapsulates single cells at a high frequency, carefully designed for researchers that want to use microfluidics efficiently as a tool and improve their controllability over experiments with limited-time samples.

The pack's user and troubleshooting guides provide all the necessary information to assemble and make the most of the encapsulation pack for your experiments. Also, the pack's flexibility allows you to easily adapt it as your needs evolve.


This solution includes all the necessary elements to create a continuous flow and monitor the flow rate applied to the cells even for long-lasting experiments.

Image: Scale bar = 400 µm  
Single cell encapsulation using a single microfluidic




**ADVANTAGES**

- Precise flow and regulation
- Easy and reproducible
- Flexibility introduction of flow



**BLANKMUSES**




### The pack contains:

- Pressure-driven flow controller
- Flow sensors
- Tubing/Adapters
- Reservoirs
- Chips (adapted to your specific needs)
- Consumables (e.g., Backfilled oil & surfactant)
- User and troubleshooting guide
- Collection Vial
- User-friendly Software


### And you can expect:

- Reliability and reproducibility of results
- High-frequency encapsulation
- High controllability over encapsulation parameters (e.g. droplet size, number of droplets per second)
- Step-by-step assembly guidance through detailed user guides.

### Who is it for?

Researchers working on (medical) encapsulation within the area

# Appendix 6 - Chapter 2. A/B Testing - High-throughput Encapsulation



**Encapsulation starter pack** | MICROFLUIDICS INNOVATION CENTER

**The perfect partner for your high-throughput encapsulation**

You need improved control and reproducibility over your high-throughput experiments? Just see our microfluidics know-how! Everything you need to start your high-throughput encapsulation experiment in one single pack!


### What is it?

It is a microfluidic droplet-based system that encapsulates samples at a high frequency, carefully designed for researchers that want to use microfluidics as a tool and improve their controllability over high-throughput experiments.

The pack's user and troubleshooting guides provide all the necessary information to assemble and make the most of the encapsulation pack for your experiments. Also, the pack's flexibility allows you to easily adapt it to your needs and/or.

This solution includes all the necessary elements to create a continuous flow and monitor the flow rate applied to the cells over for long-lasting experiments.


Image: Scale bar = 400µm  
Single cell encapsulation using digital microfluidics




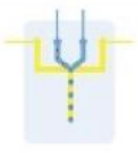
Start your encapsulation experiment with ADVANTAGES

- Pinless flow and liquidities
- High throughput flow
- Flexibility to handle several of flow

WARRANTIES







**The pack comprises:**



- Pressure-driven flow controller
- Flow sensors
- Tubing/adapters
- Reservoirs
- Chips (selected by your specific needs)
- Compression kit (e.g. Backflow kit & perfusant)
- User and troubleshooting guide
- Collection Vial
- User-Friendly Software

**And you can expect:**

- Reliability and reproducibility of results
- High-frequency encapsulation
- High controllability over encapsulation parameters (e.g. droplet size, number of droplets per second)
- Step by step assembly guidance through detailed user guides.

### Who is it for?

Researchers requiring high-throughput encapsulation experiment, for example, drug discovery or screening, willing to use microfluidics but with

# Appendix 7 - Chapter 2. A/B Testing – Cell Encapsulation



**Encapsulation starter pack** | MICROFLUIDICS INNOVATION CENTER

### The perfect partner for your cell encapsulation

(Can't achieve the level of control you want with your current setup? No problem! Just use ours!)  
Everything you need to start encapsulating cells and biological samples in droplets in one single pack.

#### What is it?

It is a microfluidic chip-based system that encapsulates cells and other biological samples in droplets at a high frequency, carefully designed for researchers that want to use microfluidics efficiently as a tool and improve their controllability over experiments.

The pack's user and troubleshooting guides provide all the necessary information to assemble and make the most of the encapsulation pack for your experiments. Also, the pack's flexibility allows you to easily adapt it as your needs evolve.

This solution includes all the necessary elements to create a continuous flow and monitor the flow rate applied to the samples even for long-lasting experiments.

Flow: Dual jet + 450µm  
Single cell encapsulation every droplet microfluidic




**ADVANTAGES**

- Precision flow control
- High frequency
- Flexibility (volume, size, etc.)

**DISADVANTAGES**

A regular price list

#### The pack comprises:

- Pressure-driven flow controller
- Flow sensors
- Solenoid Valves
- Pipettes
- Chips (excepted for your specific needs)
- Consumables (e.g. Fluorinated oil & surfactant)
- User and troubleshooting guide
- Collection Vial
- User friendly software

#### And you can expect:

- Reliability and reproducibility of results
- High frequency encapsulation
- High controllability over encapsulation parameters (e.g. droplet size, number of droplets per second)
- Step-by-step assembly guidance through detailed user guides.

#### Who is it for?

# Appendix 8 - Chapter 2. Pilot Pack - pH control without Incubator

**ELVEFLOW**  
an ELVESYS brand

About Support Contact

Search Elveflow.com

PRODUCTS APPLICATIONS OEM & CUSTOM INNOVATION RESOURCES

HOME / MICROFLUIDICS RESEARCH / BETA AND INNOVATION / MICROFLUIDICS PILOT PACKS / MICROFLUIDIC PH CONTROL WITHOUT A CO2 INCUBATOR

## BETA & INNOVATION

Time (h)	in 5% CO <sub>2</sub> (solid)	in 5% CO <sub>2</sub> (dashed)	in Room Air (dotted)	in Room Air (dash-dot)
0	7.3	7.3	7.3	7.3
5	7.7	7.7	7.7	7.7
10	7.7	7.7	7.7	7.7
20	7.7	7.7	7.7	7.7
30	7.7	7.7	7.7	7.7
40	7.7	7.7	7.7	7.7
50	7.7	7.7	7.7	7.7

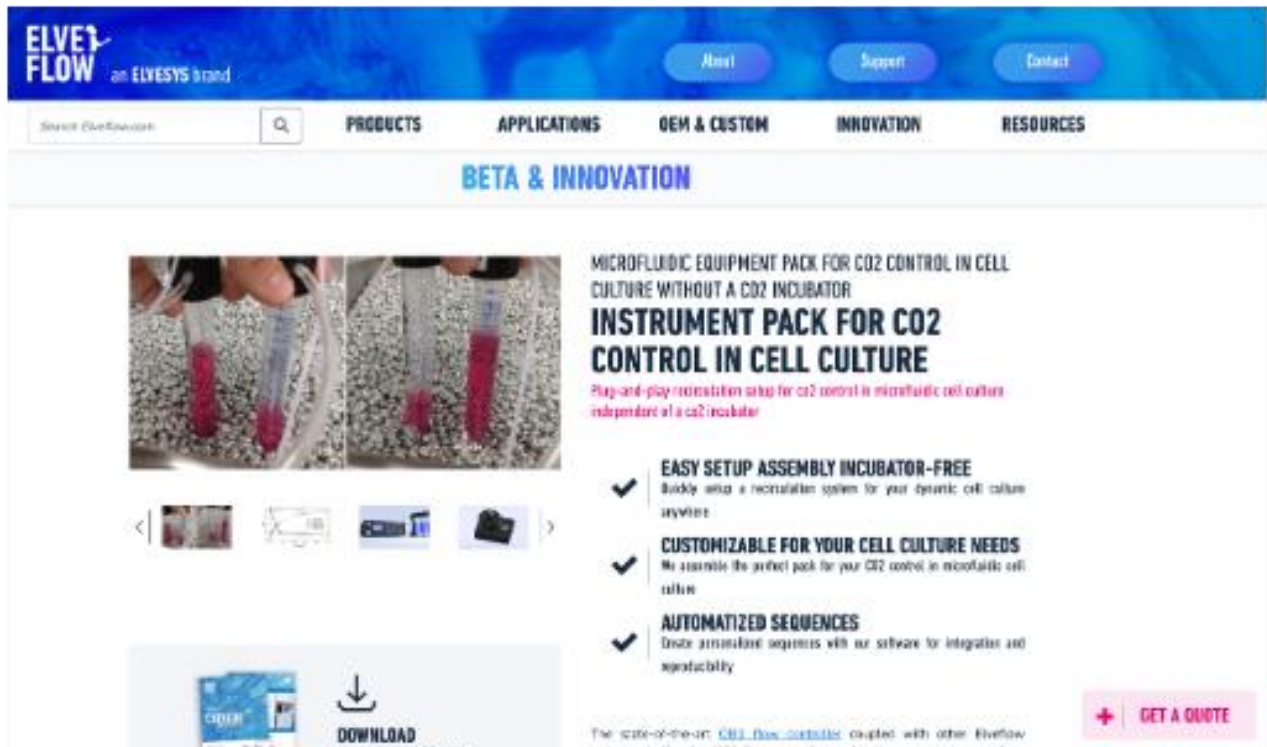
**EQUIPMENT PACK FOR PH CONTROL IN MICROFLUIDICS WITHOUT A CO2 INCUBATOR**  
**MICROFLUIDIC EQUIPMENT FOR PH CONTROL WITHOUT INCUBATOR**  
*Plug-and-play recirculation setup for pH control in microfluidic cell culture independent of a CO2 incubator*

- ✓ **EASY SETUP ASSEMBLY INCUBATOR-FREE**  
Quickly setup a recirculation system for your dynamic cell culture anywhere
- ✓ **CUSTOMIZABLE FOR YOUR CELL CULTURE NEEDS**  
We assemble the perfect pack for your CO2 control in microfluidic cell culture
- ✓ **AUTOMATIZED SEQUENCES**  
Create personalized sequences with our software for integration and reproducibility

[+ GET A QUOTE](#)



# Appendix 9 - Chapter 2. Pilot Pack - CO2 control without Incubator



The screenshot shows the Elveflow website's 'BETA & INNOVATION' section. The header includes the Elveflow logo (an ELVESYS brand), a search bar, and navigation links for Home, Support, and Contact. The main navigation menu lists PRODUCTS, APPLICATIONS, OEM & CUSTOM, INNOVATION, and RESOURCES. The featured product is the 'INSTRUMENT PACK FOR CO2 CONTROL IN CELL CULTURE', described as a 'play-and-play recirculation setup for CO2 control in microfluidic cell culture independent of a CO2 incubator'. The page highlights three key features: 'EASY SETUP ASSEMBLY INCUBATOR-FREE', 'CUSTOMIZABLE FOR YOUR CELL CULTURE NEEDS', and 'AUTOMATIZED SEQUENCES'. A 'DOWNLOAD' button is visible, and a 'GET A QUOTE' button is located in the bottom right corner.

**ELVEFLOW** an ELVESYS brand

Home Support Contact

Search Elveflow

PRODUCTS APPLICATIONS OEM & CUSTOM INNOVATION RESOURCES

### BETA & INNOVATION

**MICROFLUIDIC EQUIPMENT PACK FOR CO2 CONTROL IN CELL CULTURE WITHOUT A CO2 INCUBATOR**

## INSTRUMENT PACK FOR CO2 CONTROL IN CELL CULTURE

Play-and-play recirculation setup for CO2 control in microfluidic cell culture independent of a CO2 incubator

- EASY SETUP ASSEMBLY INCUBATOR-FREE**  
Builds into a recirculation system for your dynamic cell culture systems
- CUSTOMIZABLE FOR YOUR CELL CULTURE NEEDS**  
We assemble the perfect pack for your CO2 control in microfluidic cell culture
- AUTOMATIZED SEQUENCES**  
Create personalized sequences with our software for integration and reproducibility

The state-of-the-art [CO2 flow controller](#) coupled with other Elveflow

**DOWNLOAD**

**GET A QUOTE**

# Appendix 10 - Chapter 2. Pilot Pack - pH control for cell culture

The screenshot shows the Elveflow website's product page for a pH control equipment pack. The header includes the Elveflow logo (an ELVEYS brand), navigation buttons for 'About', 'Support', and 'Contact', and a search bar. The main navigation menu lists 'PRODUCTS', 'APPLICATIONS', 'DEM & CUSTOM', 'INNOVATION', and 'RESOURCES'. The page is titled 'BETA & INNOVATION' and features a carousel of images showing the equipment pack. The main content area is titled 'EQUIPMENT PACK FOR PH CONTROL IN MICROFLUIDICS' and 'PH CONTROL IN MICROFLUIDIC CELL CULTURE EQUIPMENT PACK'. It includes a sub-headline 'Plug-and-play recirculation setup for pH control in microfluidic cell culture' and three key features: 'CUSTOMIZABLE FOR YOUR CELL CULTURE NEEDS', 'EASY SETUP ASSEMBLY', and 'AUTOMATIZED SEQUENCES'. A 'DOWNLOAD PRODUCT CATALOG 2017' button is visible. A 'GET A QUOTE' button is located in the bottom right corner.

**ELVEFLOW**  
an ELVEYS brand

Search Elveflow.com

PRODUCTS APPLICATIONS DEM & CUSTOM INNOVATION RESOURCES

**BETA & INNOVATION**

**EQUIPMENT PACK FOR PH CONTROL IN MICROFLUIDICS**  
**PH CONTROL IN MICROFLUIDIC CELL CULTURE EQUIPMENT PACK**  
*Plug-and-play recirculation setup for pH control in microfluidic cell culture*

- ✓ **CUSTOMIZABLE FOR YOUR CELL CULTURE NEEDS**  
We assemble the perfect pack for your pH control in cell culture
- ✓ **EASY SETUP ASSEMBLY**  
Easily setup a recirculation system for your dynamic cell culture
- ✓ **AUTOMATIZED SEQUENCES**  
Create personalized sequences with our software for integrative and reusability

Easy pH in microfluidics for your pH control in dynamic cell culture with this all-included user-friendly, customizable and automatable recirculation pack

The state-of-the-art [OD1 flow controller](#) coupled with other Elveflow instruments like the [MS5 flow controller](#) and in-line sensors is enough to precisely control your cell culture parameters, such as pH, while keeping your

**DOWNLOAD**  
PRODUCT CATALOG 2017

**GET A QUOTE**

# Appendix 11 - RÉSUMÉ EN FRANÇAIS

Développement d'outils pour le contrôle précis de paramètres à intérêts biologiques utilisant la microfluidique

## 1. Introduction

La microfluidique est une technologie versatile qui couvre une grande gamme d'applications. Elle offre un niveau de contrôle sans précédent, permettant l'assemblage guidé précis de molécules en micro-compartiments, tels les émulsions de second ordre (adapté de l'anglais, émulsions doubles), qui se traduit par une efficacité d'encapsulation et une monodispersité des populations sensiblement améliorées. Outre la possibilité de contrôler ces paramètres internes, la microfluidique peut également être utilisée pour contrôler et surveiller les paramètres physiques externes d'un système, tels que le pH ou la composition en gaz de ces compartiments ou d'autres structures, comme des cellules vivantes.

Les émulsions doubles (EDs) sont des systèmes complexes de liquides non-miscibles (e.g. des gouttelettes d'eau dans l'huile dans l'eau) fréquemment utilisées dans l'industrie alimentaire pour la fabrication de produits à faible teneur en matières grasses et pour améliorer l'apport en nutriments et en arômes.<sup>1-3</sup> Historiquement, la plupart des intérêts dérivés des EDs proviennent de l'industrie pharmaceutique.<sup>1,4</sup> Les EDs ont notamment été étudiées dans le cadre de systèmes de délivrance de médicaments<sup>5-7</sup>, de substituts sanguins<sup>8,9</sup>, et de vaccins<sup>10,11</sup>, avec l'une des premières applications rapportée remontant à la fin des années 1960, visant à améliorer l'absorption d'insuline dans l'intestin.<sup>12</sup>

Les EDs sont généralement produites par un processus d'émulsification en deux étapes, dans lequel les populations ont tendance à être polydispersées et à présenter une efficacité d'encapsulation variable, allant de 10 à 98%.<sup>4,13,14</sup> La production d'émulsions simples, doubles et voire même multiples par des procédés microfluidiques a été récemment signalée<sup>15-17</sup>, démontrant des populations hautement monodispersées et des efficacités d'encapsulation de près de 100%.<sup>18,19</sup>

Le contrôle des paramètres physiques externes d'un système microfluidique tels que le pH ou la concentration en gaz dissous est également une problématique essentielle. Les incubateurs

à CO<sub>2</sub> sont les facilitateurs silencieux de la plupart des avancées modernes de la recherche dans les domaines de la biologie cellulaire et de la santé. Ils maintiennent les cellules à une température physiologique constante (37 °C), dans des niveaux d'humidité et de CO<sub>2</sub> idéaux afin de tamponner le milieu pendant la croissance cellulaire. Les organes-sur-puce (organ-on-chip, OoC, en anglais) ont gagné en pertinence ces dernières années pour ajouter de la complexité aux cultures cellulaires traditionnelles en reproduisant plus fidèlement les conditions physiologiques des stimulus mécaniques et d'interactions intercellulaires.

Toutefois, les OoC dépendent encore largement de l'infrastructure traditionnelle de la culture cellulaire comme l'incubateur à CO<sub>2</sub> pour maintenir des niveaux appropriés de CO<sub>2</sub> et de température pendant la culture sur puce à long terme. En particulier, une partie du système de culture se trouve souvent à l'intérieur de l'incubateur, principalement la puce, tandis qu'une autre partie se trouve à l'extérieur, comme les réservoirs de milieu et les tuyaux. En raison du grand rapport entre la surface d'échange et le volume typique d'un système microfluidique et de la perméabilité variable des composants du système aux gaz, cela peut entraîner des variations de température et de concentration en gaz entre la surface de culture et le reste du circuit fluidique.

Ces travaux de thèse ont d'abord consisté à explorer le potentiel de la microfluidique pour produire des émulsions doubles et en les testant dans des conditions physiologiquement pertinentes afin d'évaluer leur utilité comme systèmes de délivrance de médicaments par voie orale. Dans un second temps, les paramètres physiques d'un système microfluidique de culture cellulaire de longue durée (pH, gaz dissous) ont été caractérisés et ajustés afin que le système soit indépendant d'un incubateur à CO<sub>2</sub>.

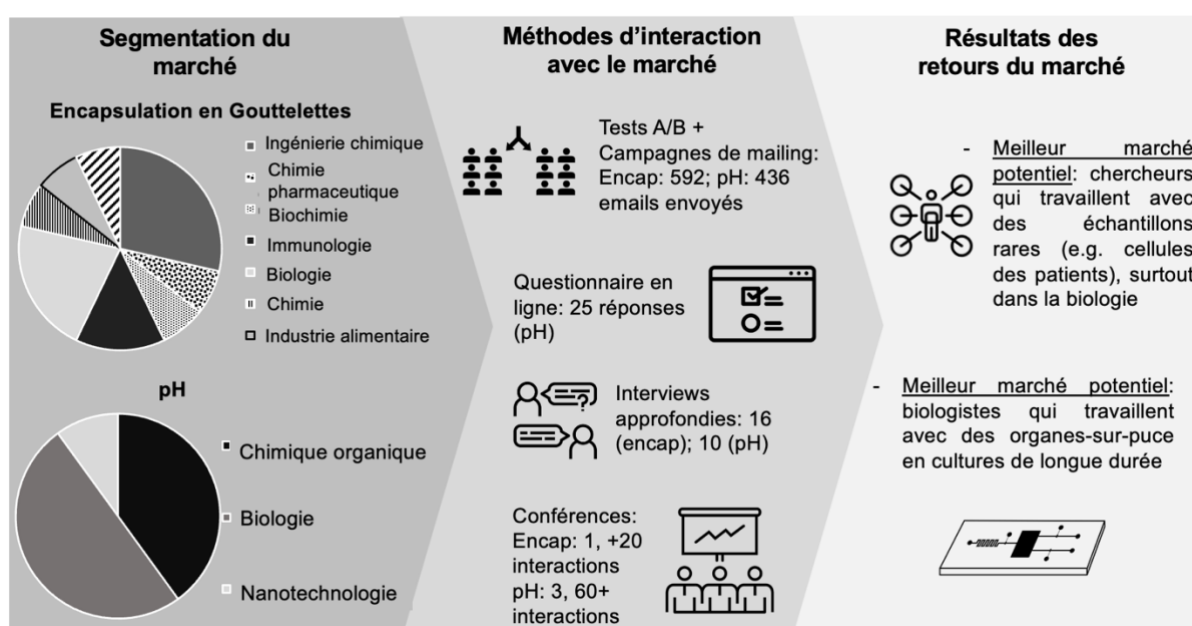
## **2. Résultats et discussions**

### **2.1. Évaluation de l'adéquation aux besoins du marché**

Dans le cadre d'un doctorat industriel, il est important d'identifier et de comprendre les enjeux actuels qui doivent être abordés dans chaque domaine d'intérêt. Ce travail est effectué avant de s'engager dans la recherche et le développement de solutions afin que les résultats puissent apporter de la valeur à une large communauté d'utilisateurs dans l'avenir. Pour ce faire, la collecte d'informations auprès de leaders d'opinion clés (key opinion leaders, KOL) a été faite dans les deux domaines d'intérêt : l'encapsulation en gouttelettes et la surveillance du pH dans les cultures cellulaires dynamiques. Le but était d'identifier les spécifications

techniques des systèmes microfluidiques à chaque niveau (i.e. puce, connecteurs, débit, tuyaux, etc.) et d'identifier les normes du domaine pour assurer la conformité et la reproductibilité de la solution.

Ces études ont été basées sur des questionnaires, des entretiens et des recherches secondaires sur la concurrence (Fig. 1) ainsi que sur des analyses financières des différents segments de marché possibles. Les idées générées par ces interactions ont permis de mieux aligner les besoins des utilisateurs avec la démarche de la recherche afin de la conduire au développement des produits potentiels. De plus, ces données ont contribué à orienter les efforts de marketing et de vente au sein de l'entreprise.



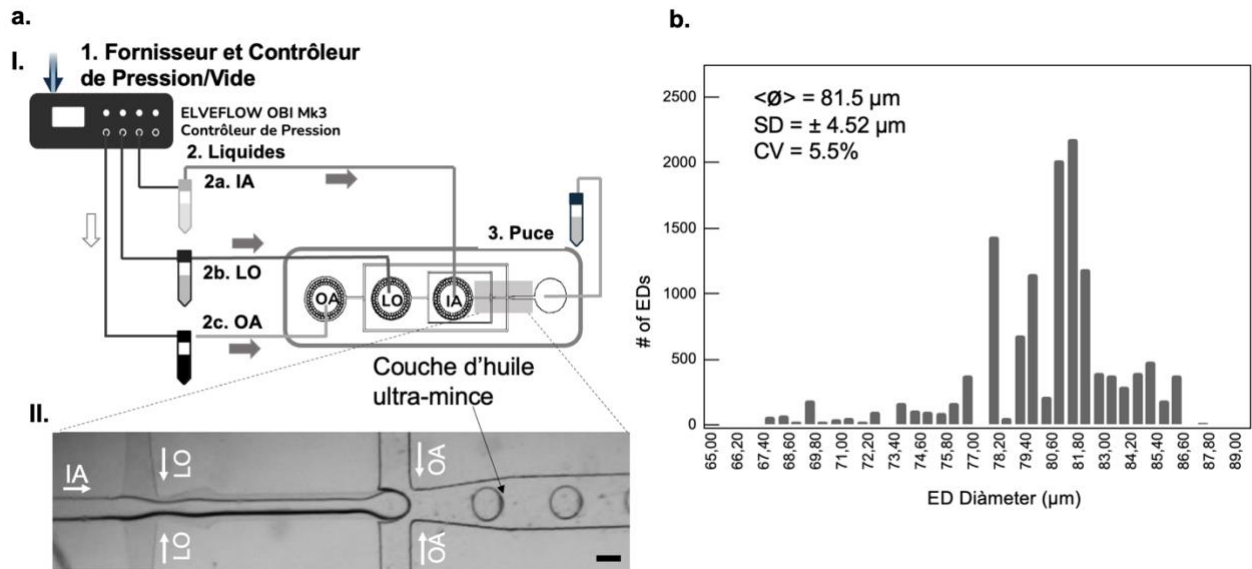
**Figure 1.** Étapes du développement de l'analyse du marché. La segmentation a permis la compréhension des applications et la définition du profil des utilisateurs pour l'étape d'interaction. Les potentiels utilisateurs ont été contactés par différents moyens et l'ensemble des interactions a donné une orientation vers le meilleur marché potentiel.

## 2.2. Émulsions Doubles

Pour étudier la production des EDs à l'aide d'une installation microfluidique, les EDs ont été produites dans des puces en polydiméthylsiloxane (PDMS) à double jonction, réalisées avec des techniques de lithographie douce standard sans salle blanche. Les solutions ont été injectées à l'aide d'un dispositif de contrôle de pression (Fig. 2a.I) depuis les réservoirs jusqu'à la première jonction, où la solution aqueuse interne a été enveloppée par la solution

intermédiaire d'huile, puis jusqu'à la deuxième jonction, où la solution aqueuse externe a pincé les EDs avec une couche d'huile ultra-mince (Fig. 2a.II).

Les EDs résultantes étaient monodispersées (coefficient de variation, CV : 5,5%), avec un diamètre moyen de 81,5  $\mu\text{m}$  ( $\pm 4,52 \mu\text{m}$  ET ; nombre total d'EDs = 14.750) (Fig 2b).



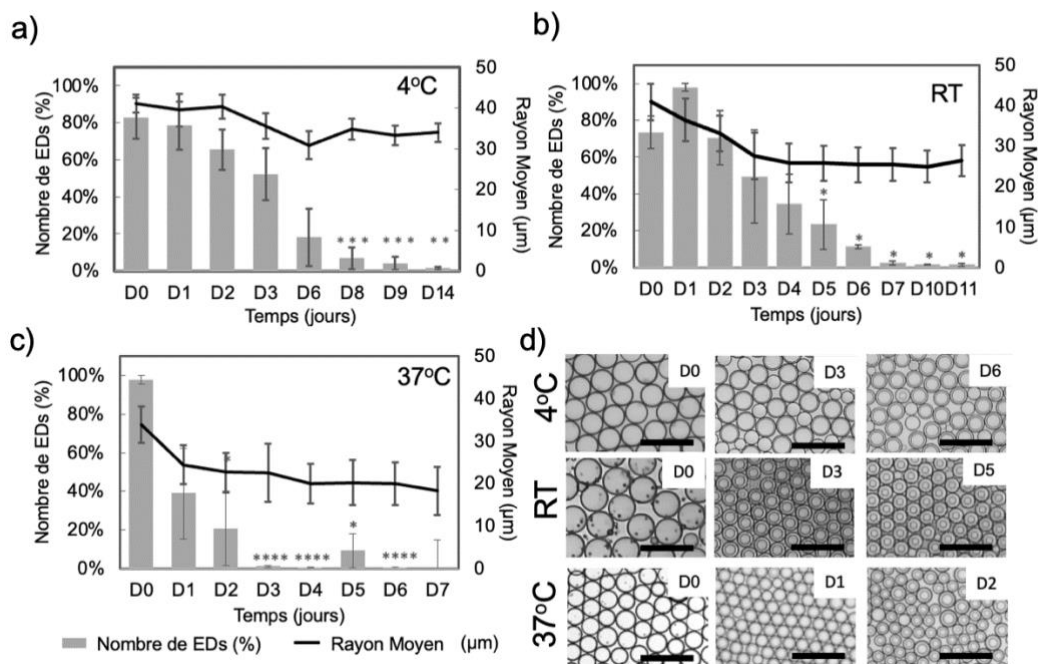
**Figure 2.** Production microfluidique des EDs et caractérisation de leur taille. **a. I.** Système microfluidique pour la production des EDs monodispersées avec des couches d'huile ultra-minces. Chaque réservoir (IA: solution interne aqueuse; LO: solution lipide-huile; OA: solution externe aqueuse) est connecté au contrôleur de débit sous-pression et à leur entrée respective dans la puce. **II.** Photo montrant les EDs pincés à la deuxième jonction et enveloppés d'une couche d'huile ultra-mince. Échelle, 100  $\mu\text{m}$ . **b.** Graphique représentant la distribution de la taille des EDs en  $\mu\text{m}$  ( $\langle \phi \rangle = 81,5 \mu\text{m}$ ,  $\pm 4,52 \mu\text{m}$  ;  $CV : 5,5\%$  ; nombre total d'EDs = 14.750).

La stabilité est un paramètre crucial pour les applications pratiques des EDs. Les émulsions de diamètres supérieurs à 0.1  $\mu\text{m}$  sont des systèmes métastables, c'est-à-dire, qu'elles sont seulement cinétiquement stables et tendent à se briser ou coalescer au fil du temps<sup>20,21</sup>. En vue d'une future application potentielle comme système de délivrance, la stabilité des EDs a été testée dans des conditions physiologiques pertinentes, en étant exposées à des plages de températures, de pH et de débits différents.

La température joue un rôle important dans les systèmes métastables en fournissant l'énergie nécessaire pour que le système quitte l'équilibre transitoire (minimum local d'énergie) et se

dirige vers un état de plus faible énergie.<sup>21</sup> Les températures expérimentales ont été choisies en fonction de leur pertinence pour le cycle de vie d'une ED thérapeutique : de la température physiologique du corps à 37 °C, aux températures pertinentes pour la manipulation et le stockage, à savoir la température ambiante (RT) et 4 °C. Ainsi, les EDs stabilisées par des lipides ont été exposées à 4 °C, à RT et à 37 °C pendant un minimum de 7 jours. Leur nombre et leur rayon moyen ont été mesurés (Fig. 3). Le nombre d'EDs a été normalisé pour chaque condition par le nombre maximal d'ED observé sur la durée de l'expérience. À 4 °C, on observe une tendance de diminution de la population d'EDs au fil du temps, avec une réduction significative observée au jour 8 par rapport au jour 0. À RT, la perte des EDs a été similaire, avec une diminution significative au jour 5 par rapport au jour 0, démontrant un effet positif des températures plus froides sur la stabilité de l'état métastable, comme prévu. Les EDs étaient considérablement moins résistantes aux températures plus chaudes, avec une forte réduction de leur nombre et une différence statistiquement significative à partir du jour 2.

Pour chaque température, le rayon externe moyen a diminué tout au long de la période d'essai (Fig. 3d) accompagné d'une nette augmentation de l'épaisseur de la couche intermédiaire dans le temps.



**Figure 3.** Stabilité et modifications morphologiques des EDs non chargées à différentes températures. a-c. Pourcentage de la valeur maximale dans le temps (axe y gauche) ; La ligne épaisse montre le rayon des EDs (μm), +/- SD (axe y droite). **a.** EDs maintenues à 4 °C (n = 4, nombre total d'EDs à D0 = 16.357 EDs, +/- SEM) ; **b.** RT (n=3, 72.245 EDs, +/- SEM) ; et **c.** 37 °C (n=4, 119.051 EDs, +/- SEM) ; **d.** Images représentatives à différents moments

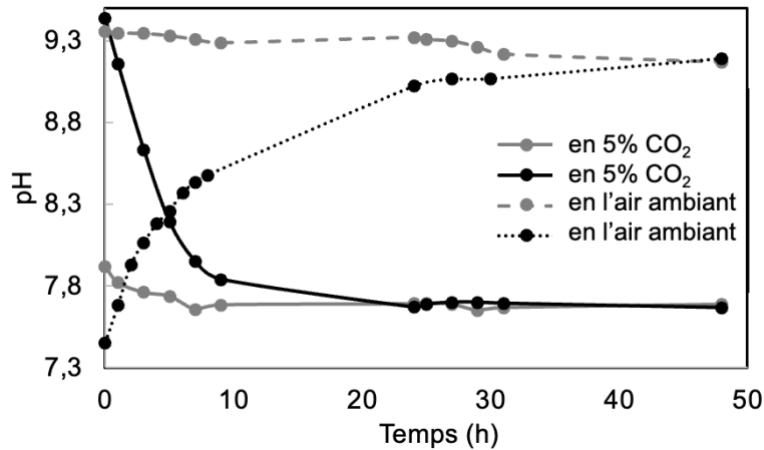
*mettant en évidence le gonflement de la phase intermédiaire ; Échelle : 200  $\mu\text{m}$ . Signification statistique par rapport à D0 (Student T-test) :  $p < 0,05$  (\*) ;  $p < 0,01$ (\*\*) ;  $p < 0,005$  (\*\*\*) ;  $p < 0,001$  (\*\*\*\*).*

La définition de la stabilité des EDs, pour qu'elles soient utilisées comme systèmes de délivrance orale de médicaments, est largement dépendante de leur chargement et de l'application finale. Par exemple, le vaccin à l'ARNm de Pfizer-BioNtech est stable jusqu'à 5 jours à 2-8°C et seulement de 2h à 6h à température ambiante.<sup>22</sup> La stabilité des EDs non chargés se situait dans l'intervalle de temps dans des conditions de stockage au réfrigérateur (8 jours, 4°C) et présentait une résistance substantielle au changement de taille ou à l'agrégation dans des conditions favorables à la distribution et à l'administration d'un produit thérapeutique (5 jours, RT). Cependant, lorsqu'elles étaient chargés, leur stabilité à température ambiante étaient considérablement réduite (Dil, 1 jour ; LUVs, 2h), ce qui démontre l'impact important du chargement sur la stabilité de l'ED. Comme l'illustre le cas de Pfizer-BioNtech, les stabilités observées pourraient être suffisantes dans des applications réelles, bien qu'elles nécessitent des chaînes de distribution complexes.

## **2.4. Surveillance de l'environnement de culture cellulaire de longue durée dans un système microfluidique**

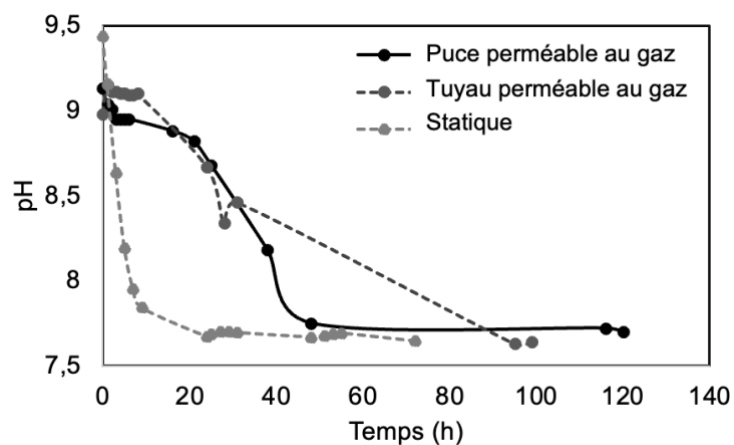
Le pH est un facteur crucial pour la survie cellulaire en culture et il est généralement maintenu dans une gamme désirée par la capacité de tampon du CO<sub>2</sub> dissous dans le milieu. Dans ce cadre, un milieu de culture cellulaire couramment utilisé – le DMEM – a été caractérisé pour établir l'effet de la concentration en CO<sub>2</sub> dissous sur le pH du milieu. D'abord, le milieu a été équilibré à différentes concentrations de CO<sub>2</sub> (~0% comme dans l'air, et 5%, comme dans un incubateur à CO<sub>2</sub>) en l'exposant à des atmosphères de composition gazeuses déterminées. Ces concentrations de CO<sub>2</sub> correspondent à des pH différents (~9,5 pour 0% de CO<sub>2</sub> et ~7,7 pour 5% de CO<sub>2</sub>). Ensuite, le taux de changement de pH a été mesuré au fil du temps avec une électrode de pH standard dans des flacons exposés au mélange gazeux correspondant. Dans les deux cas, le changement est plus rapide dans les 10 premières heures d'exposition (Fig. 4), pour atteindre un plateau où le pH est le plus élevé ou le plus bas possible après 24h.





**Figure 4.** Caractérisation de l'effet du CO<sub>2</sub> sur le pH des milieux de culture cellulaire. Lorsque le milieu est placé dans un incubateur à 5% CO<sub>2</sub> à 37 °C pour être équilibré en gaz au pH 7,7, puis placé dans un bain à 37 °C à l'air ambiant, le pH augmente à environ 9. Inversement, si le milieu est équilibré en gaz à un pH de 9,3 par exposition à l'air atmosphérique, puis placé dans l'incubateur à 5% CO<sub>2</sub>, le pH descend à 7,7.

L'effet des différentes perméabilités au gaz des puces et des tubes sur le pH du milieu a été étudié dans un système microfluidique à recirculation qui reproduit une installation de culture cellulaire. La vitesse de changement était similaire pour les systèmes ayant une puce perméable au gaz ou des tubes perméables au gaz (sans puce), quelle que soit la différence de surface entre les deux configurations (Fig 5). De plus, dans les deux cas, le taux était plus lent que celui d'un système statique comparable.



**Figure 5.** Essais de perméabilité au CO<sub>2</sub> à partir de pH 9 (équilibré à l'air ambiant, 0% de CO<sub>2</sub>). Les systèmes de recirculation utilisant une puce perméable au CO<sub>2</sub> ou des tubes en PFTE (également perméables au CO<sub>2</sub>) ont démontré un taux de changement de pH plus lent que pour l'essai statique de même volume.

La vitesse de variation du pH en raison de la diffusion des gaz est un paramètre important à considérer lors de la conception d'un système de culture cellulaire dynamique destiné à être indépendant d'un incubateur à CO<sub>2</sub>. Si le mélange gazeux idéal est une entrée contrôlée du système, soit en faisant barboter le milieu, soit en pressurant les réservoirs à l'aide d'un régulateur de débit sous pression dans le système de recirculation, l'utilisation d'un matériau imperméable aux gaz peut être une solution simple pour maintenir les paramètres dans les plages souhaitées.

### 3. Conclusion générale

Ce travail a démontré la versatilité de la microfluidique dans la création et le contrôle des paramètres internes et externes de différentes applications. Des émulsions doubles ont été produites avec succès, avec des niveaux élevés de monodispersité et d'efficacité d'encapsulation. Elles ont ensuite été caractérisées et identifiées comme des systèmes potentiels de délivrance orale de médicaments. Les résultats indiquent que les EDs pourraient être des systèmes de délivrance de médicament appropriés, mais les propriétés de chargement et l'application prévue doivent être considérées dès le début du processus de formulation.

Les paramètres externes des cultures cellulaires microfluidiques ont été caractérisés avec succès, notamment l'effet du CO<sub>2</sub> sur le pH des milieux de culture cellulaire et l'effet de la perméabilité aux gaz des composants de la culture cellulaire dynamique. Les futurs travaux se concentreront sur la compréhension de l'effet de l'O<sub>2</sub> et sur la conception d'une solution permettant de maintenir ces paramètres stables indépendamment de l'incubateur à CO<sub>2</sub>.

### 4. Références

1. Muschiolik, G. & Dickinson, E. Double Emulsions Relevant to Food Systems: Preparation, Stability, and Applications. *Compr. Rev. Food Sci. Food Saf.* **16**, 532–555 (2017).
2. Aditya, N. P. *et al.* Co-delivery of hydrophobic curcumin and hydrophilic catechin by a water-in-oil-in-water double emulsion. *Food Chem.* **173**, 7–13 (2015).
3. Moriano, M. E. & Alamprese, C. Whey Protein Concentrate and Egg White Powder as Structuring Agents of Double Emulsions for Food Applications. *Food Bioprocess Technol.* **13**, 1154–1165 (2020).

4. Ding, S., Serra, C. A., Vandamme, T. F., Yu, W. & Anton, N. Double emulsions prepared by two-step emulsification: History, state-of-the-art and perspective. *J. Control. Release* **295**, 31–49 (2019).
5. Sengupta, S. *et al.* Temporal targeting of tumour cells and neovasculature with a nanoscale delivery system. *Nature* **436**, 568–572 (2005).
6. Qi, X., Wang, L. & Zhu, J. Water-in-oil-in-water double emulsions: An excellent delivery system for improving the oral bioavailability of pidotimod in rats. *J. Pharm. Sci.* **100**, 2203–2211 (2011).
7. Yang, Y. Y., Chung, T. S. & Ping Ng, N. Morphology, drug distribution, and in vitro release profiles of biodegradable polymeric microspheres containing protein fabricated by double-emulsion solvent extraction/evaporation method. *Biomaterials* **22**, 231–241 (2001).
8. Lu, J., Jiang, F., Lu, A. & Zhang, G. Linkers Having a Crucial Role in Antibody–Drug Conjugates. *Int. J. Mol. Sci.* **17**, 561 (2016).
9. Yu, W. P. & Chang, T. M. . Submicron Polymer Membrane Hemoglobin Nanocapsules as Potential blood substitutes: Preparation and Characterization. *Artif. Cells, Blood Substitutes Immob. Biotech.* **24**, 169–183 (1996).
10. Verma, R. & Jaiswal, T. N. Protection, humoral and cell-mediated immune responses in calves immunized with multiple emulsion haemorrhagic septicaemia vaccine. *Vaccine* **15**, 1254–1260 (1997).
11. Liao, J. J., Hook, S., Prestidge, C. A. & Barnes, T. J. A lipid based multi-compartmental system: Liposomes-in-double emulsion for oral vaccine delivery. *Eur. J. Pharm. Biopharm.* **97**, 15–21 (2015).
12. Engel, R. H., Riggi, S. J. & Fahrenbach, M. J. Insulin: Intestinal Absorption as Water-in-Oil-in-Water Emulsions. *Nature* **219**, 856–857 (1968).
13. Matsumoto, S., Kita, Y. & Yonezawa, D. An attempt at preparing water-in-oil-in-water multiple-phase emulsions. *J. Colloid Interface Sci.* **57**, 353–361 (1976).
14. Frenkel, M., Shwartz, R. & Garti, N. Multiple Emulsions. I. stability, inversion, apparent and weighted HLB. *J. Colloid Interface Sci.* **94**, 174–178 (1983).
15. Chu, L. Y., Utada, A. S., Shah, R. K., Kim, J. W. & Weitz, D. A. Controllable monodisperse multiple emulsions. *Angew. Chemie - Int. Ed.* **46**, 8970–8974 (2007).
16. Cai, B. *et al.* A microfluidic platform utilizing anchored water-in-oil-in-water double emulsions to create a niche for analyzing single non-adherent cells. *Lab Chip* **19**, 422–431 (2019).
17. Trantidou, T., Elani, Y. & Ces, O. Microfluidic generation of double emulsions as multiphase compartmentalised cell-like systems. *IET Conf. Publ.* **2016**, (2016).
18. Tumarkin, E. *et al.* High-throughput combinatorial cell co-culture using microfluidics.

- Integr. Biol.* **3**, 653–662 (2011).
19. Yandrapalli, N., Petit, J., Bäumchen, O. & Robinson, T. Surfactant-free production of biomimetic artificial cells using PDMS-based microfluidics. *bioRxiv* (2020). doi:10.1101/2020.10.23.346932
  20. Zhao, C. X., Chen, D., Hui, Y., Weitz, D. A. & Middelberg, A. P. J. Controlled Generation of Ultrathin-Shell Double Emulsions and Studies on Their Stability. *ChemPhysChem* **18**, 1393–1399 (2017).
  21. Kornysushin, Y. Short Communication A Model for Metastable States. *J. Non-Equilib. Thermodyn.* **18**, 353–358 (1993).
  22. Crommelin, D. J. A., Anchordoquy, T. J., Volkin, D. B., Jiskoot, W. & Mastrobattista, E. Addressing the Cold Reality of mRNA Vaccine Stability. *J. Pharm. Sci.* **110**, 997–1001 (2021).
-

# Appendix 12 – Scientific Outreach activities

## LIST OF PRESENTATIONS

- C. B. Giuliano, J. Ayache, L. Muiznieks. Production and Stability of Microfluidic Double Emulsions for Oral Drug Delivery. Micro-Nano-Fluidics Meeting (Poster, in-person) – 23 à 24 Septembre, 2021 - Toulouse, France
  - C. B. Giuliano, J. Ayache, L. Muiznieks. Production and Stability of Microfluidic Double Emulsions for Oral Drug Delivery. NanoBioTech Conference (Poster, in-person) - Montreux – 15 à 17 Novembre, 2021 - Montreux, Switzerland
  - C. B. Giuliano, M. Kopf, L. Muiznieks. Monitoring environmental parameters in microfluidics cell culture. Microphysiological systems : from organoids to organ-on-chip Workshop (Poster, in-person) – Cargèse – 11 à 15 Avril, 2022 - Corse, France
- 

## LIST OF PUBLICATIONS

- C. B. Giuliano, N. Cvjetan, J. Ayache, P. Walde. *Multivesicular Vesicles: Preparation and Applications*. ChemSystemsChem 2021, 3, e2000049. (DOI: <https://doi.org/10.1002/syst.202000049>)
  - C.B. Giuliano, J. Ayache, J. Moran and L. Muiznieks. Stability characterization of microfluidics lipid-stabilized double emulsions under physiologically-relevant conditions. Accepted for publication.
- 

## LIST OF NON-PEER REVIEWED PUBLICATIONS

- C. B. Giuliano. Droplets encapsulation for biological applications: a review. Elveflow, 2020
- C.B. Giuliano. The origins of life meet microfluidics. Webinar, Elveflow, 2020.
- L. Muiznieks, S. Bano, C. B. Giuliano ,J.Ayache.. Automate cell seeding in a microfluidic chip for dynamic cell culture. Application Note, Elveflow, 2020.
- L. Muiznieks, S. Bano, C. B. Giuliano ,J.Ayache. An easy guide to do microfluidic perfusion for dynamic cell culture. Application Note, Elveflow, 2020.
- L. Muiznieks, S. Bano, C. B. Giuliano ,J.Ayache. Unidirectional medium recirculation for microfluidic cell culture. Application Note, Elveflow, 2020.
- L. Muiznieks, S. Bano, C. B. Giuliano ,J.Ayache.. How to stain cells cultured in a microfluidic chip for dynamic cell culture?. Application Note, Elveflow, 2020.
- C. B. Giuliano. Double emulsion for encapsulation using microfluidics. Application Note, Elveflow, 2021.
- B. Garlan, C. B. Giuliano. Microfluidic Pack for Artificial Cell Creation - Artificial Cell Droplet Microfluidics. Pilot Pack, Elveflow, 2021.
- C. B. Giuliano. Multivesicular microfluidic vesicles for drug delivery and artificial cells: a short review. Elveflow, 2022
- C. B. Giuliano. Microfluidic flow cells: off-chip pH monitoring for organ-on-chip. Elveflow, 2022

# Appendix 13 – Curriculum Vitae

## CAMILA BETTERELLI GIULIANO

PhD in Chemistry to be concluded in September

+33 (0) 7 66 37 25 57  
cb.giuliano@gmail.com  
<https://www.linkedin.com/in/camilabetterelli>  
Paris, FR  
Dual Nationality: Brazil/Italy

### WORK EXPERIENCE

#### Investment Associate

##### Startup Farm

11/2017 – 09/2018 São Paulo, Brazil  
Leading Startup Accelerator in Brazil  
– 5 investments in accelerated startups  
– 6 startup selection processes

#### Acceleration Program Coordinator

##### Startup Farm

06/2016 – 11/2017 São Paulo, Brazil  
– 200% average annual growth rate of advanced startups  
– 3 sponsored international modules to Silicon Valley  
– 7 Acceleration Programs, over 60 startups

#### Sales Trainee

##### IBM

09/2015 – 06/2016 São Paulo, Brazil  
– Global Sales School  
– Business Development for Santander Brasil

### RESEARCH EXPERIENCE

#### Microfluidics – Marie Curie Fellow

##### Elvesys – Microfluidics Innovation Center; University of Strasbourg

10/2019 – present Paris, France  
Precise control of pH and droplet size and composition within microfluidic devices

Publication: C. B. Giuliano, N. Cvjetan, J. Ayache, P. Walde, ChemSystemsChem 2021, 3, e2000049.  
★ Top 10 Most Downloaded Papers (2019-2020)

#### Drug Delivery – FAPESP Scholar

##### Biomaterials Lab, UNESP

05/2013 – 05/2014 Assis, Brazil  
– Developed a magnetic-field-controlled drug delivery system for the antibiotic Ciprofloxacin with superparamagnetic nanoparticles and latex membrane

Publication: Murbach, H., Giuliano, C. B., Herculano, R. PontodeAcesso, v.10, n.1, pg.46-61, ISSN:1981-6766(2016).

#### Biophysics – Research Intern

##### Harvard University, The Rowland Institute

06/2012 – 12/2012 Cambridge, USA  
– In-dept research of prey attraction mechanism of carnivorous plant

Publication: Giuliano, C. B., Zhang, R., Wilson, L. G. Digital Inline Holographic Microscopy (DIHM) of Weakly-scattering Subjects. *J. Vis. Exp.* (84), e50488, doi:10.3791/50488 (2014).

### MOST PROUD OF



#### Academic Excellence

Graduated as 2<sup>nd</sup> of my class (38 students) and was awarded three fully-funded scholarships for exchange programs (USA, China and Netherlands)



#### Crowdfunding Campaign

Raised £8,000 in two months from 215 people to complement the scholarship for my Masters degree. The initial goal was £6,000.



#### World Citizen

Lived in 5 countries (Brazil, USA, Netherlands, UK and France) and visited more than 25.



#### Harvard Published Paper

First academic paper as first author at the age of 22.

### EDUCATION

#### Masters in Bioscience

##### Enterprises

##### University of Cambridge, UK

10/2018 – 06/2019

GPA  
71/100

#### Innovation and Business

##### University of Groningen, NL

10/2014 – 01/2015

GPA  
7.8/10

#### Biotechnology

##### Boston University, USA

01/2012 – 12/2012

GPA  
3.91/4

#### Biotechnological

##### Engineering

##### UNESP, BR

02/2009 – 06/2015

GPA  
8.23/10

### LANGUAGES

Portuguese	English	Spanish	French
Native	Proficient	Advanced	Advanced

Camila BETTERELLI GIULIANO  
**Development of tools for  
the precise control of  
biological parameters via  
microfluidics**

## Abstract

### Résumé

La manipulation précise de fluides à l'échelle microscopique par la microfluidique est pertinente pour la biologie, en transposant une technologie originaire du domaine de la physique à un outil polyvalent pour les sciences de la vie. Cette thèse explore cette polyvalence dans deux applications biologiques : l'encapsulation dans des gouttelettes et la surveillance du microenvironnement pour la culture cellulaire microfluidique. Ces recherches se sont appuyées sur des études de marché qui ont révélé un besoin pour de telles applications. Il a été démontré que la microfluidique permet de produire des compartiments de niveaux de complexité variés, comme des émulsions doubles, dans des conditions de production accessibles. En outre, la stabilité des émulsions doubles a été étudiée dans des conditions physiologiques pertinentes en tant que système de délivrance orale de médicaments. Ensuite, une culture cellulaire microfluidique a été maintenue avec succès hors de l'incubateur à CO<sub>2</sub> pendant plus de 48h. La mesure continue du pH a été suffisamment sensible pour enregistrer une signature du métabolisme des cellules.

**Mots clés** : microfluidique, microfluidique à gouttelettes, émulsions doubles, organe sur puce, surveillance du microenvironnement ; culture cellulaire microfluidique.

### Résumé en anglais

Microfluidics precise handling of liquids in the micro-scale is particularly relevant for biology, transitioning the technology from physic-related studies to become a versatile tool in life sciences. This thesis explores this versatility in two biological applications: encapsulation in microcompartments and microenvironment monitoring for microfluidic cell culture. These investigations were supported by market studies that highlighted a demand for such applications. Microfluidics was demonstrated to produce microcompartments in varying levels of complexity, such as double emulsions, in non-specialist settings. Moreover, the stability of double emulsions was investigated under physiologically-relevant conditions as a potential oral drug delivery system. Then, a miniaturised microfluidic cell culture was successfully maintained outside the CO<sub>2</sub> incubator for over 48h. Continuous pH monitoring of the microenvironment was sensitive enough to demonstrate metabolic cell cycles.

**Keywords**: microfluidics, droplet microfluidics, double emulsions, organ-on-a-chip, microenvironment monitoring; microfluidic cell culture